12-4-2006

# Selective Recognition of Quadruplex DNA by Small Molecules

Elizabeth W. White

SELECTIVE RECOGNITION OF QUADRUPLEX DNA BY SMALL MOLECULES

by

Elizabeth W. White

Under the Direction of Dr. W. David Wilson

ABSTRACT

Structure-specific recognition of nucleic acids is a promising method to reduce the size of the recognition unit required to achieve the necessary selectivity and binding affinity for small molecules. It has been demonstrated recently that G-quadruplex DNA structures can be targeted by organic cations in a structure-specific manner. Structural targets of quadruplexes include the planar end surfaces of the G-tetrad stacked columns as well as four grooves. The significant structural differences between quadruplex DNA and duplex DNA make quadruplex DNA a very attractive target for highly selective, structure-specific drug design. We have used a variety of biophysical techniques including circular dichroism, surface plasmon resonance, thermal melting and absorbance spectroscopy to investigate small molecules that can selectively bind to the ends of human telomeric DNA as well as the ends of the G-quadruplex structure formed by the purine-rich promoter region of the c-MYC oncogene. We have also screened a library of heterocyclic diamidines, and identified one that binds selectively in the grooves of human telomeric quadruplex DNA. This compound is an excellent starting point for the design of new anti-cancer and anti-parasitic compounds with high affinity and selectivity for human telomeric DNA.

INDEX WORDS: Molecular recognition, Quadruplex DNA, Circular dichroism, Surface plasmon resonance, Telomeres, Telomerase inhibitors, i-motif, c-MYC oncogene, G-quartet

# SELECTIVE RECOGNITION OF QUADRUPLEX DNA BY SMALL MOLECULES

by

ELIZABETH W. WHITE

A Dissertation Submitted in Partial Fulfillment of the Requirements for the Degree of

Doctor of Philosophy

In the College of Arts and Sciences

Georgia State University

2006

**SELECTIVE RECOGNITION OF QUADRUPLEX DNA BY SMALL MOLECULES**

by

ELIZABETH W. WHITE

| | |
|---|---|
| Major Professor: | Dr. W. David Wilson |
| Committee: | Dr. David W. Boykin |
| | Dr. Bruce Armitage |

Electronic Version Approved:

Office of Graduate Studies
College of Arts and Sciences
Georgia State University
December 2006

Dedicated to AJB

## Acknowledgments

First of all, I would like to thank Dr. David Wilson for being brave enough to take me on as a student, and second, for all the help, patience and support he gave me throughout the years. I thank all the members of Dr. Wilson's research group for all their help and friendship, especially Rupesh Nanjunda for his assistance on this project and Binh Nguyen and Farial Tanious for being such great teachers and always helping me when I needed it (which was often). I would also like to thank Dr. Boykin and his group for their assistance and for their collaboration on this project.

I thank NIH, Gates Foundation, and Georgia Research Alliance, for financial support of this project. I would also like to thank Dr. Alfons Baumstark and the GSU Chemistry Department as well as the GSU Molecular Basis of Disease program for their support.

I would like to thank Dr. Laurence Hurley and Dr. Bruce Armitage for all their helpful advice and suggestions on this project throughout the last several years.

And last but not least… I would like to give a special thanks to Ms. Dane Marshall, my high school math teacher at Oconee County High School from 1985 to 1989. She instilled in me a lifelong love of learning and showed me that being a math geek can actually be pretty cool.

**Table of Contents**

# List of Tables

## Chapter 5



## Chapter 6

# List of Figures

## Chapter 1



## Chapter 2

**Chapter 3**

**Chapter 4**

**Chapter 5**

**Chapter 6**

## List of Abbreviations

| | |
|---|---|
| CD | Circular Dichroism |
| DNA | Deoxyribonucleic Acid |
| EDTA | Ethylenediamine Tetraacetate |
| HEPES | 4-(2-hydroxyethyl)-1-piperazineethanesulfonic Acid |
| HTel | Human Telomeric DNA |
| $IC_{50}$ | 50% Inhibitory Concentration |
| ITC | Isothermal Titration Calorimetry |
| mdeg | millidegrees |
| MES | 2-(N-morpholino)ethanesulfonic Acid |
| NMR | Nuclear Magnetic Resonance |
| RU | Response Units |
| SPR | Surface Plasmon Resonance |
| TBA | Thrombin Binding Aptamer |
| TetTel | Tetrahymena Telomere |
| Tm | Thermal Melting Temperature |
| TRIS | Tris Hydroxymethylaminoethane |
| UV | Ultraviolet |

# Chapter 1

# Overview

## Introduction

Specific recognition of double helical sequences of base pairs in DNA, for example, by transcription control proteins [1] and designed synthetic molecules [2, 3], has been thoroughly studied and many sequence-specific recognition complexes are now characterized in molecular detail. Therapeutic intervention or control of cellular function through specific recognition of a cellular duplex DNA sequence requires interaction with a large number of base pairs. This is routinely accomplished by cellular proteins but is more difficult to achieve with relatively small synthetic compounds that must have properties that allow them to pass through barriers including cell membranes in order to bind to DNA. Incorporating nucleic acid structure into the recognition motif, however, is a promising method to reduce the size of the recognition sequence required to gain the necessary specificity. Specific recognition of RNA structures by small molecules that interact with only a few bases or base pairs, for example, is well established for aminoglycoside antibiotics that target ribosomal RNA [4-6]. The recent discovery of small metabolites and analogs that bind specifically to RNA riboswitch structures is now a demonstrated method for specific control of translation [7]. Selection methods that yield nucleic acids that are capable of highly specific binding to small molecules provide an additional example of recognition by structure-specific motifs [8]. Examples of structure-specific targeting are also emerging for selective recognition of DNA. The

mitochondrial kinetoplast DNA of kinetoplastid eukaryotic parasites, which cause serious diseases that affect millions of people, for example, has a complex structure that is composed of a few large circular DNAs in an interlocked, catenated array with thousands of minicircular DNAs [9-11]. The minicircular DNAs have phased AT sequence tracts that bend the DNA duplex [12] and provide an optimum sequence-structure target for drug design [13].

Another structural target of interest is four-stranded quadruplex DNA. Guanine-rich sequences, which are capable of forming quadruplex structures, are present in biologically significant regions of the genome including telomeres [14], immunoglobulin switch regions [15], the transcriptional regulatory regions of a number of genes such as the insulin gene [16], and also the promoter regions of certain oncogenes, such as c-MYC [17, 18]. Cytosine-rich DNA, such as found in the complementary DNA strand of sequences that form G-quadruplexes, has also been shown to form four-stranded structures *in vitro*, known as i-motif DNA. The key structural feature of the G-quadruplex is a series of stacked guanine tetrads held together in a coplanar cyclic array by Hoogsteen and Watson-Crick hydrogen bonds (Figure 1.1). The quadruplex is also stabilized through π-π stacking interactions of the stacked tetrads as well as by coordination with cations located between or within the tetrads. G-quadruplexes have been shown to form a variety of secondary structures, which depend on the sequence, strand stoichiometry, and sometimes the nature of cations present. These structures can be characterized as parallel, or antiparallel, depending on strand orientation. G-quadruplexes may be intermolecular, consisting of four DNA strands (tetrameric), or two hairpin strands (dimeric), or may be intramolecular, consisting of a folded single strand.

Some examples of quadruplex conformations are shown in Figure 1.2. The significant structural differences between quadruplex DNA and duplex DNA make quadruplex DNA a very attractive target for highly selective, structure-specific drug design. Three quadruplex-forming sequences that have been studied as structure-specific targets for quadruplex-interactive compounds include human telomeric DNA, i-motif DNA formed by the pyrimidine-rich strand of the c-MYC oncogene, and G-quadruplexes formed by the purine-rich strand of the c-MYC oncogene.

**Telomeres**

Telomeres are regions of non-coding DNA located at the ends of eukaryotic chromosomes in organisms as diverse as trypanosomes and humans. Their function is to protect the ends of the chromosomes from erosion, end-end fusion, and to aid in chromosomal alignment during recombination. Human telomeres consist of a 5-15 kilobase double-stranded region with one purine-rich strand and one pyrimidine-rich stand. At the extreme 3' end, the purine-rich strand exists as a single-stranded overhang about 200 bases long. The telomeric sequence varies depending on the organism. In humans and other vertebrates, telomeres consist of tandem $T_2AG_3$ repeats. The human telomere sequence has been shown to adopt a G-quadruplex conformation *in vitro* under physiological conditions [19, 20]. The discovery of proteins such as transcription factors, nucleases and helicases that can bind to and even promote the formation of telomeric quadruplexes suggests that these structures may exist *in vivo* under certain conditions [21-23]. A very exciting recent finding by Boussin and coworkers is that a radiolabeled G-quadruplex binding ligand accumulated in nuclei of cultured cells and preferentially

bound to the terminal regions of the chromosomes, suggesting that G-quadruplexes do exist in *vivo* and are accessible to drugs [24].

Each time a cell divides, DNA polymerase is unable to replicate the extreme end of the 3'strand of the chromosome, since it is the lagging strand during replication. This "end replication problem" results in shortening of the telomere by about 30-200 bases per cell doubling. After 60-70 rounds of cell replication, the telomeres reach a critical length, and are no longer able to form secondary structures. The cells enter a non-dividing state called senescence either by activating p53 or by inducing the p16/RB pathway, which leads to apoptosis and eventually cell death [25]. However, in 85-90% of cancer cells the reverse transcription enzyme telomerase is activated [26]. The enzyme is also active in eukaryotic parasites such as trypanosomes and leishmania. This enzyme is inactive in most normal somatic cells, providing a potentially very specific target for the treatment of cancer and parasitic disease. In humans telomerase adds $T_2AG_3$ repeats to the telomere ends, which balances telomere shortening during cell division. The result is that telomere length is maintained, contributing to immortality of the cancer cells. Telomerase consists of an 11 base RNA template and an hTERT catalytic subunit with reverse transcriptase activity. Telomerase inhibition has been studied as an anti-cancer strategy. Targets for telomerase inhibition include the hTERT catalytic subunit, targeted by reverse transcriptase inhibitors and dominant negative hTERT constructs [27-32]. The RNA template has also been targeted using antisense oligonucleotides [33, 34] as well as hammerhead ribozymes [35, 36]. Our focus is on the telomere primer rather than the enzyme itself. Telomerase requires the telomere primer to be single stranded. The formation of higher-ordered structures such as G-quadruplexes, prevents hybridization of

the telomerase RNA template onto the primer and thus inhibits telomerase activity through an indirect topological mechanism [37]. Stabilization of the quadruplex conformation of telomeres, such as by binding with a small molecule, has been shown to inhibit telomerase activity. The development of small molecules that can selectively bind to and stabilize the G-quadruplex conformation of the telomere is therefore a current area of interest in anti-cancer drug design.

In eukaryotic parasites the telomere and telomerase is essential for all of the functions described above but also for additional gene control mechanisms. The enzyme telomerase is found in disease-causing unicellular protozoan parasites, such as *Plasmodium, Trypanosoma, and Leishmania* species [38, 39]. The telomeres of these organisms consist of the same sequence of tandem $T_2AG_3$ repeats as in human telomeres. These protozoa undergo very rapid cell division, but because telomere shortening is compensated for by telomerase, these cells can undergo an unlimited number of cell divisions, much like cancer cells. The protozoan pathogens cause such diseases as malaria and African sleeping sickness and are responsible for millions of deaths each year. The few available antiprotozoan therapies suffer from problems such as drug resistance and severe toxicity to the host. Telomerase inhibition through stabilization of the quadruplex conformation of the telomere offers an attractive, selective target for the design of agents which may impair the proliferation of these protozoa with decreased cytotoxicity and drug resistance.

**Promoter Region of c-MYC Oncogene**

Emerging evidence for the involvement of G-quadruplex structures in cellular processes such as transcriptional control of the c-MYC oncogene has stimulated the

development of drugs that have selectivity for different G-quadruplex structures for the purpose of controlling gene regulation. The promoter regions of some important genes, such as the insulin gene, c-MYC, PDGF, HER-2/neu, c-MYB, the human and chicken β-globin genes, the rat preproinsulin II gene, adenovirus serotype 2, and retinoblastoma susceptibility genes, have been found to contain sequences that have the ability to form G-quadruplex structures under physiological conditions [18, 40-44]. Direct evidence for the involvement of G-quadruplexes in transcriptional control has been obtained only for c-MYC and the insulin gene. The protein product of c-MYC activates telomerase and facilitates cell growth by altering the activity of certain transcription factors [45-47]. Overexpression of c-MYC results in increased cellular proliferation in a variety of human and animal malignanices, including cancers of the colon, breast, cervix, and lungs, as well as B and T cell lymphomas, osteosarcomas, glioblastomas and myeloid leukemias [48-51]. A 27-bp sequence located -142 to -115 bp upstream of the P1 promoter of c-MYC, known as the Nuclease Hypersensitivity Element, ($NHEIII_1$), controls up to 90% of the transcriptional activity of the gene, making it an attractive target for anti-cancer drug design [52-55]. This DNA sequence contains a non-coding purine-rich strand, and its complementary pyrimidine-rich coding strand. The $NHEIII_1$ exists as a duplex structure, but can interconvert in a slow equilibrium with both unwound and quadruplex structures with the aid of an accessory factor with helicase activity known as NM23-H2. The conformation of the purine-rich strand has been proposed to act as a transcriptional switch [17]. When the $NHEIII_1$ is in either the duplex or unwound single-stranded form, the gene is transcriptionally active and expression occurs. With the aid of the accessory protein, the purine-rich strand can form a highly dynamic mixture of four parallel G-

quadruplex loop isomers, all of which have been shown to act as transcriptional repressors and silence gene expression [56]. The 1:2:1 loop isomer is predominant, and the NMR structure has been solved for this isomer [57]. This transcriptionally silent state must be remodeled back to the duplex state with the aid of the accessory protein for transcription to occur. Small molecules which can bind to one of these transcriptionally silent paranemic DNA forms and prevent the conformational change back to the duplex state may act as transcriptional repressors, preventing expression of this oncogene, thus making this DNA element an attractive target for structure-specific anti-cancer drug design.

**i-motif DNA**

Under acidic pH conditions, cytosine-rich DNA sequences are capable of forming four-stranded quadruplex structures known as i-motif DNA. The i-motif structure is comprised of two parallel-stranded duplexes containing hemiprotonated C·C+ mismatch base pairs (Figure 1.3). Protonation occurs at the N3 of one cytosine, which allows three hydrogen bonds with non-protonated cytosine. The two duplexes are zipped together in an antiparallel orientation, with the C·C+ base pairs from each duplex intercalated between each other (Figure 1.3). Like G-quadruplexes, i-motif DNA can fold into monomeric, dimeric or tetrameric structures, depending on the sequence. However, the conformation of i-motif is not cation-dependent as is the case with G-quadruplex DNA, since there is no cation binding site. Sequences capable of forming i-motif structures are found throughout the genome, including in telomeres and the regulatory regions of genes such as the retinoblastoma susceptibility gene, myeloid-specific genes and the c-MYC oncogene [18, 58-60].

I-motif DNA has not received as much attention as G-quadruplex DNA as a potential drug target. The belief that these structures may not exist *in vivo* under physiological conditions has hindered research in this area. While the structure of G-quadruplex DNA is not significantly affected by changes in pH [61], i-motif conformation is pH sensitive and is favored by slightly acidic pH conditions. CD studies of C-rich oligomers have shown that sequences that form i-motif structures at low pH unfold as the pH is increased to 7.4 [61]. Although there is no direct evidence of a biological role for i-motif DNA, or that i-motif structures exist *in vivo*, proteins have been discovered which are capable of binding to i-motif sequences [62-64]. I-motif recognition proteins that have been recently discovered include ST-1 of Trypanosoma brucei, qTBP42 of rat hepatocytes and hnRNP K and ASF/SF2, which bind to the pyrimidine-rich strand of human telomeres [64-66]. It has also been hypothesized that i-motif formation could be aided *in vivo* by superhelical stress due to chromatin assembly [67]. Small molecules have been shown to promote G-quadruplex formation under unfavorable conditions (such as the absence of added cation) [68, 69] so, it seems possible that some small molecules could induce formation of i-motif structures under physiological conditions as well. These factors suggest that i-motif structures formed by pyrimidine-rich DNA sequences may indeed exist *in vivo*, have biological function, and may serve as a potential drug design target for cancer and other diseases.

**Objectives of this Dissertation**

Discovery and design of compounds that target G-quadruplex structures in DNA is a relatively new area that is now being rapidly driven by the desire to discover new anti-cancer drugs and targets. The majority of compounds that have been shown to bind

to quadruplex DNA are planar, aromatic compounds that bind via external end-stacking to the G-quartet on either one end or both ends of the quadruplex. These compounds, which include anthraquinones, cationic porphyrins, acridines, perylenes, macrocycles and related compounds have large aromatic planar chromophores that mimic the planar surface of the G-quartets [70-73]. These molecules bind non-covalently through electrostatic, van der Waals, and π-orbital overlap interactions, and generally also interact with the loop bases. Since essentially all known quadruplex DNA binders are based on or derived from prototype duplex intercalators, many exhibit little selectivity for quadruplex over duplex structures. These types of molecules exhibit non-selective binding to many sites, leading to the cytotoxic side effects generally associated with chemotherapy, such as nausea vomiting, hair loss, and heart and kidney damage. Binding to non-targeted duplex sequences can also result in significant loss of compound. Since potential quadruplex-forming sequences are common in the genome, selectivity for a particular quadruplex structure over other quadruplexes is also a concern in the design of quadruplex-binding compounds. Binding to non-targeted quadruplex sequences results in compound loss and may have unintentional effects on regulation of non-targeted genes. Thus, there is a need for new classes of compounds that can bind to quadruplex DNA via novel binding modes, with high affinity and with selectivity over duplex and other quadruplex DNA.

The goal of this dissertation is to use biophysical methods to investigate the interactions between a series of small molecules with their respective quadruplex targets in order to gain insight into how quadruplex DNA can be effectively targeted in a structure-specific manner, and to provide the basis of design of new molecules which will

bind with improved affinity and selectivity over current therapeutics in order to provide enhanced telomerase inhibition and oncogene transcriptional repression for treating cancer and microbial (e.g. protozoal) infections with fewer side effects.

Chapter 2 describes the screening of a series of commercially available compounds as well as a library of heterocyclic diamidines in order to identify compounds that bind to human telomeric DNA. A bifuryl compound, DB 832, was identified as a possible quadruplex DNA groove binder and chosen for further study, as presented in Chapter 3. Biophysical techniques including ITC, UV-Vis absorbance spectroscopy, and photocleavage were used to investigate the binding mode, and location of the binding site of DB 832 with human telomeric DNA. Chapter 4 describes the use of circular dichroism to investigate the binding of DB 832 with other DNA sequences to evaluate its selectivity for certain DNA structural types. Derivatives and analogues of DB 832 are also studied in order to develop initial structure-activity relationships to better understand how this compound binds to quadruplex DNA, and to aid in the future design of new molecules with improved binding and selectivity. Chapter 5 characterizes the interactions of a series of modified porphyrin compounds with both human telomeric DNA as well as a promoter region of the c-MYC oncogene using surface plasmon resonance. Chapter 6 examines a fluoroquinolone derivative that has been shown to have potential use as an anti-cancer therapeutic. Surface plasmon resonance is used to determine if this compound is quadruplex-interactive, and if so, to determine which quadruplex structure is the likely target for this compound.

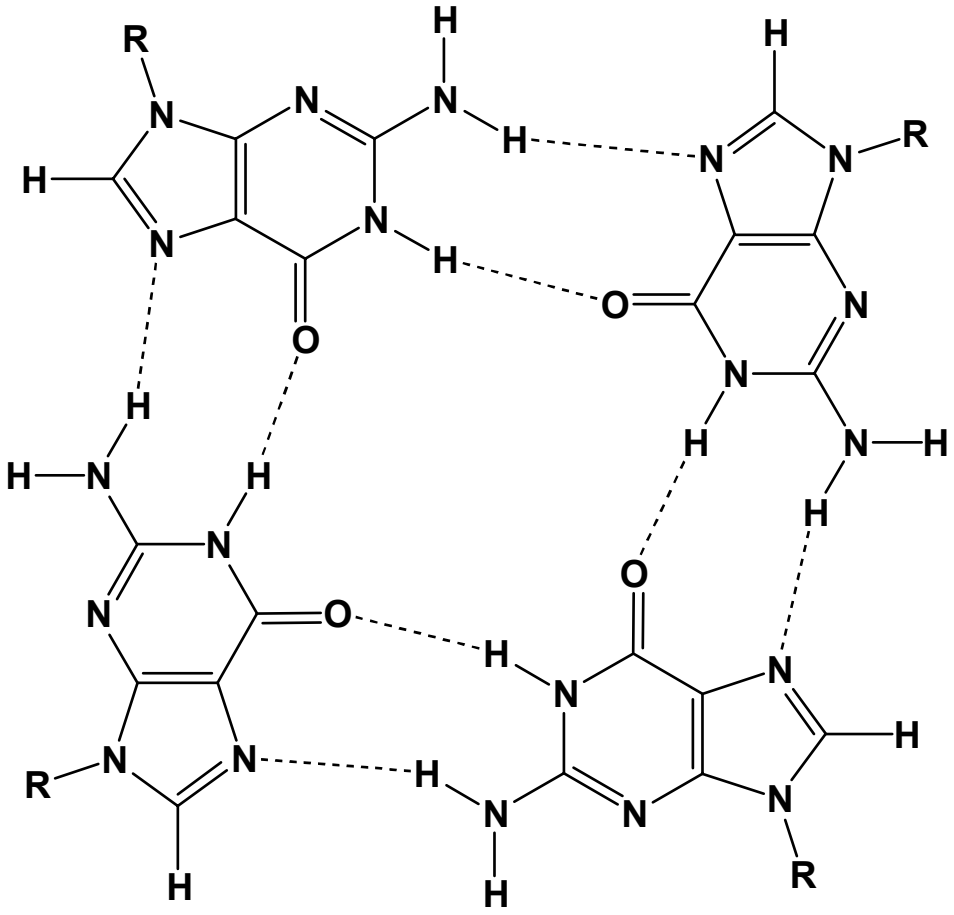


Figure 1.1 G-quartet structure. The Hoogsteen face of each guanine is hydrogen bonded to the Watson-Crick face of the adjacent guanine, resulting in a coplanar array.

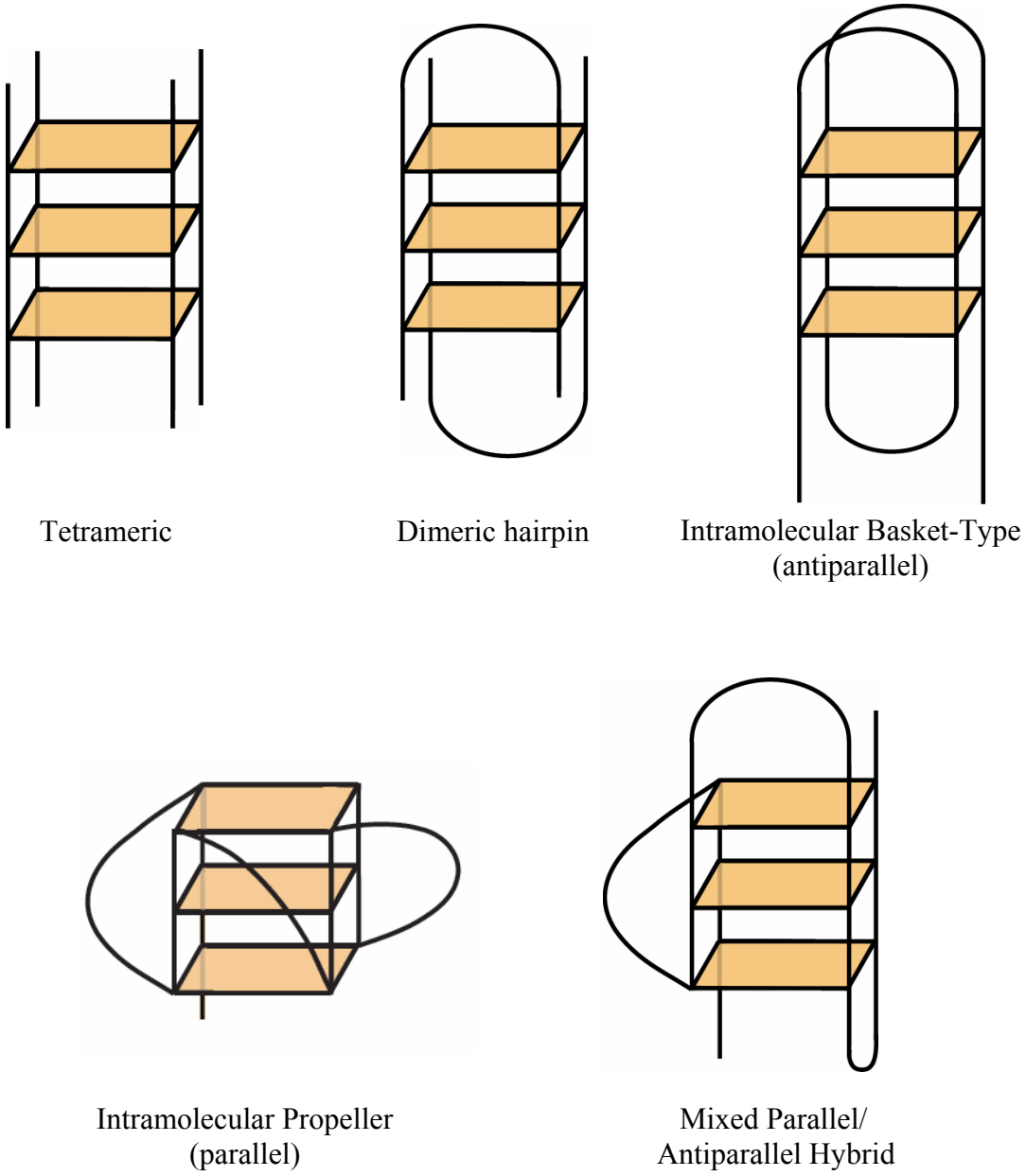


Figure 1.2 Examples of inter- and intramolecular quadruplex DNA conformations. structure-specific targets for quadruplex-interactive compounds.

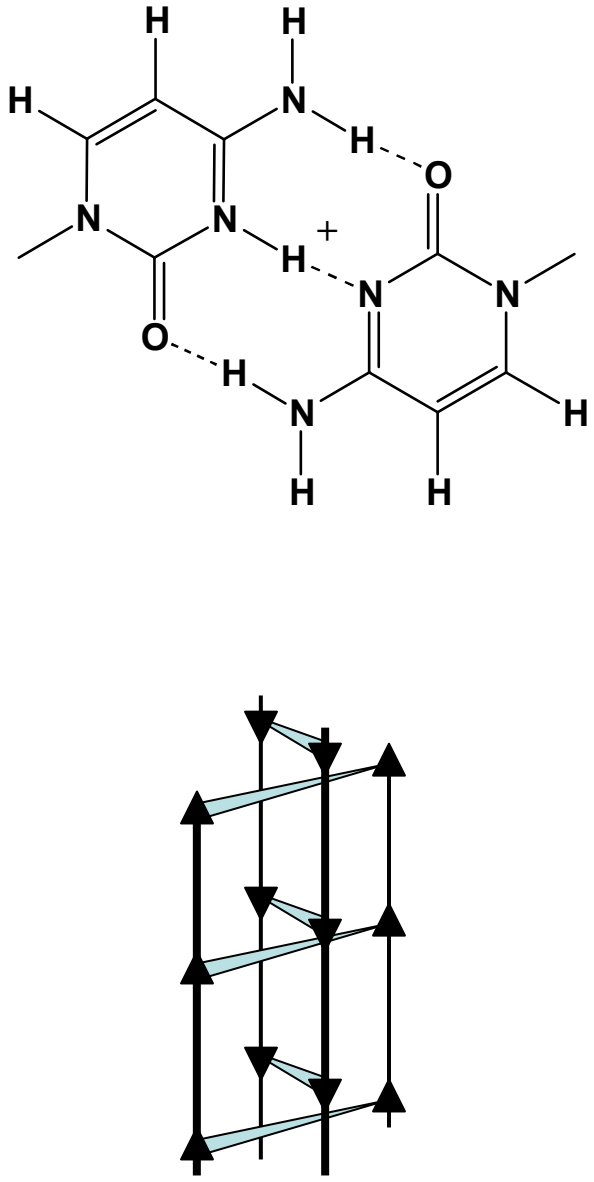


Figure 1.3 Structure of hemiprotonated C·C+ mismatch base pair as found in i-motif DNA (top) and intercalated base pairing scheme of i-motif DNA (bottom)

## References


1. Blackburn, G.M. and M.J. Gait, *Nucleic acids in chemistry and biology*. Second ed. 1996, New York: Oxford University Press. 528.
2. Dervan, P.B. and B.S. Edelson, *Recognition of the DNA minor groove by pyrrole-imidazole polyamides.* Curr. Opin. Struct. Biol., 2003. **13**(3): p. 284-99.
3. Lacy, E.R., et al., *Polyamide stacking in the DNA minor groove and recognition of T-G mismatched base pairs in DNA*, in *DNA and RNA binders*, M. Demeunynck, Bailly, C., Wilson, W.D.,, Editor. 2003, Wiley-VCH: Weinheim. p. 384-413.
4. Carter, A.P., et al., *Functional insights from the structure of the 30S ribosomal subunit and its interactions with antibiotics.* Nature, 2000. **407**(6802): p. 340-8.
5. Kaul, M., C.M. Barbieri, and D.S. Pilch, *Aminoglycoside-induced reduction in nucleotide mobility at the ribosomal RNA A-site as a potentially key determinant of antibacterial activity.* J. Am. Chem. Soc., 2006. **128**(4): p. 1261-71.
6. Moazed, D. and H.F. Noller, *Interaction of antibiotics with functional sites in 16S ribosomal RNA.* Nature, 1987. **327**(6121): p. 389-94.
7. Tucker, B.J. and R.R. Breaker, *Riboswitches as versatile gene control elements.* Curr. Opin. Struct. Biol., 2005. **15**(3): p. 342-8.
8. Gold, L., *Globular oligonucleotide screening via the SELEX process: aptamers as high-affinity, high-specificity compounds for drug development and proteomic diagnostics*. Combinatorial Chemistry and Technology, ed. S. Miertus and G. Fassina. 1999, New York: Dekker.

9. Liu, B., et al., *Fellowship of the rings: the replication of kinetoplast DNA.* Trends Parasitol., 2005. **21**(8): p. 363-9.

10. Shapiro, T.A. and P.T. Englund, *The structure and replication of kinetoplast DNA.* Annu. Rev. Microbiol., 1995. **49**: p. 117-43.

11. Shlomai, J., *The structure and replication of kinetoplast DNA.* Curr. Mol. Med., 2004. **4**(6): p. 623-47.

12. Marini, J.C., et al., *Bent Helical Structure in Kinetoplast DNA.* Proc. Natl. Acad. Sci. U S A, 1982. **79**(24): p. 7664-7668.

13. Wilson, W.D., et al., *Dications that target the DNA minor groove: compound design and preparation, DNA interactions, cellular distribution and biological activity.* Curr. Med. Chem. Anticancer Agents, 2005. **5**(4): p. 389-408.

14. Cech, T.R., *G-strings at chromosome ends.* Nature, 1988. **332**(6167): p. 777-8.

15. Sen, D. and W. Gilbert, *Formation of parallel four-stranded complexes by guanine-rich motifs in DNA and its implications for meiosis.* Nature, 1988. **334**(6180): p. 364-6.

16. Catasti, P., et al., *Structure-function correlations of the insulin-linked polymorphic region.* J. Mol. Biol., 1996. **264**(3): p. 534-45.

17. Siddiqui-Jain, A., et al., *Direct evidence for a G-quadruplex in a promoter region and its targeting with a small molecule to repress c-MYC transcription.* Proc. Natl. Acad. Sci. U S A, 2002. **99**(18): p. 11593-8.

18. Simonsson, T., P. Pecinka, and M. Kubista, *DNA tetraplex formation in the control region of c-myc.* Nucleic Acids Res., 1998. **26**(5): p. 1167-72.

19. Parkinson, G.N., M.P. Lee, and S. Neidle, *Crystal structure of parallel quadruplexes from human telomeric DNA.* Nature, 2002. **417**(6891): p. 876-80.

20. Wang, Y. and D.J. Patel, *Solution structure of the human telomeric repeat d[AG3(T2AG3)3] G-tetraplex.* Structure, 1993. **1**(4): p. 263-82.

21. Giraldo, R., et al., *Promotion of parallel DNA quadruplexes by a yeast telomere binding protein: a circular dichroism study.* Proc. Natl. Acad. Sci. U S A, 1994. **91**(16): p. 7658-62.

22. Fang, G. and T.R. Cech, Biochemistry, 1993. **32**: p. 11646-11657.

23. Fang, G. and T.R. Cech, Cell, 1993. **74**: p. 875-885.

24. Granotier, C., et al., *Preferential binding of a G-quadruplex ligand to human chromosome ends.* Nucleic Acids Res., 2005. **33**(13): p. 4182-4190.

25. Harley, C.B., A.B. Futcher, and C.W. Greider, *Telomeres shorten during ageing of human fibroblasts.* Nature, 1990. **345**(6274): p. 458-60.

26. Kim, N.W., et al., *Specific association of human telomerase activity with immortal cells and cancer.* Science, 1994. **266**(5193): p. 2011-5.

27. Zhang, X., et al., *Telomere shortening and apoptosis in telomerase-inhibited human tumor cells.* Genes Dev., 1999. **13**(18): p. 2388-2399.

28. Hahn, W.C. and e. al, *Inhibition of telomerase limits the growth of human cancer cells* Nat. Med. , 1999. **5**: p. 1164-1170.

29. Strahl, C. and E.H. Blackburn, *Effects of reverse transcriptase inhibitors on telomere length and telomerase activity in two immortalized human cell lines.* Mol. Cell Biol., 1996. **16**(1): p. 53-65.

30. Melana, S.M. and e. al., *Inhibition of cell growth and telomerase activity of breast cancer cells in vitro by 3'-azido-3'-deoxythymidine.* Clin. Cancer Res., 1997. **4**: p. 693-696.

31. Murakami, J., et al., *Inhibition of telomerase activity and cell proliferation by a reverse transcriptase inhibitor in gynaecological cancer cell lines.* Eur. J. Cancer, 1998. **35**: p. 1027-1034.

32. Gomez, D.E. and e. al, *Irreversible telomere shortening by 3'-azido-2',3'-dideoxythymidine (AZT) treatment.* Biochem. Biophys. Res. Commun., 1998. **246**: p. 107-110.

33. Schindler, A., et al., *Human telomerase reverse transcriptase antisense treatment downregulates the viability of prostate cancer cells in vitro.* Int. J. Oncol., 2001. **19**(1): p. 25-30.

34. Fu, W., et al., *The catalytic subunit of telomerase is expressed in developing brain neurons and serves a cell survival-promoting function.* J. Mol. Neurosci., 2000. **14**(1-2): p. 3-15.

35. Yokoyama, Y., et al., *The 5'-end of hTERT mRNA is a good target for hammerhead ribozyme to suppress telomerase activity.* Biochem. Biophys. Res. Commun., 2000. **273**(1): p. 316-21.

36. Ludwig, A., et al., *Ribozyme cleavage of telomerase mRNA sensitizes breast epithelial cells to inhibitors of topoisomerase.* Cancer Res., 2001. **61**: p. 3053-3061.

37. Zahler, A.M., et al., *Inhibition of telomerase by G-quartet DNA structures.* Nature, 1991. **350**(6320): p. 718-20.

38. Bottius, E., N. Bakhsis, and A. Scherf, *Plasmodium falciparum telomerase: de novo telomere addition to telomeric and nontelomeric sequences and role in chromosome healing.* Mol. Cell Biol., 1998. **18**(2): p. 919-25.

39. Cano, M.I., et al., *Telomerase in kinetoplastid parasitic protozoa.* Proc. Natl. Acad. Sci. U S A, 1999. **96**(7): p. 3616-21.

40. Catasti, P., et al., *Structure-function correlations of the insulin-linked polymorphic region.* J Mol Biol, 1996. **264**(3): p. 534-45.

41. Evans, T., et al., *S1-hypersensitive sites in eukaryotic promoter regions.* Nucleic Acids Res, 1984. **12**(21): p. 8043-58.

42. Howell, R.M., et al., *The chicken beta-globin gene promoter forms a novel "cinched" tetrahelical structure.* J Biol Chem, 1996. **271**(9): p. 5208-14.

43. Kilpatrick, M.W., et al., *Unusual DNA structures in the adenovirus genome.* J Biol Chem, 1986. **261**(24): p. 11350-4.

44. Murchie, A.I. and D.M. Lilley, *Retinoblastoma susceptibility genes contain 5' sequences with a high propensity to form guanine-tetrad structures.* Nucleic Acids Res, 1992. **20**(1): p. 49-53.

45. Hahn, W.C. and M. Meyerson, *Telomerase activation, cellular immortalization and cancer.* Ann Med, 2001. **33**(2): p. 123-9.

46. Wang, J., et al., *Myc activates telomerase.* Genes Dev, 1998. **12**(12): p. 1769-74.

47. Wu, K.J., et al., *Direct activation of TERT transcription by c-MYC.* Nat Genet, 1999. **21**(2): p. 220-4.

48. Facchini, L.M. and L.Z. Penn, *The molecular role of Myc in growth and transformation: recent discoveries lead to new insights.* Faseb J, 1998. **12**(9): p. 633-51.

49. Marcu, K.B., S.A. Bossone, and A.J. Patel, *myc function and regulation.* Annu Rev Biochem, 1992. **61**: p. 809-60.

50. Pelengaris, S., B. Rudolph, and T. Littlewood, *Action of Myc in vivo - proliferation and apoptosis.* Curr Opin Genet Dev, 2000. **10**(1): p. 100-5.

51. Spencer, C.A. and M. Groudine, *Control of c-myc regulation in normal and neoplastic cells.* Adv Cancer Res, 1991. **56**: p. 1-48.

52. Boles, T.C. and M.E. Hogan, *DNA structure equilibria in the human c-myc gene.* Biochemistry, 1987. **26**(2): p. 367-76.

53. Cooney, M., et al., *Site-specific oligonucleotide binding represses transcription of the human c-myc gene in vitro.* Science, 1988. **241**(4864): p. 456-9.

54. Sakatsume, O., et al., *Binding of THZif-1, a MAZ-like zinc finger protein to the nuclease-hypersensitive element in the promoter region of the c-MYC protooncogene.* J Biol Chem, 1996. **271**(49): p. 31322-33.

55. Siebenlist, U., et al., *Chromatin structure and protein binding in the putative regulatory region of the c-myc gene in Burkitt lymphoma.* Cell, 1984. **37**(2): p. 381-91.

56. Seenisamy, J., et al., *The dynamic character of the G-quadruplex element in the c-MYC promoter and modification by TMPyP4.* J Am Chem Soc, 2004. **126**(28): p. 8702-9.

57. Yang, D. and L.H. Hurley, *Structure of the biologically relevant G-quadruplex in the c-MYC promoter.* Nucleosides Nucleotides Nucleic Acids, 2006. **25**(8): p. 951-68.

58. Manzini, G., N. Yathindra, and L.E. Xodo, *Evidence for intramolecularly folded i-DNA structures in biologically relevant CCC-repeat sequences.* Nucleic Acids Res, 1994. **22**(22): p. 4634-40.

59. Postel, E.H., et al., *Human NM23/nucleoside diphosphate kinase regulates gene expression through DNA binding to nuclease-hypersensitive transcriptional elements.* J Bioenerg Biomembr, 2000. **32**(3): p. 277-84.

60. Xu, Y. and H. Sugiyama, *Formation of the G-quadruplex and i-motif structures in retinoblastoma susceptibility genes (Rb).* Nucleic Acids Res, 2006. **34**(3): p. 949-54.

61. Miyoshi, D., et al., *Structural polymorphism of telomeric DNA regulated by pH and divalent cation.* Nucleosides Nucleotides Nucleic Acids, 2003. **22**(2): p. 203-21.

62. Cornuel, J.F., A. Moraillon, and M. Gueron, *Participation of yeast inosine 5'-monophosphate dehydrogenase in an in vitro complex with a fragment of the C-rich telomeric strand.* Biochimie, 2002. **84**(4): p. 279-89.

63. Gueron, M. and J.L. Leroy, *The i-motif in nucleic acids.* Curr Opin Struct Biol, 2000. **10**(3): p. 326-31.

64. Lacroix, L., et al., *Identification of two human nuclear proteins that recognise the cytosine-rich strand of human telomeres in vitro.* Nucleic Acids Res, 2000. **28**(7): p. 1564-75.

65. Eid, J.E. and B. Sollner-Webb, *ST-1, a 39-kilodalton protein in Trypanosoma brucei, exhibits a dual affinity for the duplex form of the 29-base-pair subtelomeric repeat and its C-rich strand.* Mol Cell Biol, 1995. **15**(1): p. 389-97.

66. Sarig, G., et al., *Purification and characterization of qTBP42, a new single-stranded and quadruplex telomeric DNA-binding protein from rat hepatocytes.* J Biol Chem, 1997. **272**(7): p. 4474-82.

67. Patel, D., et al., *Structures of guanine-rich and cytosine-rich quadruplexes formed in vitro by telomeric, centromeric, and triplet repeat disease DNA sequences*, in *Oxford Handbook of Nucleic Acid Structure*, N. Stephen, Editor. 1999, Oxford University Press. p. 389-453.

68. Kim, M.Y., et al., *The different biological effects of telomestatin and TMPyP4 can be attributed to their selectivity for interaction with intramolecular or intermolecular G-quadruplex structures.* Cancer Res., 2003. **63**(12): p. 3247-56.

69. Rezler, E.M., et al., *Telomestatin and diseleno sapphyrin bind selectively to two different forms of the human telomeric G-quadruplex structure.* J. Am. Chem. Soc., 2005. **127**(26): p. 9439-47.

70. Fedoroff, O.Y., et al., *NMR-Based model of a telomerase-inhibiting compound bound to G-quadruplex DNA.* Biochem., 1998. **37**(36): p. 12367-74.

71. Han, F.X., R.T. Wheelhouse, and L.H. Hurley, *Interactions of TMPyP4 and TMPyP2 with Quadruplex DNA. Structural Basis for the DIfferential Effects on Telomerase Inhibition.* J. Am. Chem. Soc., 1999. **121**(15): p. 3561-3570.

72. Read, M., et al., *Structure-based design of selective and potent G quadruplex-mediated telomerase inhibitors.* Proc. Natl. Acad. Sci. U S A, 2001. **98**(9): p. 4844-9.

73. Teulade-Fichou, M.P., et al., *Selective recognition of G-Quadruplex telomeric DNA by a bis(quinacridine) macrocycle.* J. Am. Chem. Soc., 2003. **125**(16): p. 4732-40.

# Chapter 2

## Search for Compounds that Bind to Quadruplex Grooves

### Introduction

Stabilization of the quadruplex conformation of telomeres, such as by binding small molecules, has been shown to be an effective method to inhibit telomerase activity [1-9]. The development of small molecules that can selectively bind to and stabilize the G-quadruplex conformation of the telomere is therefore a current area of interest in anticancer as well as antiparasitic drug design. Compounds that have been shown to bind to quadruplex DNA have traditionally been planar, aromatic compounds that bind via external end-stacking to the G-quartet on either one end or both ends of the quadruplex [1-8]. These compounds, which include anthraquinones, cationic porphyrins, acridines, macrocyclic compounds and analogs have planar aromatic surface areas that mimic the large planar surface of the G-tetrads in quadruplex DNA [10-13]. Since essentially all known quadruplex DNA binders are based on, or derived from duplex intercalators, many exhibit little selectivity for quadruplex over duplex structures and this can result in nonspecific cytotoxicity. Increasing the selectivity of telomerase inhibitors for their quadruplex targets is an important focus of research.

Groove binding has been a useful way to selectively recognize duplex DNA with relatively low nonspecific toxicity [14-19], but groove binding is an under-exploited design mode with DNA quadruplexes. The structural differences between duplex and quadruplex DNA grooves offer an attractive strategy for development of compounds to

differentiate between these two structures. Since groove dimensions vary according to the type of quadruplex [20], groove binding also offers the opportunity for obtaining increased selectivity for a particular quadruplex structure. Groove-binding has been proposed as a binding mode for some small molecule/ quadruplex DNA combinations. Shafer et al. obtained spectroscopic data suggesting that the dye 3,3'-diethyloxadicarbocyanine (DODC) binds in the quadruplex grooves of a dimeric hairpin G-quadruplex [21]. Satellite hole spectroscopy studies support the groove-binding model for this particular compound/DNA pair [22, 23]. Electrospray mass spectrometry fragmentation patterns upon ionization also indicate that the carbocyanine dye DTC binds in the quadruplex grooves [24]. However, in spite of extensive experiments with quadruplex DNA, no compounds to date have been found which bind to the grooves of the intramolecular human or parasite telomeres or to oncogene control quadruplexes. Thus, although G-quadruplex end-stacking is a well-established and documented recognition mode, binding in the G-quadruplex grooves is an area that lacks adequate models for drug design and development.

Since typical screening techniques such as thermal denaturation and surface plasmon resonance (SPR) are not capable of distinguishing between groove binding and intercalating-type end-stacking interactions, an alternate technique such as circular dichroism (CD) must be employed to evaluate the binding mode. Circular dichroism pattern recognition has been used as a technique for determination of binding mode with duplex DNA-binding compounds [25]. Induced circular dichroism (CD) signals of molecules bound to duplex DNA have provided a very powerful method to distinguish intercalation-stacking type interactions from groove binding [25]. Non-chiral molecules

exhibit no CD signal in solution. However, when an achiral ligand binds tightly to a chiral host, such as DNA, a CD signal is induced in the wavelength region corresponding to the absorbance of the bound compound. Intercalating compounds usually produce negative induced CD signals or very small positive signals. Groove binding is generally indicated by the presence of a large positive induced CD signal upon titration of compound into duplex DNA. However, pattern recognition of induced CD signals has not been established for small molecules binding to quadruplex DNA.

Circular dichroism is also useful for evaluation of small molecule binding to quadruplex DNA because it not only can yield information about mode of binding, but can also provide information about the conformation of the DNA. Due to the polymorphism of quadruplex DNA, small molecules may trap out certain quadruplex conformations out of a mixture, or even induce a conformational change in the quadruplex structure. Since it has been proposed that some conformations of quadruplex DNA may be more biologically relevant than others [26, 27], it is especially important to have information about the conformation of the DNA.

Stacked species are of particular interest for recognition of quadruplexes since studies with duplex DNAs show that compounds that bind as stacked dimers have increased binding affinity and selectivity over similar compounds that bind as monomers [14, 15, 17, 18, 28-30]. Similar stacking in the grooves of quadruplex DNA structures would appear to be a favorable way to selectively recognize quadruplexes with optimum interactions, perhaps employing an induced fit component, between the stacked heterocycles and the G bases of the quadruplex tetrads.

To initiate a search for compounds that can bind as stacked species to quadruplex DNA grooves we have used CD spectroscopy and induced CD signals to distinguish end stacking from stacked groove complexes. For quantitative comparison of binding affinities of quadruplex-binding agents under a defined set of conditions, we have used SPR. SPR is a powerful technique to monitor molecular reactions in real time and has been used previously to study the interaction of compounds with the G-quadruplex formed in the human telomeric sequence [12, 13]. This method uses very little material and is applicable to a very large variety of small molecules with quite different properties, binding modes and affinities.

We report CD results for a number of compounds of quite different structure, including a cyanine dye that exhibits CD spectral characteristics consistent with groove binding as a stacked species. Based on the CD results, a library of diamidines synthesized by Boykin and coworkers at Georgia State University was screened against the human telomeric sequence using circular dichroism. Diamidines were chosen because they have favorable cell uptake properties and low general toxicity, making them ideal for possible therapeutic use. Of the compounds evaluated, DB 832 was identified as a potential quadruplex groove-binder and selected for further study. This molecule serves as a paradigm to show that the grooves of the human telomere can indeed be targeted and also serves as the starting point for the design of new molecules that may have therapeutic use as anti-cancer or anti-trypanosomal agents.

## Materials and Methods

### Sample Preparation

The oligonucleotides d[$AG_3(T_2AG_3)_3$] and d($AG_3TG_4AG_3TG_4A$) were purchased with HPLC purification from Midland Certified Reagent Company. The G-quadruplex DNA samples were dissolved in buffer to the desired concentrations, heated to 85 $^0$C and cooled slowly to insure the folding of the quadruplexes prior to each experiment. The concentration of each DNA sample was determined spectrophotometrically at 260 nm using the nearest neighbor extinction coefficient at 80°C and extrapolated to 20°C. Stock solutions containing 1 mM each of compound were prepared in double distilled water and diluted to working concentrations immediately before use with buffer. Ethidium bromide, distamycin A, neomycin, thionin, chromomycin A3, mithramycin, DODC, DOC, DTDC and DTC were obtained from Sigma Aldrich. fImImIm was synthesized by the Lee group at Furman University [31]. The synthesis of all DB compounds will be described elsewhere.

### CD Measurements

CD measurements were performed at 20°C in a 10 mM HEPES buffer (pH 7.4) containing 3 mM EDTA and 50 mM KCl, NaCl or 50 mM KCl plus 50 mM $MgCl_2$. For CD measurements obtained in the presence of 50 mM LiCl or in the absence of added salt, a 10 mM TRIS buffer containing 3 mM EDTA acid and pH adjusted to 7.4 using TRIS was used. CD spectra were recorded using a Jasco J-810 spectrapolarimeter in a 1-cm cell using an instrument scanning speed of 50 nm/min with a response time of 1 s. The spectra were averaged over four scans. Appropriate amounts of compound were added sequentially to increase the molar ratio. A buffer baseline scan was collected in the

same cuvette and subtracted from the average scan for each CD experiment. Data manipulation and plotting was performed using the program Kaleidagraph version 3.6.

**Immobilization of DNA and Biosensor SPR Experiments**

Biosensor SPR experiments were performed with a four-channel BIAcore 3000 optical biosensor system (BIAcore, Inc.) and streptavidin-coated sensor chips (BIAcore SA with linked streptavidin). The concentration in all cases refers to the strand concentration, which is also the quadruplex concentration. The chips were prepared for use by conditioning with three to five consecutive 1 min injections of 1 M NaCl in 50 mM NaOH followed by extensive washing with buffer. 5'-Biotinylated DNA samples (25 nM) in HBS buffer were immobilized on the flow cell surface by noncovalent capture as previously described [17, 18, 31, 32]. Three flow cells were used to immobilize DNA oligomer samples, and a fourth cell was left blank as a control. Interaction analysis was performed by steady-state methods with multiple injections of different compound concentrations over the immobilized DNA surface at 25 ºC. DNA-binding experiments were performed in sterile filtered and degassed HBS buffers: 0.01 M HEPES, (pH 7.4), 3 mM EDTA, and 0.005% surfactant P20 with 0.2 M KCl. Compound solutions were prepared in the desired buffer by serial dilutions from stock solution and injected from 7 mm plastic vials with pierceable plastic crimp caps (BIAcore, Inc.) at a flow rate of 25 μL/min. To remove any remaining bound compound after the dissociation phase of the sensorgram, a low-pH glycine regeneration buffer was used (10 mM glycine at pH 2). The baseline was then reestablished, and the next compound concentration sample was injected.

The instrument response (RU) in the steady-state region is proportional to the amount of bound drug and was typically determined by linear averaging over a 10-20 s or longer time span, depending on the length of the steady-state plateau. The predicted maximum response per bound compound in the steady-state region ($RU_{max}$) was determined from the DNA molecular weight, the amount of DNA on the flow cell, the compound molecular weight, and the refractive index gradient ratio of the compound and DNA, as previously described [17, 18, 31, 32]. The number of binding sites was estimated fitting plots of RU versus $C_{free}$. These methods can also be used to determine an empirical $RU_{max}$ value. The $RU_{max}$ value is required to convert the observed response (RU) to the standard binding parameter *r* (moles of drug bound per moles of DNA)

$$r = RU/RU_{max}$$

which is useful for comparison of a compound binding to different DNAs. To obtain the affinity constants, the data were fitted to the following interaction model using Kaleidagraph for nonlinear least-squares optimization of the binding parameters:

$$r = (K_1C_{free} + 2K_1K_2C_{free}^2)/(1 + K_1C_{free} + K_1K_2C_{free}^2)$$

where $K_1$ and $K_2$ are equilibrium constants for two types of binding sites and $C_{free}$ is the concentration of the compound in equilibrium with the complex and is fixed by the concentration in the flow solution. For a single dominant binding site model, $K_2$ is equal to zero.

## Results and Discussion

### Duplex DNA Binders

To develop a paradigm for groove-binding, a series of compounds that bind to duplex DNA were evaluated. The compounds cover a range of structural types and each compound interacts with duplex DNA in a different manner. The compounds were evaluated against the human telomere using circular dichroism to determine if any unusual induced CD signature existed which could be used for pattern recognition in the screening of potential quadruplex DNA-binding compounds. As a control for the CD analysis, a titration was first performed with a well-characterized quadruplex end-stacking compound, ethidium [33, 34]. With this compound there are no significant induced signals as seen in Figure 2.1.

Distamycin binds as a stacked dimer to the minor groove of AT-rich duplex DNA sequences. It has previously been suggested distamycin may bind to the grooves of certain quadruplex DNA sequences [21-24, 35], although more recent NMR results indicate that distamycin stacks on the ends of quadruplexes [36]. The CD spectra of human telomeric DNA does not show any change when titrated with distamycin (Figure 2.2) suggesting that it binds very weakly, if at all to this sequence. SPR results confirm the weak binding ($Ka < 10^5\ M^{-1}$) to the human telomere and binding is likely to only be seen in high concentration experiments such as NMR.

Since the minor groove binder, distamycin, does not bind to the grooves of the human telomere, neomycin, an aminoglycoside antibiotic that binds in the major groove of DNA duplexes was studied to see if it binds to the human telomere. Figure 2.3 shows

the CD spectra of neomycin titrated into human telomeric DNA. Like distamycin, this compound does not appear to interact with human telomeric DNA.

The minor-groove binding polyamide fImImIm (Figure 2.4) selectively binds to GC-rich duplex DNA through hydrogen binding interactions [31]. The CD spectra of fImImIm titrated into human telomeric DNA do not reveal any significant quadruplex interactions. It seems unlikely that traditional polyamides will interact significantly with telomere, and probably other, DNA quadruplex structures due to the differences in geometry of the grooves.

Thionin is a cationic dye that has been shown to intercalate with duplex DNA. It can form a dimer and has been shown to bind to some quadruplex sequences and exhibit exciton splitting in the induced region [37]. In these cases, it is believed to stack on the quartet ends. The CD spectra of thionin titrated into the human telomeric sequence is shown in Figure 2.5. There is no change in the CD spectra in either the DNA region or the induced region up to a 4:1 ratio, indicating that thionin likely does not bind to this quadruplex sequence.

Chromomycin A3 and mithramycin are commercially available aureolic acid antibiotics. Chromomycin A3 is produced from *Streptomyces grieus,* while mithramycin is produced from *Streptomyces plicatus.* These compounds bind as $Mg^{2+}$-mediated dimers through hydrogen bonding with 2-amino groups on guanines in the minor grooves of GC-rich sequences [38, 39]. They disrupt replication and transcription processes through inhibition of DNA and RNA polymerases [38-40]. It was speculated that these compounds may bind to quadruplex grooves since they selectively recognize the grooves of guanine-containing sequences. CD titrations of chromomycin added to human

telomeric DNA and the c-MYC sequence in the presence of 50 mM $K^+$ and 50 mM $Mg^{2+}$ are shown in Figures 2.6 and 2.7, respectively. Chromomycin and mithramycin are chiral, and therefore optically active. Both compounds produce CD signals even in the absence of DNA. Because these compounds have absorbance bands in the visible region of the spectrum as well as in the near-UV, where DNA absorbs, the signals of these compounds overlap with the CD signal from the DNA, which may mask any changes in the CD spectrum of the DNA. The chirality of these compounds therefore makes it difficult to ascertain whether any CD signal is being induced or even whether the compound is binding to the DNA at all. However, since there appears to be a significant difference in the c-MYC and human telomere spectra when titrated with chromomycin A3, it suggests that this compound may be selective for one of these DNAs.

The $Mg^{2+}$-mediated mithramycin dimer is more flexible than the chromomycin dimer due to a high degree of plasticity in its trisaccharide segment [40, 41]. This flexibility makes it less sensitive to groove width which may result in better binding to quadruplex sequences. This is supported by the CD spectra of mithramycin titrated into the human telomeric sequence (Figure 2.8) and the c-MYC sequence (Figure 2.9). The much larger magnitude of CD signal with the human telomeric sequence as well as the c-MYC sequence suggests that mithramycin may interact more favorably with quadruplexes than chromomycin does. Spectra were also obtained for mithramycin with the human telomere in the presence of sodium (Figure 2.10) as well as lithium (Figure 2.11) to see if the starting conformation of the DNA had any effect on binding. The human telomere has an antiparallel basket-type structure in sodium [42], and the structure

is unfolded in the presence of lithium [43]. The spectra are of similar shape and magnitude regardless of the starting conformation of the human telomeric DNA.

To differentiate between the contribution to the CD signal due to binding and the inherent CD signal of mithramycin, the highest concentration spectrum in Figure 2.8 was shown on the same graph as the CD signal of identical amount of mithramycin in the absence of DNA. The difference in these curves suggests that at least some of the CD signal is due to actual binding interactions, or possibly a change in the spectral properties of mithramycin over the duration of the titration. To determine if the large change in CD signal upon titration was due to any time-dependent change in the spectral properties of mithramycin, a CD spectrum was obtained for mithramycin in the absence of DNA, and the same sample was run again after a period of one hour (Figure 2.13). There is no change in the CD signal at any wavelength, suggesting that the CD signal of mithramycin is not time-dependent and that binding between mithramycin and the human telomere may be occurring. However, SPR results show that mithramycin does not bind to any significant extent with the human telomere as demonstrated by the sensorgrams shown in Figure 2.14. Although the results with chromomycin and mithramycin are interesting, the problems with the inherent circular dichroism of the compounds makes it difficult to study, and even if these compounds do bind in the grooves of quadruplex DNA, they are not useful as a paradigm for groove-binding.

Cyanine derivatives, which form stacked complexes in the minor groove of duplex DNAs, exhibit strong exciton splitting in their induced CD spectra with duplexes [29, 30, 44]. CD titrations were performed on the intramolecular human telomere DNA with four different cyanine compounds: DODC, DOC, and their sulfur analogs, DTDC

and DTC (Figures 2.15-2.18). Although each of the cyanines appears to interact with the human telomere, DODC appears to have the strongest interaction. The titration spectra for DODC show a strong induced CD signal in the DODC absorption region (Figure 2.15). Exciton splitting in the induced spectra indicates that DODC binds to the quadruplex grooves as one or more stacked species. Since DODC is also the only one of the four compounds that is water soluble, it was chosen for further study by surface plasmon resonance to quantify the binding of DODC with the intramolecular human telomeric DNA sequence. The binding curve is shown in Figure 2.19. Because DODC has an absorbance band that overlaps with the light used by the SPR instrument, an enhancement of signal occurs which results in artificially high response unit values. Therefore, the stoichiometry of binding cannot be determined by RUmax from the SPR experiments. Since DODC dimerizes in solution, even at the low concentrations used in SPR, it can be assumed that binding is occurring as a series of dimers. Since the binding curve is sigmoidal in shape, it suggests that two (or more) dimers are binding to the sequence with positive cooperativity. For the analysis of binding constants, we assume that DODC is binding as a set of two dimers. A fit of the data gives the equilibrium binding constants for each of the two dimers to be $K_1 = 3.3 \times 10^4\ M^{-1}$ and $K_2 = 2.2 \times 10^6\ M^{-1}$. The positive cooperativity suggests that the binding of the first dimer may cause a distortion to one of the other grooves that makes it a better binding site for the second dimer.

**Screening of Library of Heterocyclic Diamidines**

The DODC results are quite exciting and indicate that compound stacking in the quadruplex grooves is a promising approach for the design of highly selective

quadruplex-targeting agents. The results also indicate that the presence of an induced exciton CD signal can be used as a method to distinguish among binding modes. Boykin and coworkers have designed a series of unfused aromatic heterocycles with terminal amidine substituents that are excellent groove-binding agents with duplex DNA [45]. The compounds also get into cells and are promising antiparasitic drug development candidates [19]. Over 150 compounds from this library were screened against the intramolecular human telomeric sequence using circular dichroism. The spectral patterns of the compounds tended to fall into several main categories. To try to establish an interpretation of these patterns of CD signals, SPR studies were conducted on several compounds from each category. An example of each type of spectral pattern is shown along with its equilibrium binding constant for the strong, first binding site (if applicable) in Figures 2.20 through 2.28.

A number of compounds such as DB 860 (Figure 2.20) showed no change in CD signal when the compound was titrated into the DNA. As expected, these compounds typically did not show any binding as measured by surface plasmon resonance.

Several of the compounds, including DB 185 (Figure 2.21), showed increases in CD signal across all wavelengths, with no isoelliptic points. These compounds generally had very high SPR signals, but binding to the control flow cell was equal to or larger than binding to the cell containing DNA. This behavior is consistent with non-specific aggregation of the compound onto the DNA, and not actual binding.

Upon titration, several compounds caused a decrease in the CD signal of the DNA at 260 nm. A negative peak at 260 nm has been associated with formation of a basket or chair-type antiparallel quadruplex conformation [46]. One example, DB 1065 (Figure

2.22) has $K_1 = 4.4 \times 10^5\ M^{-1}$. The CD spectra of DB 634 (Figure 2.23) also show a decrease at 260 nm when it was titrated into the DNA. However, the 295 nm peak increases during the titration. The $K_1$ for this compound with human telomere is $2.3 \times 10^5\ M^{-1}$, which is lower than the binding constant for DB 1065. In general, changes in CD signal at 295 nm do not seem to have a significant effect on the binding constant. It has been suggested that changes in signal at this wavelength are caused by conformational changes in the loops. Since these compounds likely are binding on the quadruplex ends or in the grooves, it is likely that the binding constant would be unaffected by conformational changes in the loops.

The spectra of compounds such as DB 587 (Figure 2.24) show the formation of a peak around 270 nm as the titration proceeds. This spectral pattern is associated with the formation of a parallel quadruplex structure [46]. For this compound, since the peak at 295 does not change, it suggests that the compound is inducing or trapping out a mixed parallel/antiparallel hybrid quadruplex structure. $K_1$ for this compound is $9.7 \times 10^4\ M^{-1}$.

Compounds that exhibited induced CD signals generally had the highest binding constants among those screened. Two examples of compounds that exhibit a positive induced CD signal when titrated into the human telomeric DNA are DB 989 (Figure 2.25) and DB 210 (Figure 2.26). Based on established pattern recognition for DNA, DB 989 appears to be binding to an antiparallel conformation of DNA and DB 210 appears to bind to a mixed parallel/antiparallel hybrid conformation. $K_1$ for DB 989 is $5.1 \times 10^6\ M^{-1}$. $K_1$ for DB 210 is $1.6 \times 10^6\ M^{-1}$. In studies with duplex DNA, a positive induced signal is usually indicative of groove binding [47]. It is likely that these compounds are binding in the grooves of the human telomere as monomers. This library of compounds was

designed as potential DNA groove binders. They generally have the crescent-type shape that has been shown to fit into the grooves of DNA. The compounds do not have the large, planar, aromatic surfaces required for extensive π- π stacking with quadruplex ends. It is likely that any strong binding compounds are therefore binding in the quadruplex grooves.

DB 1300 (Figure 2.27) and several compounds with similar structures bind to the human telomere with strong induced exciton CD signals, suggesting binding as a stacked complex or complexes. $K_1$ for this compound with the human telomere is $2.7 \times 10^6$ $M^{-1}$. The CD signal in the DNA region shows a dramatic decrease as the titration progresses. The resulting spectrum for the DNA does not follow any established CD pattern for the conformation of quadruplex DNA. Although this group of compounds appear to bind to the telomere as stacked species with a fairly high level of affinity, this group of compounds was not chosen for further study, due to the difficulty in analyzing the DNA conformation.

A bifuryl compound, DB832, also exhibited strong induced exciton CD signals when titrated into telomeric DNA (Figure 2.28). The large magnitude of the signal suggests that it probably forms stacked complexes in more than one groove. Due to the high stoichiometry of the system, a reliable binding constant was not able to be measured using surface plasmon resonance. Addition of this compound results in a CD pattern for the DNA region that is indicative of formation of a mixed parallel/antiparallel hybrid structure. Since this appears to bind in the quadruplex grooves as a stacked species, and interacts with the DNA in a well-defined manner, it was chosen for further study as presented in Chapters 3 and 4.

**Conclusion**

Since the grooves of quadruplex DNA structures have different geometries than with duplex DNAs as well as different patterns of donor-acceptor, hydrogen-bonding sites [20, 48], compounds that bind only in the grooves should be able to achieve excellent structure-specific recognition affinity and specificity. CD results for a cyanine dye, DODC, established that the grooves of telomeric DNA can be targeted by small molecules as stacked species.

Based on these results, a library of heterocyclic diamidine dications was investigated using CD spectroscopy. The screening process yielded a variety of CD patterns, both in the induced region as well as the DNA region. CD patterns in the DNA region show that different conformations of the human telomere including antiparallel and mixed parallel/antiparallel hybrids can be selectively targeted by small molecules. Patterns in the induced region suggest that a positive induced CD is indicative of binding in the grooves as a monomer, and an induced exciton signal indicates binding in the grooves as one or more stacked species. Binding as a stacked species is of particular interest since studies with duplex DNA have shown that stacked species can have improved binding affinity and selectivity over monomer binding.

Through the screening process, a heterocyclic diamidine molecule, DB 832, was identified as a possible quadruplex groove binder. This compound exhibited the characteristic strong exciton induced CD signals associated with groove binding. The large magnitude of the signals suggests that it may bind as a series of stacked species. This compound may serve as the starting point for the design of a new class of highly

selective quadruplex DNA groove binders and is the subject of further investigation in Chapters 3 and 4.

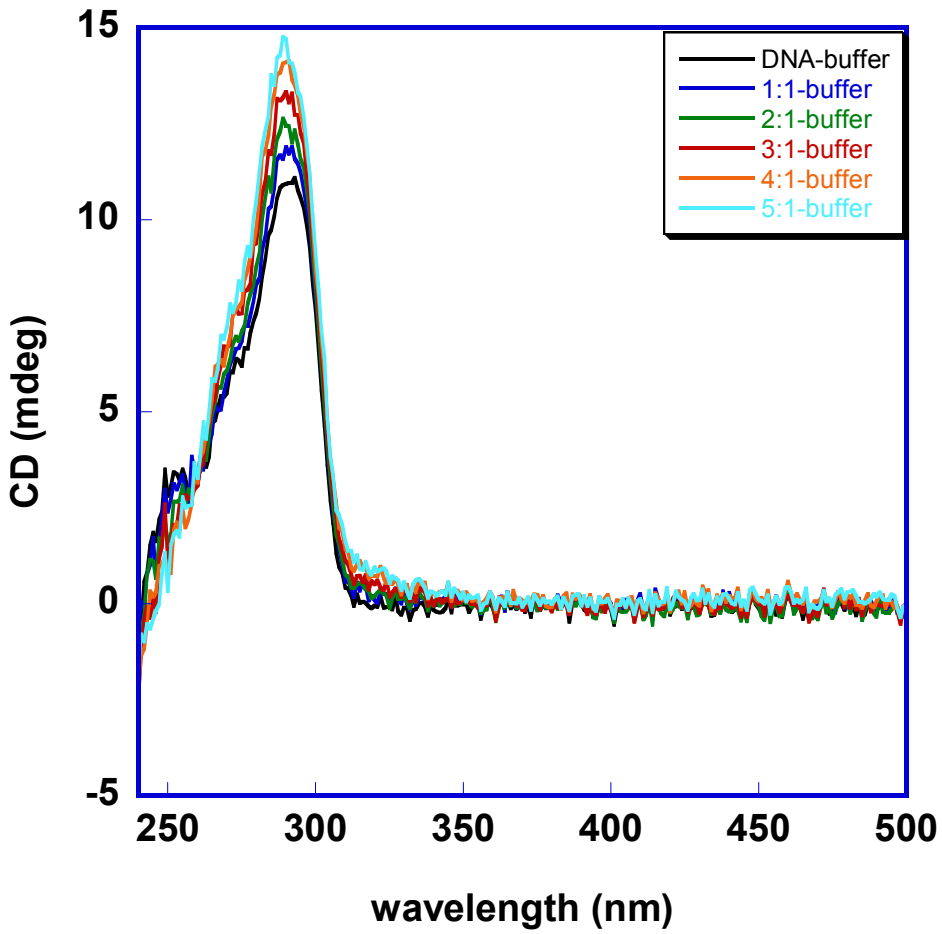


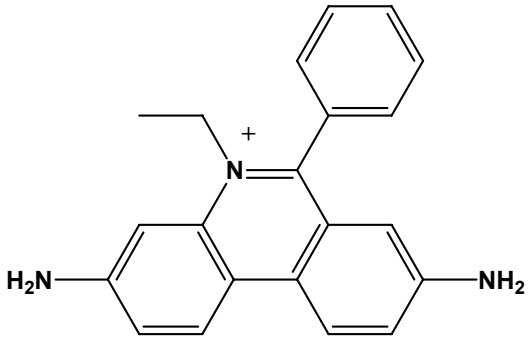


Figure 2.1 CD spectra of ethidium bromide titrated into 3.0 μM of d[$AG_3(T_2AG_3)_3$] in HEPES buffer containing 50 mM KCl. Compound:DNA ratios ranged from 1:1 to 5:1.

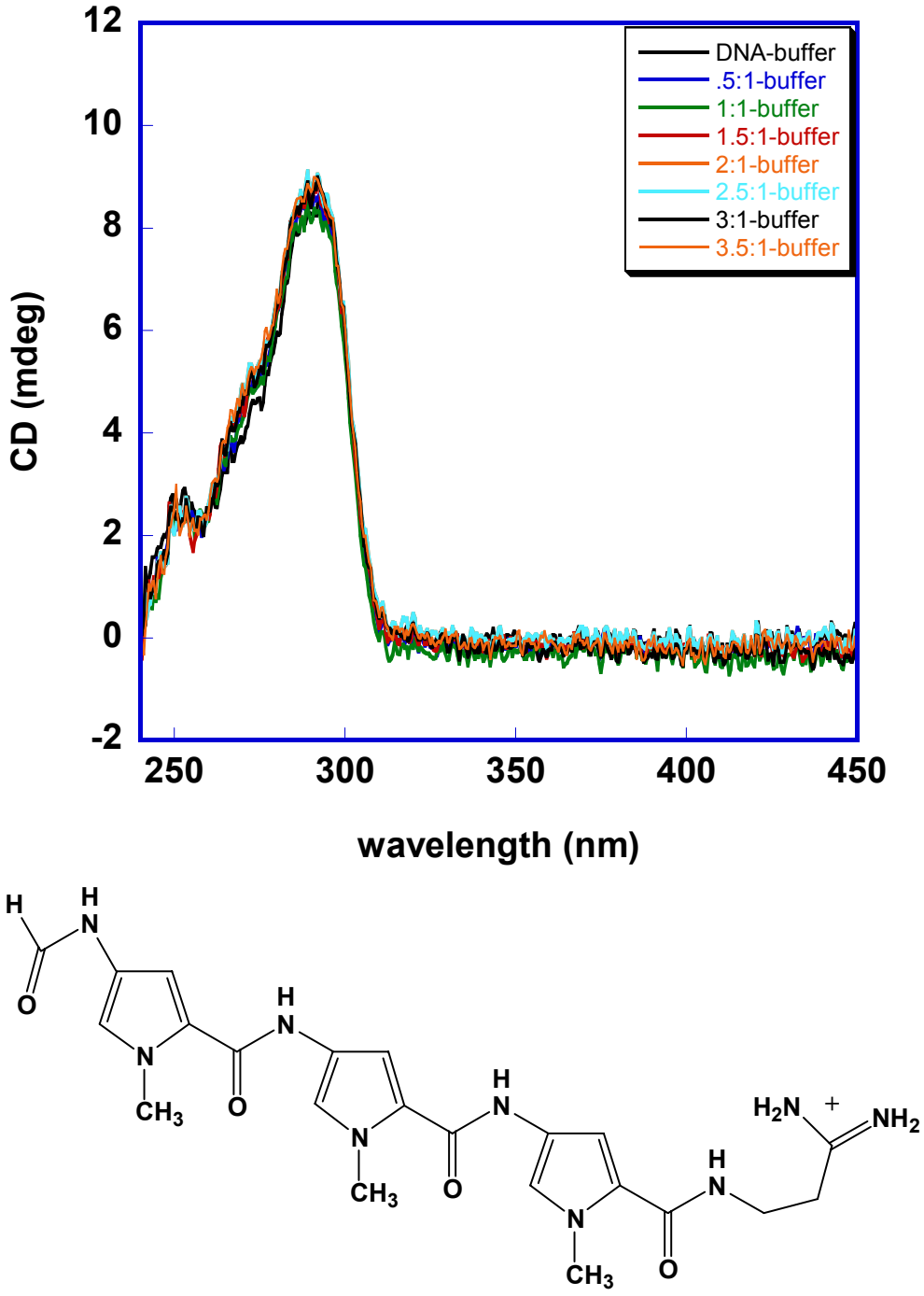


Figure 2.2 CD spectra of distamycin A titrated into 3.0 μM of d[$AG_3(T_2AG_3)_3$] in HEPES buffer containing 50 mM KCl. Compound:DNA ratios ranged from 1:1 to 3.5:1.

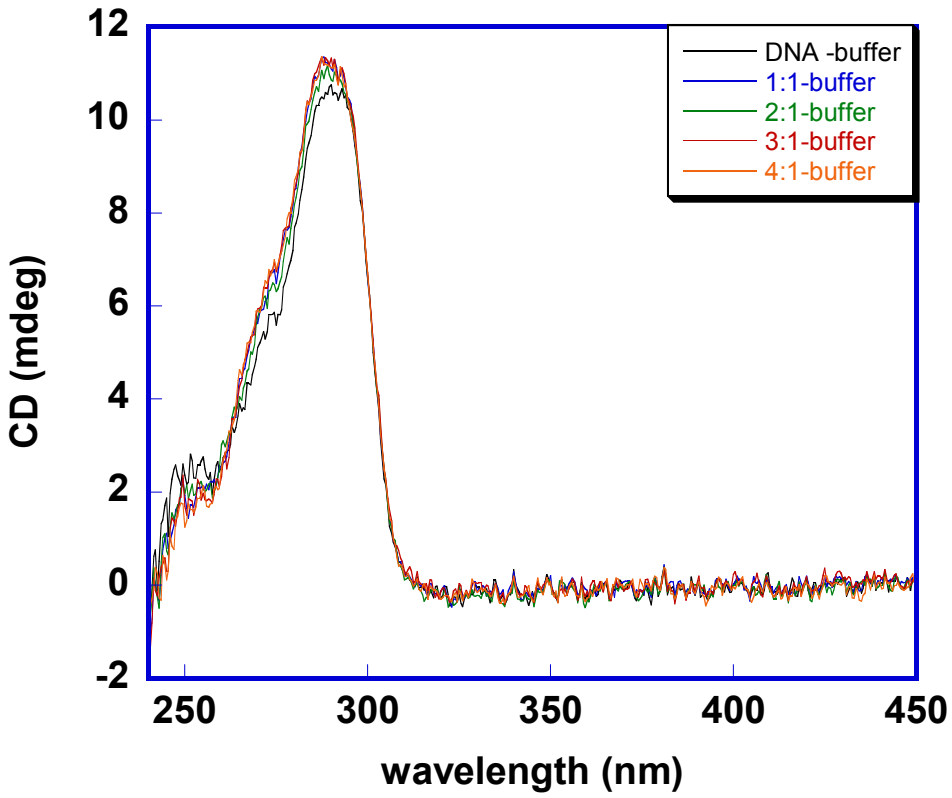


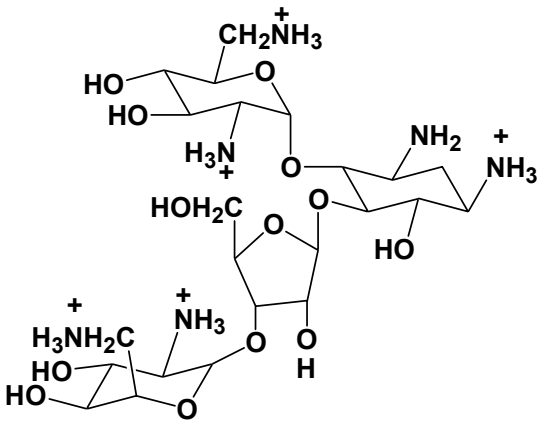


Figure 2.3 CD spectra of neomycin titrated into 3.8 μM of d[$AG_3(T_2AG_3)_3$] in HEPES buffer containing 50 mM KCl. Compound:DNA ratios ranged from 1:1 to 4:1.

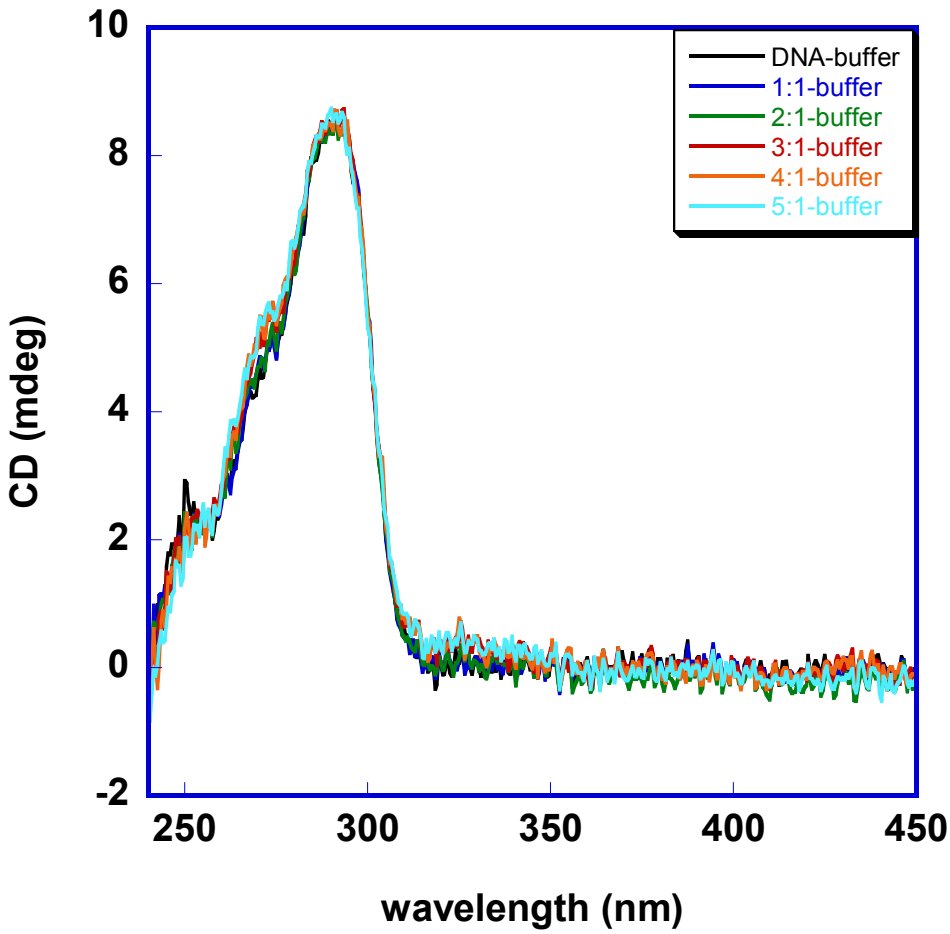


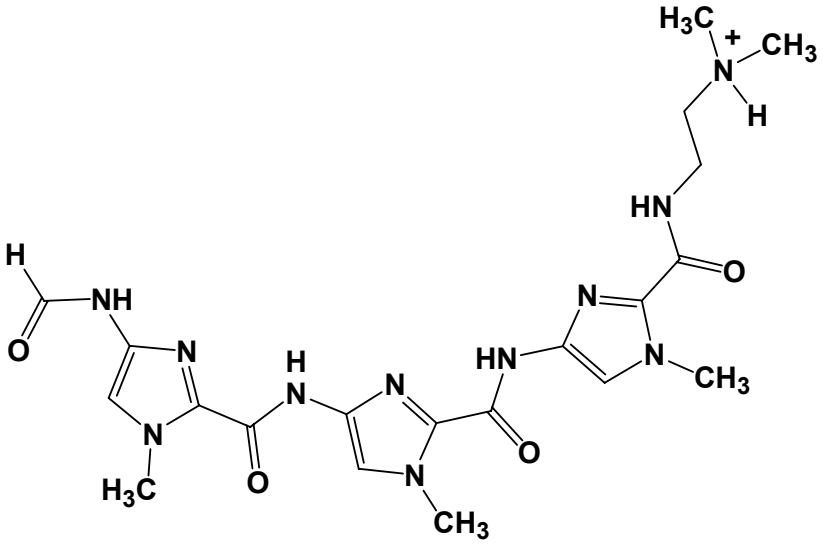


Figure 2.4 CD spectra of fImImIm titrated into 2.9 μM of d[$AG_3(T_2AG_3)_3$] in HEPES buffer containing 50 mM KCl. Compound:DNA ratios ranged from 1:1 to 5:1.

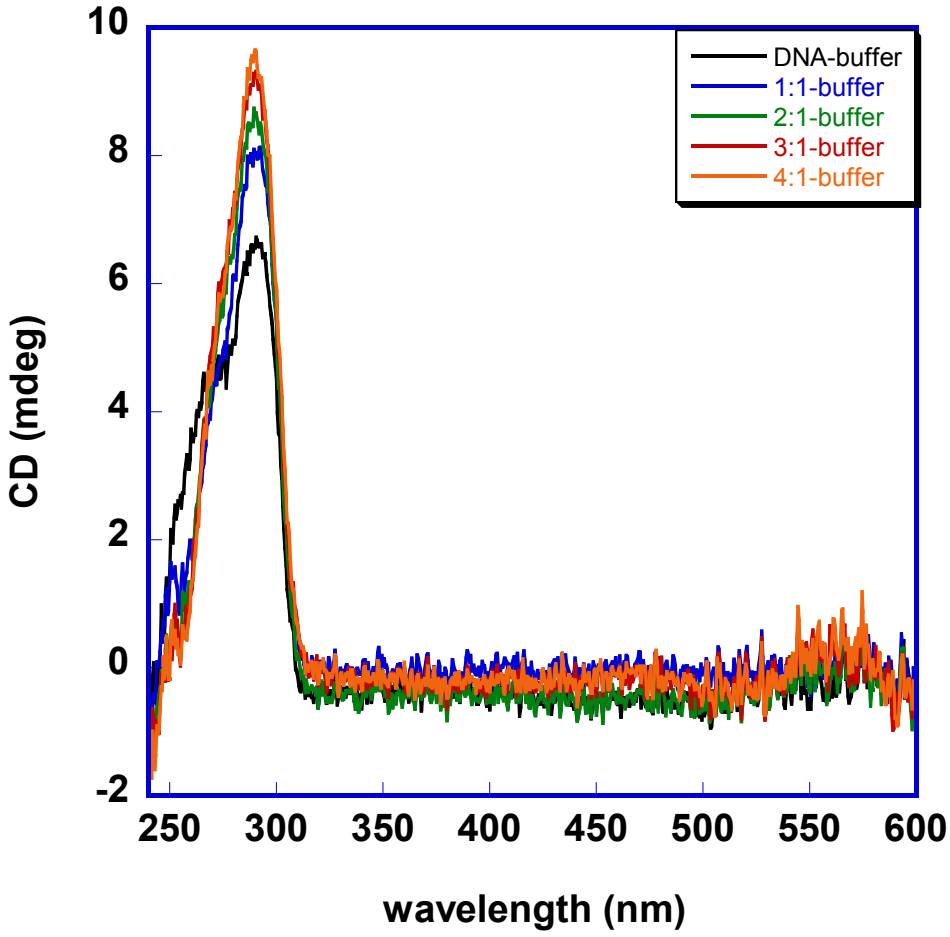


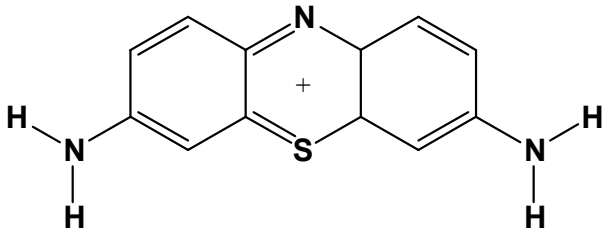


Figure 2.5 CD spectra of thionin titrated into 3.0 μM of d[$AG_3(T_2AG_3)_3$] in HEPES buffer containing 50 mM KCl. Compound:DNA ratios ranged from 1:1 to 4:1.

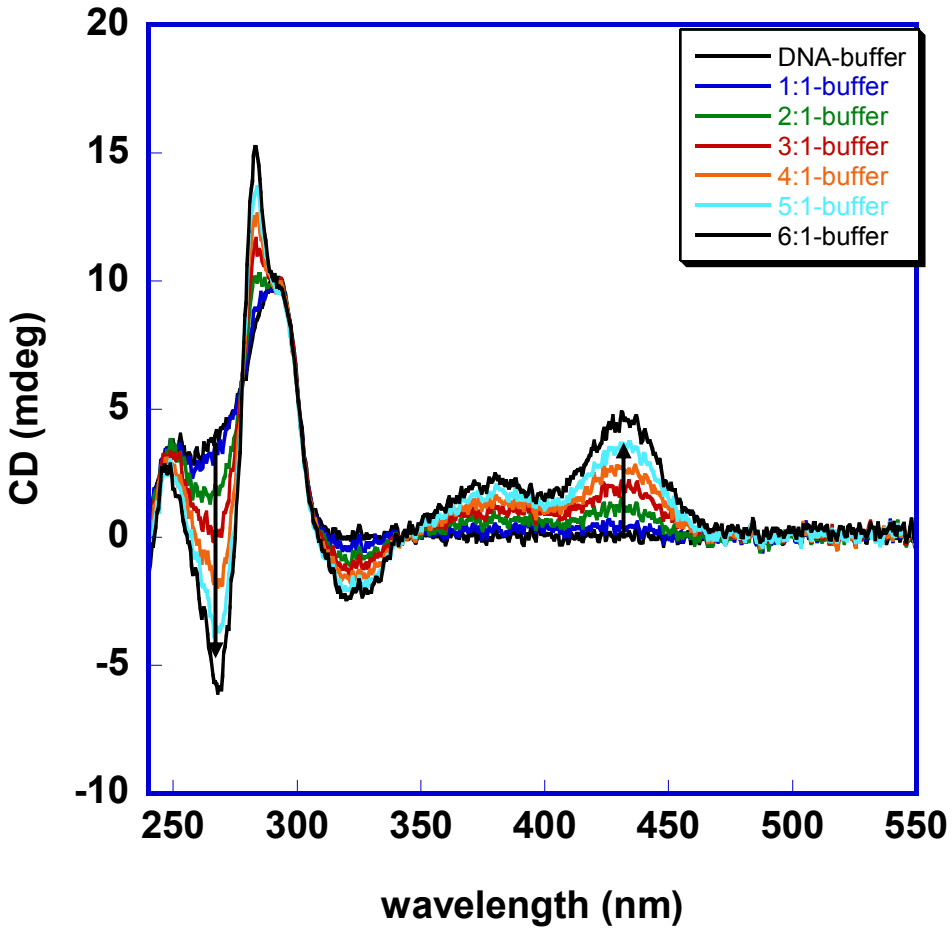


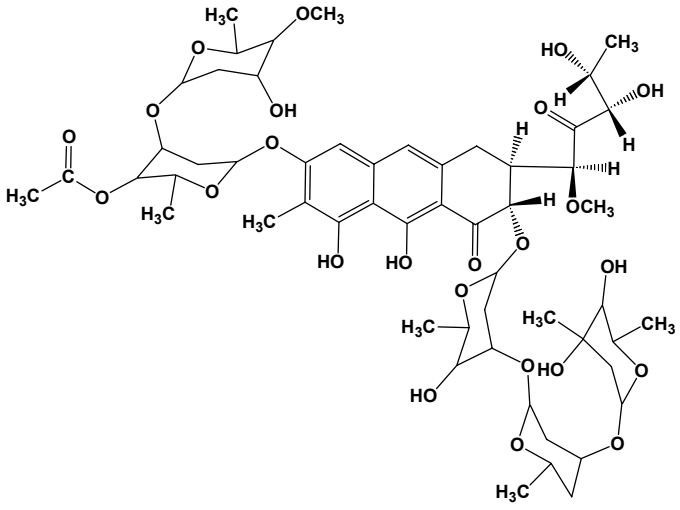

Figure 2.6 CD spectra of chromomycin A3 titrated into 3.9 μM of d[$AG_3(T_2AG_3)_3$] in HEPES buffer containing 50 mM KCl and 50 mM $MgCl_2$. Compound:DNA ratios ranged from 1:1 to 6:1.

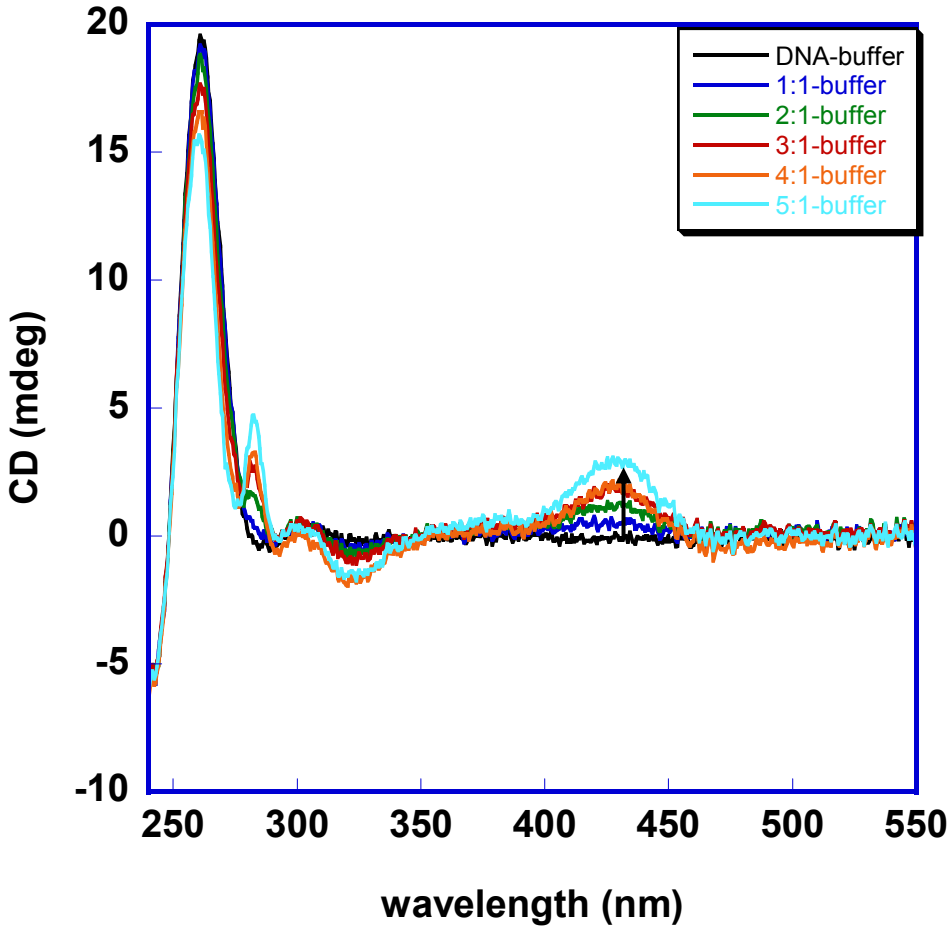


Figure 2.7 CD spectra of chromomycin A3 titrated into 2.9 μM of d[$AG_3TG_4AG_3TG_4A$] in HEPES buffer containing 50 mM KCl and 50 mM $MgCl_2$. Compound:DNA ratios ranged from 1:1 to 5:1.

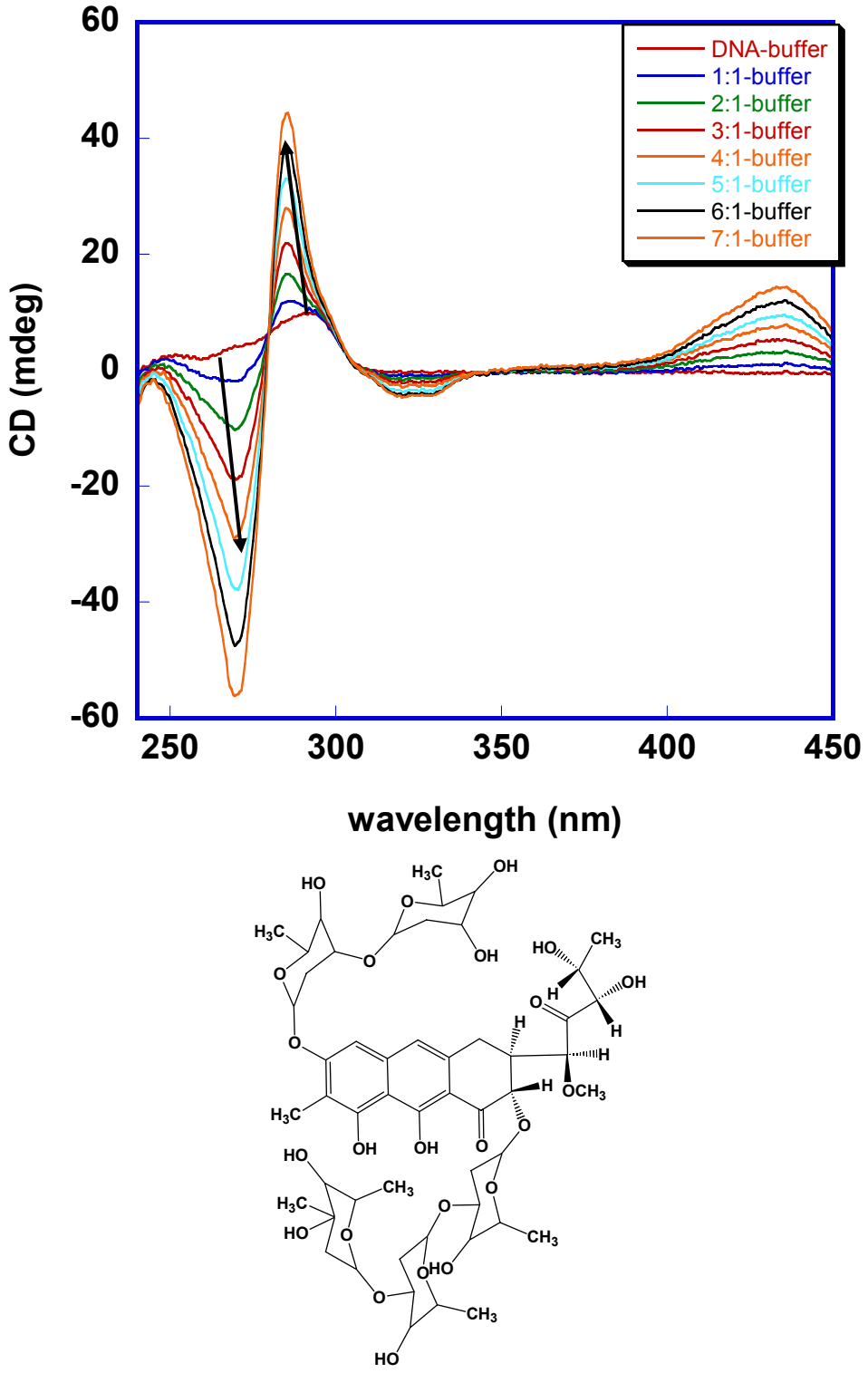


Figure 2.8 CD spectra of mithramycin titrated into 4.5 μM of d[$AG_3(T_2AG_3)_3$] in HEPES buffer containing 50 mM KCl and 50 mM $MgCl_2$. Compound:DNA ratios ranged from 1:1 to 7:1.

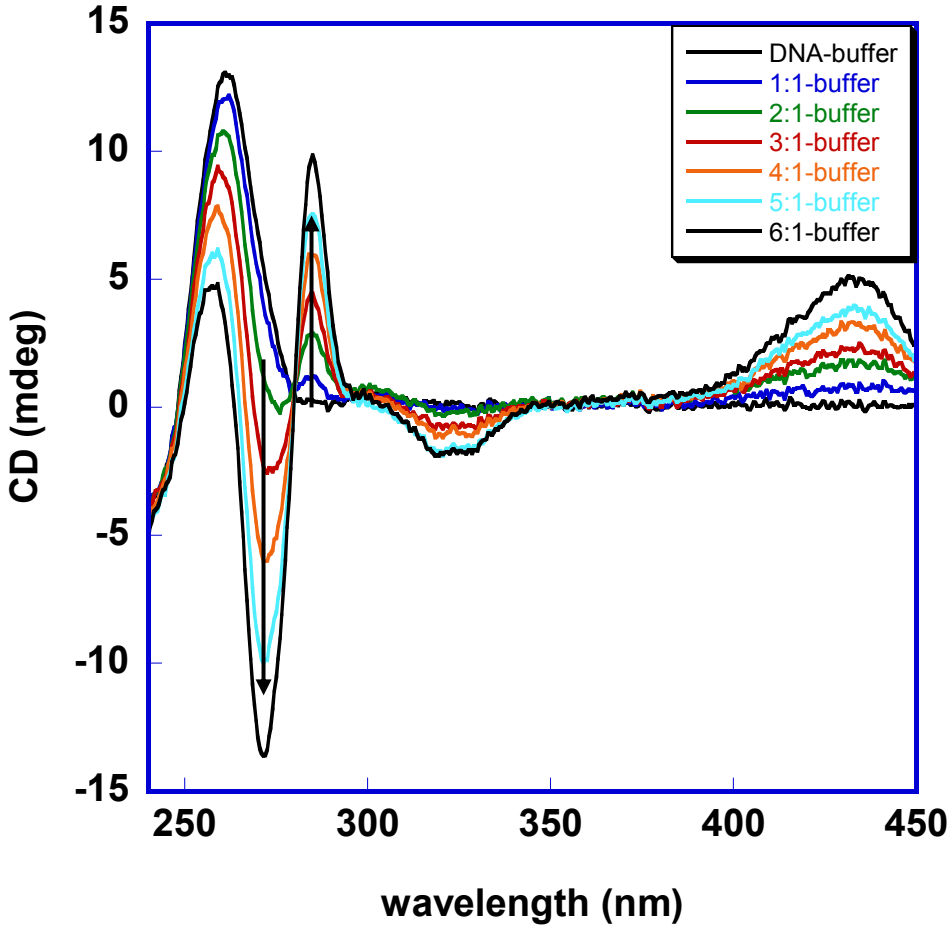


Figure 2.9 CD spectra of mithramycin titrated into 1.7 μM of d[$AG_3TG_4AG_3TG_4A$] in HEPES buffer containing 50 mM KCl and 50 mM $MgCl_2$. Compound:DNA ratios ranged from 1:1 to 6:1.

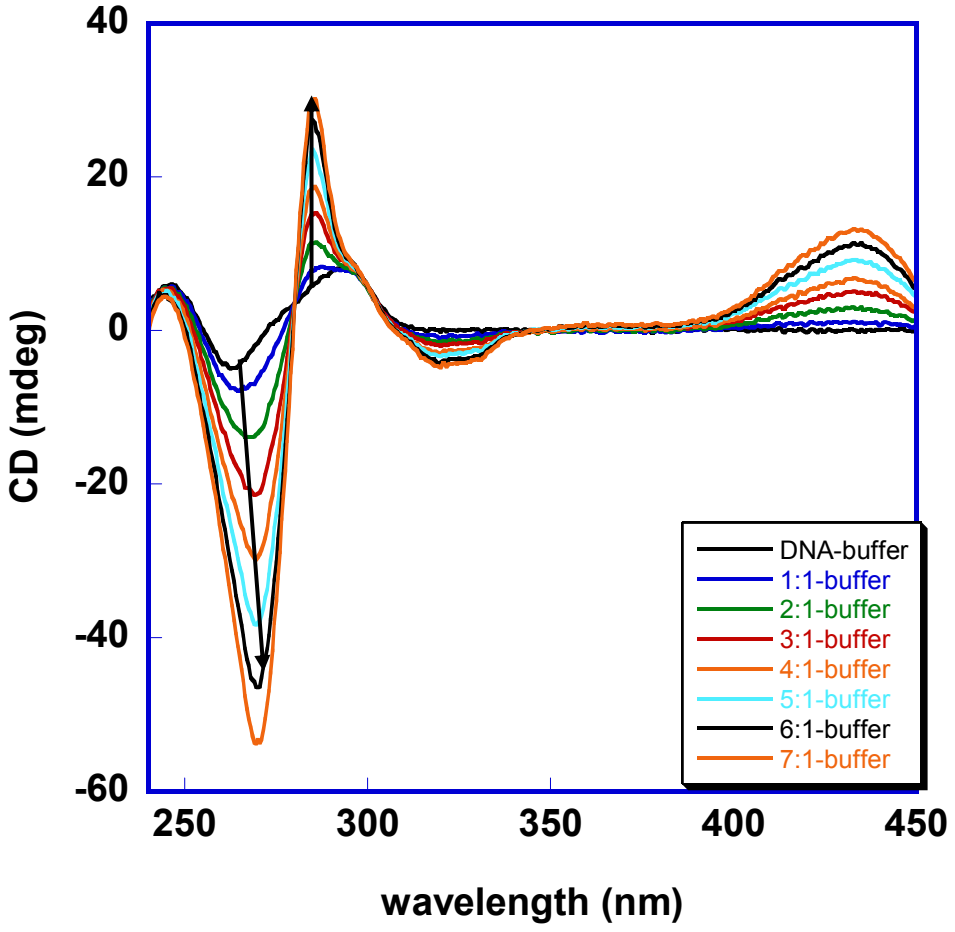


Figure 2.10 CD spectra of mithramycin titrated into 4.1 μM of d[$AG_3(T_2AG_3)_3$] in HEPES buffer containing 50 mM NaCl and 50 mM $MgCl_2$. Compound:DNA ratios ranged from 1:1 to 7:1.

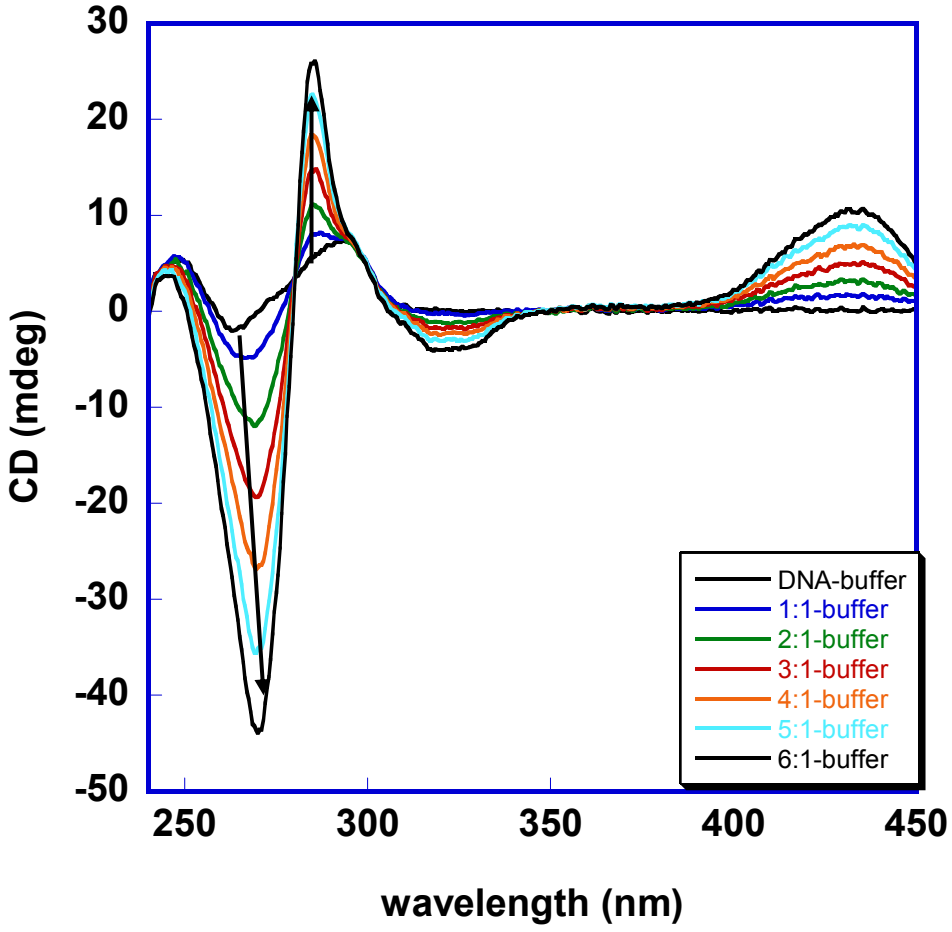


Figure 2.11 CD spectra of mithramycin titrated into 4.0 μM of d[$AG_3(T_2AG_3)_3$] in HEPES buffer containing 50 mM LiCl and 50 mM $MgCl_2$. Compound:DNA ratios ranged from 1:1 to 6:1.

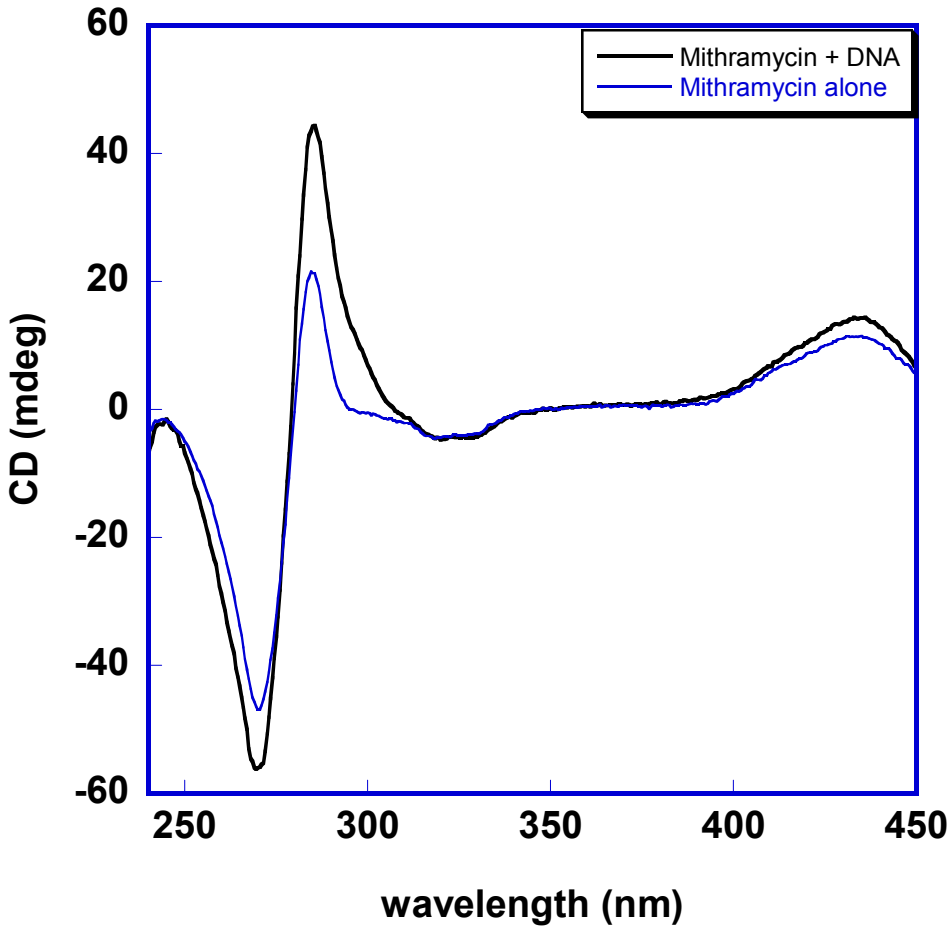


Figure 2.12 CD spectrum of 31.7 mM mithramycin added to 4.5 μM of d[$AG_3(T_2AG_3)_3$] minus the CD spectrum of 31.7 mM mithramycin alone. Both samples were prepared in HEPES buffer containing 50 mM KCl and 50 mM $MgCl_2$.

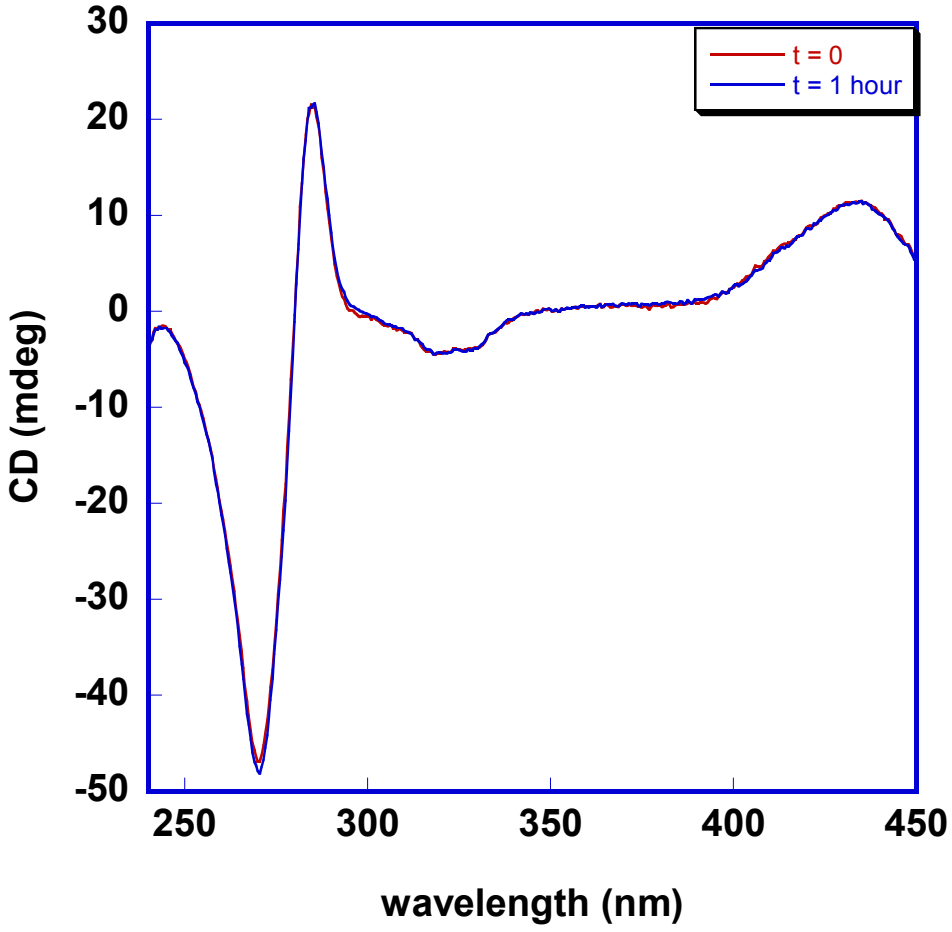


Figure 2.13 CD spectra of 31.7 mM mithramycin in HEPES buffer containing 50 mM KCl and 50 mM $MgCl_2$ at zero and one hour.

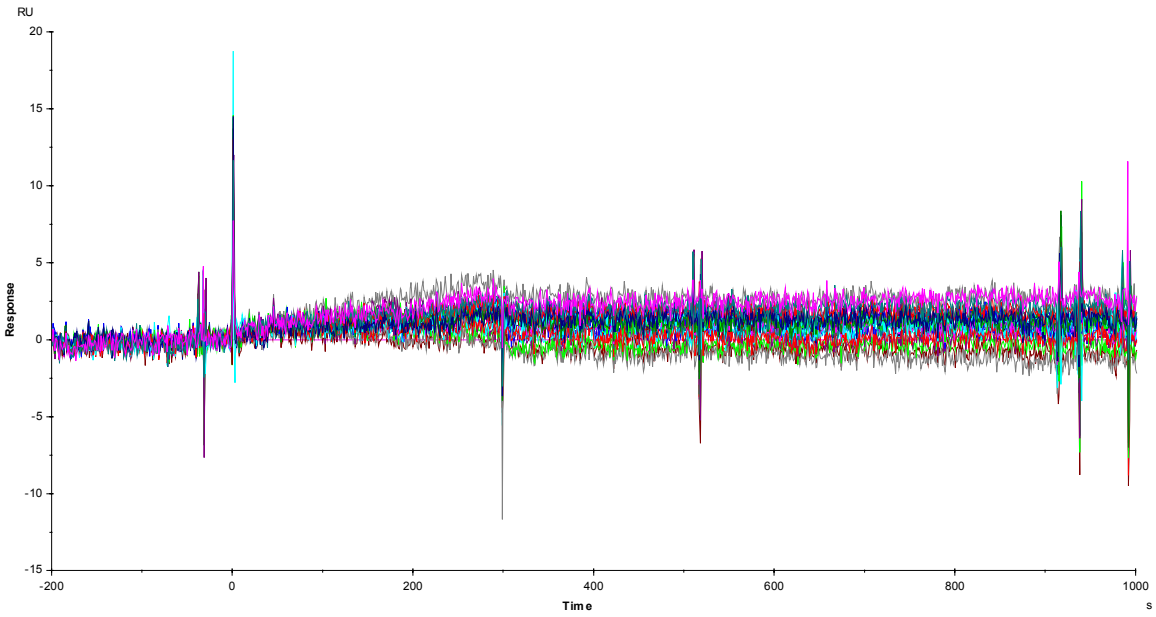


Figure 2.14 Sensorgrams for mithramycin binding to the human telomere, d[$AG_3(T_2AG_3)_3$], in HEPES buffer containing 50 mM $K^+$ and 10 mM $Mg^{2+}$. The concentration ranges from 0.0 μM to 2.0 μM.

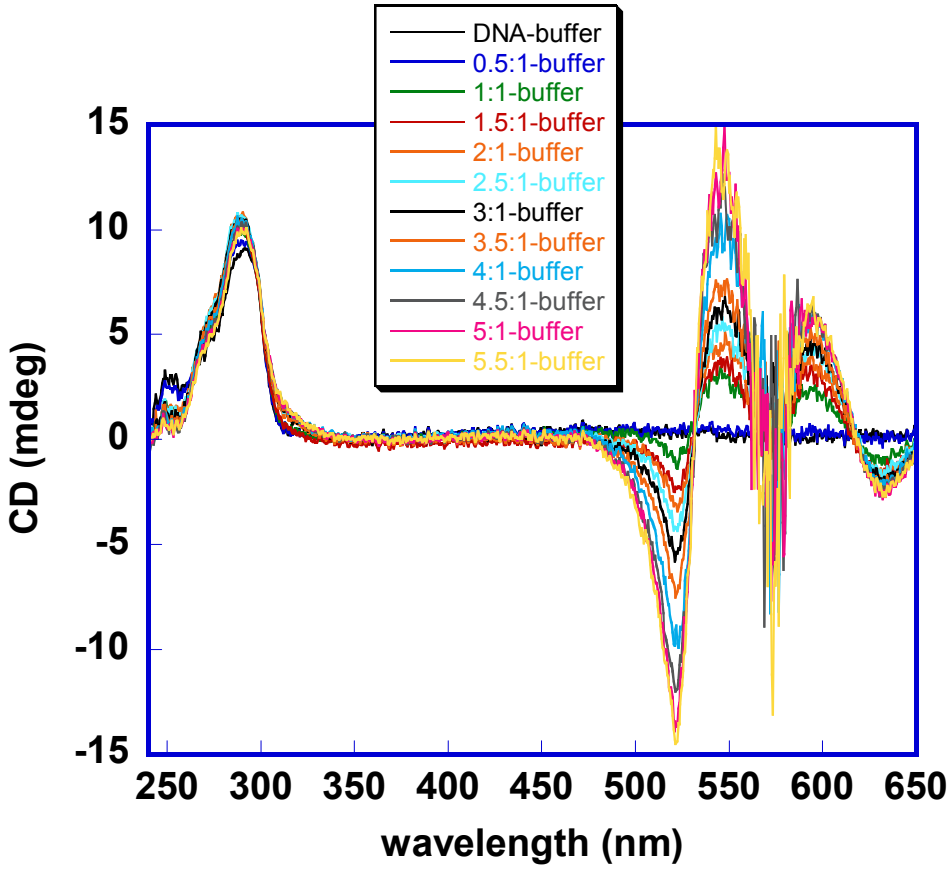


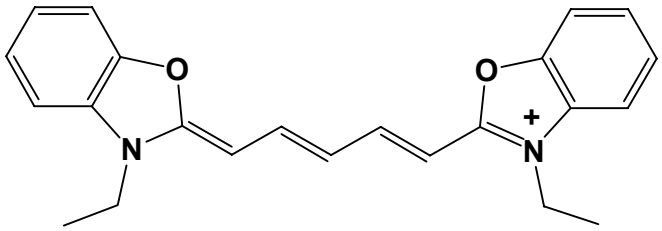


Figure 2.15 CD spectra of diethyloxadicarbocyanine (DODC) titrated into 3.1 μM of d[$AG_3(T_2AG_3)_3$] in HEPES buffer containing 50 mM KCl. Compound:DNA ratios ranged from 0.5:1 to 5.5:1.

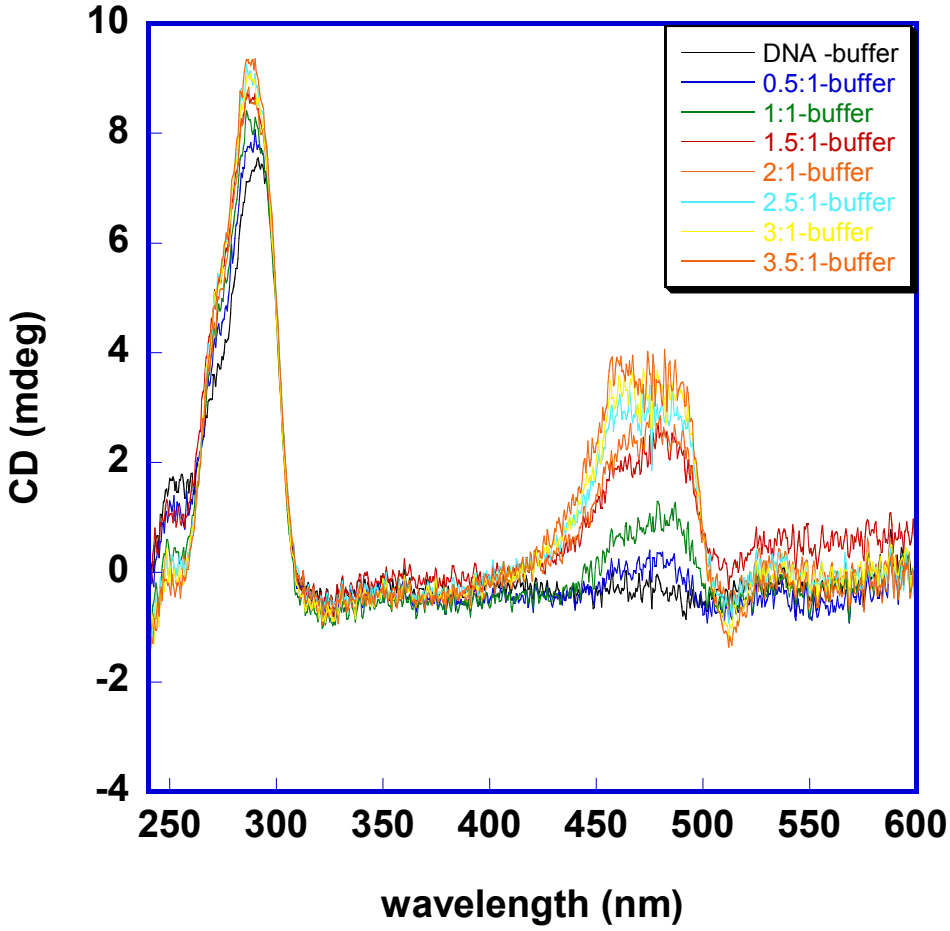


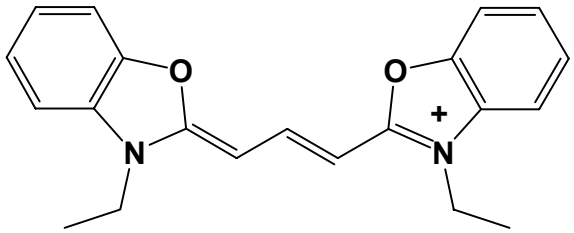


Figure 2.16 CD spectra of (DOC) titrated into 2.8 μM of d[$AG_3(T_2AG_3)_3$] in HEPES buffer containing 50 mM KCl. Compound:DNA ratios ranged from 0.5:1 to 3.5:1.

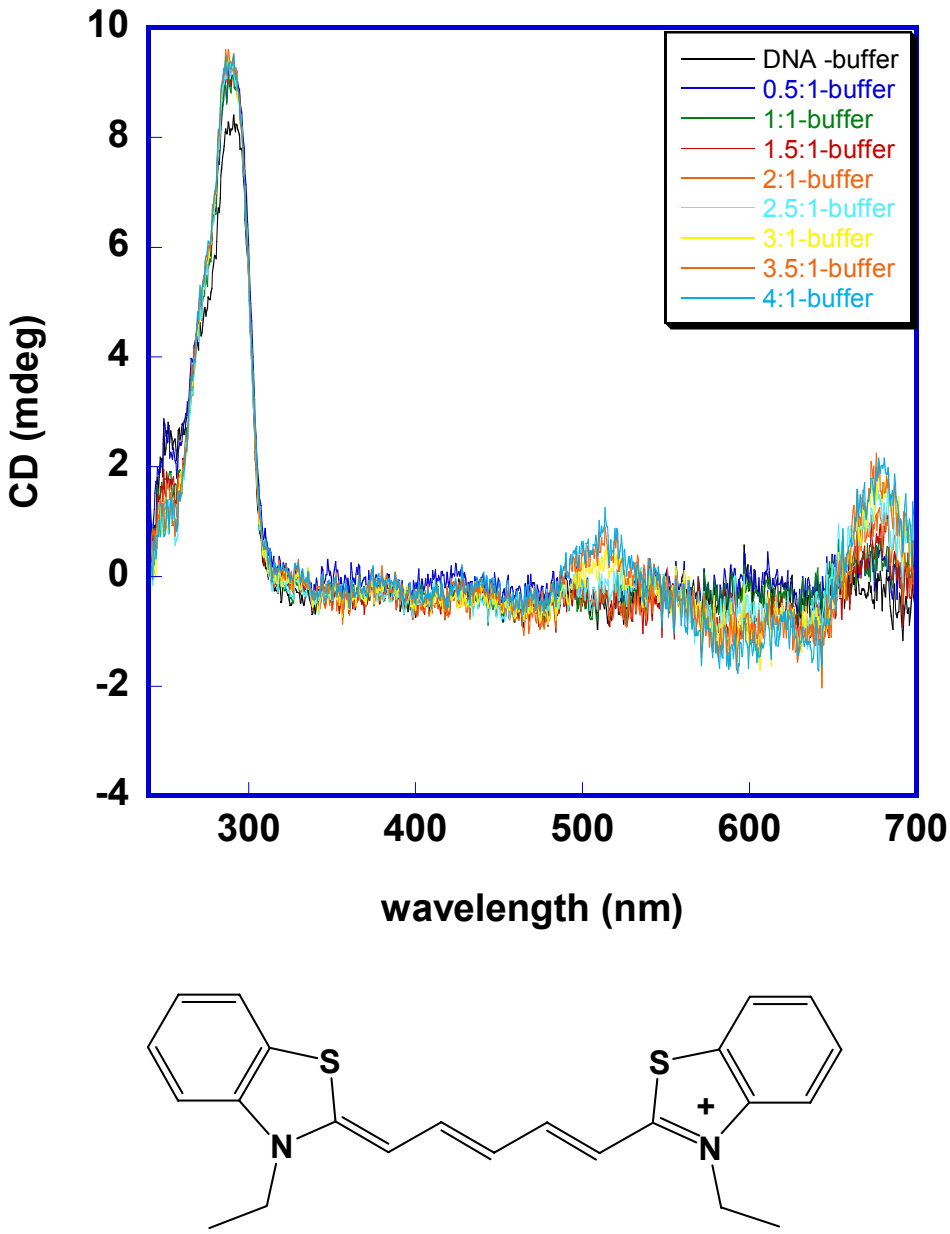


Figure 2.17 CD spectra of (DTDC) titrated into 3.2 μM of d[$AG_3(T_2AG_3)_3$] in HEPES buffer containing 50 mM KCl. Compound:DNA ratios ranged from 0.5:1 to 4:1.

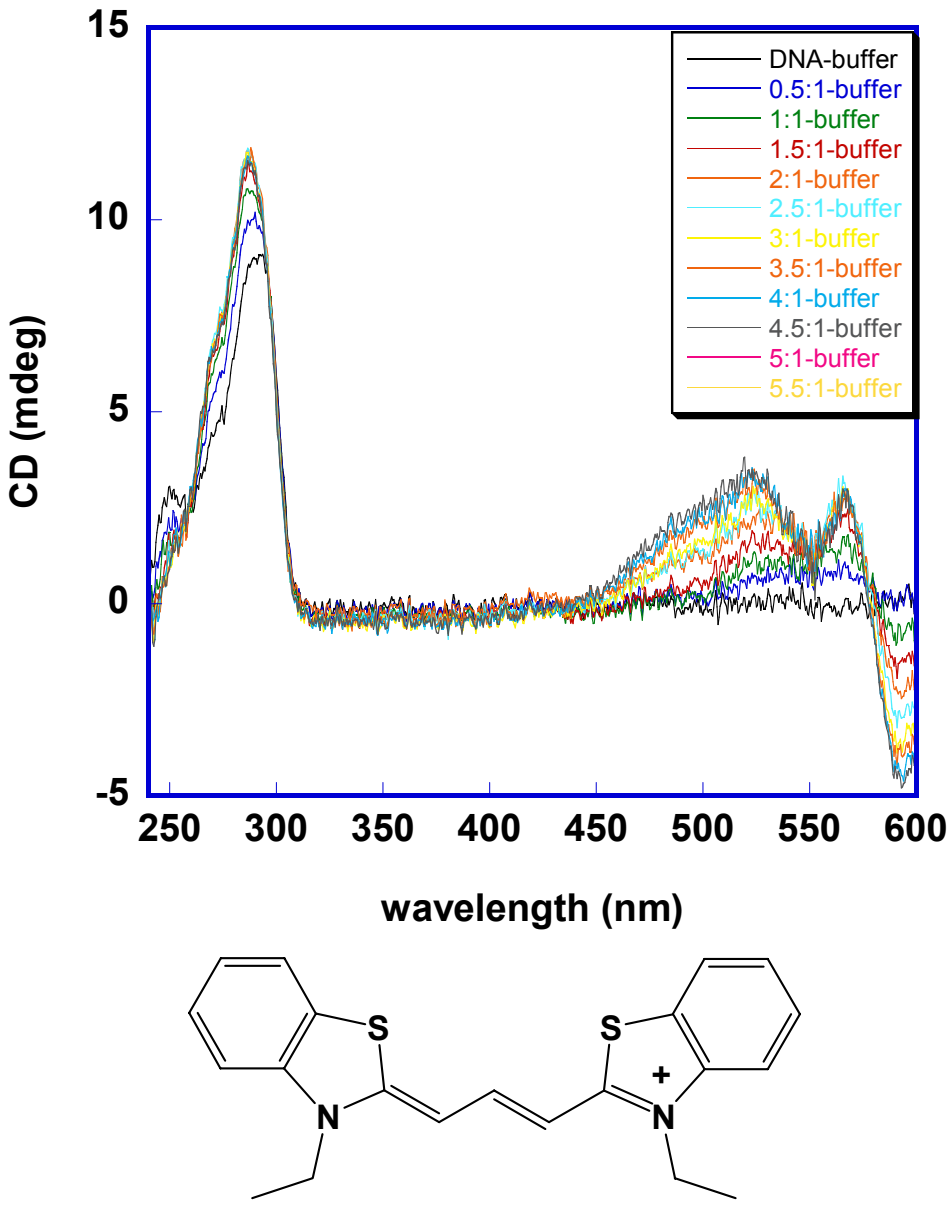


Figure 2.18 CD spectra of (DTC) titrated into 3.2 μM of d[$AG_3(T_2AG_3)_3$] in HEPES buffer containing 50 mM KCl. Compound:DNA ratios ranged from 0.5:1 to 5.5:1.

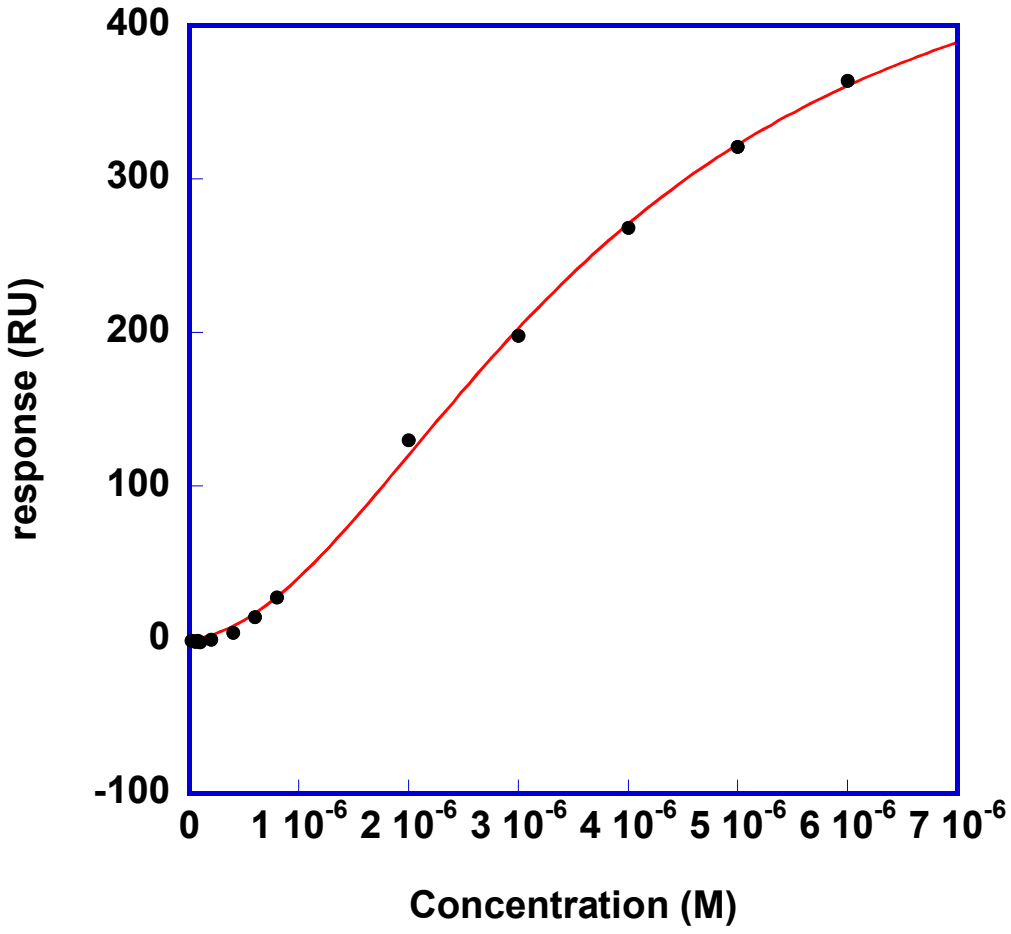


Figure 2.19 Direct binding plot for DODC to the human telomere, d[$AG_3(T_2AG_3)_3$], in HEPES buffer containing 200 mM $K^+$ fitted to a two-site model. The concentration axis is for unbound DODC concentration in the flow solution.

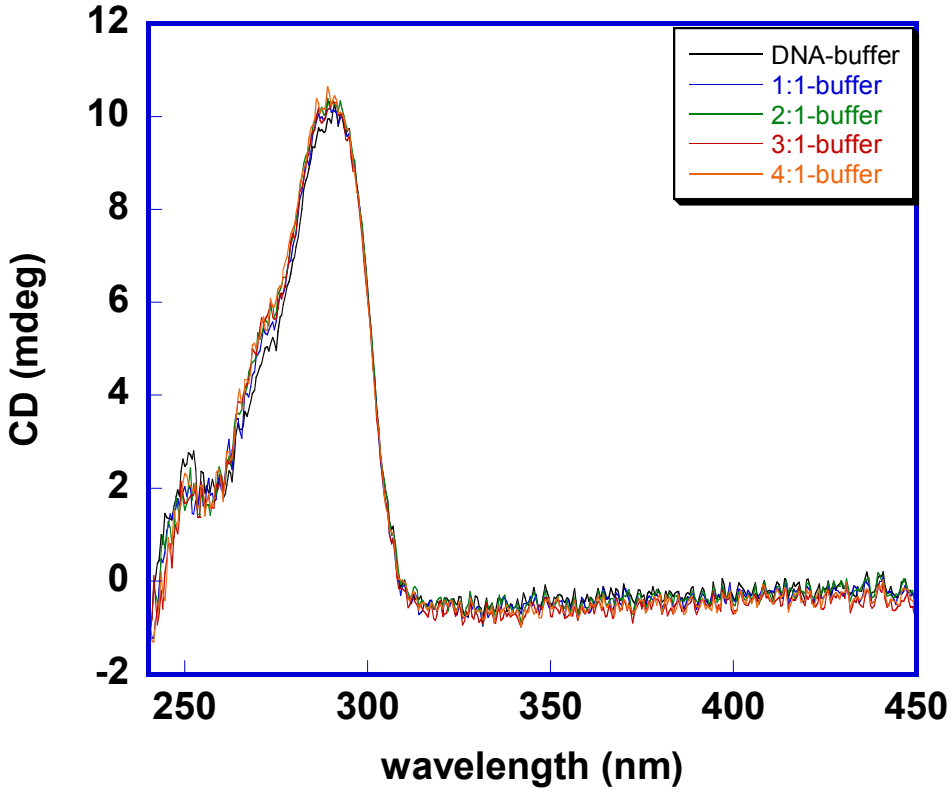


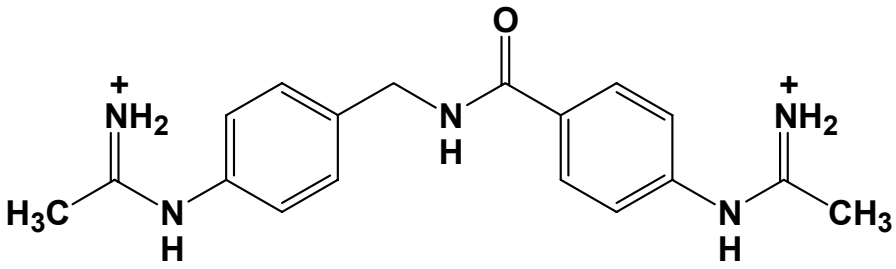


Figure 2.20 CD spectra of DB 860 titrated into 3.8 μM of d[$AG_3(T_2AG_3)_3$] in HEPES buffer containing 50 mM KCl. Compound:DNA ratios ranged from 1:1 to 4:1.

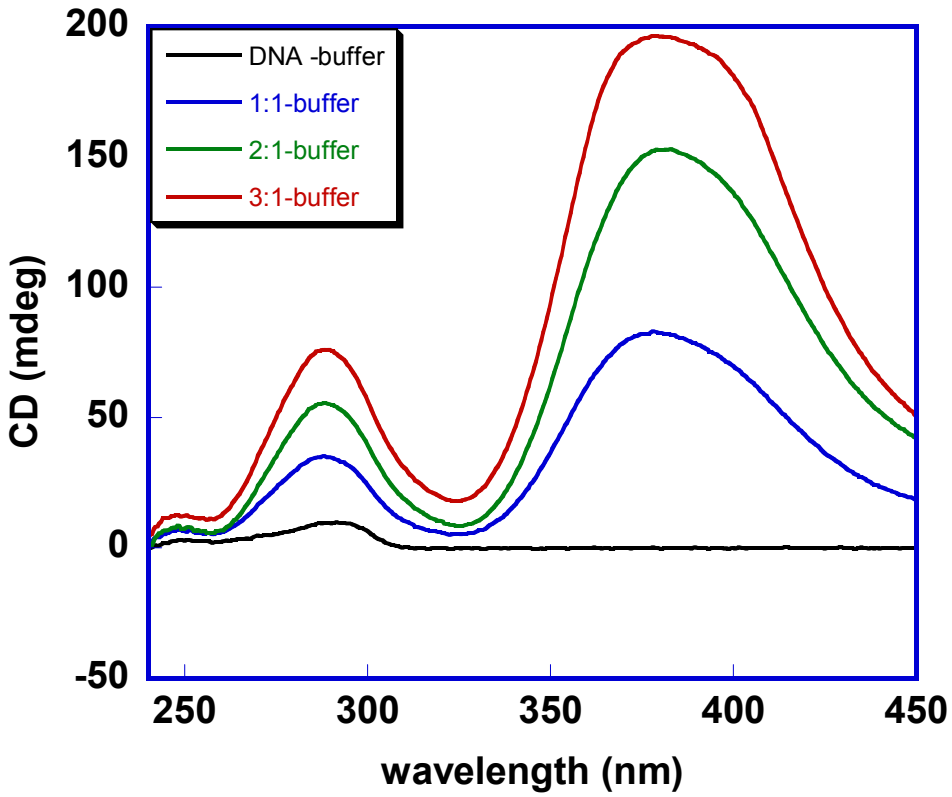


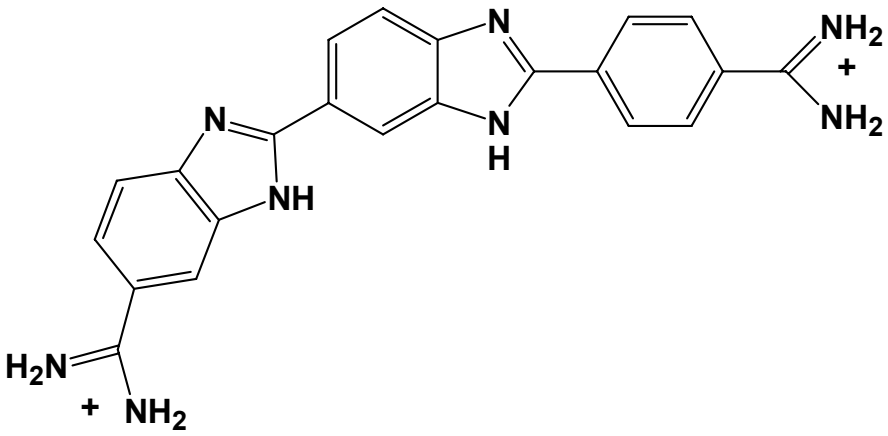


Figure 2.21 CD spectra of DB 185 titrated into 3.6 μM of d[$AG_3(T_2AG_3)_3$] in HEPES buffer containing 50 mM KCl. Compound:DNA ratios ranged from 1:1 to 3:1.

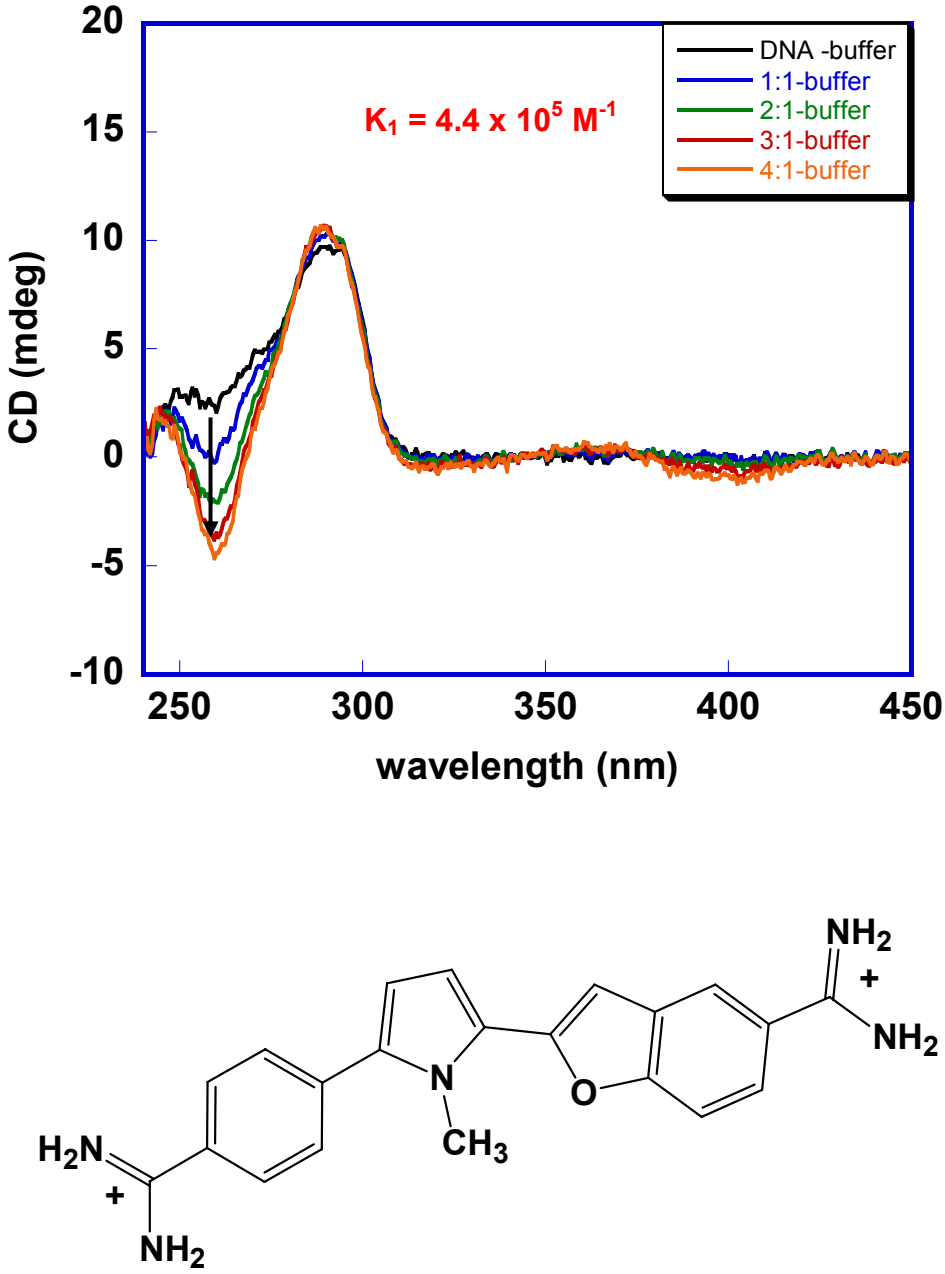


Figure 2.22 CD spectra of DB 1065 titrated into 3.4 μM of d[$AG_3(T_2AG_3)_3$] in HEPES buffer containing 50 mM KCl. Compound:DNA ratios ranged from 1:1 to 4:1.

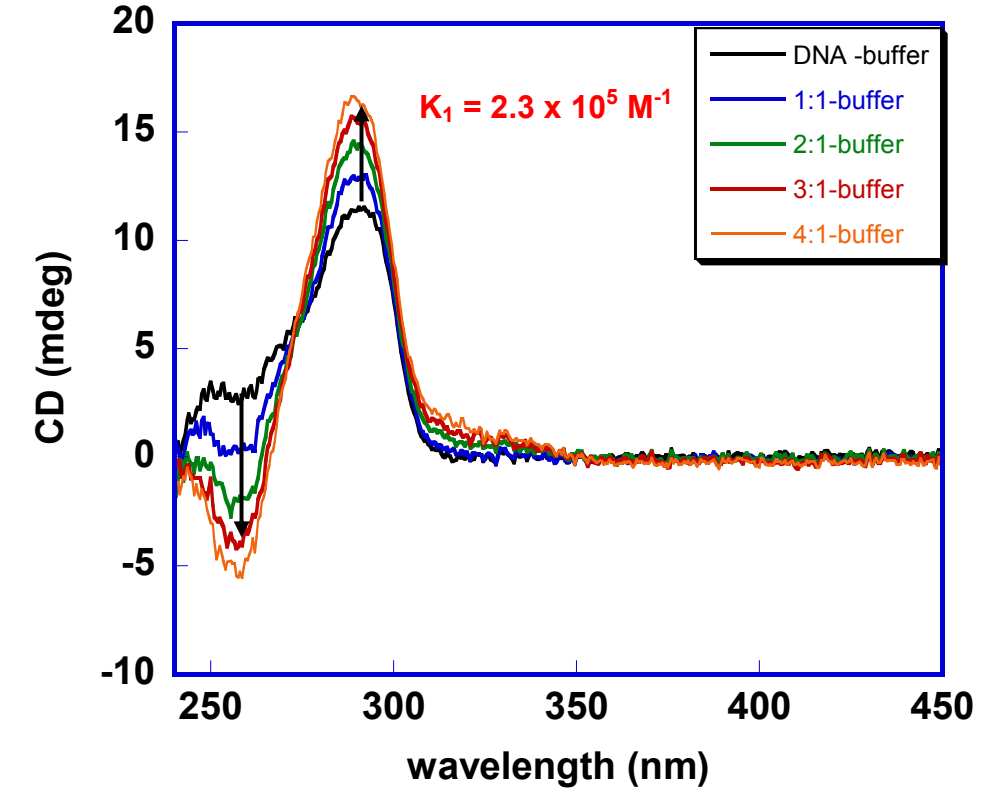


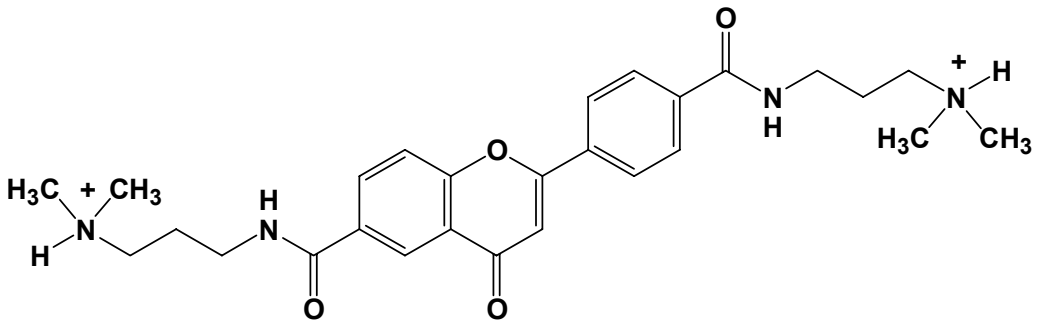


Figure 2.23 CD spectra of DB 634 titrated into 4.1 μM of d[$AG_3(T_2AG_3)_3$] in HEPES buffer containing 50 mM KCl. Compound:DNA ratios ranged from 1:1 to 4:1.

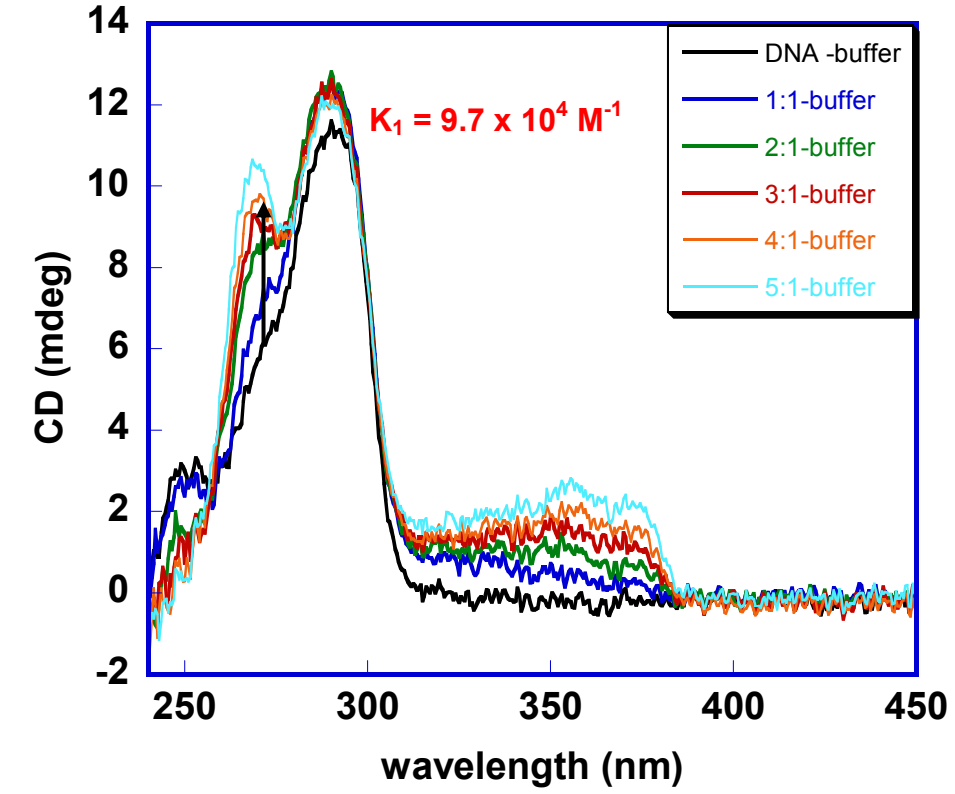


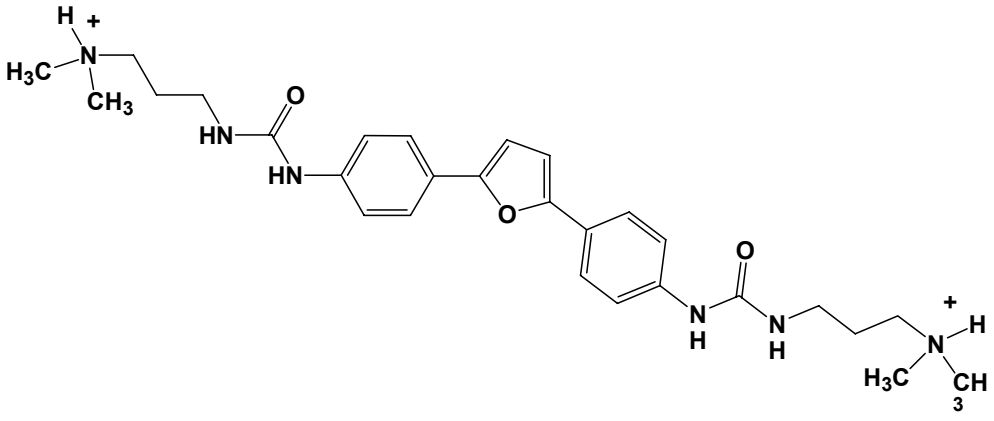


Figure 2.24 CD spectra of DB 587 titrated into 3.9 μM of d[$AG_3(T_2AG_3)_3$] in HEPES buffer containing 50 mM KCl. Compound:DNA ratios ranged from 1:1 to 5:1.

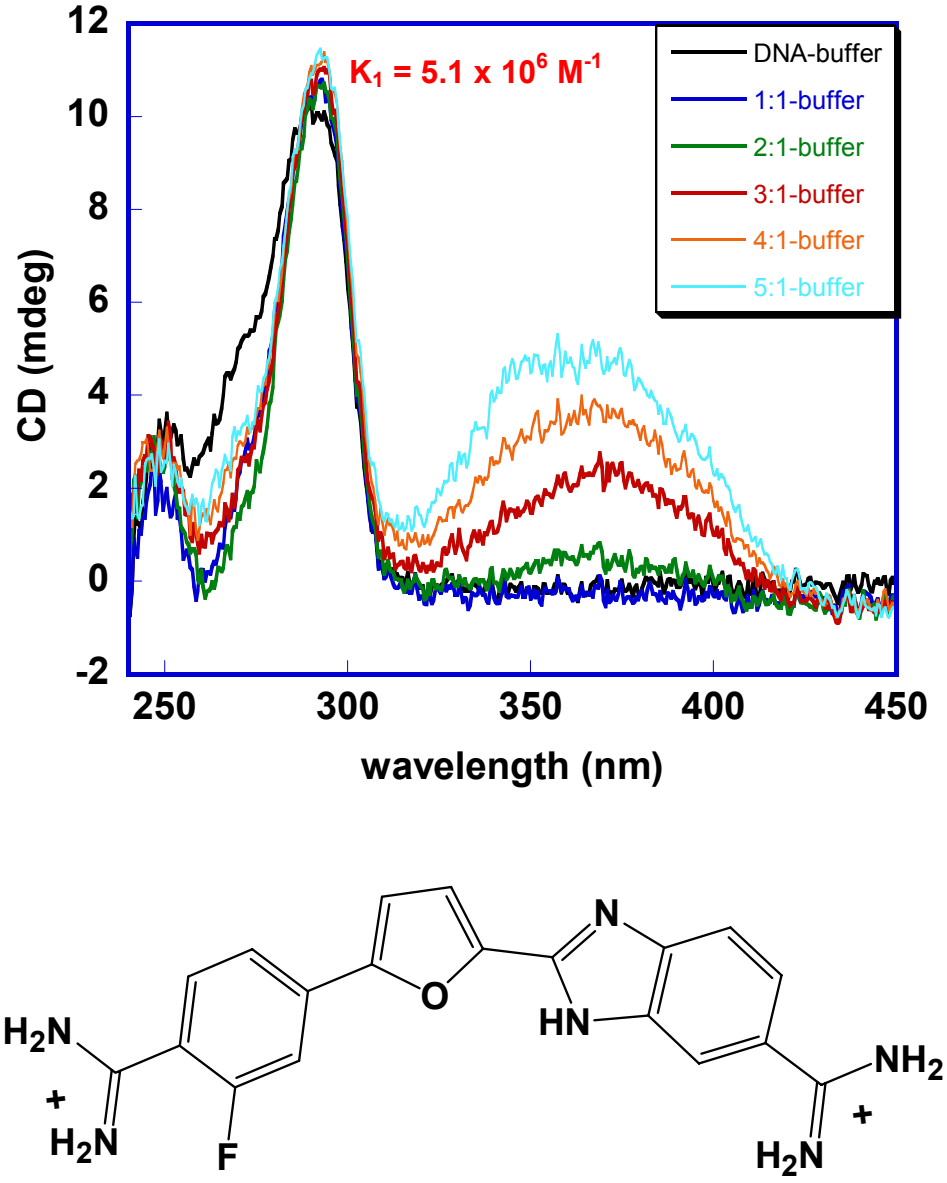


Figure 2.25 CD spectra of DB 989 titrated into 3.7 μM of d[$AG_3(T_2AG_3)_3$] in HEPES buffer containing 50 mM KCl. Compound:DNA ratios ranged from 1:1 to 5:1.

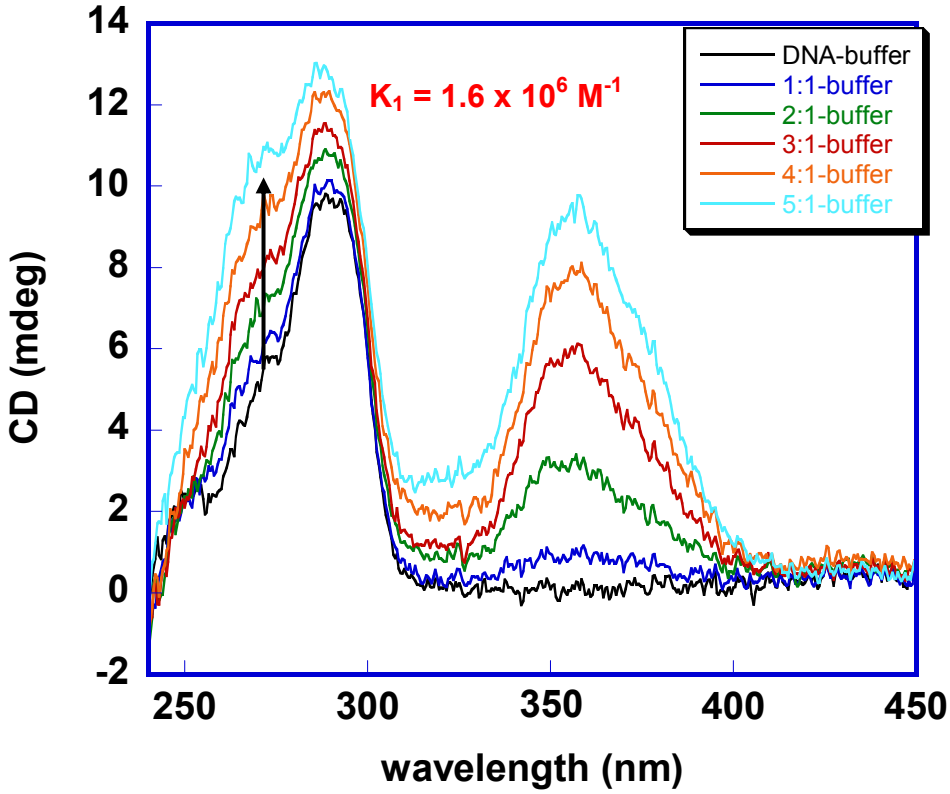


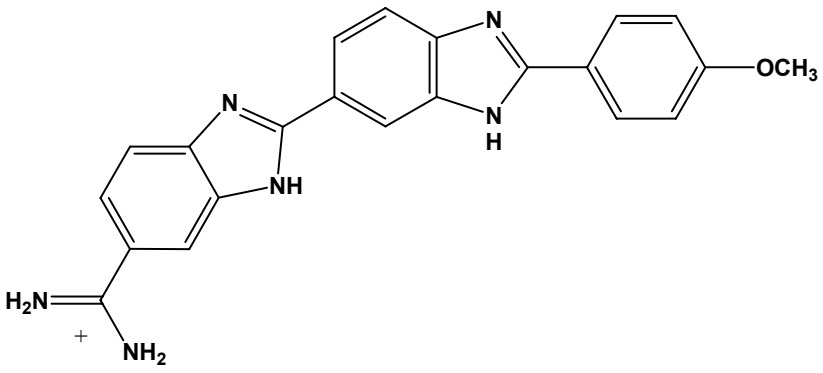


Figure 2.26 CD spectra of DB 210 titrated into 3.3 μM of d[$AG_3(T_2AG_3)_3$] in HEPES buffer containing 50 mM KCl. Compound:DNA ratios ranged from 1:1 to 5:1.

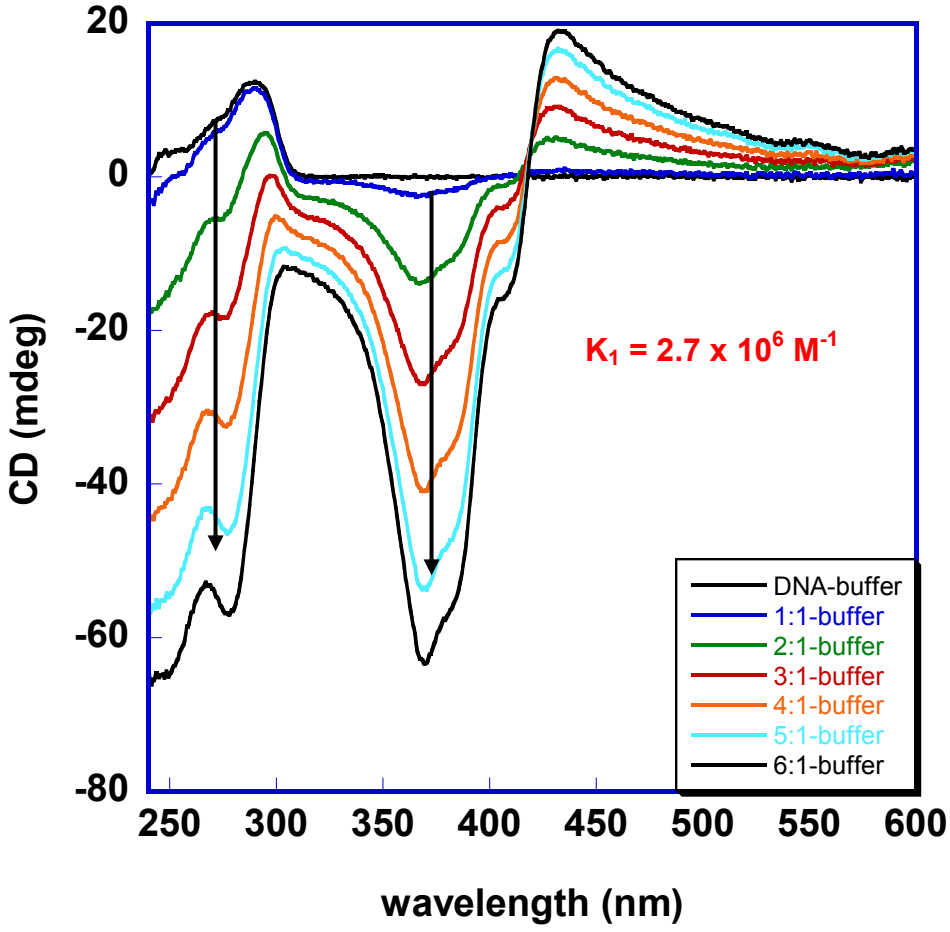


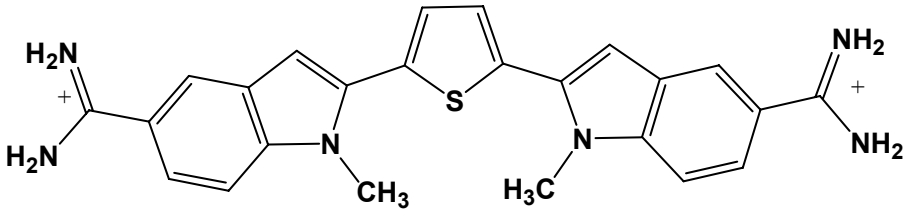


Figure 2.27 CD spectra of DB 1300 titrated into 4.2 μM of d[$AG_3(T_2AG_3)_3$] in HEPES buffer containing 50 mM KCl. Compound:DNA ratios ranged from 1:1 to 6:1.

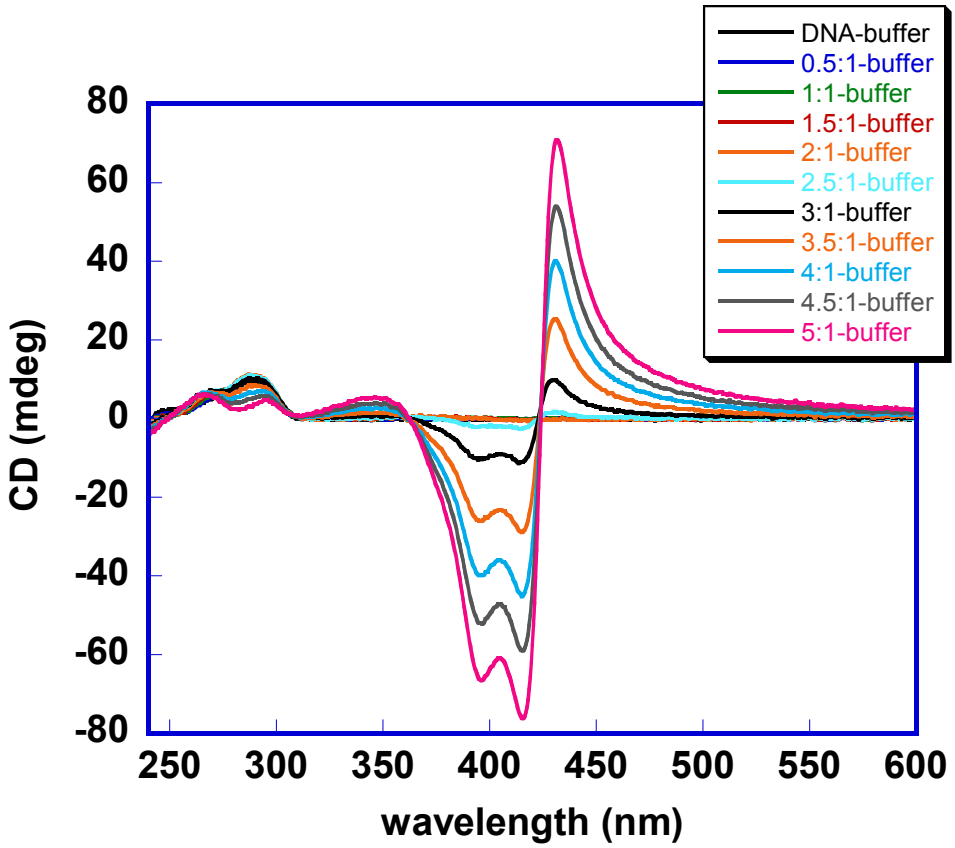


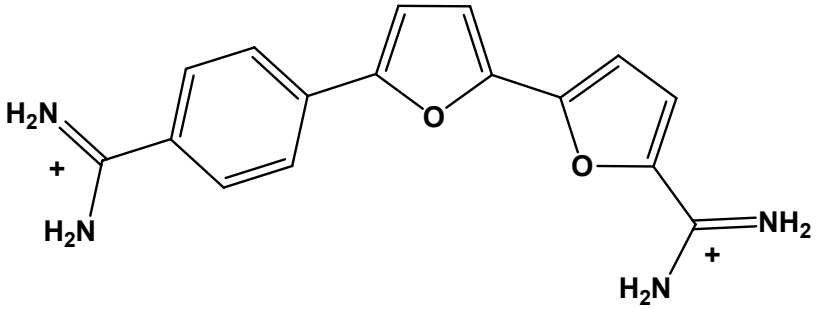


Figure 2.28 CD spectra of DB 832 titrated into 3.0 μM of d[$AG_3(T_2AG_3)_3$] in HEPES buffer containing 50 mM KCl. Compound:DNA ratios ranged from 0.5:1 to 5:1.

## References


1. Incles, C.M., C.M. Schultes, and S. Neidle, *Telomerase inhibitors in cancer therapy: current status and future directions.* Curr. Opin. Investig. Drugs, 2003. **4**(6): p. 675-85.
2. Kelland, L.R., *Overcoming the immortality of tumour cells by telomere and telomerase based cancer therapeutics--current status and future prospects.* Eur. J. Cancer, 2005. **41**(7): p. 971-9.
3. Mergny, J.L., et al., *Natural and pharmacological regulation of telomerase.* Nucleic Acids Res., 2002. **30**(4): p. 839-65.
4. Olaussen, K.A., et al., *Telomeres and telomerase as targets for anticancer drug development.* Crit. Rev. Oncol. Hematol., 2006. **57**(3): p. 191-214.
5. Rezler, E.M., D.J. Bearss, and L.H. Hurley, *Telomeres and telomerases as drug targets.* Curr. Opin. Pharmacol., 2002. **2**(4): p. 415-23.
6. Rezler, E.M., D.J. Bearss, and L.H. Hurley, *Telomere inhibition and telomere disruption as processes for drug targeting.* Annu. Rev. Pharmacol. Toxicol., 2003. **43**: p. 359-79.
7. Saretzki, G., *Telomerase inhibition as cancer therapy.* Cancer Lett., 2003. **194**(2): p. 209-19.
8. Shin-Ya, K., *Novel antitumor and neuroprotective substances discovered by characteristic screenings based on specific molecular targets.* Biosci. Biotechnol. Biochem., 2005. **69**(5): p. 867-72.
9. Sun, D., et al., *Inhibition of human telomerase by a G-quadruplex-interactive compound.* J. Med. Chem., 1997. **40**(14): p. 2113-6.

10. Fedoroff, O.Y., et al., *NMR-Based model of a telomerase-inhibiting compound bound to G-quadruplex DNA.* Biochem., 1998. **37**(36): p. 12367-74.

11. Han, F.X., R.T. Wheelhouse, and L.H. Hurley, *Interactions of TMPyP4 and TMPyP2 with Quadruplex DNA. Structural Basis for the DIfferential Effects on Telomerase Inhibition.* J. Am. Chem. Soc., 1999. **121**(15): p. 3561-3570.

12. Read, M., et al., *Structure-based design of selective and potent G quadruplex-mediated telomerase inhibitors.* Proc. Natl. Acad. Sci. U S A, 2001. **98**(9): p. 4844-9.

13. Teulade-Fichou, M.P., et al., *Selective recognition of G-Quadruplex telomeric DNA by a bis(quinacridine) macrocycle.* J. Am. Chem. Soc., 2003. **125**(16): p. 4732-40.

14. Dervan, P.B. and B.S. Edelson, *Recognition of the DNA minor groove by pyrrole-imidazole polyamides.* Curr. Opin. Struct. Biol., 2003. **13**(3): p. 284-99.

15. Lacy, E.R., et al., *Polyamide stacking in the DNA minor groove and recognition of T-G mismatched base pairs in DNA*, in *DNA and RNA binders*, M. Demeunynck, Bailly, C., Wilson, W.D.,, Editor. 2003, Wiley-VCH: Weinheim. p. 384-413.

16. Neidle, S., *DNA minor-groove recognition by small molecules.* Nat. Prod. Rep., 2001. **18**(3): p. 291-309.

17. Wang, L., et al., *Specific molecular recognition of mixed nucleic acid sequences: an aromatic dication that binds in the DNA minor groove as a dimer.* Proc. Natl. Acad. Sci. U S A, 2000. **97**(1): p. 12-6.

18. Wang, L., et al., *Evaluation of the influence of compound structure on stacked-dimer formation in the DNA minor groove.* Biochem., 2001. **40**(8): p. 2511-21.

19. Wilson, W.D., et al., *Dications that target the DNA minor groove: compound design and preparation, DNA interactions, cellular distribution and biological activity.* Curr. Med. Chem. Anticancer Agents, 2005. **5**(4): p. 389-408.

20. Kerwin, S.M., *G-Quadruplex DNA as a target for drug design.* Curr. Pharm. Des., 2000. **6**(4): p. 441-78.

21. Chen, Q., I.D. Kuntz, and R.H. Shafer, *Spectroscopic recognition of guanine dimeric hairpin quadruplexes by a carbocyanine dye.* Proc. Natl. Acad. Sci. U S A, 1996. **93**: p. 2635-2639.

22. Cheng, J.-Y., S.-H. Lin, and T.-C. Chang, *Vibrational Investigation of DODC Cation for Recognition of Guanine Dimeric Hairpin Quadruplex Studied by Satellite Holes.* J. Phys. Chem., 1998. **102**: p. 5542-5546.

23. Chiang, C.-C., J.-Y. Cheng, and T.-C. Chang, *Satellite Hole Spectral Method and Its Applications to Dye-DNA Complexes.* Proc. Natl. Sci. Coun. ROC (A), 1999. **23**(6): p. 679-694.

24. Kerwin, S.M., et al., *G-Quadruplex DNA Binding by a Series of Carbocyanine Dyes.* Bioorg. Med. Chem. Letters, 2001. **11**: p. 2411-2414.

25. Rodger, A. and B. Norden, *Circular Dichroism and Linear Dichroism*. Oxford Chemistry Masters, ed. R.G. Compton, S.G. Davies, and J. Evans. 1997, New York: Oxford University Press. 150.

26. Xu, Y., Y. Noguchi, and H. Sugiyama, *The new models of the human telomere d[AGGG(TTAGGG)3] in K+ solution.* Bioorg Med Chem, 2006. **14**(16): p. 5584-91.

27. Yu, H.Q., D. Miyoshi, and N. Sugimoto, *Characterization of structure and stability of long telomeric DNA g-quadruplexes.* J Am Chem Soc, 2006. **128**(48): p. 15461-8.

28. Blackburn, G.M. and M.J. Gait, *Nucleic acids in chemistry and biology*. Second ed. 1996, New York: Oxford University Press. 528.

29. Cao, R., C.F. Venezia, and B.A. Armitage, *Investigation of DNA binding modes for a symmetrical cyanine dye trication: effect of DNA sequence and structure.* J. Biomol. Struct. Dyn., 2001. **18**(6): p. 844-56.

30. Garoff, R.A., et al., *Helical Aggregation of Cyanine Dyes on DNA Templates: Effect of Dye Structure on Formation of Homo- and Heteroaggregates.* Langmuir, 2002. **18**(16): p. 6330-6337.

31. Lacy, E.R., et al., *Influence of a terminal formamido group on the sequence recognition of DNA by polyamides.* J. Am. Chem. Soc., 2002. **124**(10): p. 2153-63.

32. Mazur, S., et al., *A thermodynamic and structural analysis of DNA minor-groove complex formation.* J. Mol. Biol., 2000. **300**(2): p. 321-37.

33. Koeppel, F., et al., *Ethidium derivatives bind to G-quartets, inhibit telomerase and act as fluorescent probes for quadruplexes.* Nucleic Acids Res., 2001. **29**(5): p. 1087-96.

34. Rosu, F., et al., *Selective interaction of ethidium derivatives with quadruplexes: an equilibrium dialysis and electrospray ionization mass spectrometry analysis.* Biochem., 2003. **42**(35): p. 10361-71.

35. Randazzo, A., et al., *Interaction of distamycin A and netropsin with quadruplex and duplex structures: a comparative 1H-NMR study.* Nucleosides Nucleotides Nucleic Acids, 2002. **21**(8-9): p. 535-45.

36. Cocco, M.J., et al., *Specific interactions of distamycin with G-quadruplex DNA.* Nucleic Acids Res., 2003. **31**(11): p. 2944-51.

37. Wu, J.Y., et al., *Structural isomers and binding sites of guanine-rich quadruplexes investigated by induced circular dichroism of thionin: loops and tails.* J Biomol Struct Dyn, 2003. **21**(1): p. 135-40.

38. Aich, P. and D. Dasgupta, *Role of magnesium ion in mithramycin-DNA interaction: binding of mithramycin-Mg2+ complexes with DNA.* Biochemistry, 1995. **34**(4): p. 1376-85.

39. Aich, P., R. Sen, and D. Dasgupta, *Role of magnesium ion in the interaction between chromomycin A3 and DNA: binding of chromomycin A3-Mg2+ complexes with DNA.* Biochemistry, 1992. **31**(11): p. 2988-97.

40. Chakrabarti, S., D. Bhattacharyya, and D. Dasgupta, *Structural basis of DNA recognition by anticancer antibiotics, chromomycin A(3), and mithramycin: roles of minor groove width and ligand flexibility.* Biopolymers, 2000. **56**(2): p. 85-95.

41. Sastry, M., R. Fiala, and D.J. Patel, *Solution structure of mithramycin dimers bound to partially overlapping sites on DNA.* J Mol Biol, 1995. **251**(5): p. 674-89.

42. Wang, Y. and D.J. Patel, *Solution structure of the human telomeric repeat d[AG3(T2AG3)3] G-tetraplex.* Structure, 1993. **1**(4): p. 263-82.

43. Sen, D. and W. Gilbert, *Guanine quartet structures.* Methods Enzymol., 1992. **211**: p. 191-199.

44. Wang, M., G.L. Silva, and B.A. Armitage, *DNA-Templated Formation of a Helical Cyanine Dye J-Aggregate.* J. Am. Chem. Soc., 2000. **122**(41): p. 9977-9986.

45. Tidwell, R.R., Boykin, W.D, *DNA and RNA Binders: from Small Molecules to Drugs;*, ed. M. Demeunynck, Bailly, C., Wilson, W.D., and Eds. Vol. Vol. 2, Chapter 16. 2003: Wiley-VCH. 414-460.

46. Balagurumoorthy, P., et al., *Hairpin and parallel quartet structures for telomeric sequences.* Nucleic Acids Res., 1992. **20**(15): p. 4061-7.

47. Nguyen, B., et al., *Characterization of a novel DNA minor-groove complex.* Biophys J, 2004. **86**(2): p. 1028-41.

48. Neidle, S. and M.A. Read, *G-quadruplexes as therapeutic targets.* Biopolymers, 2001. **56**(3): p. 195-208.

# Chapter 3

## Evaluation of a Heterocyclic Diamidine that Binds to the Grooves of Quadruplex DNA as a Stacked Species

### Introduction

Discovery and design of compounds that target G-quadruplex structures in DNA is a relatively new area that is now being rapidly driven by the desire to discover new anti-cancer drugs and targets. Many small molecules known to bind quadruplex DNA are planar, aromatic compounds that are based on or derived from or are quite similar to duplex intercalators. These molecules generally bind to the quadruplex via end-stacking on either or both of the terminal G-tetrads. Because of the structural similarity to intercalators, many of these quadruplex-binding molecules exhibit limited selectivity for quadruplex over duplex structures. Binding to non-targeted duplex sequences can result in significant loss of compound with potential nonselective cytotoxicity. Since potential quadruplex-forming sequences are common in the genome, selectivity for a particular quadruplex structure over other quadruplexes is also a concern in the design of quadruplex-binding compounds. Binding to non-targeted quadruplex sequences results in compound loss and may have unintentional effects on regulation of non-targeted genes. Increasing selectivity of telomerase inhibitors for their targets is therefore an important focus of research.

Other modes of binding, including intercalation between tetrads as well as groove-binding have been proposed. Ethidium bromide has been proposed to intercalate

between tetrads, although structural evidence to support this claim is lacking [1]. G-quadruplex intercalation is not considered to be a generally viable binding mode due to its high energetic cost and similarity to duplex intercalation [2]. Shafer et al. have investigated the interaction of the carbocyanine dye 3,3'-diethyloxadicarbocyanine (DODC) with a dimeric hairpin G-quadruplex [3]. Spectroscopic data suggests that this molecule binds in one or more of the quadruplex grooves. Satellite hole spectroscopy studies by Chang et al. support the groove-binding model for this particular ligand/DNA pair [4, 5]. Kerwin and coworkers have used electrospray mass spectrometry to investigate the interaction of the carbocyanine dye DTC with a different four-stranded intermolecular quadruplex [6]. The fragmentation pattern upon ionization suggests that this molecule binds in the grooves of this quadruplex as well. Randazzo et al. have investigated the interaction of distamycin with a four-stranded intermolecular quadruplex [7]. Their NMR results suggest that distamycin binds in one quadruplex groove as a dimer, but is capable of binding to two grooves at higher concentrations. However, Maizels and coworkers have shown with NMR that distamycin binds via an end-stacking mechanism to several four-stranded intermolecular quadruplexes, including one formed from the human telomeric sequence [8]. Thus, although G-quadruplex end-stacking is a well-established and documented recognition mode, binding in the G-quadruplex grooves is an area that lacks adequate models for drug design and development.

Quadruplex groove-binding may offer an attractive strategy for exploiting the structural differences between duplex and quadruplex DNA, leading to possible increased selectivity of recognition over traditional planar end-stacking molecules. Since groove dimensions vary significantly according to the type of quadruplex, groove-binding also

offers the opportunity for obtaining increased selectivity for a particular quadruplex structure. The geometry of the G-quartet is not greatly affected by the glycosidic (syn/anti) conformation or the strand orientation of the quadruplex [9]. However, groove dimensions are strongly dependent on these factors, resulting in a wide variety of possible groove geometries. The groove structural variation allows for the targeting of certain quadruplex sequences with a high degree of selectivity. In spite of extensive experiments on telomeres, no compounds to date have been found which bind to the grooves of the human telomere sequence. A library of diamidines synthesized by Boykin and coworkers at Georgia State University was screened against the human telomeric sequence using circular dichroism as described in Chapter 2. DB 832 was identified as a potential stacked quadruplex groove-binder and selected for further study. In this chapter, we use several biochemical methods to show that the heterocyclic diamidine DB 832 binds selectively as a stacked species with high (yet discrete) stoichiometry to a mixed parallel/antiparallel hybrid quadruplex structure. This molecule serves as a paradigm to show that the grooves of the human telomere can indeed be targeted and it can also serve as the starting point for the design of new molecules that may have therapeutic use as anti-cancer or anti-trypanosomal agents.

## Materials and Methods

### Sample Preparation

The oligonucleotides d[$AG_3(T_2AG_3)_3$], d($AG_3TG_4AG_3TG_4A$), d(GCGAATTCGC), d(TAGGGUTAGGGT), and d(TAGGGUUAGGGT) were purchased with HPLC purification from Midland Certified Reagent Company. The oligonucleotide d($A^{Br}GGTTA^{Br}GGTTAGGGTTA^{Br}GG$) was purchased with HPLC

purification from IDT. The oligonucleotides d(TAATACGACTCACTATAGCAATTGCGTG), and d[TCCAACTATGTATAC(TTAGGG)$_4$TTAGCGGCACGCAATTGCTATAGTGAGTCGTATTA], were purchased from Biosearch Technologies. The G-quadruplex DNA samples were dissolved in buffer to the desired concentrations, heated to 85 $^0$C and cooled slowly to insure the folding of the quadruplexes prior to each experiment. The concentration of each DNA sample was determined spectrophotometrically at 260 nm using the nearest neighbor extinction coefficient at 80°C and extrapolated to 20°C. pUC19 plasmid DNA was purchased from Sigma. Stock solutions containing 1 mM each of DB 832 and Se2SAP were prepared in double distilled water and diluted to working concentrations immediately before use with buffer. The synthesis of DB 832 will be described elsewhere. The synthesis of Se2SAP has been previously described [10].

**Absorbance and CD Measurements**

Absorbance and CD measurements were performed at 20°C in a 10 mM HEPES buffer (pH 7.4) containing 3 mM EDTA and 50 mM KCl or NaCl. For CD measurements obtained in the presence of 50 mM LiCl or in the absence of added salt, a 10 mM TRIS buffer containing 3 mM EDTA acid and pH adjusted to 7.4 using TRIS was used. CD spectra were recorded using a Jasco J-810 spectrapolarimeter in a 1-cm cell using an instrument scanning speed of 50 nm/min with a response time of 1 s. The spectra were averaged over four scans. Absorbance spectra were obtained on a Cary Varian 300 BIO UV-visible spectrophotometer in a quartz cell with a 1 cm pathlength. Appropriate amounts of stock solution of DB 832 or DNA were added sequentially to increase the molar ratio. A buffer baseline scan was collected in the same cuvette and subtracted from

the average scan for each absorbance and CD experiment. In the case of reverse absorbance titration, a second cuvette containing buffer was titrated with DB 832 in the absence of DNA. The absorbance spectrum of the free DB 832 was subtracted from the spectrum of the DB 832-DNA complex at each concentration. Data manipulation and plotting was performed using the program Kaleidagraph version 3.6.

**Isothermal Titration Calorimetry**

ITC experiments were performed with a MicroCal VP-ITC (MicroCal Inc., Northampton, MA, USA). HEPES buffer containing 10 mM HEPES, 3 mM EDTA, and 50 mM KCl and pH adjusted to 7.4 was used for the ITC experiments. The compound was injected into the DNA in the sample cell in 5 μL increments. The observed heat for each injection was determined by integration of the injection peak areas with respect with time. Blank titrations were conducted by injecting the compound into the sample cell containing only buffer under the same conditions. The corrected interaction heat was determined by subtracting the blank heat from that for the compound/DNA titration. Number of binding sites was determined by fitting with Origin.

**Nuclear Magnetic Resonance Studies**

DNA samples were prepared in phosphate buffer containing 50 mM KCl, 10 mM $K_2HPO_4$, 0.1 mM EDTA and 0.01 mM DSS as an internal reference. Quadruplex DNA concentration for the U6 and U6U7 sequences were 0.1mM for 1D experiments and 0.5mM for 2D experiments in 90% $H_2O$:10% $D_2O$ (Cambridge Isotope Laboratories, Inc.) The final DNA samples were adjusted to pH 7.0 using 1M HCl or 1M KOH solutions and were heated past their transition temperature and annealed to room temperature for several hours before collecting the spectra. Experiments on U6 and

U6U7 sequences were performed on Bruker AMX-600 and Varian Unity600 spectrometers respectively. DB832 was titrated with quadruplex DNA with DB832:DNA ratios varying from 0.5 to 2. Temperature dependent 1D spectra were recorded from 15°C to 50°C using jump-return [11] and WATERGATE [12] methods for solvent suppression; whereas homonuclear TOCSY [13, 14] on U6U7 was performed at 35°C using WATERGATE solvent suppression method with a mixing time of 60ms. All NMR data were processed and analyzed with the programs XWINNMR (Bruker Instruments), VNMR (Varian Inc.) and SPARKY [15].

**Taq Polymerase Stop Assay**

The DNA primer P28 was 5'-end-labeled with [$\gamma$-$^{32}$P] ATP according to manufacturer's protocol (New England Biolabs, Ipswich, MA) and purified with a Bio-Spin 6 chromatography column (Bio-Rad, Hercules, CA) to remove free $\gamma$-$^{32}$P. The 5'-end-labeled primer P28 (100 nM) and the human telomeric template DNA (100 nM) were annealed in the annealing buffer (50μM Tris-HCl, 10μM NaCl, pH7.5) by heating at 95°C and slowly cooling down to room temperature. The primer-annealed DNA template was purified using electrophoresis on a 12% native polyacrylamide gel. The purified primer-template DNA was counted and 5000 counts/min of DNA was used in a primer extension assay. In the primer extension assay, 5000 counts/min of DNA was mixed with 2μl of 10x reaction buffer (provided with the Klenow fragment, Hanover, MD), 1μl of 10mM dNTP, 2μl of 1M KCl (to a final concentration of 100mM in 20μl total volume) and different concentrations of compounds (DB 832 and Se2SAP). The reaction mixtures were incubated at room temperature for 30 min, and then Klenow fragment was added to each sample. All samples were incubated at 37°C for 30min, and were stopped by adding

same volume of stop buffer (10mM EDTA, 0.1% xylene cyanole, 0.1% bromophenol blue in formamide solution). The samples were resolved on a 16% denaturing polyacrylamide gel.

**pUC19 Photocleavage**

Individual reactions contained 38 μM bp pUC19 plasmid DNA in the presence or absence of 10μM DB 832. The buffer concentration for each reaction was 20 mM in a total volume of 20 μL. Reactions were kept in the dark or were irradiated at 419 nm for 50 min at 22 °C in 1.7 mL microcentrifuge tubes with eight fluorescent lamps located 6 cm above the opened tubes. Aerobic ventilation was achieved by placing a table fan directly adjacent to the lamps. Half the samples were treated with 0.3% piperdine at 65°C for 30 minutes, and half left untreated as a control. Cleavage products were electrophoresed on a 1.0% nondenaturing agarose gel stained with ethidium bromide (0.5 μg/mL). The gel was then visualized on a transilluminator set at 302 nm, photographed, and scanned.

**Quadruplex Photocleavage**

The DNA was 5'-labeled with $^{32}P$ and stored in buffer (10 mM Tris-HCl, 1 mM EDTA, pH 8.0) at 3000 cpm/μl. For each photocleavage reaction, 10 μl of DNA (~5 ng) was mixed with 10 μl of 100 mM KCl, boiled for 10 minutes and cooled to room temperature. The DNAs used were a 74-mer human telomeric sequence, and a 77-mer c-MYC G-quadruplex sequence. For the control experiments, 10 μl of distilled water was added instead of the KCl solution. The mixtures were transferred to a 96 well plate and varying amounts of DB 832 or telomestatin stock solution were added. The samples were then exposed to a 24 W fluorescent lamp under a glass filter. The reactions were stopped

with 100 µl of calf thymus DNA (0.1 µg/µl) and after phenol-choloroform extraction, the samples were subjected to piperdine to induce strand breakage and then precipitated with ethanol. The DNA samples were separated using electrophoresis on a 12% polyacrylamide gel and visualized using a phosphorimager.

**Fluorescence Measurements**

A Fluorescence energy transfer experiment was performed using a Cary Eclipse fluorescence spectrometer. All measurements were conducted at 20°C in a 10 mM HEPES buffer (pH 7.4) containing 3 mM EDTA and 50 mM KCl. A quartz cell with a 1.0 cm pathlength was used. The emission wavelength was set to 469 nm with an excitation slit width of 5 nm. The excitation spectrum was scanned from 230 to 330 nm for DB 832 alone and in the presence of $d[AG_3(T_2AG_3)_3]$. The DB 832 concentration was 0.3 µM and the DNA concentration was 8 µM.

**TRAP Assay**

A TRAP (Telomeric Repeat Amplification Protocol) assay was performed using a TRAPese Telomerase Dectection Kit S7700 (Chemicon International). The resulting products were run on a 12% non-denaturing polyacrylamide gel in 0.5x TBE buffer and visualized with a phosphorimager.

**Results and Discussion**

**DB 832 Binds to the Human Telomere as a Stacked Species**

Achiral molecules, such as DB 832, exhibit no CD signal in solution. However, when an achiral ligand binds tightly to a chiral host, such as DNA, a CD signal is generally induced in the wavelength region corresponding to the absorbance of the ligand [16]. Figure 3.1 shows the CD spectra of the human telomeric sequence titrated with DB

832 in the presence of $K^+$. The spectra show an induced CD signal, which indicates that DB 832 is binding to the DNA. As compound is added to DNA the induced signal exhibits exciton-type splitting with a positive band centered at 432 nm, a negative band centered at 416 nm, and an isoelliptic point at 424 nm, which is also the absorbance maximum of the dye when bound to DNA. An additional negative band centered at 395 nm overlaps with the higher energy exciton band. The exciton band indicates that DB 832 is binding to the DNA as a stacked species, likely located in a quadruplex groove.

The addition of DB 832 to the human telomeric DNA model sequence also affects the CD signal in the wavelength region of DNA absorbance (Figure 3.2). The interpretation of CD spectra is based heavily on pattern recognition. Many parallel-type quadruplexes, for example, have a characteristic strong positive CD band at 264 nm and a negative band at 240 nm, whereas antiparallel quadruplexes usually have a positive band between 290 and 295 nm and a negative band at 260-265 nm [17]. Upon addition of DB 832, a peak appears around 265 nm, which is characteristic of parallel quadruplexes. The presence of a residual peak at 295 nm suggests the presence of an antiparallel structure. This data suggests that DB 832 either induces the formation of a mixed parallel/antiparallel hybrid quadruplex, or binds to a mixture of quadruplex conformations.

An absorbance titration was performed to monitor changes in the spectral properties of DB 832 when bound to human telomeric DNA (Figure 3.3). Prior to addition of the DNA, the absorbance peak of the DB 832 monomer appears at 370 nm. As the DNA is added, this monomer peak decreases in intensity and a new peak is formed at around 425 nm, corresponding to the formation of the stacked species. This

bathochromic shift is indicative of the formation of a J-aggregate. In a J-aggregate, the transition dipole moments of the two chromophores within a dimer are oriented with a translational offset. Electronic transitions to the lowest exciton state are allowed, resulting in the red shift of the absorbance maximum [18, 19]. In the case of DB 832, the offset of this dimer structure allows the terminal positively-charged amidines to have a larger distance between the amidines on the adjacent molecule decreasing the electronic repulsion that would exist in an H-aggregate (non-offset) structure. The titration spectra also reveal an isosbestic point at 395 nm, indicative of a two-state transition. This suggests that the DB 832 is binding to the DNA with a discrete binding mode.

An absorbance titration in which compound is titrated into the DNA was performed in order to further characterize the spectral properties of DB 832 upon binding to the telomeric DNA (Figure 3.4). Since the absorbance of free DB 832 is subtracted from the absorbance of the DB 832-DNA complex, the resulting signal can be positive or negative. The reverse titration also confirms that DB 832 binds to the human telomere with a discrete binding mode.

In order to determine if DB 832 stacks in solution, or whether the stacking is DNA-mediated, the extinction coefficient of DB 832 was calculated in both buffer as well as ethanol (Figure 3.5) by calculating the slope of the absorbance versus concentration for each plot. The molar extinction of DB 832 was found to be $4.7 \times 10^4$ $M^{-1}cm^{-1}$ in buffer and $5.9 \times 10^4$ $M^{-1}cm^{-1}$ in ethanol at 371 nm. In both cases, the extinction curve was linear over a wide concentration range, suggesting that no aggregation is occurring in solution as the concentration is increased. The difference between the two extinction coefficients is also not significant enough relative to experimental error to

suggest that the DB 832 molecules are aggregating in solution. DODC is a well-studied cyanine dye that has been previously shown to stack in solution [20, 21]. The observed extinction coefficient for DODC monitored at 582 nm is 2.7 x $10^5$ $M^{-1}cm^{-1}$ in ethanol and 5.7 x $10^4$ $M^{-1}cm^{-1}$ in buffer, illustrating the dramatic effect that stacking in solution can have on the extinction coefficient. The absence of observed DB 832 stacking in solution is supported by the fact that the molecule is dicationic, and therefore unlikely to stack in solution in the absence of a template due to repulsion from the positively charged amidine groups. The single charge on each DODC molecule is delocalized, and thus electrostatic repulsion between the molecules is much smaller than with DB 832.

**DB 832 Binds to the Human Telomere Cooperatively with High Stoichiometry**

Titration curves can be obtained from the spectroscopic titration data by plotting signal as a function of compound concentration for a given wavelength. Figures 3.6 and 3.7 show titration curves for DB 832 with the human telomeric sequence d[$AG_3(T_2AG_3)_3$] using data obtained from the circular dichroism titration and the absorbance titration with DB 832 titrated into the DNA, respectively. Due to the high stoichiometry of the system, it is difficult to mathematically fit the data in order to obtain the exact stoichiometry or binding constants. However, a rudimentary fit of both curves reveals that there are approximately 12 molecules of DB 832 bound per quadruplex strand. Both curves are sigmoidal in shape, indicating that the binding of the DB 832 molecules to this DNA sequence occurs with positive cooperativity, or two modes of binding. However, the absorbance titration data suggests that there is only one mode of binding, so it is likely that the binding of the DB 832 molecules is positively cooperative. A titration curve was also obtained for DB 832 using isothermal titration calorimetry.

Interaction heats for the titration of DB 832 into a DNA solution are shown in Figure 3.8. Plots of the observed net binding heat/mol versus molar ratio were obtained by subtracting the integrated peak areas for the blank titration from the areas in the DNA interaction titration. Due to the high stoichiometry, it was difficult to obtain a precise quantitative fit to the data using the Origin software. The best fit to the data arose from using a stoichiometry of n=10. This is in agreement with the high stoichiometry obtained from the CD and absorbance binding plots.

The high stoichiometry suggests that DB 832 may actually be binding as a trimer, rather than a dimer. Since each quadruplex contains four grooves, one trimer located in each groove would produce a stoichiometry of 12, in agreement with our experimental results. A distinct break point occurs in all three binding curves at n=4. In the case of the CD titration spectra, no exciton splitting occurs until after four equivalents are present. Experiments by Armitage and coworkers have shown that for some cyanine compounds, exciton splitting does not occur between monomers within a single dimer, but is due to end-to-end interactions between the molecules [22, 23]. The exciton splitting that arises from end-to-end interactions has also been shown to produce CD signals of large magnitude [22] , in agreement with the large signals obtained for DB 832. This further suggests that DB 832 may be binding as a series of trimers.

Some compounds, such as porphyrins, can aggregate onto the surface of quadruplex DNA, resulting in artificially high observed stoichiometries. The fact that each of the DB 832 binding curves distinctly levels off suggests that the high stoichiometry is not due to non-specific surface interactions. The isosbestic points observed in the absorbance titration and reverse absorbance titration further suggest that

the binding of DB 832 to the telomeric DNA is indeed a discrete binding mode, and not surface aggregation.

**Effect of Salt on DB 832 Binding**

The CD spectrum for the human telomeric sequence has previously been shown to differ in the presence of sodium ions versus potassium ions [24]. This suggests that this DNA sequence exhibits a different conformation in the presence of each of these counterions. Differing NMR and crystal structures which were obtained in the presence of sodium ions and potassium ions, respectively, support this idea. The NMR structure of $d[AG_3(T_2AG_3)_3]$ in the presence of potassium ions is an antiparallel basket-like structure [25]. The crystal structure of this sequence obtained in the presence of sodium ions consists of a parallel, propeller-like structure [26]. Other structures have been proposed to exist in solution in the presence of potassium, including a mixed parallel/antiparallel hybrid [27-30]. Lithium has been shown to have a destabilizing effect on quadruplex structure [31]. To investigate the effect of DNA structure on the binding of DB 832, CD titrations were performed with human telomeric DNA under different salt conditions to determine if DB 832 would bind as a stacked species to different conformations of this DNA sequence. Figure 3.9 shows the CD spectra for $d[AG_3(T_2AG_3)_3]$ titrated with DB 832 in the presence of 50 mM sodium, and 50 mM lithium, respectively. Regardless of the cation present, upon addition of DB 832 exciton splitting occurs in the induced wavelength region of the CD spectra. Figure 3.10 shows the DNA region for the spectra in Figure 3.9. Peaks occur in the DNA region at 265 and 295 nm, in the presence of sodium or lithium, as is the case when potassium is present. This suggests that regardless

of the starting conformation of the DNA, DB 832 induces the formation of a specific conformation of DNA to form an optimum binding site for the DB 832 stacked species.

It is generally believed that salt is required to facilitate the formation of quadruplex structures from G-rich DNA [32]. The cations act to neutralize charge repulsion between the four negatively charged DNA strands as well as stabilize the quartets by coordinating with the carbonyl oxygen atoms from the guanines. Only telomestatin has previously been shown to induce quadruplex formation in human telomeric DNA in the absence of added salt [30, 33]. Figure 3.11 shows the DNA region of the CD spectra of the human telomeric DNA titrated with DB 832 in the absence of added salt. Peaks appear around 265 and 295 nm, resulting in the same CD pattern that the DNA produces when titrated by DB 832 in the presence of $K^+$, $Na^+$ or $Li^+$, suggesting that the compound induces the same quadruplex conformation that is formed in the presence of these cations. In addition to a change in the CD spectra in the DNA region, DB 832 produces an induced CD signal when titrated into the DNA in the absence of salt. This confirms that the compound is binding to the DNA. However, the absence of exciton splitting indicates that the compound is binding as a monomer and not a stacked species under these conditions. Since DB 832 is a dication, it is reasonable to assume that stacking of the compound is not energetically favorable in the absence of salt due to charge repulsion from the amidine groups. The absorbance titration of DB 832 into human telomeric DNA exhibits a different spectral pattern in the absence of salt (Figure 3.12) than in the presence of salt, further suggesting a different binding mode.

**DB 832 Induces the Formation of a Single Quadruplex Structure**

To determine whether DB 832 is inducing the formation of a mixed parallel/antiparallel hybrid quadruplex structure or binding to a mixture of DNA conformations, 1-D NMR studies were performed by Rupesh Nanjunda using a modified human telomeric sequence previously described by Patel et al [34]. The sequence, d(TAGGGUTAGGGT), has been shown to exist in solution as a mixture of both parallel (major species) and antiparallel (minor species) dimeric hairpin quadruplexes. This sequence is suitable as a model system for studying interactions with DB 832, since the CD spectra of DB 832 titrated into this DNA exhibits the same patterns in both the induced wavelength region as well as the DNA region as with the intramolecular sequence $d[AG_3(T_2AG_3)_3]$ (Figure 3.13). The imino proton spectra of DB 832 titrated into d(TAGGGUTAGGGT) are shown in Figure 3.14. As the molar ratio of DB 832 is increased, the NMR peaks become fewer and sharper, suggesting that the compound is binding to a single DNA conformation, and not a mixture of species. Another substitution was made to the U6 sequence at T7 position (T7-->U7) to determine if DB832 has similar effects on this sequence. CD and NMR results have shown that this sequence, d(TAGGGUUAGGGT), also exists as a mixture of both parallel and antiparallel dimeric hairpin quadruplex in solution (Figure 3.13). The CD and imino region spectra of U6U7 with DB832 exhibited similar patterns as in U6 sequence suggesting that DB832 is selectively binding to a single conformation from a mixture of species (Figure 3.14). This is further supported by the TOCSY spectra of uracil region of free U6U7 sequence and with DB832 at 2:1 ratio (Figure 3.15). The four peaks correspond to the two uracil protons from the mixture of parallel and antiparallel conformation. In the absence of

DB832, all the peaks are of similar intensity indicating the heterogeneity of the sequence. After titrating with DB832, there is a significant decrease in the intensity of peaks at 7.70 and 7.52 ppm indicating that the compound is favorably binding to a particular conformation from the mixture.

**DB 832 Binds to the Same Human Telomere Hybrid Quadruplex as Se2SAP**

Diseleno Sapphyrin (Se2SAP) is a modified porphyrin compound which has been previously shown to bind via end-stacking to a mixed parallel/antiparallel hybrid conformation of intramolecular human telomeric quadruplex DNA [30]. To determine whether DB 832 and Se2SAP bind to the same quadruplex conformation of the human telomere, a *Taq* polymerase stop assay was performed by Laurence Hurley's group at the University of Arizona. In a polymerase stop assay, G-quadruplex structures block primer extension by DNA polymerase, resulting in shortened DNA fragments known as stop products. The presence of stop products as determined by gel electrophoresis indicates quadruplex stabilization by the compound. The assay was performed for human telomeric DNA with DB 832, Se2SAP, and DB 832 and Se2SAP in combination. The assay shows that DB 832 interacts with and stabilizes the G-quadruplex in the human telomeric sequence in a dose-dependent manner (Figure 3.16, lanes 7-11). Figure 3.17 shows the normalized fold increase in stop product versus compound concentration for this set of compounds. The graph shows that DB 832 and Se2SAP have an additive effect on quadruplex stabilization. This indicates that these two compounds are not competing for binding sites or competing to trap out or induce different quadruplex conformations. This suggests that DB 832 binds to the same hybrid quadruplex conformation as Se2SAP, which is consistent with the CD and NMR results which show that DB 832 induces the

formation of a single conformation, which has both parallel and antiparallel characteristics. Furthermore, the absence of any major stop products at the primer site indicates that DB 832 does not bind duplex DNA (the primer and template heterodimer) at concentrations even as high as 25 μM (data not shown) which supports the premise that DB 832 selectively binds to quadruplex DNA. A CD competition titration of DB 832 titrated into human telomeric DNA in the presence of Se2SAP is shown in Figure 3.18. The large magnitude of exciton splitting confirms that DB 832 and Se2SAP are not in competition for conformation or binding site.

**DB 832 Binds in the Grooves of Telomeric Quadruplex DNA**

Photoactive molecules can catalyze the oxidation of DNA upon exposure to light, causing strand breakage in the vicinity of their binding sites. Photocleavage of DNA has been used as an assay to determine the location of binding sites for photoactive molecules such as porphyrins [35-39]. In order to determine if DB 832 is photoactive, and therefore suitable for study using photocleavage experiments, its photoactivity was first assessed using pUC19 plasmid DNA (Figure 3.19). When the supercoiled circular pUC19 DNA is cleaved by a photoactive molecule, it becomes linear and travels slower on an electrophoretic gel. In the presence of light and treatment with piperdine, DB 832 cleaves the DNA in a dose-dependent manner. By 50 μM, no DNA bands appear on the gel, suggesting that the DNA is completely degraded by that point. In the presence of light, but absence of piperdine treatment, DB 832 still cleaves the DNA, but to a lesser extent. The DNA band disappears by 100 μM DB 832 concentration. The experiments were also conducted in the absence of light, as a control, as shown in the right side of Figure 3.19.

Since the pUC19 experiment shows that DB 832 is highly photoactive, a photocleavage assay with quadruplex DNA was performed by the Hurley group at the University of Arizona (Figure 3.20). In the presence of KCl, DB 832 cleaves the human telomeric sequence in a dose-dependent manner specifically at each run of guanines, which suggests that DB 832 binds in the grooves of this quadruplex sequence. As a control, the experiment was also performed in the absence of salt. Since quadruplex DNA sequences generally require salt to fold, any cleavage in the absence of salt is normally attributed to free compound in solution. In the absence of salt, DB 832 exhibits the same cleavage pattern as in the presence of salt. However, since DB 832 is capable of inducing quadruplex formation in the absence of salt, it is probable that this cleavage is due to actual binding and not from free DB 832 in solution. This is supported by the photocleavage results when the c-MYC sequence is treated with DB 832. In the presence of salt, DB 832 only cleaves at specific guanines, instead of all guanines, suggesting that free DB 832 in solution does not indiscriminantly cleave all guanines. This cleavage pattern also suggests that DB 832 is likely binding to the c-MYC sequence through an end-stacking interaction. The CD spectra of DB 832 with c-MYC (to be presented in Chapter 4) indeed does not show any induced signal, supporting the photocleavage results that suggest that DB 832 does not bind in the grooves of c-MYC, and therefore must be end-stacking. The photocleavage of the DNA sequences was also monitored in the presence of telomestatin. In the presence of KCl and telomestatin, DB 832 does not appear to cleave the telomeric DNA, which indicates that it is not binding under these conditions. Telomestatin has been shown to bind very strongly to a basket quadruplex structure in the human telomeric sequence in the presence of potassium ions [40]. Since

DB 832 has been shown to bind to a mixed parallel/antiparallel structure and not the antiparallel basket-type structure, it is therefore expected that DB 832 would not bind under these conditions. However, in the absence of KCl, DB 832 does cleave the telomeric DNA at every guanine. Like DB 832, telomestatin can also induce quadruplex formation in the absence of salt [30, 33]. Since telomestatin is an uncharged molecule, while DB 832 is a dication, it is likely in the absence of salt that DB 832 has a stronger binding affinity to the negatively charged DNA than telomestatin does because of the favorable electrostatic interactions that are shielded in the presence of salt.

Fluorescence energy transfer between the bases of the quadruplex DNA and the bound compound can also be used to provide evidence of the binding site location. When a compound stacks on the quadruplex ends or intercalates between tetrads, energy transfer from the DNA bases to the bound compound can occur. The fluorescence energy transfer between bound DB 832 and the human telomeric DNA was assessed by setting the emission wavelength to 469 nm (the emission $\lambda_{max}$ for bound DB 832) and scanning the excitation spectrum of DB 832 in the presence and absence of DNA (Figure 3.21). In the case of intercalation or end-stacking, a peak would appear at 260 nm in the excitation spectrum due to the absorbance of the DNA, indicating that energy transfer is occurring. However, when DNA is added to DB 832, the fluorescence decreases across all wavelengths, and a peak at 260 nm does not appear. This suggests that the DB 832 molecules are located in the quadruplex grooves, at an orientation which prevents energy transfer from the DNA.

The oligonucleotide d($A^{Br}$GGTTA$^{Br}$GGTTAGGGTTA$^{Br}$GG) is a modified human telomeric sequence in which three of the guanines have been substituted with the

modified nucleobase 8-bromoguanine, which blocks the quadruplex grooves. Substitution with 8-bromoguanine also causes the glycosidic conformation of the sugar associated with that base to adopt the *syn* conformation [41]. By selectively modulating the glycosidic orientations within the DNA sequence, the overall fold of the quadruplex can be controlled. Sugyiama and coworkers recently showed that the modified d($A^{Br}$GGTTA$^{Br}$GGTTAGGGTTA$^{Br}$GG) folds in a mixed parallel/antiparallel hybrid conformation, which is likely the structure the unmodified human telomere adopts in solution in the presence of $K^+$ [42]. NMR data from Yang and coworkers showed that a different modified human telomeric structure also forms this same hybrid quadruplex structure [43], further suggesting that this structure is the one adopted by the human telomere in potassium, and thus the one that DB 832 binds to as a stacked species. The CD spectra of DB 832 titrated into this sequence is shown in Figure 3.22. The spectra show a positive band centered at 371 nm, and a small negative band centered at 419 nm. These bands likely are not due to exciton splitting, but are rather two separate bands. When DB 832 binds to the quadruplex as a stacked species, the negative band is the higher energy band and the positive band is the lower energy band. The two peaks are shifted an equal number of nanometers from the crossover point, which is also the maximum wavelength of DB 832 when it is bound to the human telomere. In the case of this modified DNA, the positive band is at higher energy and the negative band is at lower energy. If this were an exciton signal, it would suggest that the compound (and hence the DNA) was oriented with an opposite-handed helicity than when DB 832 is bound to the unmodified sequence. Since we know that both DNAs have the same structure, it makes exciton splitting in this case unlikely. The peak of the positive band

also occurs 21 nm from the apparent crossover point, while the negative peak is located 27 nm from the crossover point. The small magnitude of these bands suggests that this difference is not due to overlapping bands. The crossover point for this sequence occurs at 392 nm, which is not the maximum absorbance wavelength of DB 832 bound as a stacked species to the human telomere. Also, DB 832 does not exhibit a wavelength shift with this DNA, which suggests it is not binding as a stacked species. Since DB 832 does not exhibit any exciton splitting with this hybrid quadruplex structure when the grooves are blocked, it provides evidence that the mode of binding of this compound to the human telomere is groove binding as a stacked species.

**DB 832 Inhibits Telomerase**

In order to assess the biological activity of DB 832, a TRAP (Telomerase Repeat Amplification Protocol) assay was performed by the Hurley group at the University of Arizona. The TRAP assay is a PCR-based assay that measures telomerase-mediated primer extension. In the first step of the reaction, telomerase adds telomeric repeats onto the 3' end of a substrate oligonucleotide (TS). The extended products are then amplified with PCR using the TS and reverse (RP) primers. The gel from the TRAP assay is shown in Figure 3.23. The relative densities of the telomeric bands for each concentration of DB 832 were expressed relative to the untreated control. The plot showing the concentration-dependent inhibition of telomerase by DB 832 is shown in Figure 3.24. A fit of this plot reveals the $IC_{50}$ (concentration required for 50% inhibition of the protein) to be 10.8 μM, showing that DB 832 is an effective telomerase inhibitor. In comparison, the carbocyanine dye, DODC, which was also shown to bind the grooves of the human telomere (Chapter 2), does not inhibit telomerase at concentrations less than 50 μM [6].

**Conclusions**

Many DNA-targeted anti-cancer drugs act by intercalating between base pairs of duplex DNA, which causes a disruption in transcription and replication and leads to cell death. These types of small molecules typically exhibit non-selective binding to many sites, leading to the cytotoxic side effects generally associated with chemotherapy. Antiparastic therapeutics in use today also have significant toxicity to the host and can also cause debilitating side-effects. Telomeres and some oncogenes have been shown to form quadruplex structures in vitro, and may serve as structure-specific targets for anticancer as well as antiparastic therapeutics. The unique structural features of quadruplexes offer a way to target DNA in a structure-specific manner, leading to increased selectivity for quadruplex over duplex DNA, as well as selectivity for a particular quadruplex structure over other quadruplexes.

DB 832 is a heterocyclic diamidine that binds to human telomeric DNA as a stacked species. Regardless of the starting conformation of the human telomeric DNA, DB 832 is capable of inducing the formation of a mixed parallel/antiparallel hybrid quadruplex structure, and can even induce formation of this structure in the absence of salt. Nonintercalating, stacked species, such as DB 832, offer unique opportunities for drug design. The monomer units can potentially be covalently linked, resulting in extremely increased affinity and selectivity for their quadruplex targets.

Photocleavage and fluorescence energy transfer experiments suggest that DB 832 is a groove-binding agent in the human telomere. The compound does not have the large planar surface area of well-known end-stacking agents, such as anthraquinones, acridines, porphyrins, perelynes, macrocycles and related molecules. The fact that DB 832 binds to

the human telomere as a stacked complex also makes a groove complex more likely. There is little advantage to multiple stacking on the end of a quadruplex, but stacking in a groove can optimize the fit of cationic heterocycles to DNA. Stacked dimers that bind to duplex DNA grooves are quite well known and can yield exceptionally stable complexes. Structural studies are currently in progress to determine the exact orientation of DB 832 molecules with respect to each other as well to the DNA.

DB 832 may provide a starting point for the design of unique compounds with high affinity and selectivity for human telomeric DNA, leading to improved therapeutics for treating cancer and parasitic infections with decreased side effects.

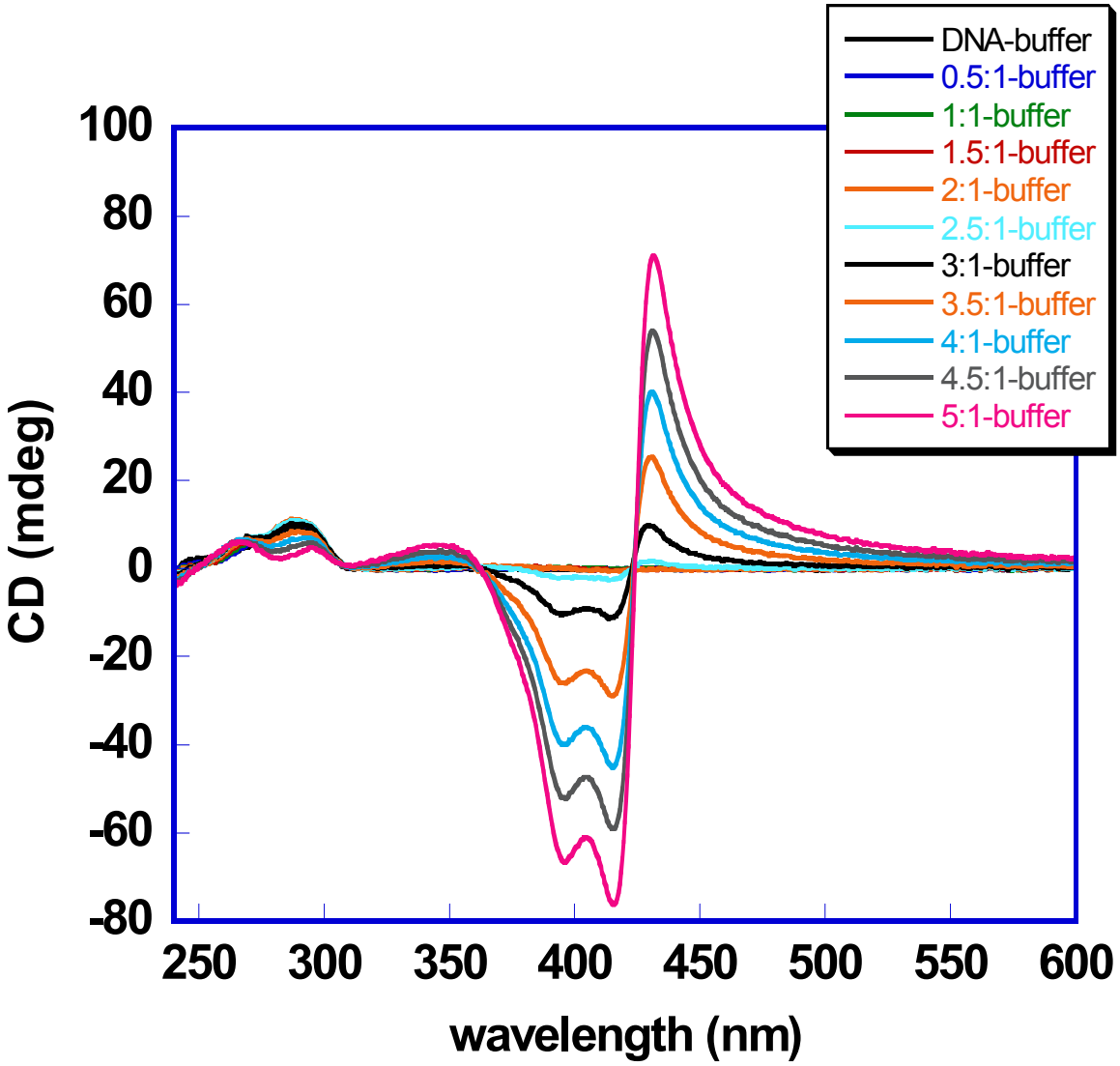


Figure 3.1 CD spectra of DB 832 titrated into 3.0 μM d[$AG_3(T_2AG_3)_3$] in HEPES buffer containing 50 mM KCl. Compound:DNA ratios ranged from 1:1 to 5:1.

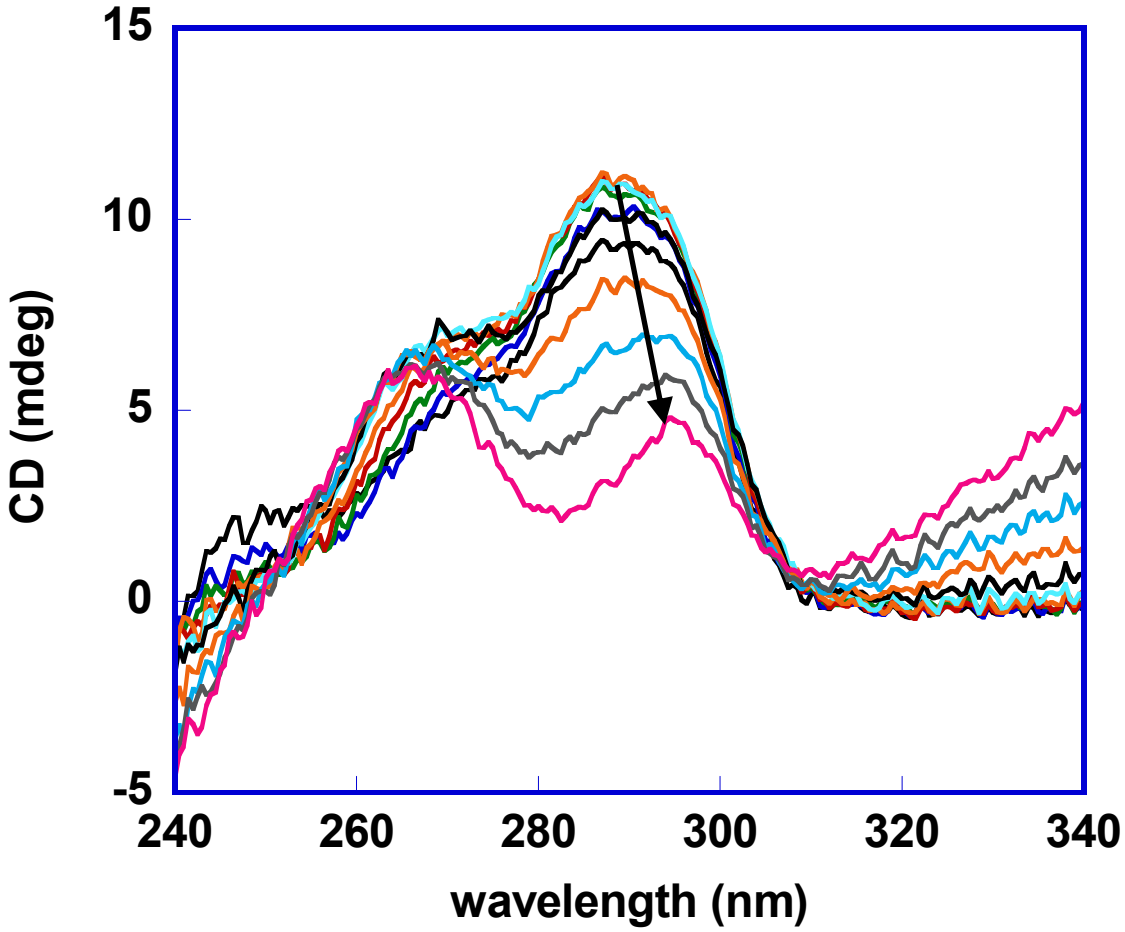


Figure 3.2 Close-up of the wavelength region of DNA absorbance for the spectra shown in Figure 3.1 of of DB 832 titrated into 3.0 μM d[$AG_3(T_2AG_3)_3$] in HEPES buffer containing 50 mM KCl. The arrow indicates increasing DB 832 concentration. Compound:DNA ratios ranged from 1:1 to 5:1.

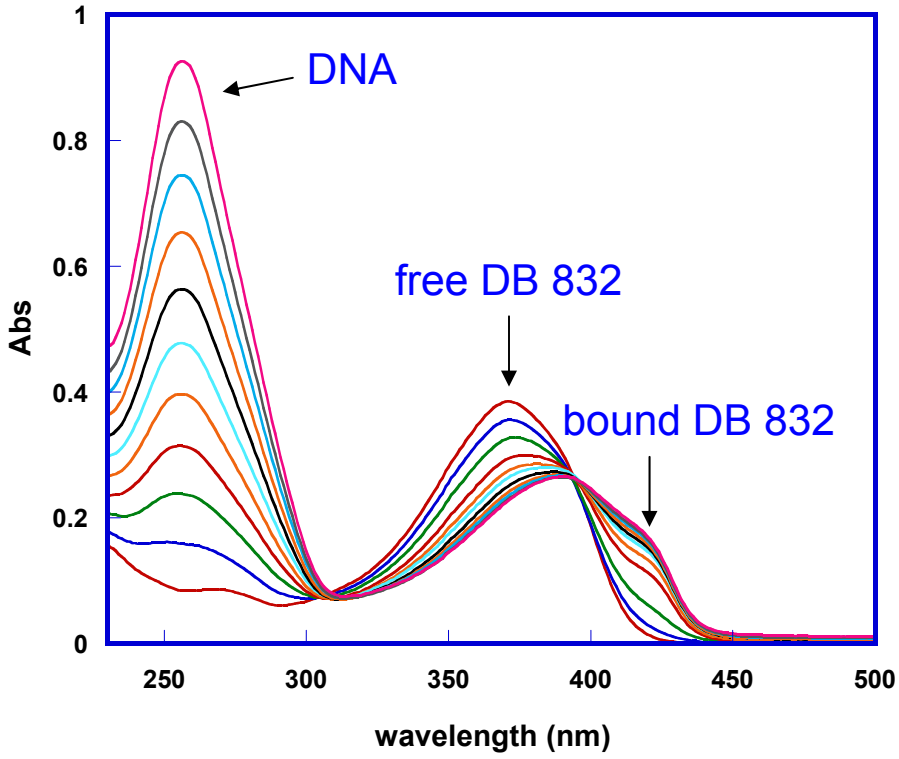


Figure 3.3 Absorbance spectra of d[$AG_3(T_2AG_3)_3$] titrated 8.2 μM DB 832 in a HEPES buffer containing 50 mM KCl, up to a final DNA concentration of 4.4 μM.

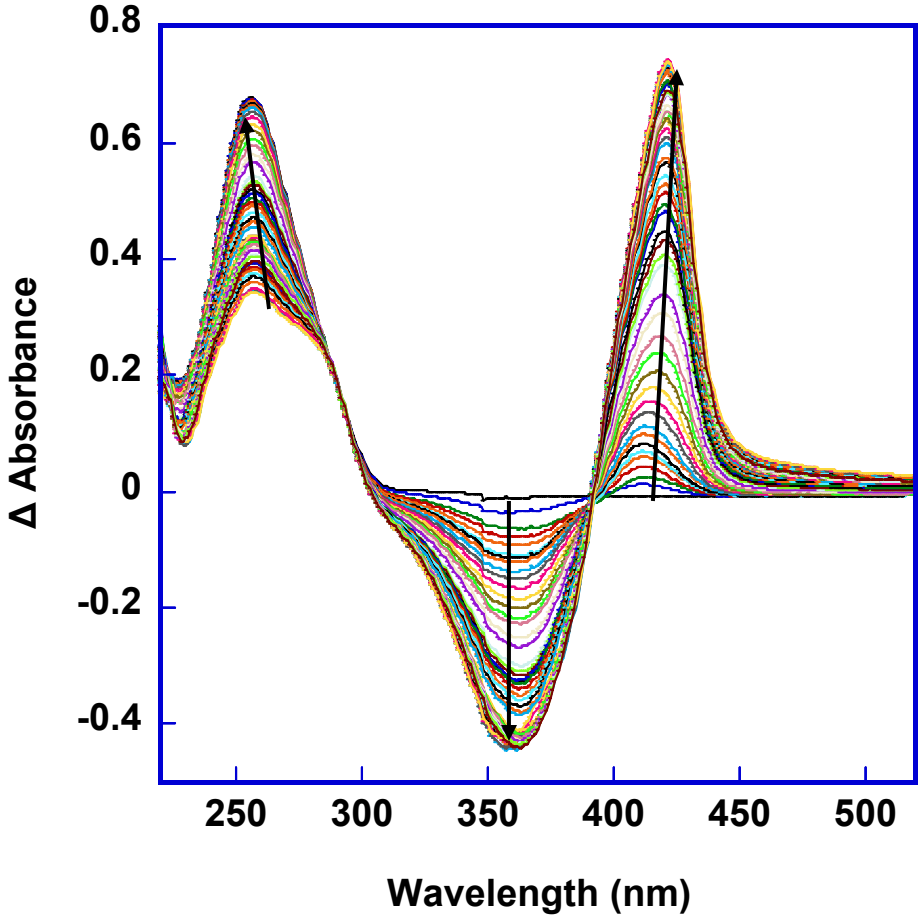


Figure 3.4 Absorbance spectra of DB 832 titrated into 3.8 μM d[$AG_3(T_2AG_3)_3$] in HEPES buffer containing 50 mM KCl up to a final DB 832/DNA ratio of 26:1. The arrows indicates increasing DB 832 concentration

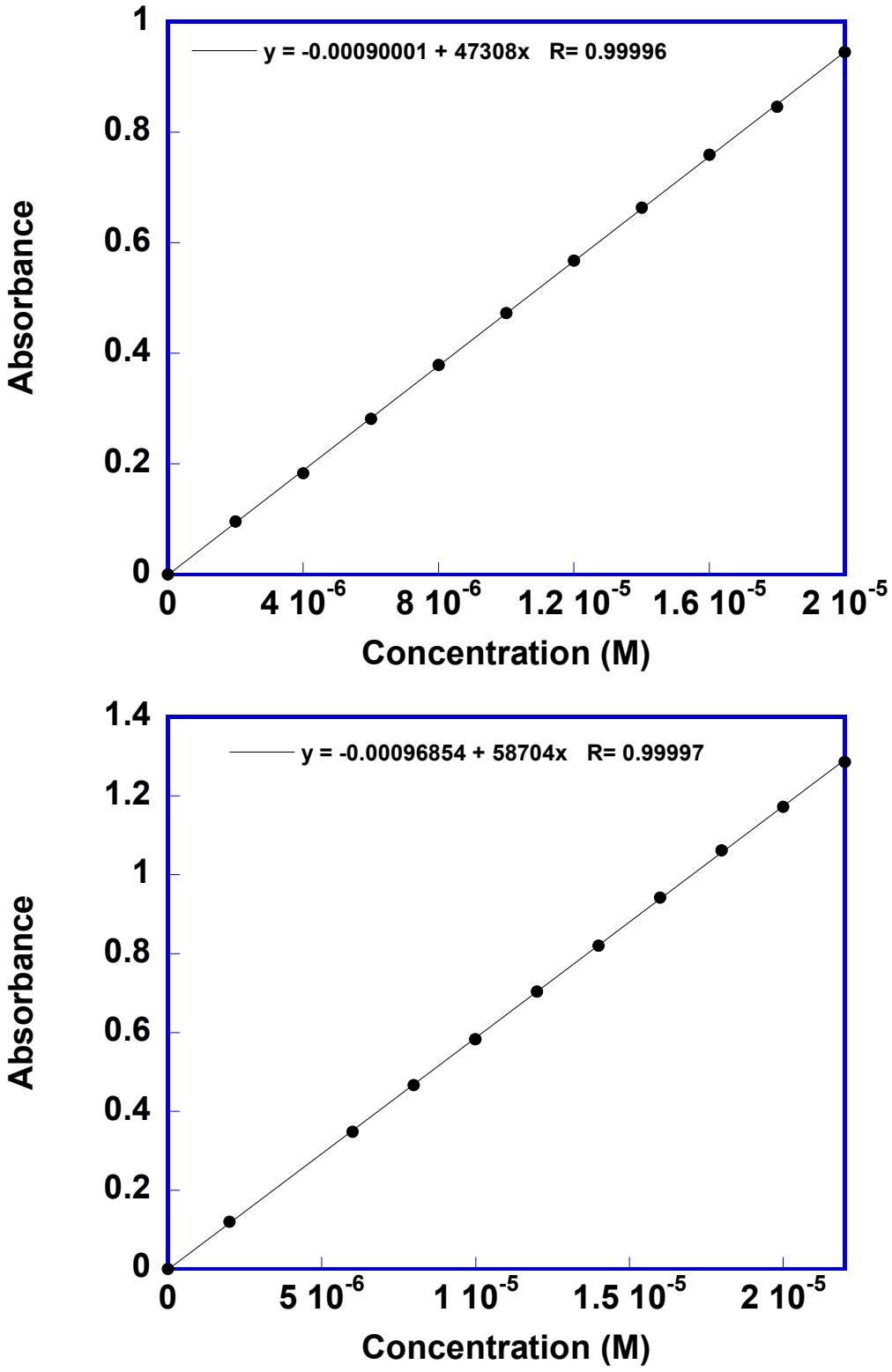


Figure 3.5 Extinction coefficient determination for DB 832 in HEPES buffer containing 50 mM KCl (top) and ethanol (bottom) monitored at 371 nm.

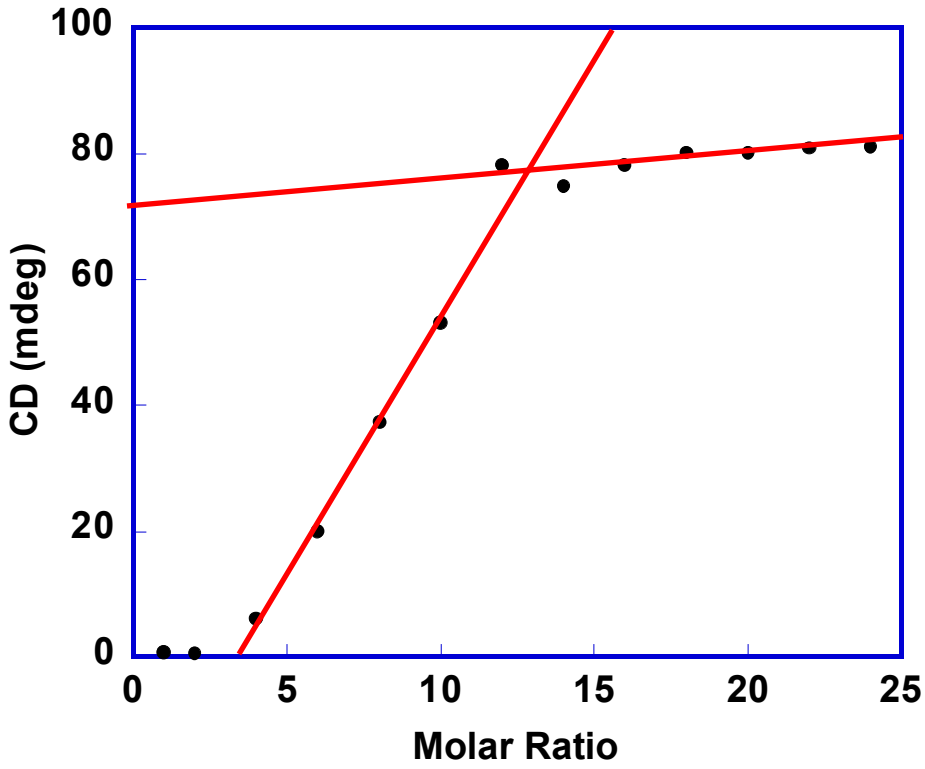


Figure 3.6 Titration curve for DB 832 obtained by plotting CD signal at 431 nm as a function of DB 832 added molar ratio. DB 832 was added to 3.5 μM d[$AG_3(T_2AG_3)_3$] up to a compound/DNA ratio of 24:1, in phosphate buffer containing 70 mM $K^+$.

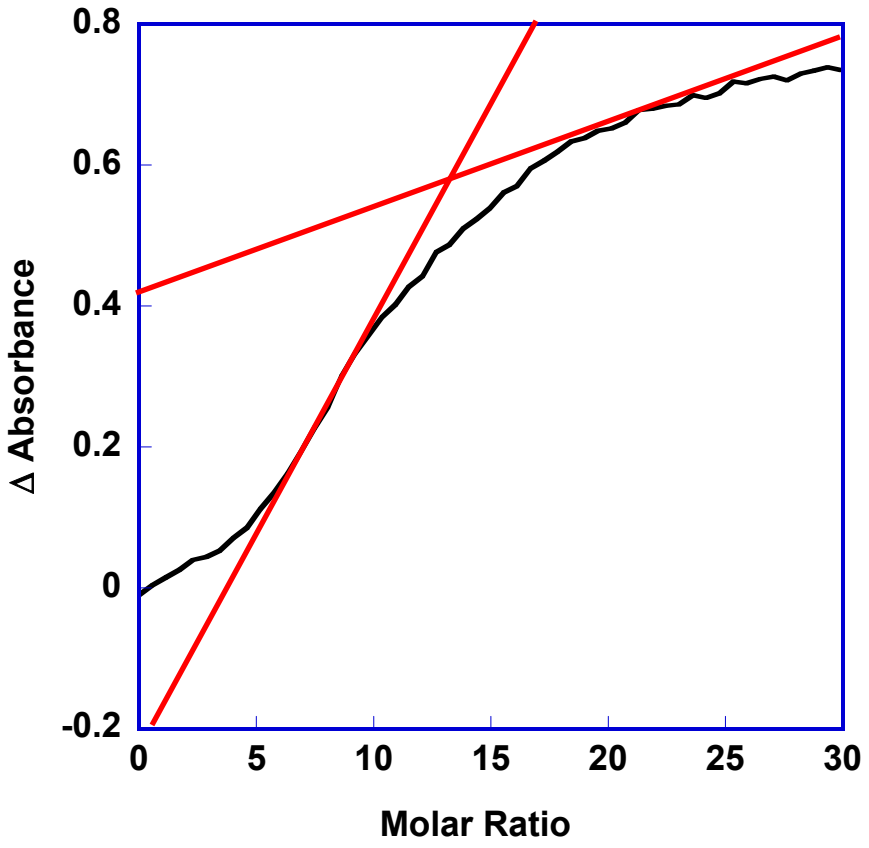


Figure 3.7 Titration curve for DB 832 obtained by plotting ΔA at 422 nm as a function of added DB 832 molar ratio. DB 832 was.titrated into 3.8 μM d[$AG_3(T_2AG_3)_3$] in HEPES buffer containing 50 mM KCl up to a final DB 832/DNA ratio of 26:1.

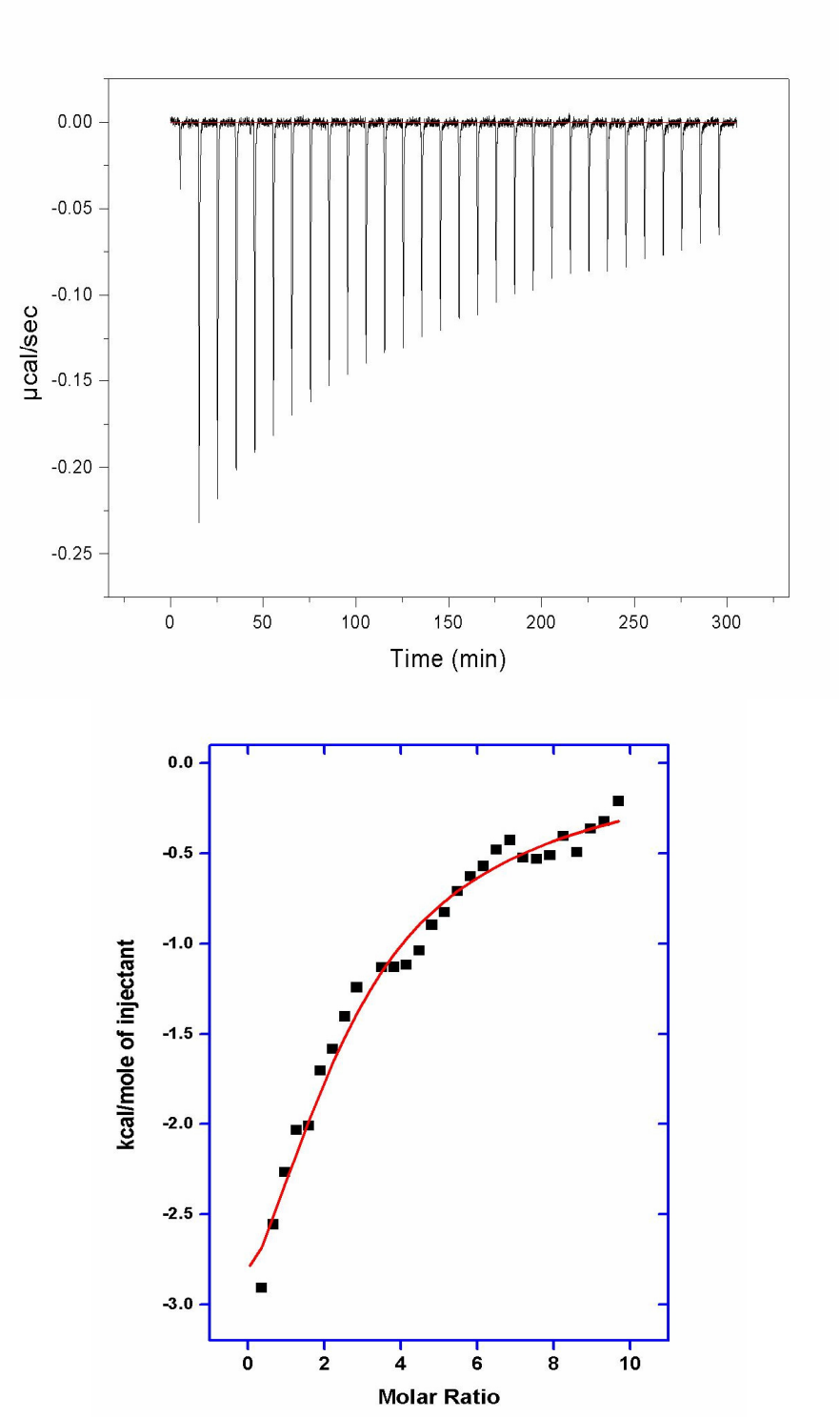


Figure 3.8 Isothermal titration calorimetry plot of DB 832 titrated into a 5 µM d[$AG_3(T_2AG_3)_3$] solution (top) in HEPES buffer containing 50 mM KCl. Plot of heat versus molar ratio (bottom) was obtained by subtracting the integrated peak areas for the blank, buffer titration from the DNA interaction titration.

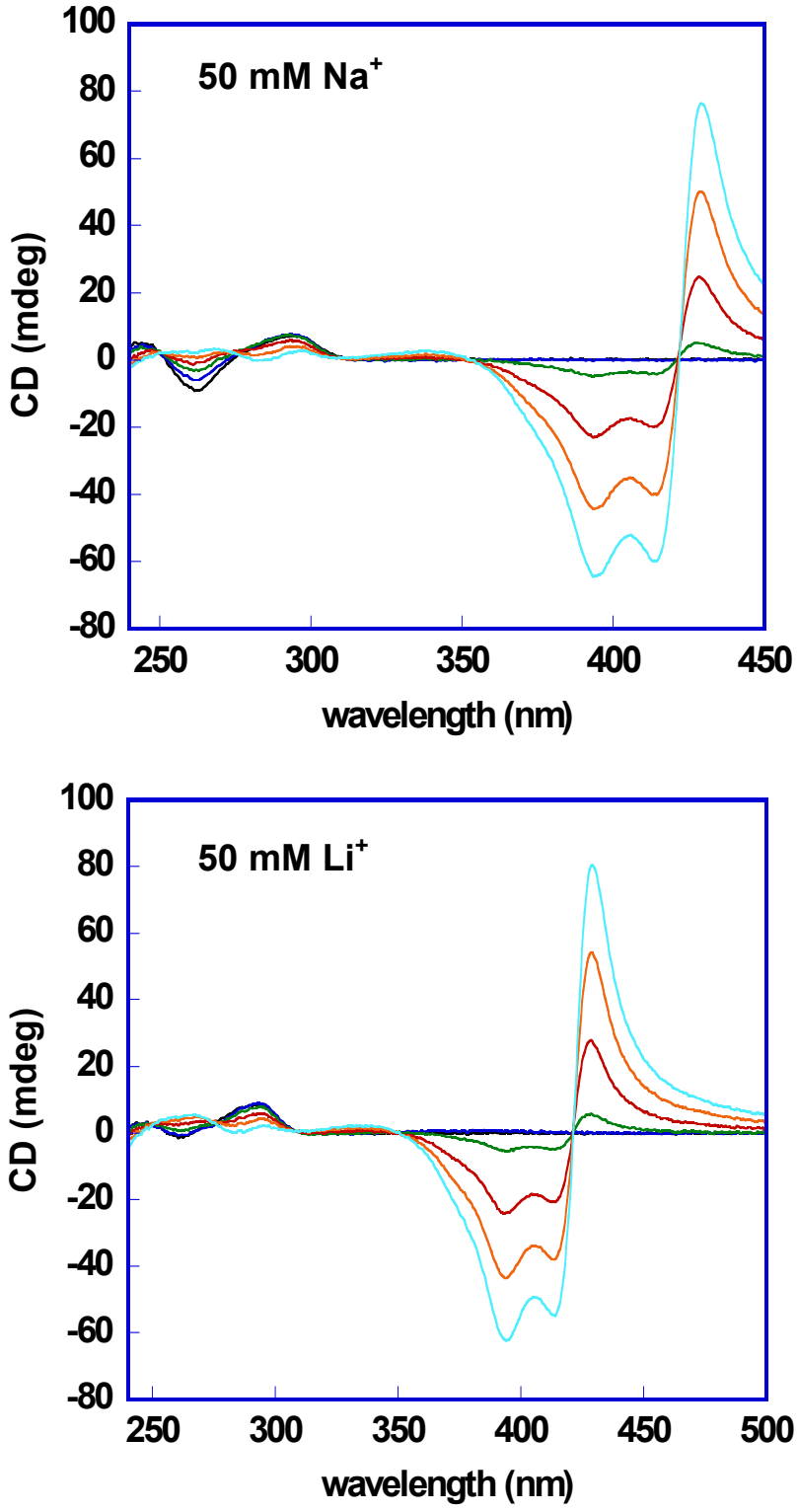


Figure 3.9 CD spectra of DB 832 titrated into 3.0 μM d[$AG_3(T_2AG_3)_3$] in buffer containing 50 mM NaCl (top) and 50 mM LiCl (bottom). Compound:DNA ratios ranged from 1:1 to 5:1.

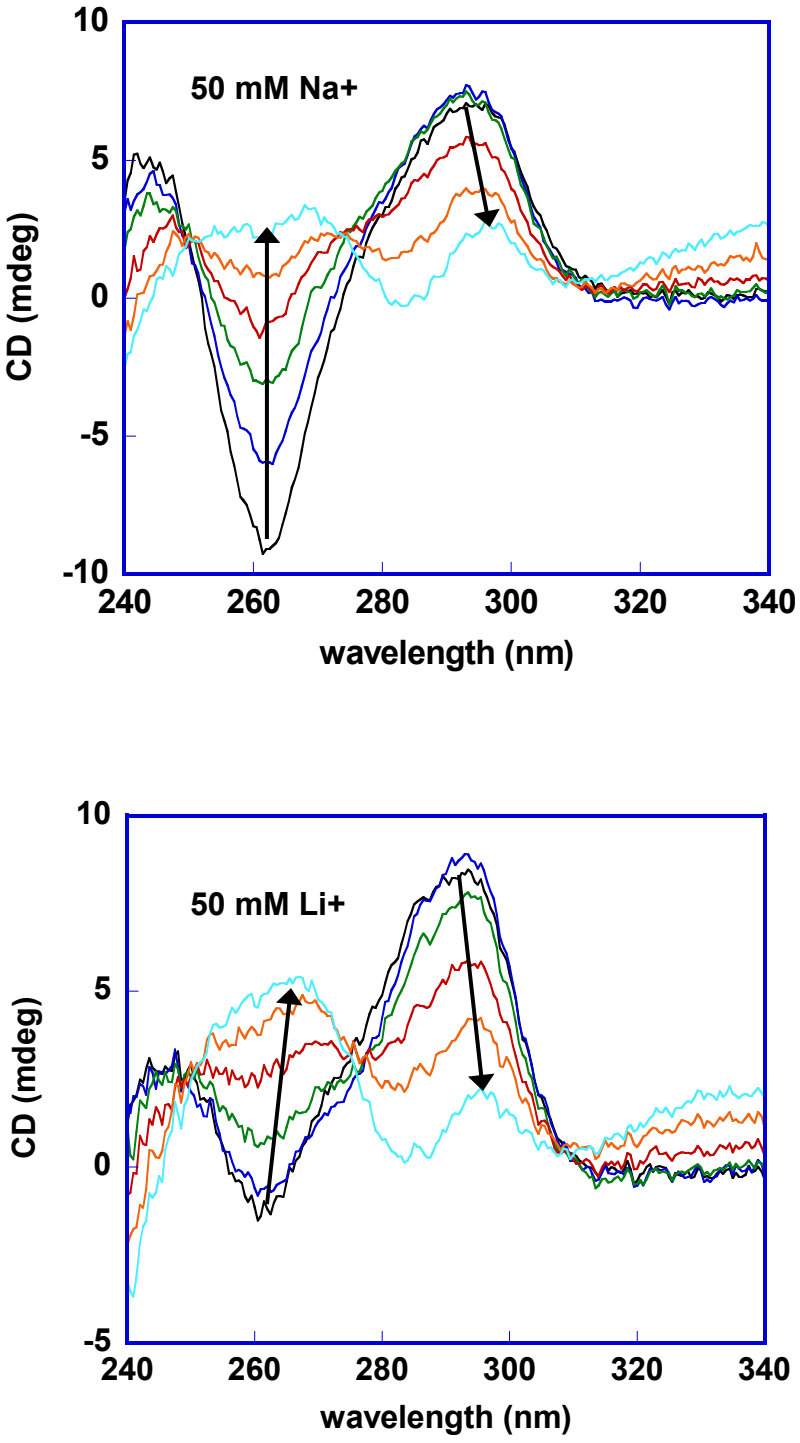


Figure 3.10 Close-up of the wavelength region of DNA absorbance for the spectra shown in Figure 3.9. The arrows indicate increasing DB 832 concentration.

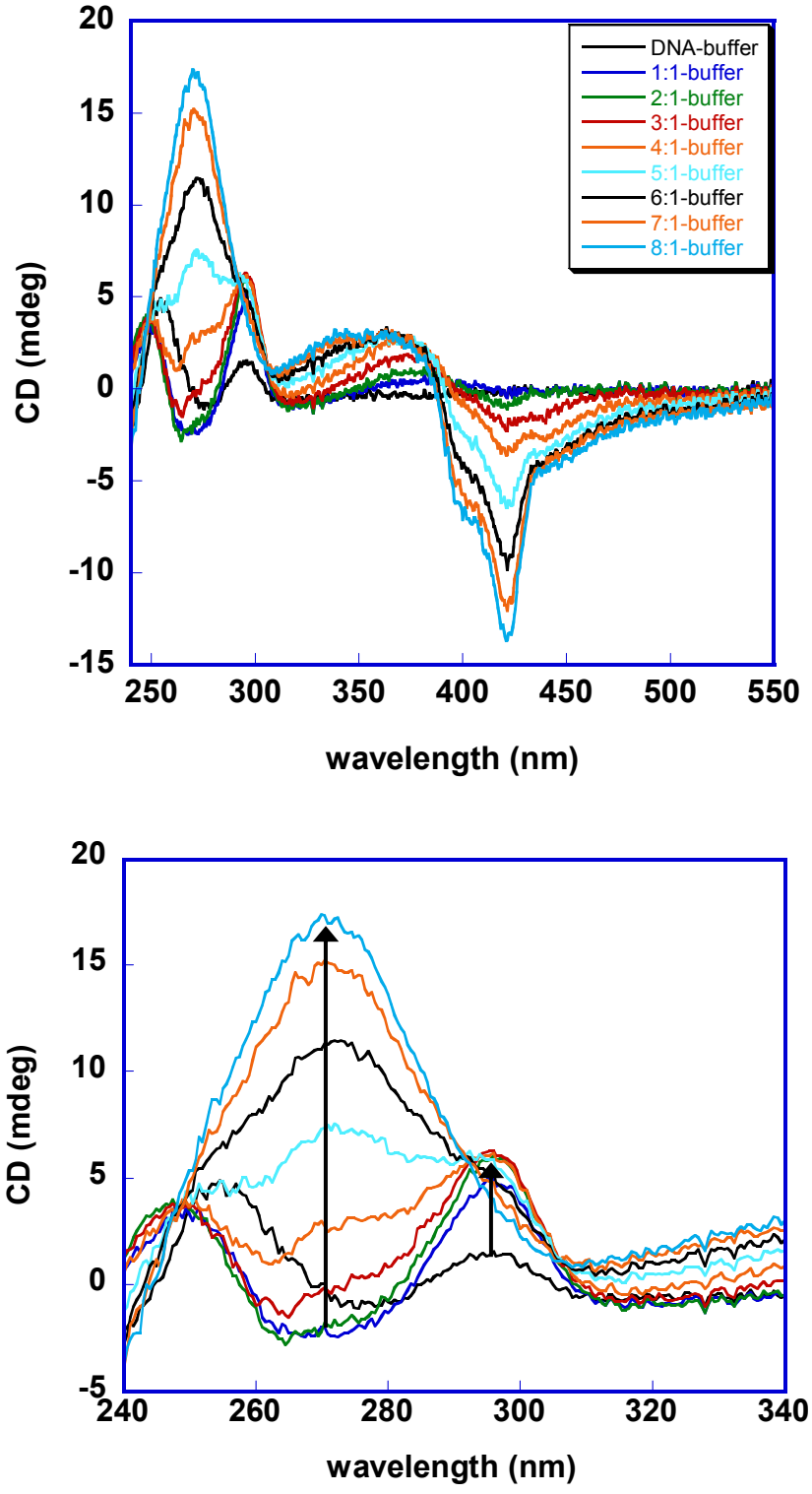


Figure 3.11 CD spectra of DB 832 titrated into 3.9 μM d[$AG_3(T_2AG_3)_3$] in 10 mM TRIS buffer in the absence of added salt. Compound:DNA ratios ranged from 1:1 to 8:1. The arrow represents increasing DB 832 concentration.

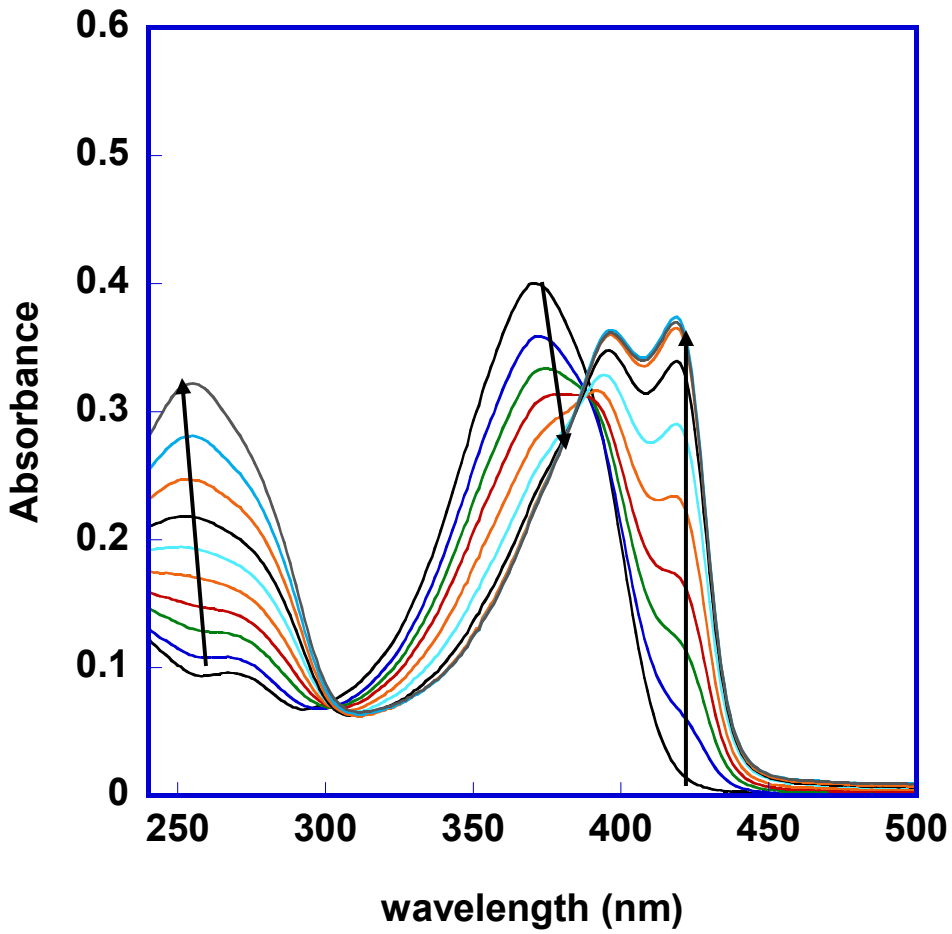


Figure 3.12 Absorbance spectra of d[$AG_3(T_2AG_3)_3$] titrated 8.0 μM DB 832 in 10 mM TRIS buffer in the absence of added salt, up to a final DNA concentration of 1.1μM. The arrows indicates increasing DB 832 concentration

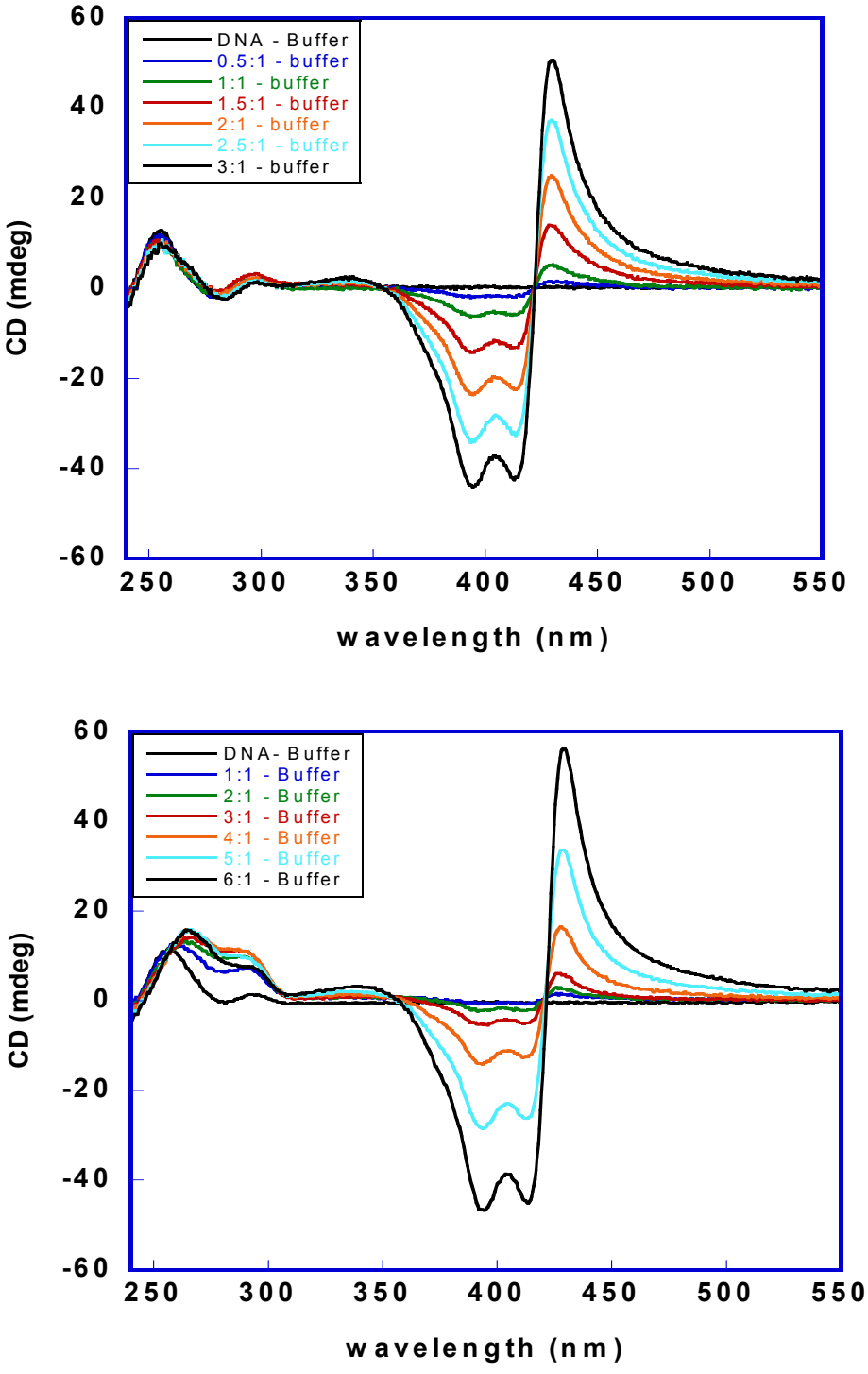


Figure 3.13 CD spectra of DB 832 titrated into 4.0 µM d[TAGGGUTAGGGT] hairpin dimer up to a compound/DNA ratio of 3:1 (top) and d[TAGGGUUAGGGT] (bottom) up to a compound/DNA ratio of 6:1 in phosphate buffer containing 70 mM $K^+$.

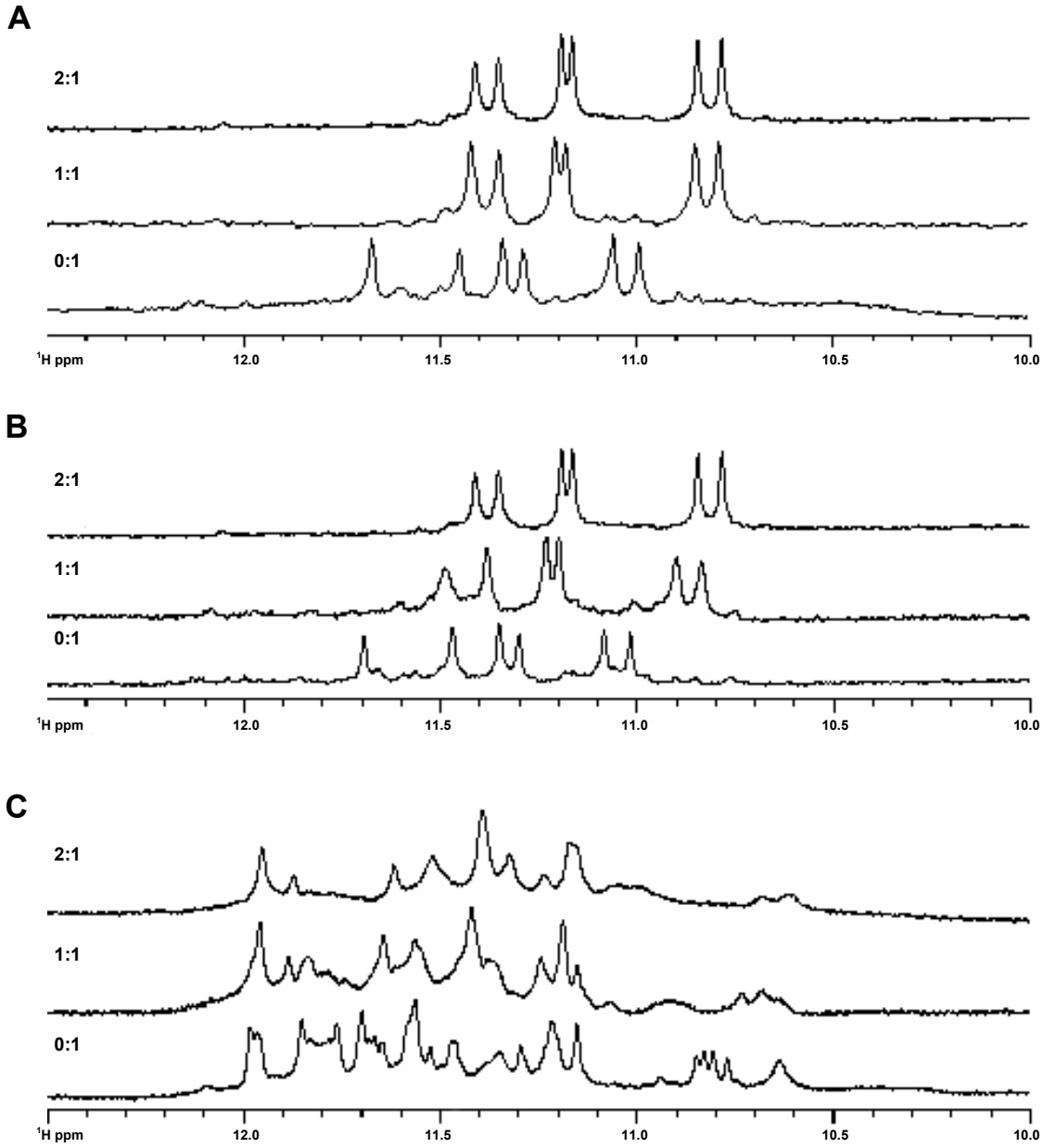


Figure 3.14 NMR imino proton titrations of (A) d(TAGGGUTAGGGT) and (B) d(TAGGGUUAGGGT) dimeric hairpin quadruplexes with DB 832 at 308 K and (C) d[$AG_3(T_2AG_3)_3$] at 298 K in the presence of phosphate buffer containing 70 mM $K^+$.

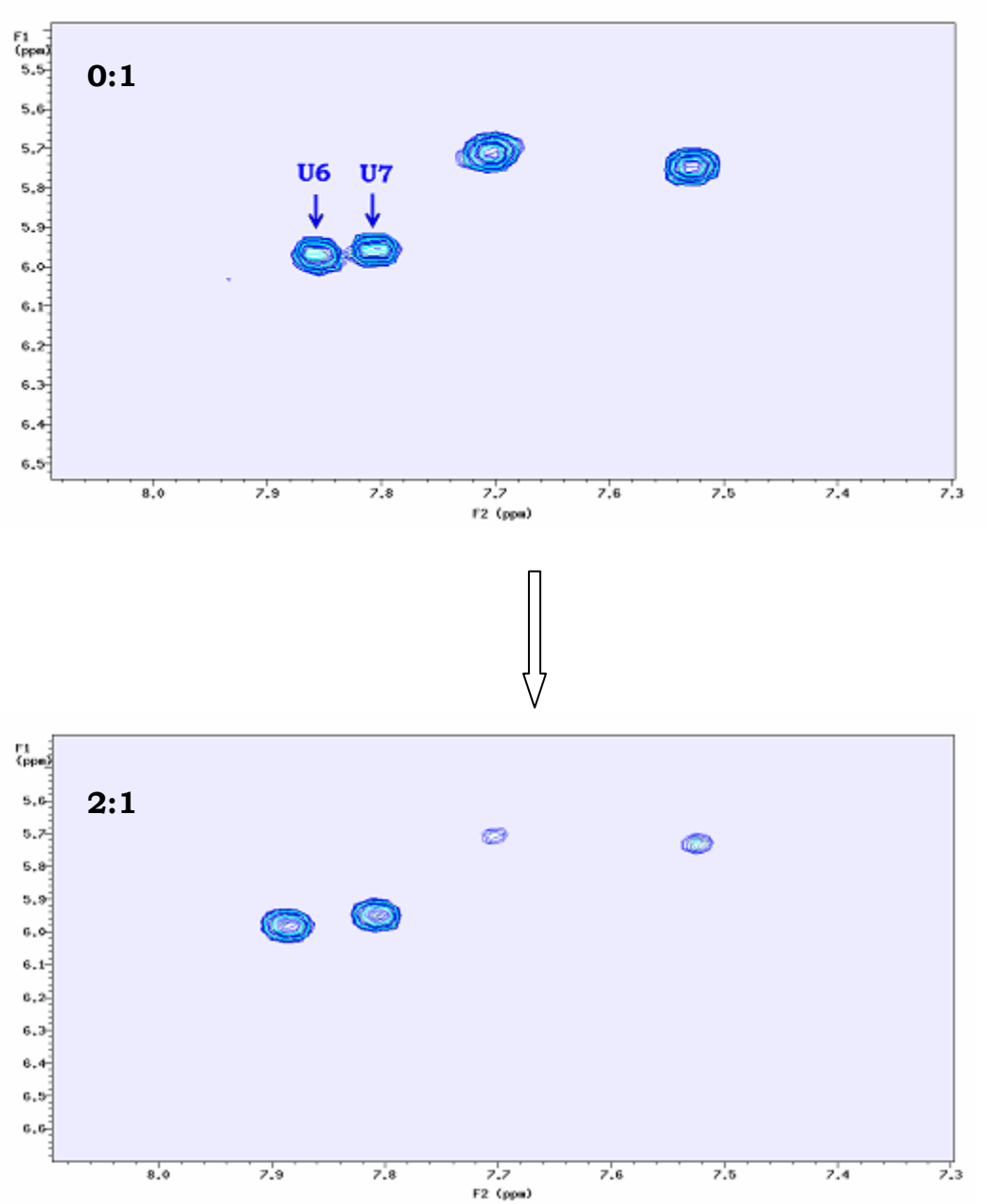


Figure 3.15 TOCSY spectra of uracil H5-H6 cross-peaks for 0.5 mM d[TAGGGUUAGGGT] at 0:1 and 2:1 DB 832 molar ratios. Spectra were obtained with a 60 ms mixing time at 35°C in phosphate buffer containing 70 mM $K^+$.

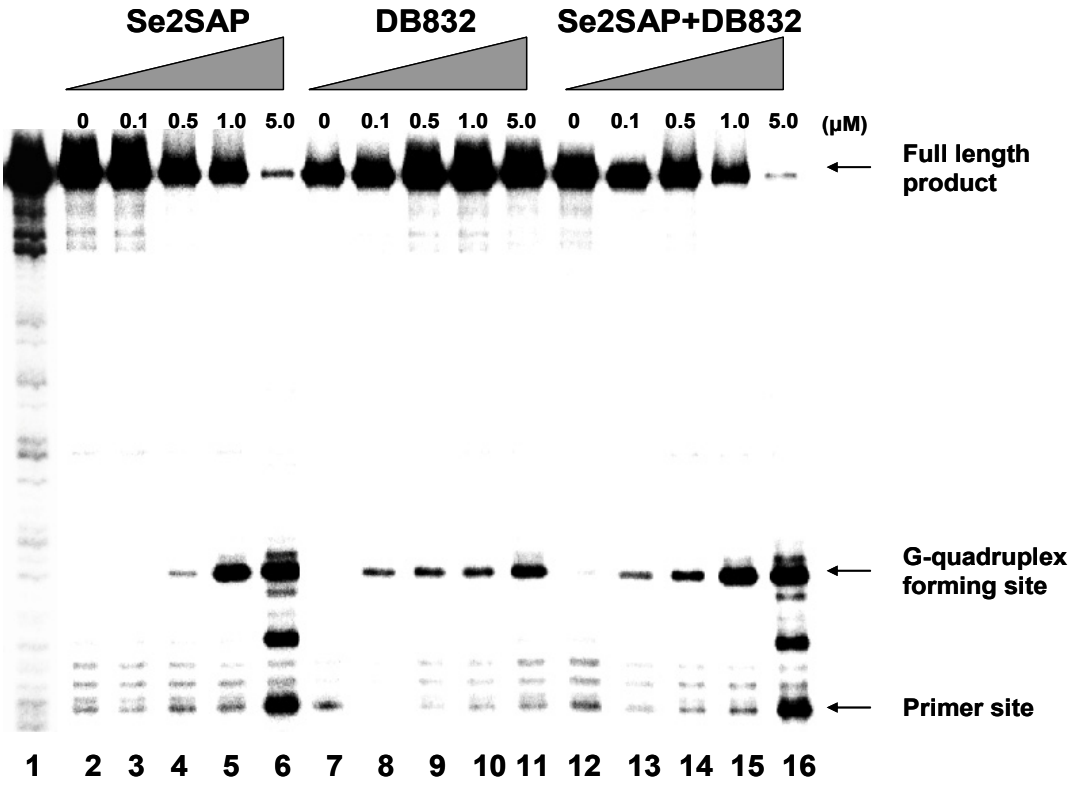


Figure 3.16 Concentration-dependent inhibition of *Taq* polymerase DNA synthesis by stabilization of the human telomeric G-quadruplex structure with Se2SAP (0-5μM), DB 832 (0-5 μM), or both (0-5 μM), using a DNA template containing the telomeric sequence at 37ºC in 100 mM KCl.

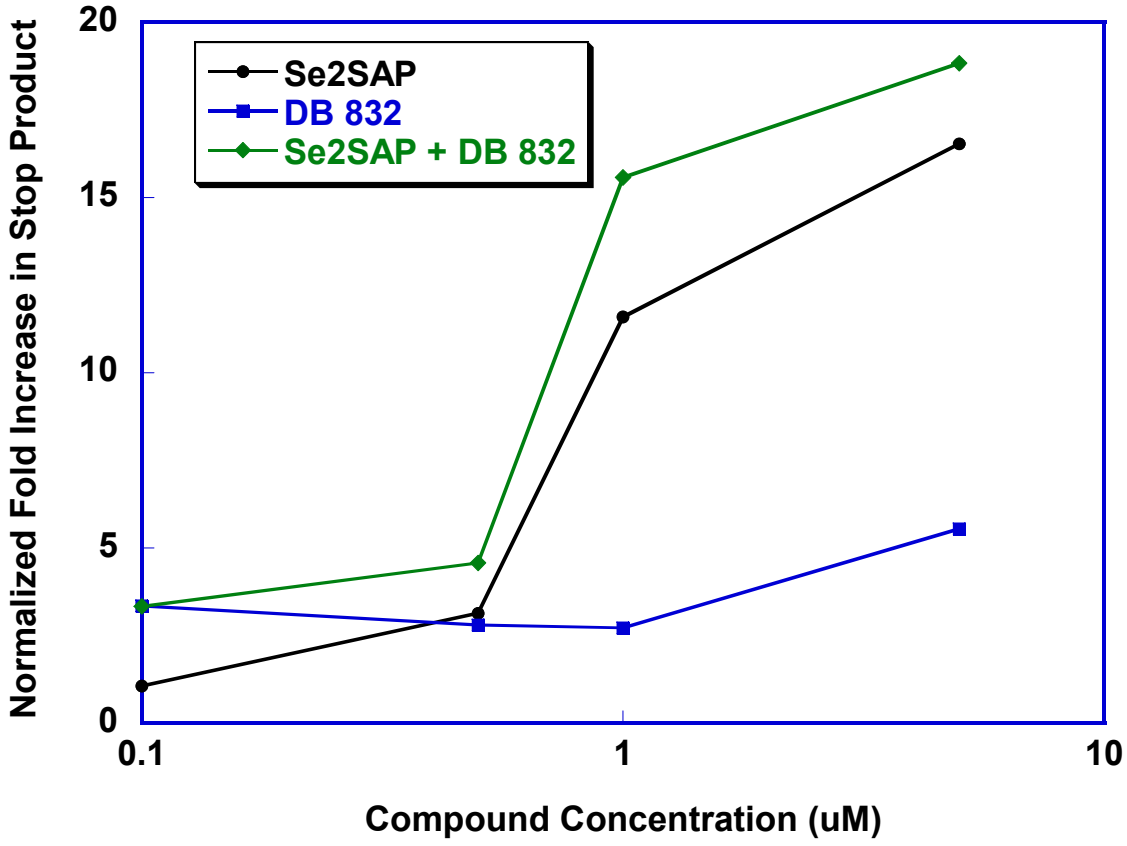


Figure 3.17 Graphical representation of the quantification of the autoradiogram in Figure 3.16 showing the normalized fold increase of stop product versus concentration.

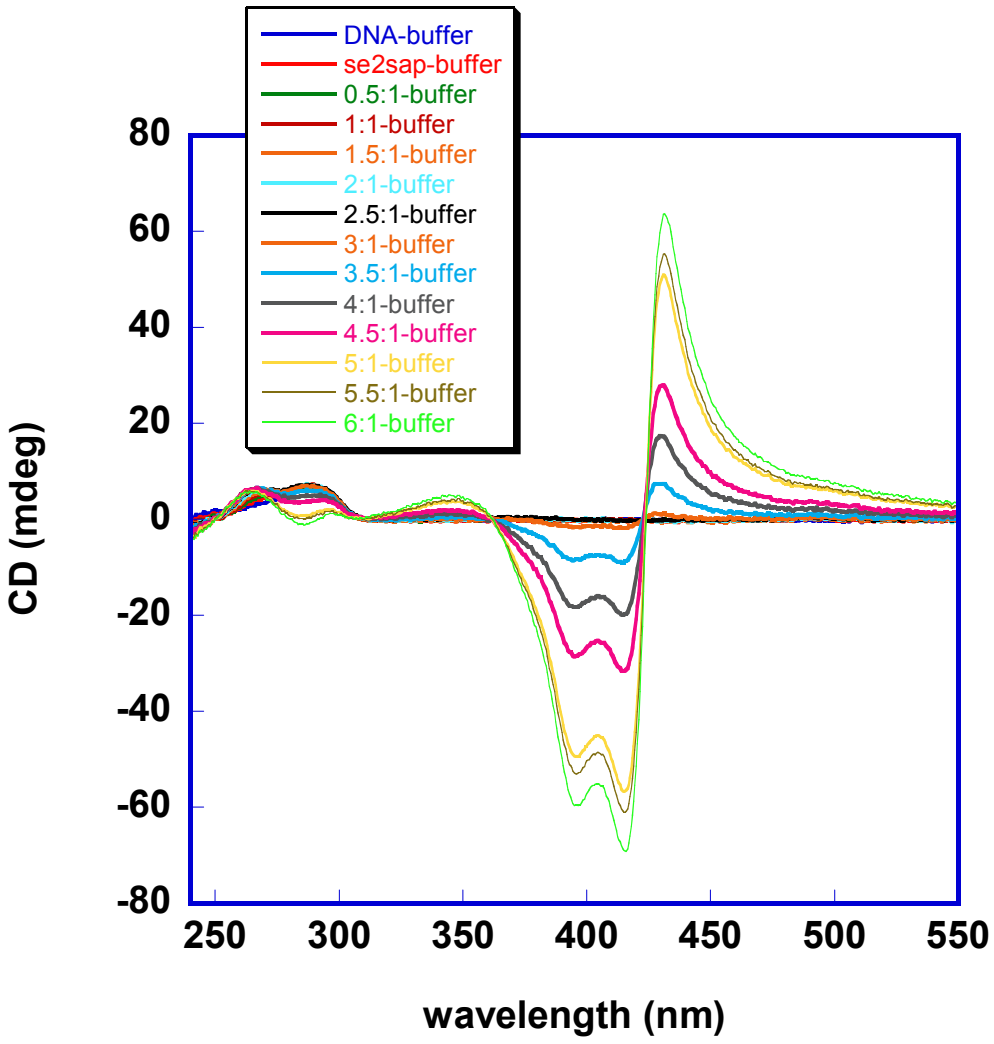


Figure 3.18 CD spectra of DB 832 titrated into 2.3 µM d[$AG_3(T_2AG_3)_3$] containing 2.7 µM Se2SAP in HEPES buffer with 50 mM KCl. DB 832:DNA ratios ranged from 0.5:1 to 6:1.

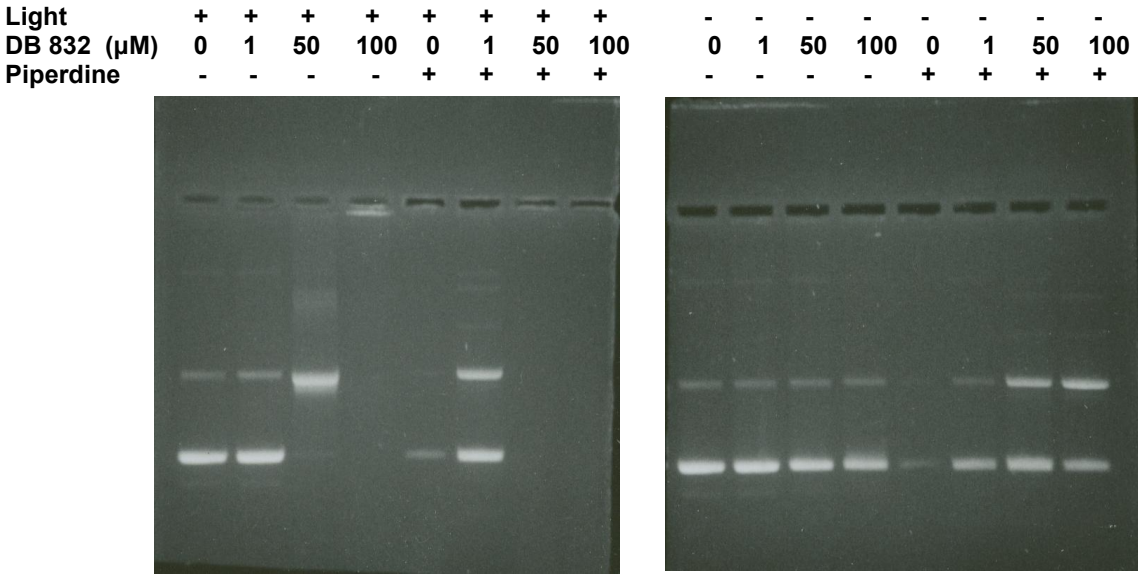


Figure 3.19 Photocleavage of puC19 plasmid DNA by DB 832 in the presence and absence of piperdine. The samples in the left gel were illuminated for 50 minutes at 419 nm. The samples on the right were left in the dark as a control.

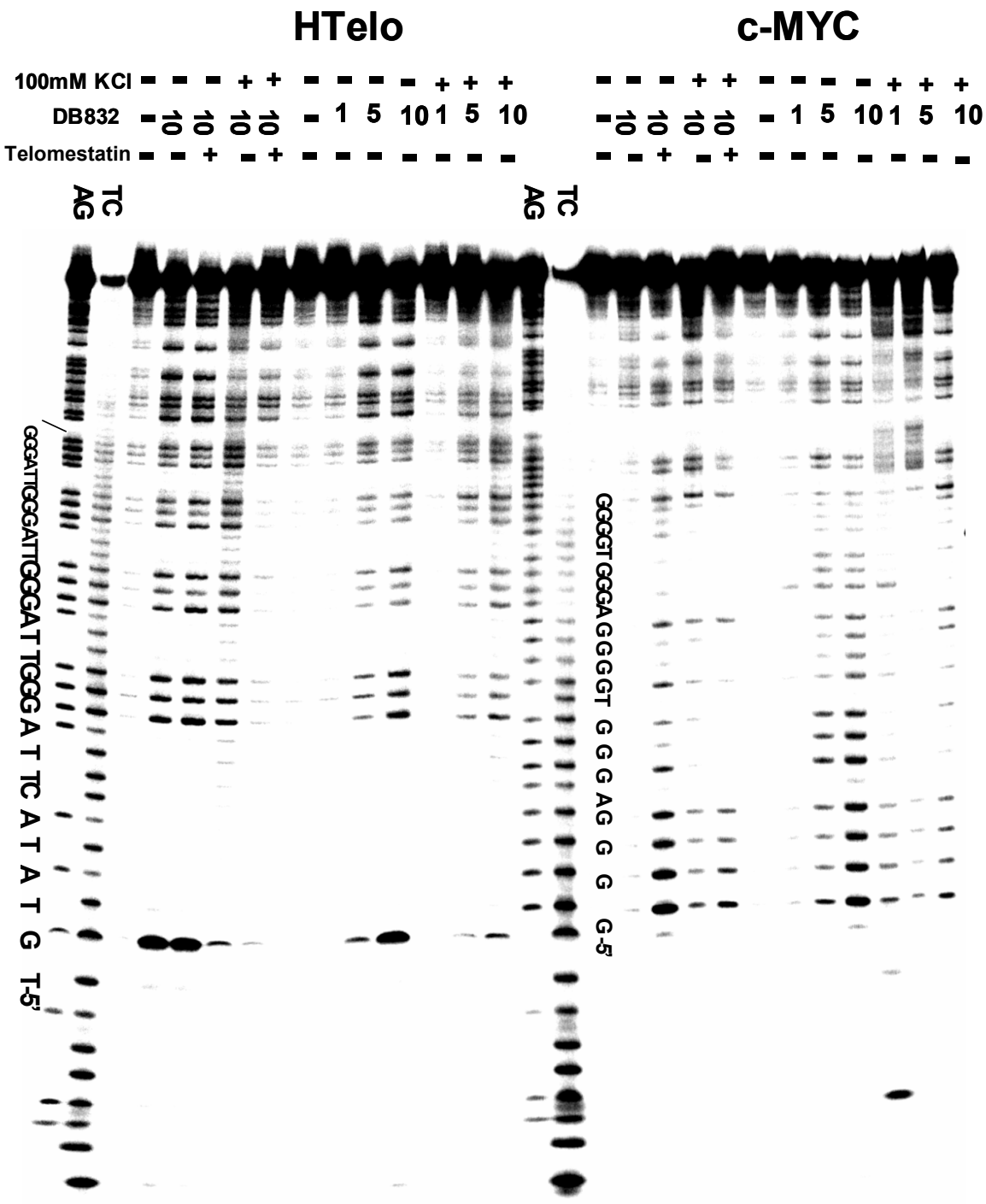


Figure 3.20 Photocleavage of 74-mer human telomeric DNA and 77-mer c-MYC DNA sequences by DB 832, telomestatin, or DB 832 and telomestatin in the presence and absence of KCl.

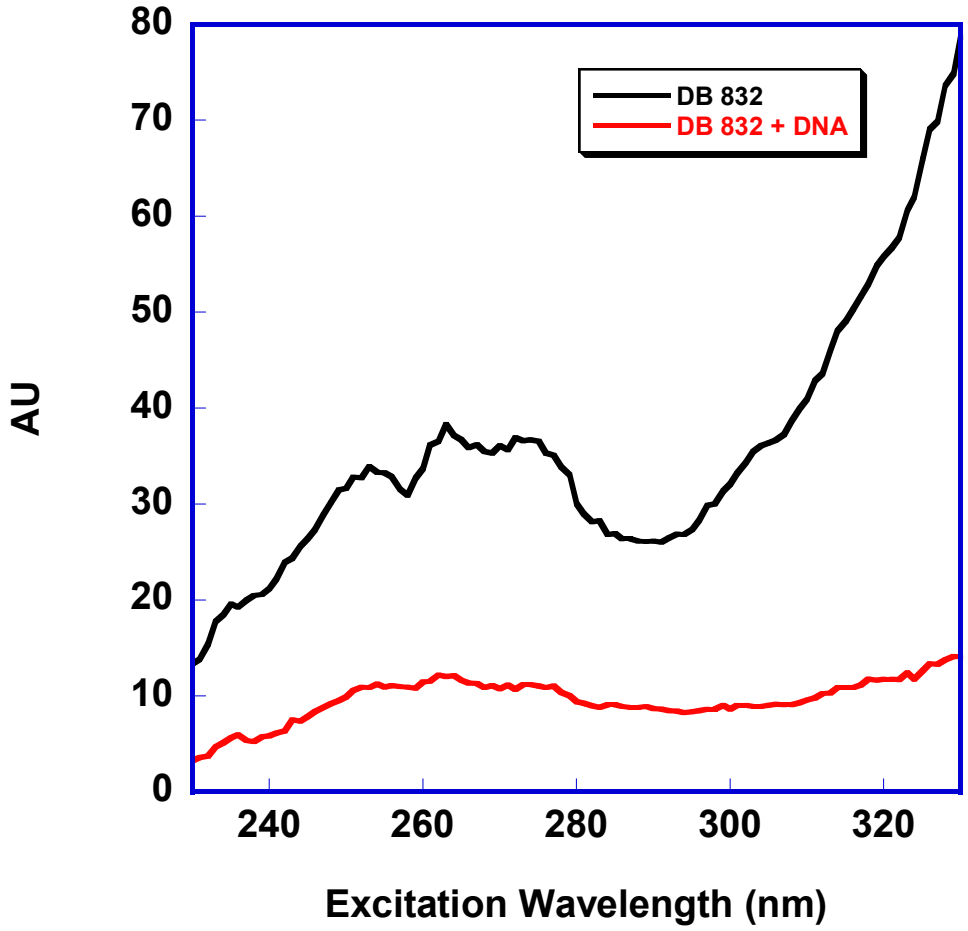


Figure 3.21 DB 832 fluorescence excitation spectra of 0.3 μM DB 832 alone and in the presence of 8 μM d[$AG_3(T_2AG_3)_3$] in HEPES buffer containing 50 mM KCl. The emission wavelength was set at 469 nm.

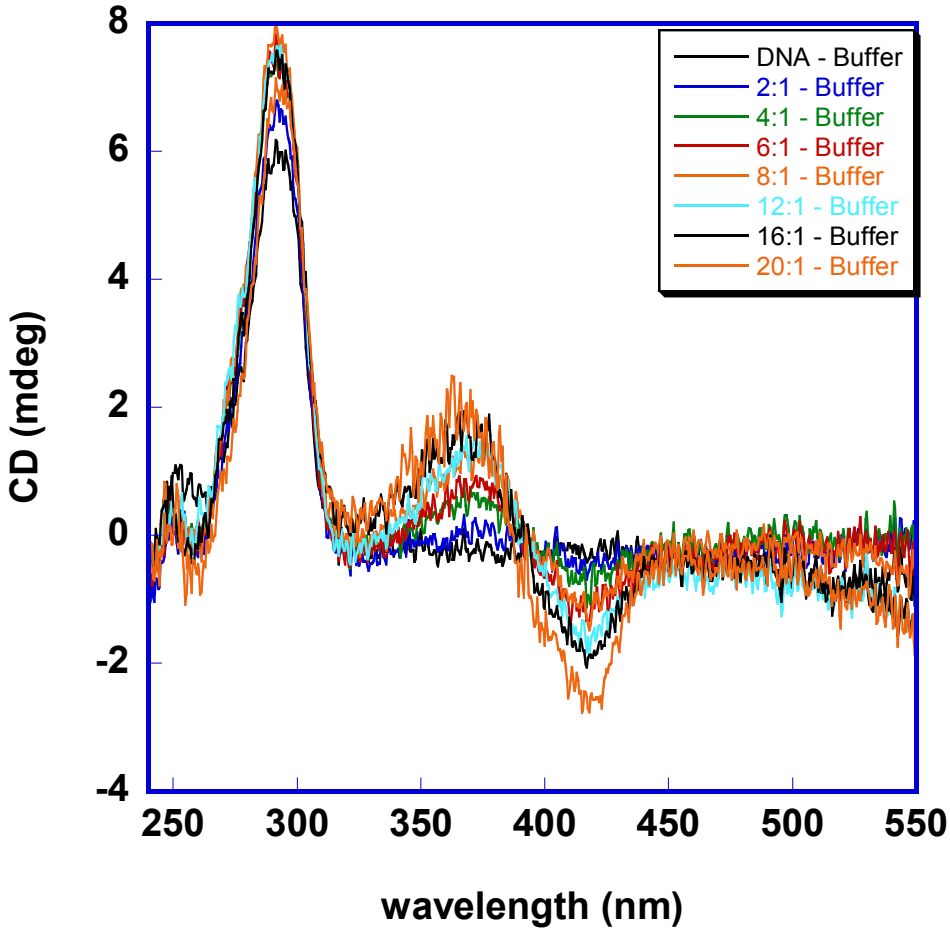


Figure 3.22 CD spectra of DB 832 titrated into 2.1 μM d(A$^{Br}$GGTTA$^{Br}$GGTTAGGGTTA$^{Br}$GG), in phosphate buffer containing 70 mM KCl. Compound:DNA ratios ranged from 2:1 to 20:1.

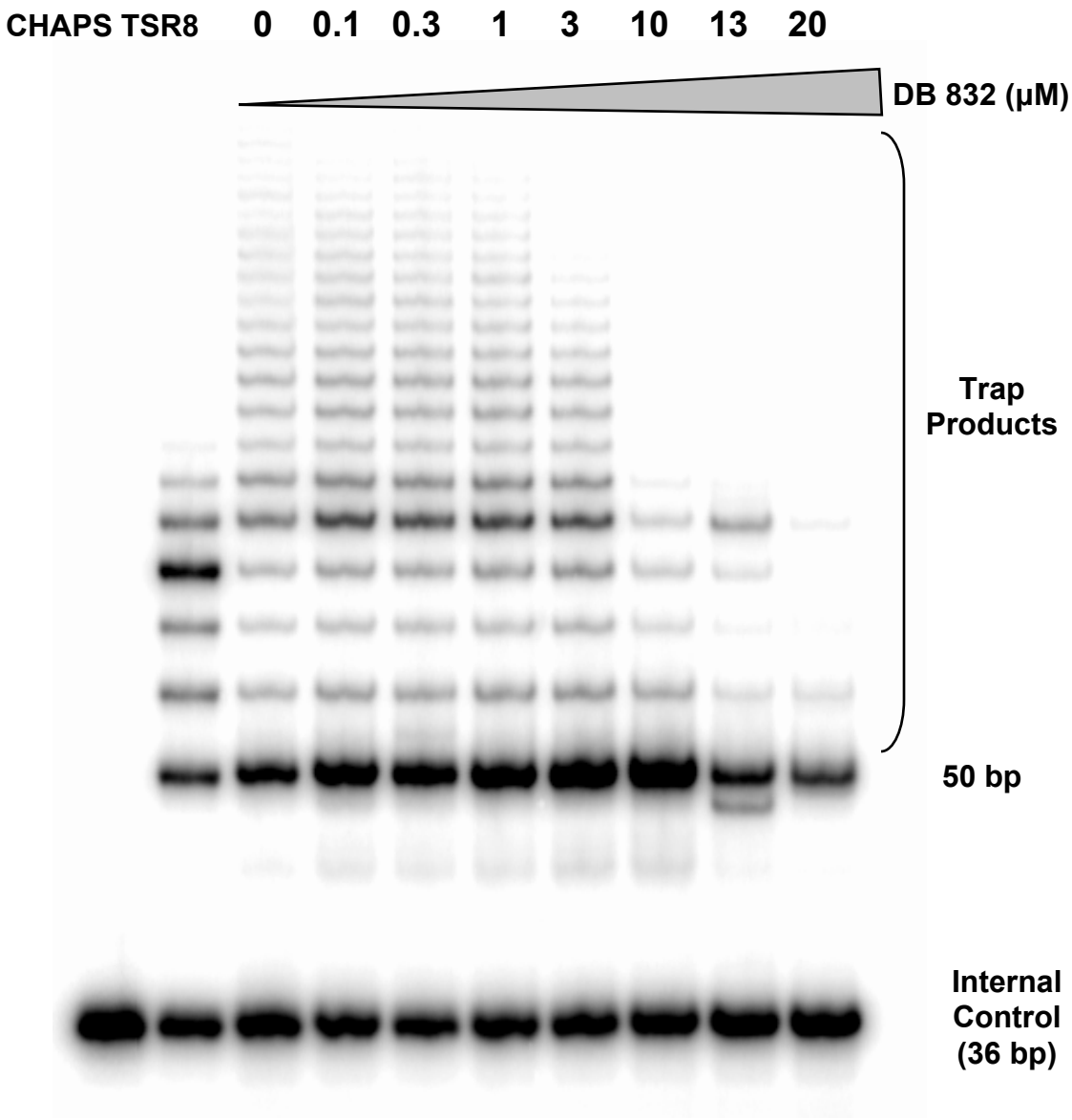


Figure 3.23 Gel showing TRAP assay extension products for DNA treated with different concentrations of DB 832. Lane 1 is a 1x cell lysis buffer control and lane 2 is the untreated TSR8 control template.

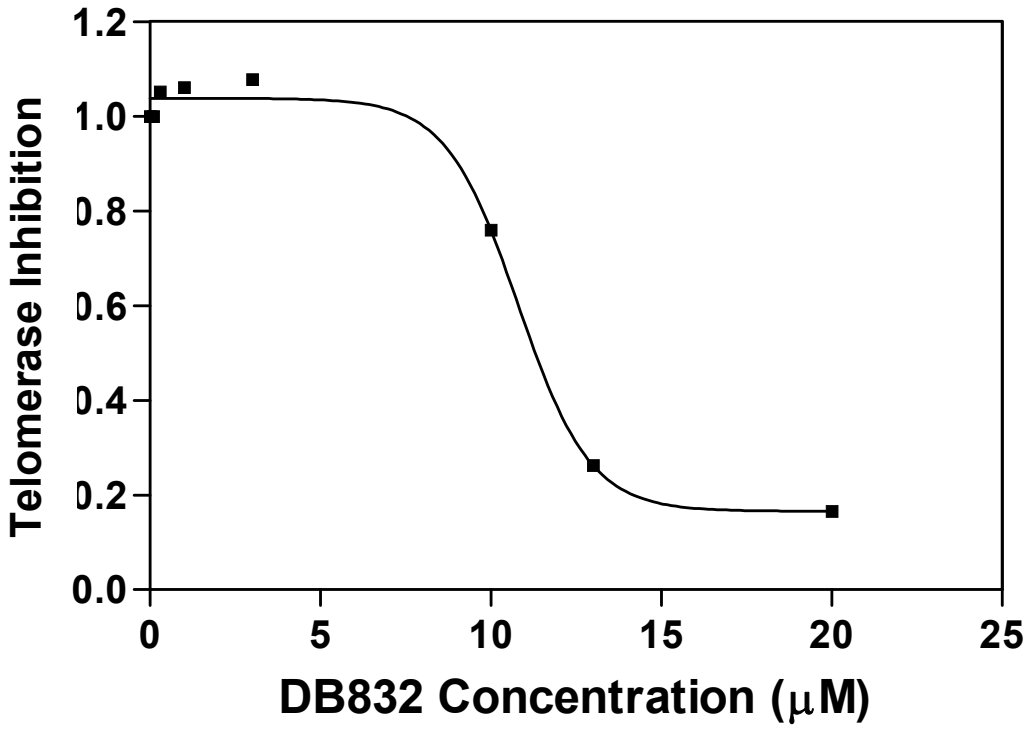


Figure 3.24 Plot showing telomerase inhibition by DB 832 relative to the untreated control as a function of concentration as determined from the TRAP assay.

## References


1. Guo, Q., et al., *Interaction of the dye ethidium bromide with DNA containing guanine repeats.* Biochem., 1992. **31**(9): p. 2451-5.
2. Han, H., et al., *Selective interactions of cationic porphyrins with G-quadruplex structures.* J. Am. Chem. Soc., 2001. **123**(37): p. 8902-13.
3. Chen, Q., I.D. Kuntz, and R.H. Shafer, *Spectroscopic recognition of guanine dimeric hairpin quadruplexes by a carbocyanine dye.* Proc. Natl. Acad. Sci. U S A, 1996. **93**: p. 2635-2639.
4. Cheng, J.-Y., S.-H. Lin, and T.-C. Chang, *Vibrational Investigation of DODC Cation for Recognition of Guanine Dimeric Hairpin Quadruplex Studied by Satellite Holes.* J. Phys. Chem., 1998. **102**: p. 5542-5546.
5. Chiang, C.-C., J.-Y. Cheng, and T.-C. Chang, *Satellite Hole Spectral Method and Its Applications to Dye-DNA Complexes.* Proc. Natl. Sci. Coun. ROC (A), 1999. **23**(6): p. 679-694.
6. Kerwin, S.M., et al., *G-Quadruplex DNA Binding by a Series of Carbocyanine Dyes.* Bioorg. Med. Chem. Letters, 2001. **11**: p. 2411-2414.
7. Randazzo, A., et al., *Interaction of distamycin A and netropsin with quadruplex and duplex structures: a comparative 1H-NMR study.* Nucleosides Nucleotides Nucleic Acids, 2002. **21**(8-9): p. 535-45.
8. Cocco, M.J., et al., *Specific interactions of distamycin with G-quadruplex DNA.* Nucleic Acids Res., 2003. **31**(11): p. 2944-51.
9. Mergny, J.L., et al., *The development of telomerase inhibitors: the G-quartet approach.* Anticancer Drug Des., 1999. **14**(4): p. 327-39.

10. Seenisamy, J., et al., *Design and synthesis of an expanded porphyrin that has selectivity for the c-MYC G-quadruplex structure.* J. Am. Chem. Soc., 2005. **127**(9): p. 2944-59.

11. Hore, P.J., *Solvent supression in Fourier transform NMR.* J. Magn. Reson., 1983. **55**: p. 283-300.

12. Sklenar, V., et al., *Gradient-tailored water supression for 1H-15N HSQC experiments optimized to retain full sensitivity.* J. Magn. Reson., 1993. **102**: p. 241-245.

13. Davis, D.G. and A. Bax, *Separation of chemical exchange and cross-relaxation effects in two-dimensional NMR spectroscopy.* J. Magn. Reson., 1982. **64**: p. 533-535.

14. Levitt, M.H., R. Freeman, and T.A. Frenkiel, *Broadband heteronuclear dicoupling.* J. Magn. Reson., 1985. **47**: p. 328.

15. Goddard, T.G. and D.G. Kneller, *SPARKY 3*, University of California, San Francisco.

16. Rodger, A. and B. Norden, *Circular Dichroism and Linear Dichroism*. Oxford Chemistry Masters, ed. R.G. Compton, S.G. Davies, and J. Evans. 1997, New York: Oxford University Press. 150.

17. Balagurumoorthy, P., et al., *Hairpin and parallel quartet structures for telomeric sequences.* Nucleic Acids Res., 1992. **20**(15): p. 4061-7.

18. Jelley, E.E., Nature, 1936. **138**: p. 1009.

19. Schiebe, G., Angew. Chem., 1937. **50**: p. 212.

20. Herz, A.H., Photogr. Sci. Eng., 1974. **18**: p. 323.

21. West, W. and S.J. Pearce, J Phys Chem, 1965. **69**: p. 1894.

22. Seifert, J.L., et al., *Spontaneous assembly of helical cyanine dye aggregates on DNA nanotemplates.* J Am Chem Soc, 1999. **121**: p. 2987-2995.

23. Tomlinson, A., et al., *A structural model for cyanine dyes templated into the minor groove of DNA.* Chem Phys, 2006. **325**: p. 36-47.

24. Sen, D. and W. Gilbert, Nature, 1990. **344**: p. 410.

25. Wang, Y. and D.J. Patel, *Solution structure of the human telomeric repeat d[AG3(T2AG3)3] G-tetraplex.* Structure, 1993. **1**(4): p. 263-82.

26. Parkinson, G.N., M.P. Lee, and S. Neidle, *Crystal structure of parallel quadruplexes from human telomeric DNA.* Nature, 2002. **417**(6891): p. 876-80.

27. He, Y., R.D. Neumann, and I.G. Panyutin, *Intramolecular quadruplex conformation of human telomeric DNA assessed with 125I-radioprobing.* Nucleic Acids Res., 2004. **32**(18): p. 5359-67.

28. Li, J., et al., *Not so crystal clear: the structure of the human telomere G-quadruplex in solution differs from that present in a crystal.* Nucleic Acids Res., 2005. **33**(14): p. 4649-59.

29. Qi, J. and R. Shafer, H., *Covalent ligation studies on the human telomere quadruplex.* Nucleic Acids Res., 2005. **33**(10): p. 3185-3192.

30. Rezler, E.M., et al., *Telomestatin and diseleno sapphyrin bind selectively to two different forms of the human telomeric G-quadruplex structure.* J. Am. Chem. Soc., 2005. **127**(26): p. 9439-47.

31. Sen, D. and W. Gilbert, *Guanine quartet structures.* Methods Enzymol., 1992. **211**: p. 191-199.

32. Williamson, J.R., M.K. Raghuraman, and T.R. Cech, *Monovalent cation-induced structure of telomeric DNA: the G-quartet model.* Cell, 1989. **59**(5): p. 871-80.

33. Kim, M.Y., et al., *The different biological effects of telomestatin and TMPyP4 can be attributed to their selectivity for interaction with intramolecular or intermolecular G-quadruplex structures.* Cancer Res., 2003. **63**(12): p. 3247-56.

34. Phan, A.T. and D.J. Patel, *Two-repeat human telomeric d(TAGGGTTAGGGT) sequence forms interconverting parallel and antiparallel G-quadruplexes in solution: distinct topologies, thermodynamic properties, and folding/unfolding kinetics.* J. Am. Chem. Soc., 2003. **125**(49): p. 15021-7.

35. Armitage, B., *Photocleavage of Nucleic Acids.* Chem Rev, 1998. **98**(3): p. 1171-1200.

36. Croke, D.T., et al., *Structure-activity relationships for DNA photocleavage by cationic porphyrins.* J Photochem Photobiol B, 1993. **18**(1): p. 41-50.

37. Nussbaum, J.M., et al., *Structure-specific binding and photosensitized cleavage of branched DNA three-way junction complexes by cationic porphyrins.* Photochem Photobiol, 1994. **59**(5): p. 515-28.

38. Pushpan, S.K., et al., *Porphyrins in photodynamic therapy - a search for ideal photosensitizers.* Curr Med Chem Anticancer Agents, 2002. **2**(2): p. 187-207.

39. Seenisamy, J., et al., *The dynamic character of the G-quadruplex element in the c-MYC promoter and modification by TMPyP4.* J Am Chem Soc, 2004. **126**(28): p. 8702-9.

40. Kim, M.Y., et al., *Telomestatin, a potent telomerase inhibitor that interacts quite specifically with the human telomeric intramolecular g-quadruplex.* J Am Chem Soc, 2002. **124**(10): p. 2098-9.

41. Dias, E., J.L. Battiste, and J.R. WIlliamson, *Chemical Proble for Glycosidic Conformation in Telomeric DNAs.* J Am Chem Soc, 1994. **116**: p. 4479-4480.

42. Xu, Y., Y. Noguchi, and H. Sugiyama, *The new models of the human telomere d[AGGG(TTAGGG)3] in K+ solution.* Bioorg Med Chem, 2006. **14**(16): p. 5584-91.

43. Ambrus, A., et al., *Human telomeric sequence forms a hybrid-type intramolecular G-quadruplex structure with mixed parallel/antiparallel strands in potassium solution.* Nucleic Acids Res., 2006. **34**(9): p. 2723-35.

# Chapter 4

## Selectivity of Quadruplex Binding as a Stacked Species: Effect of DNA and Compound Structure

### Introduction

G-quadruplex DNA differs from Watson-Crick duplex DNA in that the structures of quadruplexes are very sensitive to conditions and can be highly polymorphic. Quadruplex DNA can form different structures depending on sequence, length, concentration, nature of cations present, presence of crowding agents and other factors [1-5]. Shorter sequences can form intermolecular two-or four strand structures. Longer sequences can form intramolecular quadruplex structures including antiparallel basket and chair quadruplexes, parallel propeller quadruplexes, and mixed parallel/antiparallel hybrid structures [6-12]. Some intramolecular sequences can also form intermolecular quadruplex structures known as "G-wires" under certain conditions [13]. Some quadruplex-forming sequences can exist as a mixture of structures in solution, and even interconvert. The promoter region of the c-MYC oncogene has been shown to exist as mixture of four loop isomers [14]. The bcl-2 proto-oncogene has been shown to exist as a mixture of three different quadruplex structures [15, 16]. A two-repeat human telomeric sequence has been shown to form interconverting parallel and antiparallel G-quadruplexes in solution [17]. Evidence suggests that the intramolecular human telomeric sequence may exist as a mixture of structures in the presence of potassium [17-19]. Some small molecules have been shown to induce a conformation change of quadruplex DNA upon binding [14, 20]. In the case of the purine-rich strand of the promoter region of the

c-MYC oncogene, it has been proposed that binding of a small molecule is not sufficient to modulate transcription; a conformation change in the quadruplex must occur for effective down-regulation of the gene [14].

The extensive variation among quadruplex structures, combined with the fact that some small molecules can induce or trap out a particular conformation may allow the design of compounds that can target particular quadruplex structures with a high degree of selectivity. Selectivity of a compound for quadruplex over duplex DNA is important because indiscriminant duplex-binding is associated with cytotoxicity and can also result in significant loss of compound. However, selectivity for a certain quadruplex structure over other non-targeted quadruplexes is also a very important consideration in design of quadruplex-interactive agents. Potential quadruplex-forming sequences are common in the genome. Telomeric DNA, immunoglobulin switch region sequences, the fragile X repeat sequence, promoter regions of some oncogenes, the insulin gene and other genomic sequences have been shown to form quadruplex structures *in vitro* [10, 11, 21-25]. Binding to non-targeted quadruplex sequences results in compound loss and may have unintentional effects on regulation of non-targeted genes. Increasing selectivity of telomerase inhibitors for their targets is therefore an important focus of research.

DB 832 is a heterocyclic diamidine that has been shown in Chapter 3 to bind to human telomeric DNA as a stacked species. Regardless of the starting conformation of the human telomeric DNA, DB 832 is capable of inducing the formation of a mixed parallel/antiparallel hybrid quadruplex structure, and can even induce formation of this structure in the absence of salt. In this chapter, the selectivity of this compound for its DNA target will be investigated. Thermal melting will be used to quantify the selectivity

of DB 832 for quadruplex vs. duplex DNA binding. Circular dichroism will be used to determine selectivity for DB 832 binding as a stacked species to the mixed parallel/antiparallel hybrid DNA structure formed by the human telomere. CD studies will also be used to investigate the binding of analogs and derivatives of DB 832 to the human telomere to help better understand how the structural features of DB 832 contribute to its selectivity for binding as a stacked species.

**Materials and Methods**

**Sample Preparation**

The oligonucleotides d[$AG_3(T_2AG_3)_3$], d($G_3CGCG_3AG_2A_2T_2G_3CG_3$), d($AG_3TG_4AG_3TG_4A$), d[$A_3(G_3T_2A)_3G_3A_2$], d[$G_4(T_4G_4)_3$], d[$(T_2G_4)_4$], d($G_2T_2G_2TGTG_2T_2G_2$), d $(GC)_7$, d (GCGTTAACGC), d(CGAGATCAAAAGATCTCG) and d(TG4T) were purchased with HPLC purification from Midland Certified Reagent Company or Integrated DNA Technologies, Inc. The G-quadruplex DNA samples were dissolved in buffer to the desired concentrations, heated to 85 $^0$C and cooled slowly to insure the folding of the quadruplexes prior to each experiment. The concentration of each DNA sample was determined spectrophotometrically at 260 nm using the nearest neighbor extinction coefficient at 80°C and extrapolated to 20°C. A stock solution containing 1 mM of each compound was prepared in double distilled water and diluted to working concentrations immediately before use with buffer. The synthesis of all DB compounds will be described elsewhere.

**Thermal Denaturation Studies**

Thermal denaturation studies were conducted on a Cary Varian 300 BIO UV-visible spectrophotometer in quartz cells with a 1 cm pathlength. A thermistor fixed into

a reference cuvette was used to monitor the temperature. The absorbance of the human telomeric oligomer d[$AG_3(T_2AG_3)_3$] was monitored at 295 nm, while the hairpin duplex sequence d(CGAGATCAAAAGATCTCG) was monitored at 260 nm. Melting curves were obtained for both DNA sequences in the presence and absence of DB 832. For both oligomers the DNA concentration was 2.7 x $10^{-6}$ M and the DB 832: DNA ratio was 2:1. Data manipulation and plotting was performed using the program Kaleidagraph version 3.6.

**CD Measurements**

CD measurements were performed at 20°C in a 10 mM HEPES buffer (pH 7.4) containing 3 mM EDTA and 50 mM KCl, except the CD titration with d($TG_4T$), which was prepared in phosphate buffer containing 50 mM KCl, 10 mM $K_2HPO_4$ and 0.1 mM EDTA. CD spectra were recorded using a Jasco J-810 spectrapolarimeter in a 1-cm cell using an instrument scanning speed of 50 nm/min with a response time of 1 s. The spectra were averaged over four scans. A buffer baseline scan was collected in the same cuvette and subtracted from the average scan for each sample. Appropriate amounts of stock solution of compound were added sequentially to increase the molar ratio. Data manipulation and plotting was performed using the program Kaleidagraph version 3.6.

**Results and Discussion**

**DB 832 is Highly Selective for Quadruplex DNA over Duplex DNA**

In order to determine the selectivity of DB 832 for human telomeric DNA over duplex DNA, melting curves were obtained for the intramolecular human telomeric sequence d[$AG_3(T_2AG_3)_3$] as well as a random sequence hairpin duplex d(CGAGATCAAAAGATCTCG) (Figure 4.1). The melting temperature of the telomeric

DNA in the absence of DB 832 is 59.6 °C. Upon addition of DB 832, the melting temperature of the DNA increases by approximately 10°C, indicating that the compound is stabilizing the quadruplex conformation of the DNA. This is comparable to the ΔTm for the human telomere in the presence of the well-studied porphyrin compound, TMPyP4, under similar conditions [26]. In contrast, when DB 832 is added to the duplex sequence at the same ratio and conditions, there is no detectable change in Tm. This indicates that DB 832 binds much more strongly to quadruplex than to mixed-sequence duplex DNAs, making it ideal for further study as a highly selective G-quadruplex interactive compound.

**DB 832 Binds Selectively to Mixed Parallel/Antiparallel Hybrid Quadruplex DNA**

DB 832 has been shown to bind to or induce the formation of a mixed parallel/antiparallel conformation of human telomeric DNA (Chapter 3). To determine if the stacked binding of this compound is selective for this particular DNA structure, CD spectra were obtained for DB 832 added to DNA sequences that form a variety of structures, including antiparallel chair and basket quadruplexes, a parallel quadruplex, an intermolecular quadruplex sequence, and duplex DNA sequences.

Thrombin Binding Aptamer, d($G_2T_2G_2TGTG_2T_2G_2$), forms an antiparallel chair-type quadruplex as determined by NMR [27]. Before the addition of DB 832, the spectrum in the DNA wavelength region has a maximum at 295 nm, with a minimum at 260 nm, confirming the presence of the antiparallel (chair) conformation (Figure 4.2). The addition of DB 832 increases the signal at 260 nm and decreases the signal at 295 nm, indicating a conformation change in the DNA as the compound binds. In the wavelength region of DB 832 absorbance, a slight induced exciton splitting is observed,

but only after the compound: DNA ratio reaches 8:1. Compound concentrations this high, however, are not biologically relevant and would not be observed in therapeutic use of the compound.

The oligomer d[$(G_2T_4)_3G_2$] has been characterized as a basket-type antiparallel quadruplex by 1-D NMR [28]. Before the addition of DB 832, the spectrum in the DNA wavelength region has a maximum at 295 nm, and a minimum at 260 nm, indicative of an antiparallel conformation of DNA (Figure 4.3). The addition of DB 832 does not cause a significant change in the shape of the spectra in the DNA region, indicating that DB 832 does not significantly rearrange the conformation of the DNA. No induced exciton splitting is observed in the wavelength region of DB 832 absorbance, indicating that binding is occurring as a monomer and not a stacked species.

The G-rich strand of the promoter region of the c-MYC oncogene, d($AG_3TG_3TAG_3TG_3T$), forms a parallel propeller-type quadruplex in solution [29]. Before the addition of DB 832, the spectrum in the DNA wavelength region has a maximum at 260 nm, consistent with a parallel conformation of DNA (Figure 4.4). The addition of DB 832 causes a decrease in signal at 260 nm, but still results in a positive peak at that wavelength, indicating that DB 832 does not significantly rearrange the conformation of the DNA. No induced exciton splitting is observed in the wavelength region of DB 832 absorbance, indicating that binding is occurring as a monomer and not a stacked species.

d($TG_4T$) forms a four-stranded intermolecular quadruplex [30]. The addition of DB 832 does not change the CD spectrum of this DNA, suggesting that this compound does not bind to intermolecular quadruplexes (Figure 4.5). Binding to intermolecular

quadruplexes can result in undesirable genomic effects including end-end fusion of chromosomes.

CD spectra were also obtained with two duplex sequences, an AT-rich sequence, d(GCGAATTCGC) (Figure 4.6), and a GC-rich sequence, d $(GC)_7$ (Figure 4.7). AT-rich duplexes have been shown to have narrower grooves than GC-rich sequences [31]. In both cases, a small induced signal was observed, but the lack of exciton splitting suggests that binding as a stacked species is not occurring.

The absence of any significant exciton splitting when DB 832 is titrated into these DNA sequences suggests that DB 832 binds as a stacked species to mixed parallel/antiparallel quadruplex DNA with a high degree of selectivity.

**DB 832 Binds Selectively as a Stacked Species to a Mixed Parallel/Antiparallel Quadruplex with 5'- Diagonal/Lateral/Lateral-3' Loop Orientation**

In order to further examine the selectivity of DB 832 for the mixed parallel/antiparallel type of quadruplex structure, CD spectra were obtained for DB 832 with other DNA sequences that form hybrid quadruplex structures in solution.

Tel26, d$[A_3(G_3T_2A)_3G_3A_2]$, is a modified human telomeric sequence that has a mixed parallel/antiparallel hybrid structure as determined by NMR [32]. The structure of this sequence is identical to the hybrid conformation of the unmodified human telomere (Tel22) in the presence of postassium [18]. The CD spectrum of this sequence (Figure 4.8) has peaks at both 260 and 295 nm, suggesting the DNA has a hybrid structure, which is consistent with the NMR data. Upon addition of DB 832, the CD signal at both peaks initially increases slightly (up to a 2:1 compound:DNA ratio), then decreases, resulting in a final conformation similar in shape to the initial conformation, indicating that DB 832

does not cause significant rearrangement of DNA conformation upon binding. In the wavelength region of DB 832 absorbance, induced exciton splitting is observed, indicating that the compound is binding to this sequence as a stacked species.

Two other quadruplex DNA sequences have been shown by NMR to form mixed parallel/antiparallel structures in solution. bcl2MidG4Pu23-G15T/G16T, $d(G_3CGCG_3AG_2A_2T_2G_3CG_3)$, is a dual mutant sequence that forms the major quadruplex product found in the promoter region of the bcl-2 proto-oncogene sequence [15, 16]. Before the addition of DB 832, the spectrum in the DNA wavelength region has peaks at both 260 and 295 nm (Figure 4.9), suggesting the DNA has a mixed parallel/antiparallel structure, which is consistent with the NMR structure and previously published CD data [15, 16]. However, the 260 nm peak is larger relative to the 295 nm peak than is seen with the Tel22 or Tel26 sequences. The addition of DB 832 doesn't significantly change the shape of the spectra in the DNA region, indicating that the compound does not change the conformation of the DNA upon binding. In the wavelength region of DB 832 absorbance, a small induced CD signal is observed. However, the absence of exciton splitting indicates that the compound is likely binding as a monomer and not a stacked species.

The Tetrahymena telomeric sequence, $d(T_2G_4)_4$, has also been shown by NMR to form a mixed parallel/antiparallel quadruplex structure [10]. Before the addition of DB 832, the spectrum in the DNA wavelength region has peaks at both 260 and 295 nm, consistent with the formation of a mixed parallel/antiparallel structure. Like the bcl-2 proto-oncogene sequence, the signal at 260 nm is large relative to the signal at 295 nm. Upon addition of DB 832, the peak at 260 nm shifts to higher wavelength and has a large

decrease in magnitude (Figure 4.10). The presence of a residual peak suggests that the final structure is still a mixed hybrid conformation. An induced exciton is seen in the wavelength region of DB 832 absorbance. However, it is much smaller in magnitude than the signal seen when DB 832 is titrated with either Tel22 or Tel26.

Although these two sequences form mixed parallel/antiparallel hybrid quadruplex structures, they are not identical to the hybrid conformation formed by the human telomeric sequences Tel22 and Tel 26 [18, 32]. The three loops of the Tel22 and Tel26 sequences are oriented diagonal/lateral/lateral as read from the 5' to 3' direction. The loops of the TetTel and bcl2MidG4Pu23-G15T/G16T sequences are oriented lateral/lateral/diagonal from 5' to 3'. These two sequences also have a different pattern of glycosidic orientation of the sugars than Tel22 and Tel26. The relative difference in magnitude of the CD signals at 260 nm vs. 295 nm for TetTel and bcl2MidG4Pu23-G15T/G16T as compared to Tel22 and Tel26 may be indicative of this difference in structure. If this is the case, the fact that the addition of DB 832 to TetTel results in a smaller signal at 260 nm as compared to 295 nm, suggests that DB 832 may be inducing a conformation change of TetTel from a 5'-lateral/lateral/diagonal-3' hybrid to a 5'-diagonal/lateral/lateral-3' hybrid quadruplex. The small amount of exciton splitting seen with this sequence may be due to DB 832 binding as a stacked species to the rearranged conformation.

These results suggest that DB 832 binds selectively as a stacked species to the specific 5'-diagonal/lateral/lateral-3' type of mixed parallel/antiparallel structure formed by the human telomere and modified human telomeric sequences.

**Recognition of Quadruplex DNA as a Stacked Species is Sensitive to Compound Structure**

A series of DB 832 analogs was studied to determine how structural variations affect binding as a stacked species to the human telomere. The induced exciton CD signal is sensitive to the relative placement of the heterocyclic rings on the compound. DB 1093 is an isomer of DB 832 in which the furan groups are not adjacent. This compound does not exhibit any change in CD signal when titrated into human telomeric DNA (Figure 4.11). This suggests that recognition of the quadruplex grooves may occur via a bifurcated hydrogen bond between the two adjacent furan oxygens and a G-$NH_2$ amino group hydrogen in the quadruplex grooves.

DB 914, a derivative of DB 832 with an additional phenyl ring, exhibits a similar, but somewhat weaker, CD pattern than DB 832 when titrated into human telomeric DNA (Figure 4.12). This observation further suggests that the adjacent furans are involved in H-bonding interactions for recognition of quadruplex grooves. Additional recognition sites between DB 832 and DB 914 and the quadruplex groove may arise from hydrogen bonding between N3 of the guanine and an amidine hydrogen from the DB 832 molecule, as well as electrostatic interaction between amidines and phosphate groups on the DNA backbone. DB 1324 is an analog of DB 914 in which the amidine groups are replaced with guanidinium groups. When DB 1324 is titrated into human telomeric DNA, large changes in the CD spectra occur in the DNA region, suggesting a major structural change is occurring in the DNA (Figure 4.13). However, no exciton splitting in the induced region occurs, suggesting that this compound binds as a monomer. This further suggests that the amidine groups are involved in recognition of the groove as a stacked species.

Thiophene analogs of DB 832 and DB 914 were also studied. DB 1438 (Figure 4.14) and DB 1463 (Figure 4.15) are DB 832 analogs that have one furan replaced by a thiophene, and DB 1450 (Figure 4.16) is a DB 832 analog with both furans replaced by thiophenes. DB 1255 (Figure 4.17) is a dithiophene analog of DB 914. Sulfur is not as electronegative as oxygen and therefore has weaker hydrogen bonding interactions than oxygen. All four sulfur analogs exhibit a smaller magnitude of exciton splitting than the respective bifuryl compounds, which may be due to lower binding affinity from decreased hydrogen-bonding interactions or from decreased stacking interactions due to the slight change in the curvature of the compounds. However, the disubstituted DB 1450 has a significantly higher amount of exciton splitting than the monosubstituted compounds DB 1438 and DB1463. Thiophene compounds are known to have better stacking properties than furan, which may account for this difference.

Other bifuryl compounds were studied, including DB 1256 (Figure 4.18), DB 1246 (Figure 4.19), DB 934 (Figure 4.20) and DB 1003 (Figure 4.21) None of these compounds exhibited exciton splitting with human telomeric DNA at a 4:1 compound/DNA ratio. DB 934 and 1246 are analogs of DBA 832 and DB 914, respectively, in which a pyridine has been substituted for the phenyl ring. The fact that substitution of a single atom eliminates the stacking interaction of the compound shows that recognition of the quadruplex groove as a stacked species is extremely sensitive to the compound structure.

CD titrations with human telomeric DNA were also performed with the trifuran compounds DB 657 (Figure 4.22), DB 659 (Figure 4.23), and DB 1315 (Figure 4.24). DB 1315 is the only one that exhibits exciton splitting. It has an amidine-phenyl-furan-furan

arrangement. Every compound studied that contained this motif exhibited some degree of exciton splitting. This sequence of heterocycles could serve as a starting point for the design of other compounds that recognize quadruplex DNA as a stacked species.

**Conclusions**

The unique structural features of quadruplexes present an opportunity to target DNA in a structure-specific manner, leading to increased selectivity for quadruplex over duplex DNA, as well as selectivity for a particular quadruplex structure over other quadruplexes. Selectivity of a compound for its target quadruplex structure is important in order to reduce cytotoxicity from duplex-binding as well as prevent drug loss from binding to non-targeted quadruplex sites.

DB 832 is a heterocyclic diamidine that binds to human telomeric DNA as a stacked species. It is highly selective for quadruplex binding, showing virtually no binding to duplex DNA. DB 832 also binds very selectively as a stacked species to the 5'-diagonal/lateral/lateral-3' hybrid quadruplex structure which is preformed or induced by DB 832 in human telomere and modified human telomeric DNA sequences. The induced CD signals produced by DB 832 are very sensitive to DNA and compound structure. DB 832 does not exhibit exciton splitting with either AT- or GC-rich duplex DNA sequences (d[GCGAATTCGC] and d[$(GC)_7$], respectively) nor does it exhibit any significant induced CD signal with sequences that form parallel (c-MYC), antiparallel chair (TBA), antiparallel basket (d[$(G_2T_4)_3G_2$]) or intermolecular ($TG_4T$) quadruplexes or with the 5'-lateral/lateral/diagonal-3' hybrid structure formed by bcl2MidG4Pu23-G15T/G16T. DB 832 does induce a small amount of exciton splitting with TetTel which forms the 5'-lateral/lateral/diagonal-3' hybrid quadruplex. However, the change in CD

signal in the DNA region suggests that DB 832 may be inducing a conformation change to the 5'-diagonal/lateral/lateral-3' hybrid, consistent with the selectivity of DB 832 binding as a stacked species to this particular quadruplex conformation.

Circular dichroism studies with a series of DB 832 analogs show that the binding mode of these compounds is very sensitive to the relative placement and orientation of the heterocyclic systems. The results suggest that this series of compounds must contain two adjacent furan groups, possibly for H-bonding recognition of the grooves as a stacked species. Additional recognition sites between DB 832 and the quadruplex groove may arise from hydrogen bonding between N3 of the guanine and an amidine hydrogen from the DB 832 molecule, as well as electrostatic interaction between amidines and phosphate groups on the DNA backbone. NMR studies to determine the orientation of the DB 832 molecules relative to quadruplex groove are currently in progress.

The unique binding mode of DB 832 as well as its selectivity for its DNA target may allow it to serve as the starting point for the design of a new class of highly selective groove-binding molecules. Nonintercalating, stacked species are of particular interest for recognition of quadruplexes since studies with duplex DNAs show that compounds that bind as stacked dimers have increased binding affinity and selectivity over similar compounds that bind as monomers. Similar stacking in the grooves of quadruplex DNA structures would appear to be a favorable way to selectively recognize quadruplexes with optimum interactions, perhaps employing an induced fit component, between the stacked heterocycles and the G bases of the quadruplex tetrads.

Potentially, the individual monomer units could be covalently linked, dramatically increasing the affinity and selectivity of the compound for human telomeric DNA,

leading to enhanced telomerase inhibition and anti-protozoan activity with decreased cytotoxic side effects.

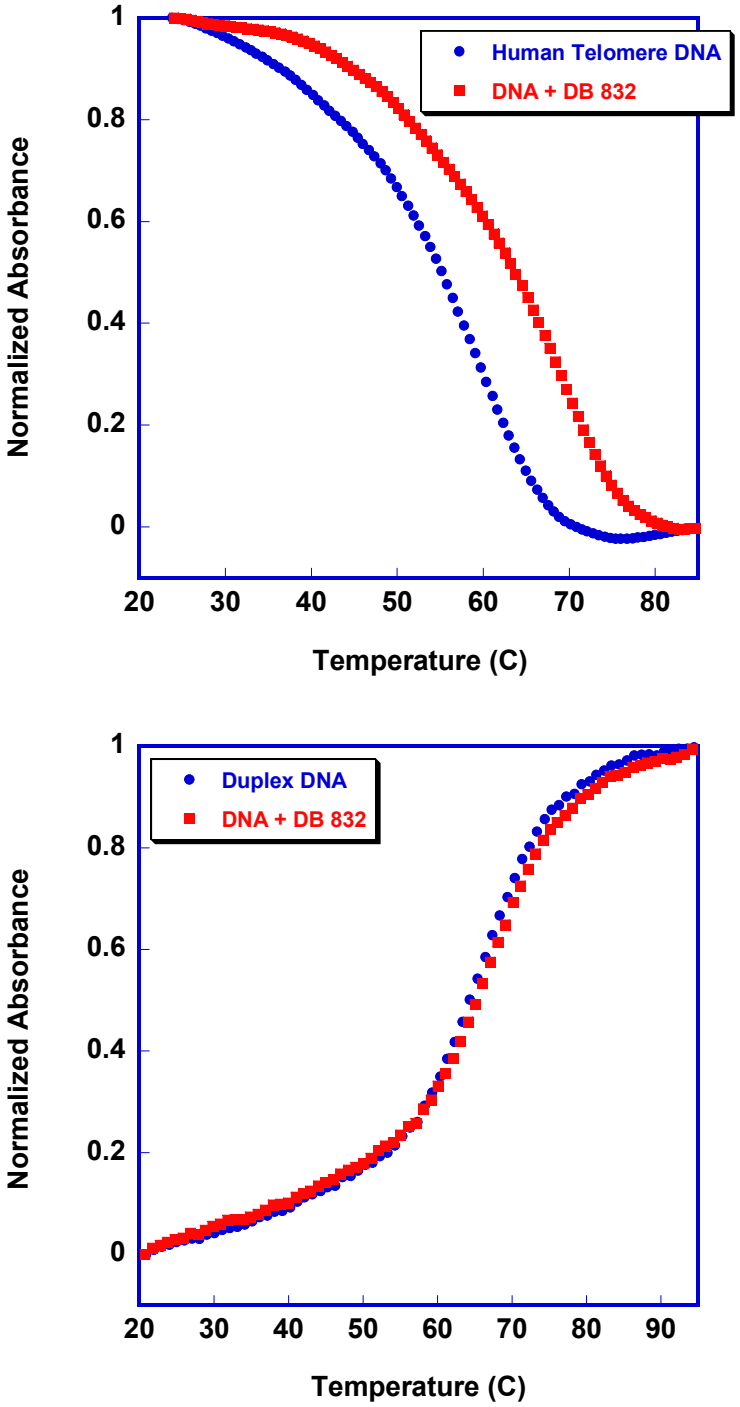


Figure 4.1 UV melting profiles of the human telomere sequence, d[$AG_3(T_2AG_3)_3$], monitored at 295 nm (top) and the hairpin duplex, d(CGAGATCAAAAGATCTCG), monitored at 260 nm (bottom) in the absence and presence of DB 832 in 50 mM KCl. DNA concentration was 2.7 μM and DB 832:DNA ratio was 2:1 for both DNAs. DB 832 increases the melting temperature of the human telomere sequence by approximately 10°C, while it has a negligible effect on the melting temperature of the duplex sequence.

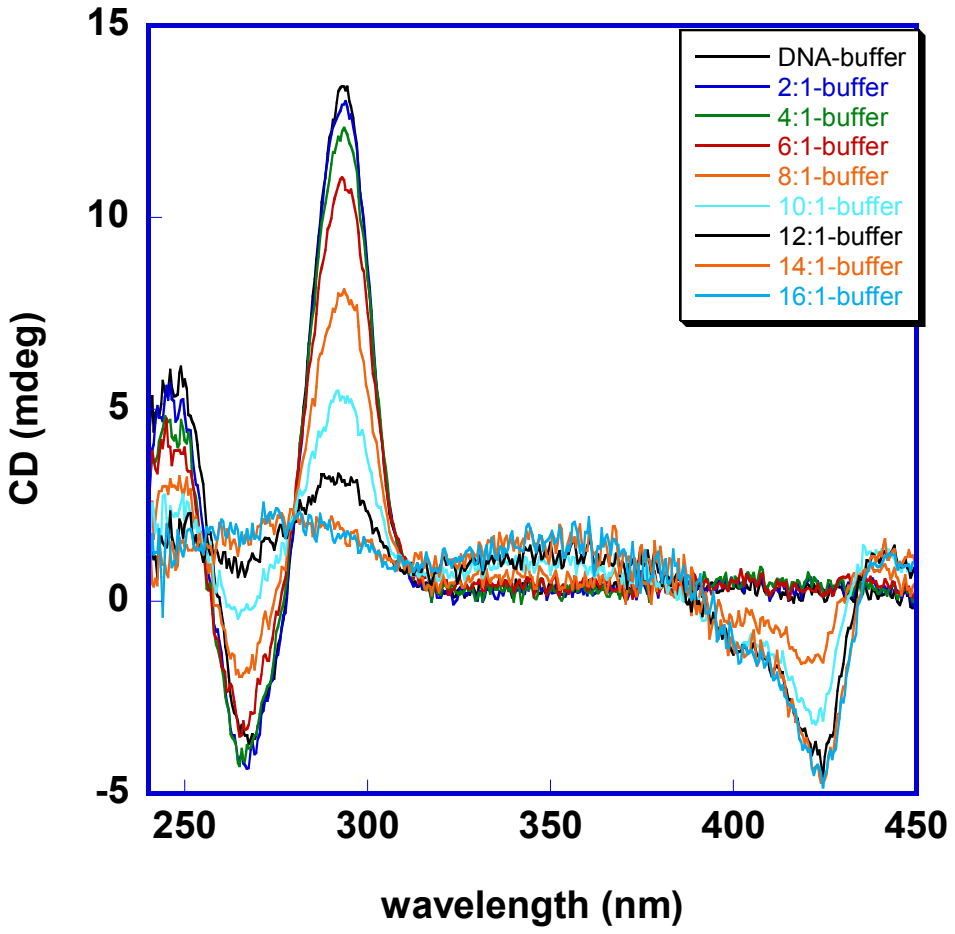


Figure 4.2 CD spectra of DB 832 titrated into 2.3 μM Thrombin Binding Aptamer, d($G_2T_2G_2TGTG_2T_2G_2$), in HEPES buffer containing 50 mM KCl. Compound:DNA ratios ranged from 2:1 to 16:1.

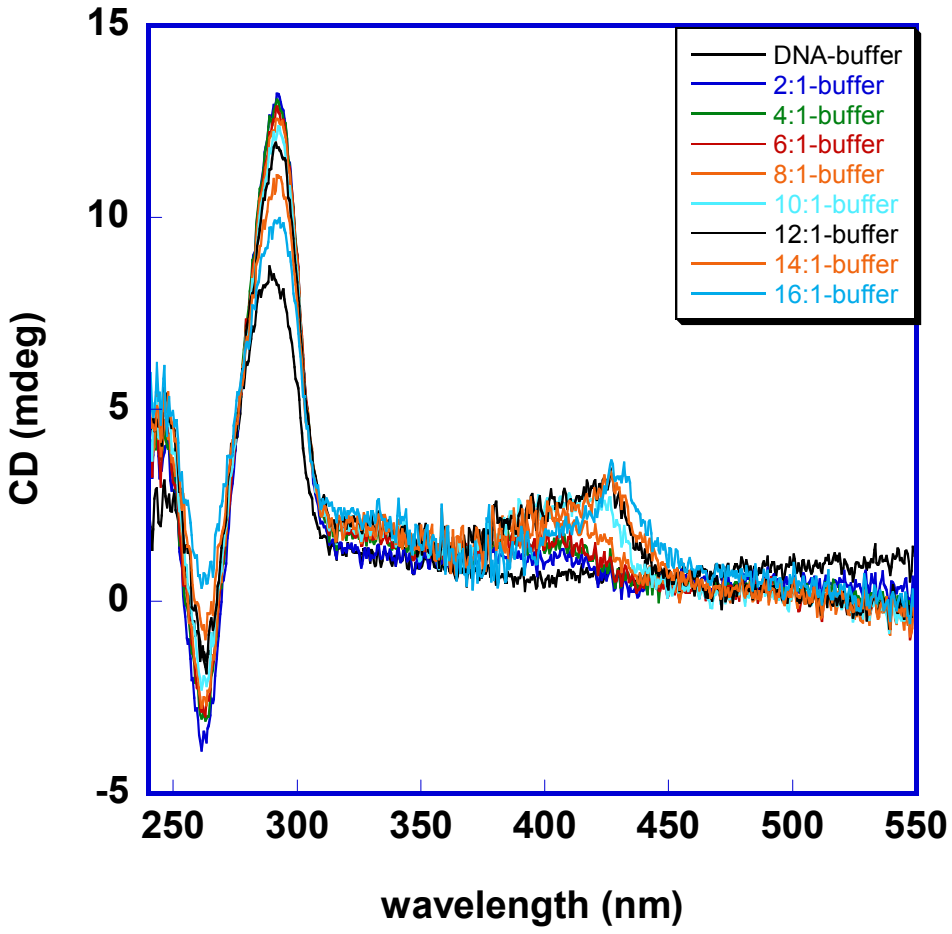


Figure 4.3 CD spectra of DB 832 titrated into 2.7 μM $d(G_2T_4)_3G_2$, in HEPES buffer containing 50 mM KCl. Compound:DNA ratios ranged from 2:1 to 16:1

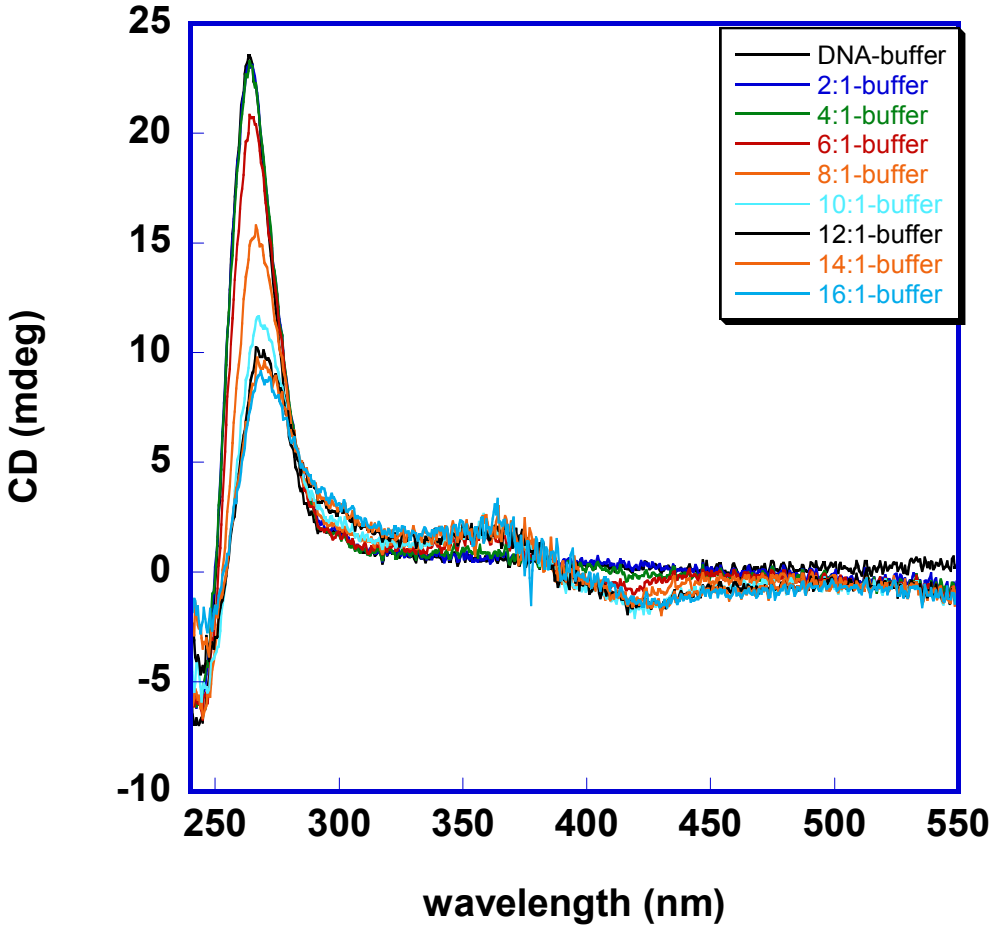


Figure 4.4 CD spectra of DB 832 titrated into 3.4 μM Pu18, promoter region of the c-MYC oncogene, d($AG_3TG_3TAG_3TG_3T$), in HEPES buffer containing 50 mM KCl. Compound:DNA ratios ranged from 2:1 to 16:1.

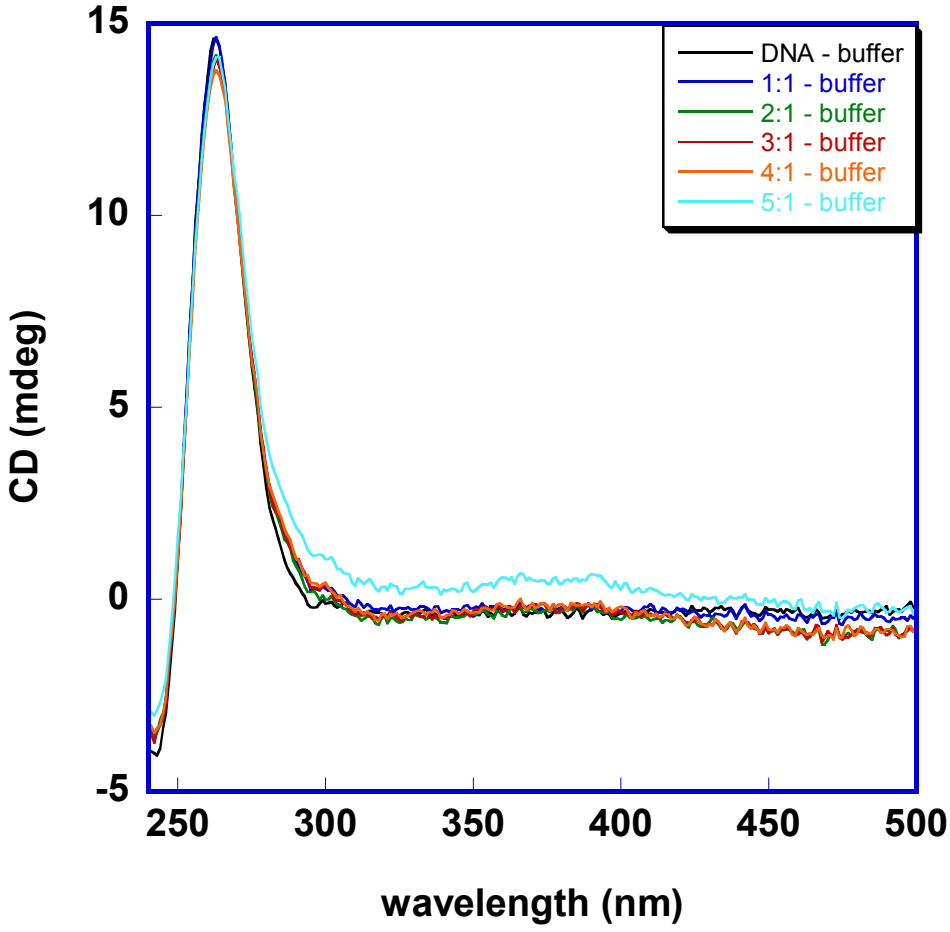


Figure 4.5 CD spectra of DB 832 titrated into d[TGGGGT] (single strand conc. 16 μM) in phosphate buffer containing 70 mM $K^+$. Compound:DNA ratios ranged from 1:1 to 5:1.

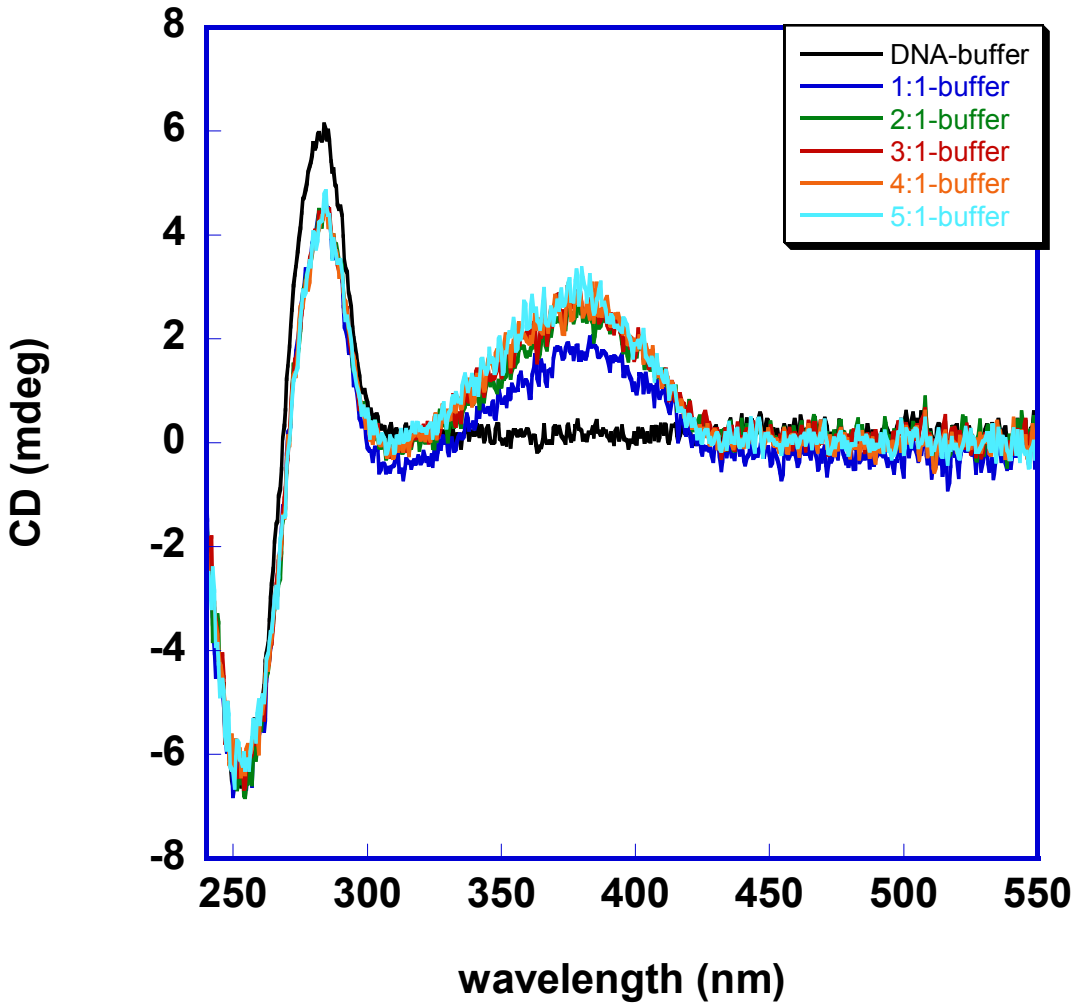


Figure 4.6 CD spectra of DB 832 titrated into 4.6 µM d[GCGAATTCGC] in HEPES buffer containing 50 mM KCl. Compound:DNA ratios ranged from 1:1 to 5:1.

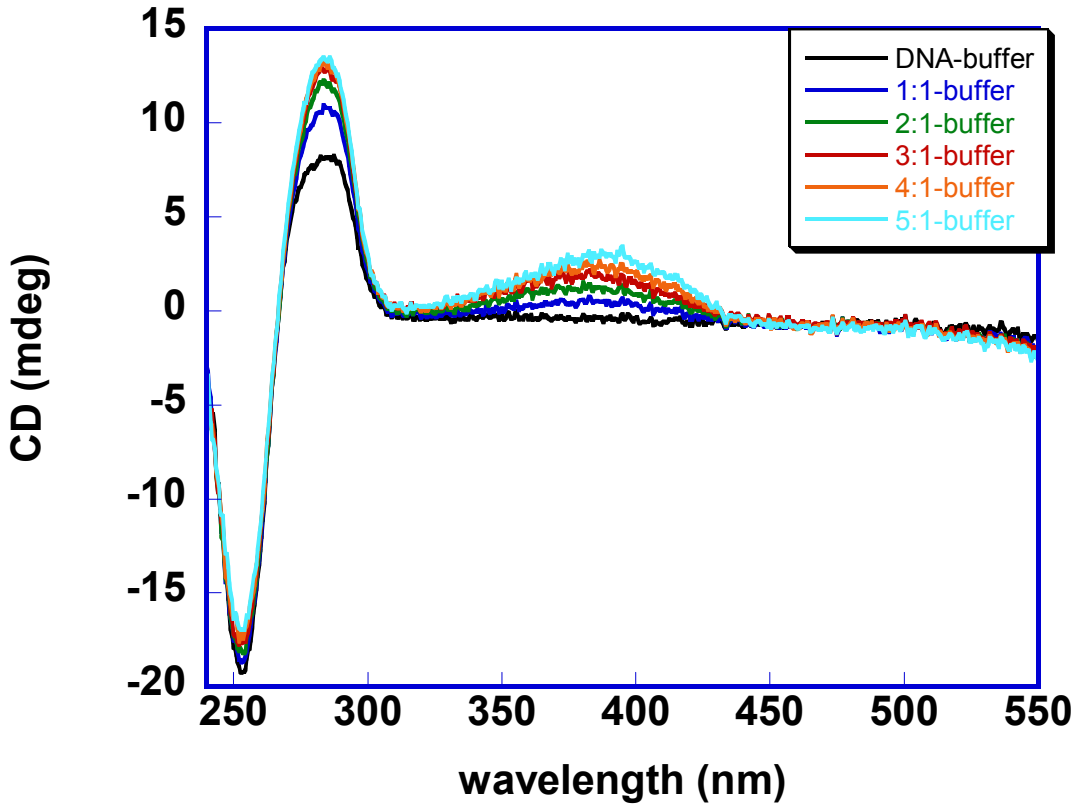


Figure 4.7 CD spectra of DB 832 titrated into 5.6μM d[$(GC)_7$] in HEPES buffer containing 50 mM KCl. Compound:DNA ratios ranged from 1:1 to 5:1.

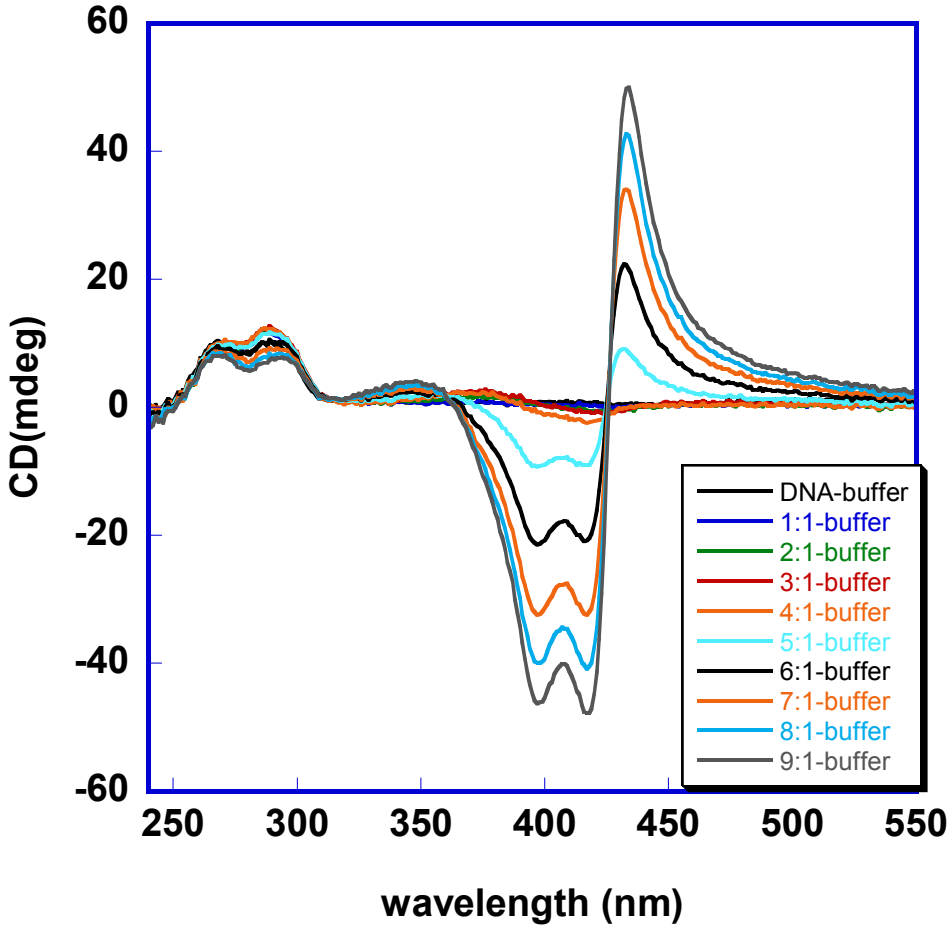


Figure 4.8 CD spectra of DB 832 titrated into 3.1 μM Tel26 modified human telomeric sequence, d[$A_3(G_3T_2A)_3G_3A_2$], in HEPES buffer containing 50 mM KCl. Compound:DNA ratios ranged from 1:1 to 9:1.

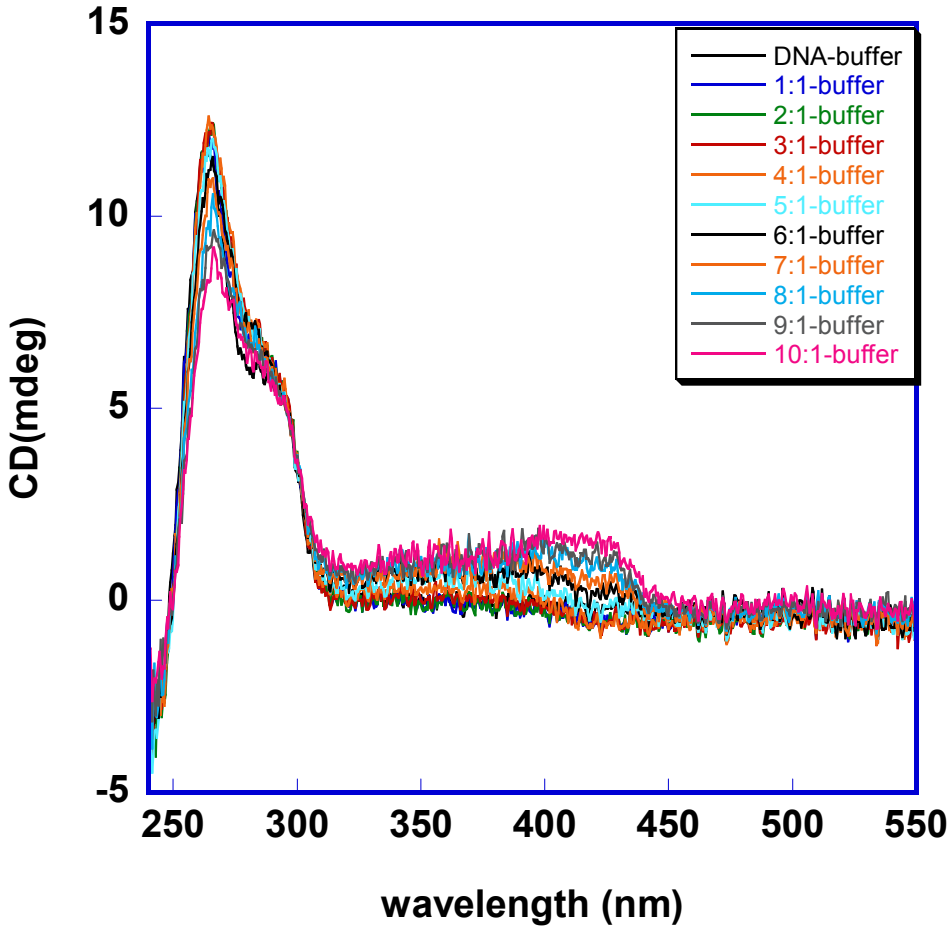


Figure 4.9 CD spectra of DB 832 titrated into 2.3 μM bcl2MidG4Pu23-G15T/G16T, d($G_3CGCG_3AG_2A_2T_2G_3CG_3$), a dual mutant sequence that forms the major quadruplex product found in the promoter region of the bcl-2 proto-oncogene sequence, in HEPES buffer containing 50 mM KCl. Compound:DNA ratios ranged from 1:1 to 10:1

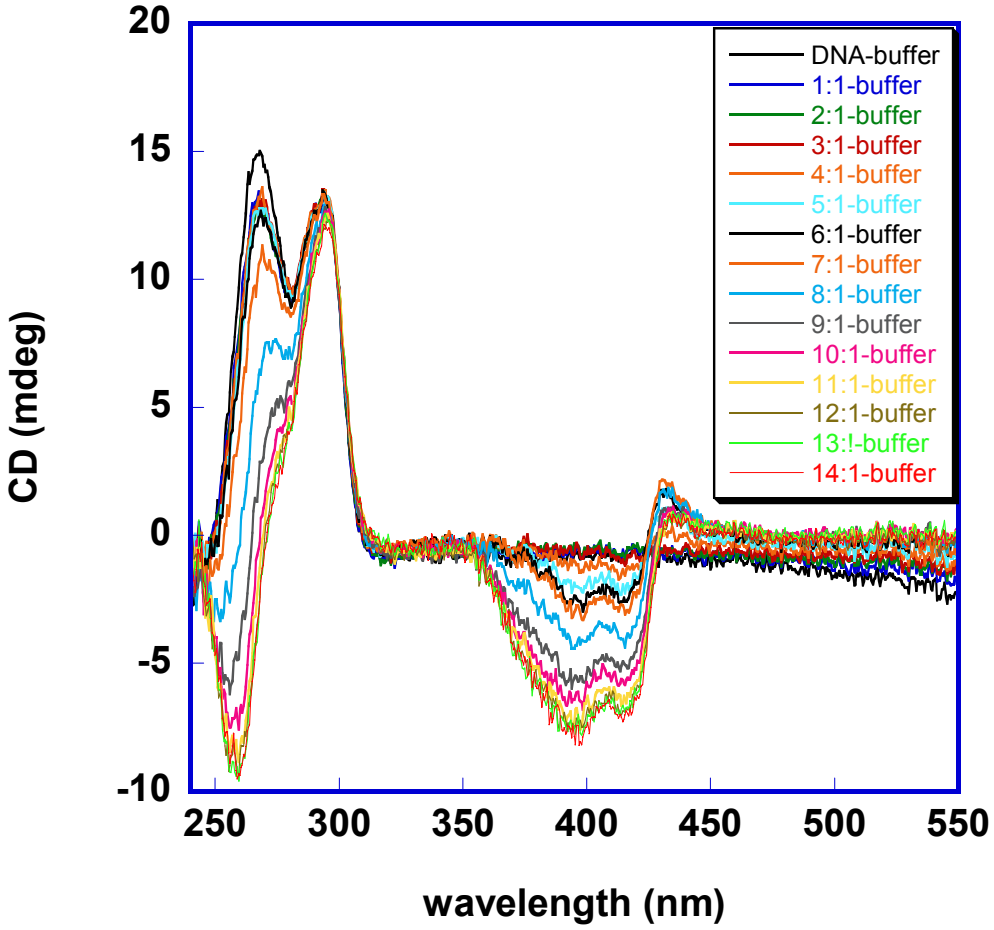


Figure 4.10 CD spectra of DB 832 titrated into 3.9 μM Tetrahymena telomeric sequence, $d(T_2G_4)_4$, in HEPES buffer containing 50 mM KCl. Compound:DNA ratios ranged from 1:1 to 14:1.

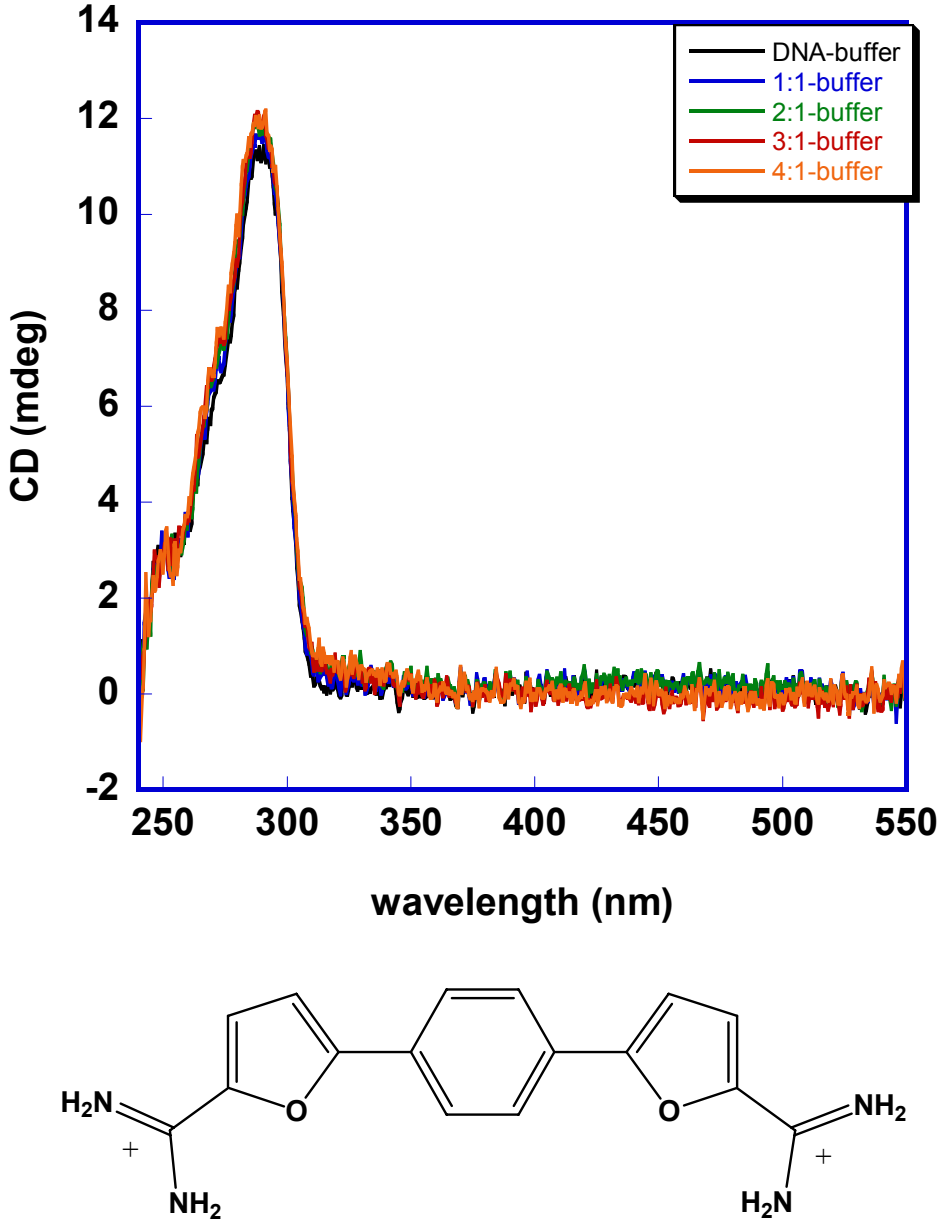


Figure 4.11 CD spectra of DB 1093 titrated into 3.8 μM human telomeric sequence, d[$AG_3(T_2AG_3)_3$], in HEPES buffer containing 50 mM KCl. Compound:DNA ratios ranged from 1:1 to 4:1.

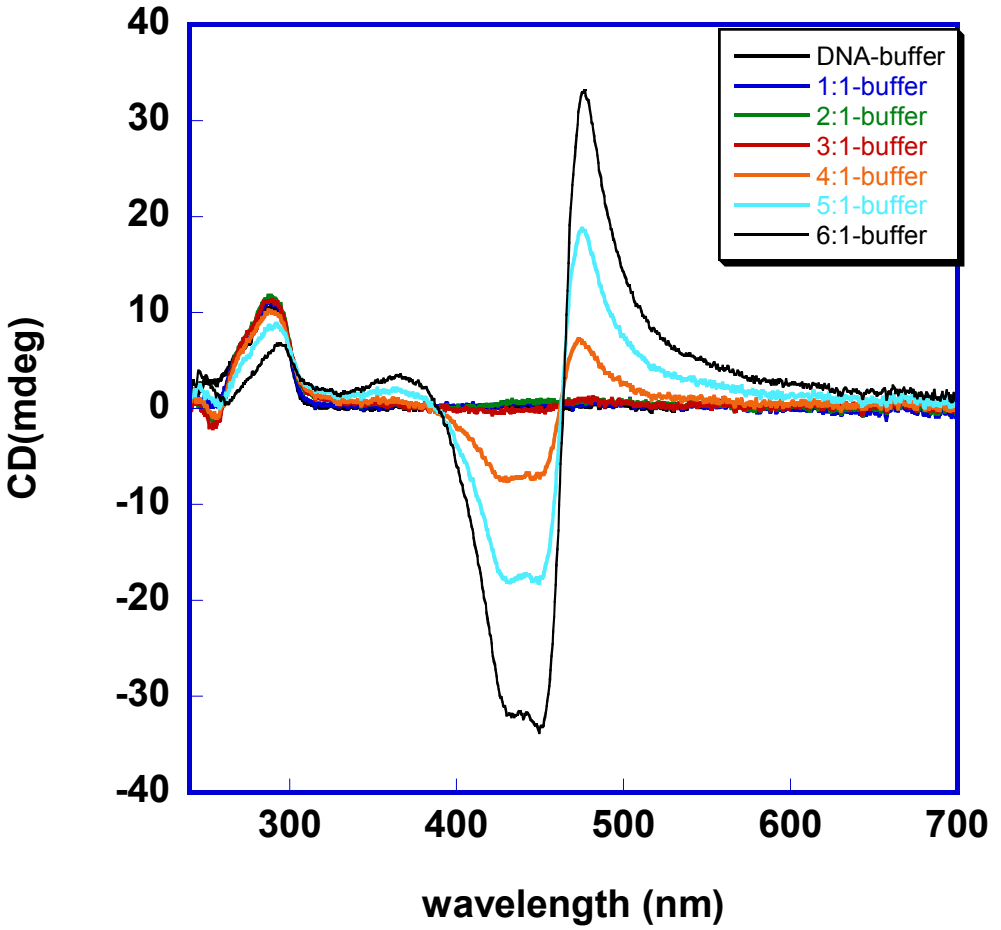


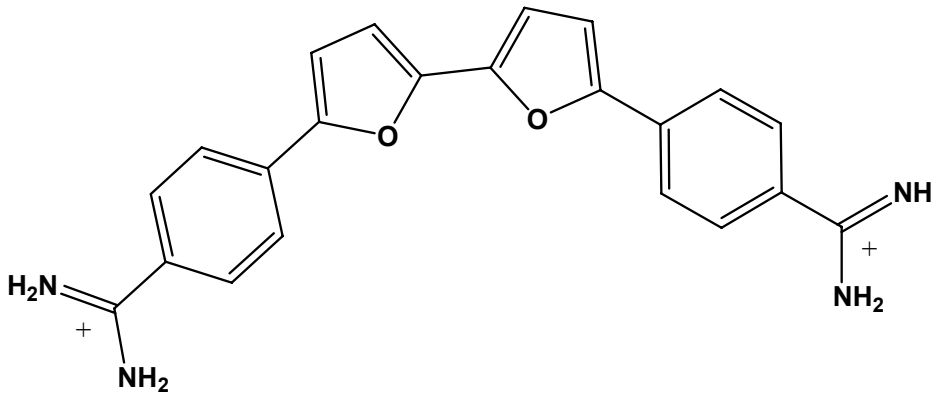


Figure 4.12 CD spectra of DB 914 titrated into 3.5 μM human telomeric sequence, $d[AG_3(T_2AG_3)_3]$, in HEPES buffer containing 50 mM KCl. Compound:DNA ratios ranged from 1:1 to 6:1.

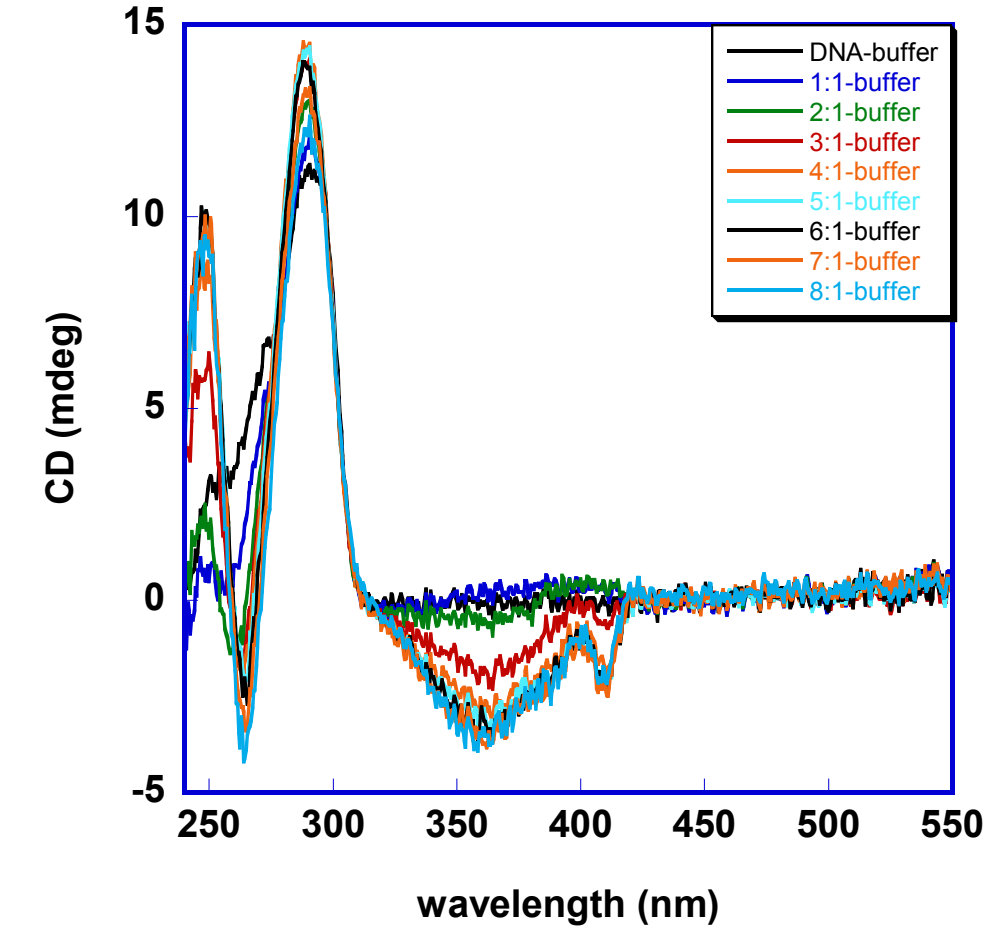


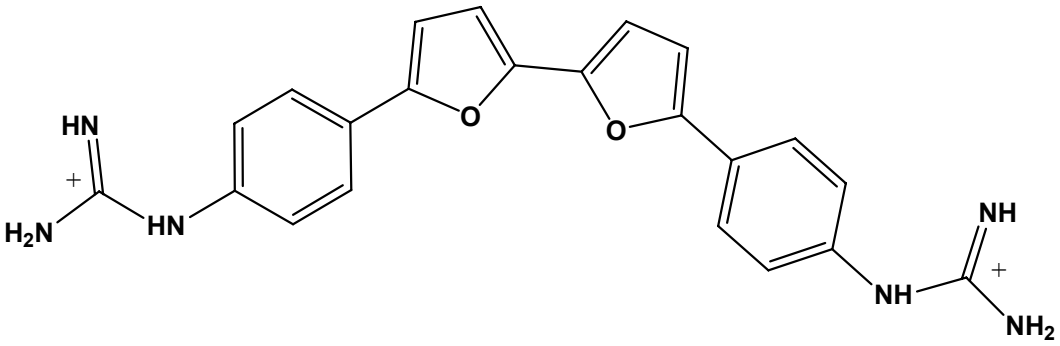


Figure 4.13 CD spectra of DB 1324 titrated into 3.6 μM human telomeric sequence, d[$AG_3(T_2AG_3)_3$], in HEPES buffer containing 50 mM KCl. Compound:DNA ratios ranged from 1:1 to 8:1.

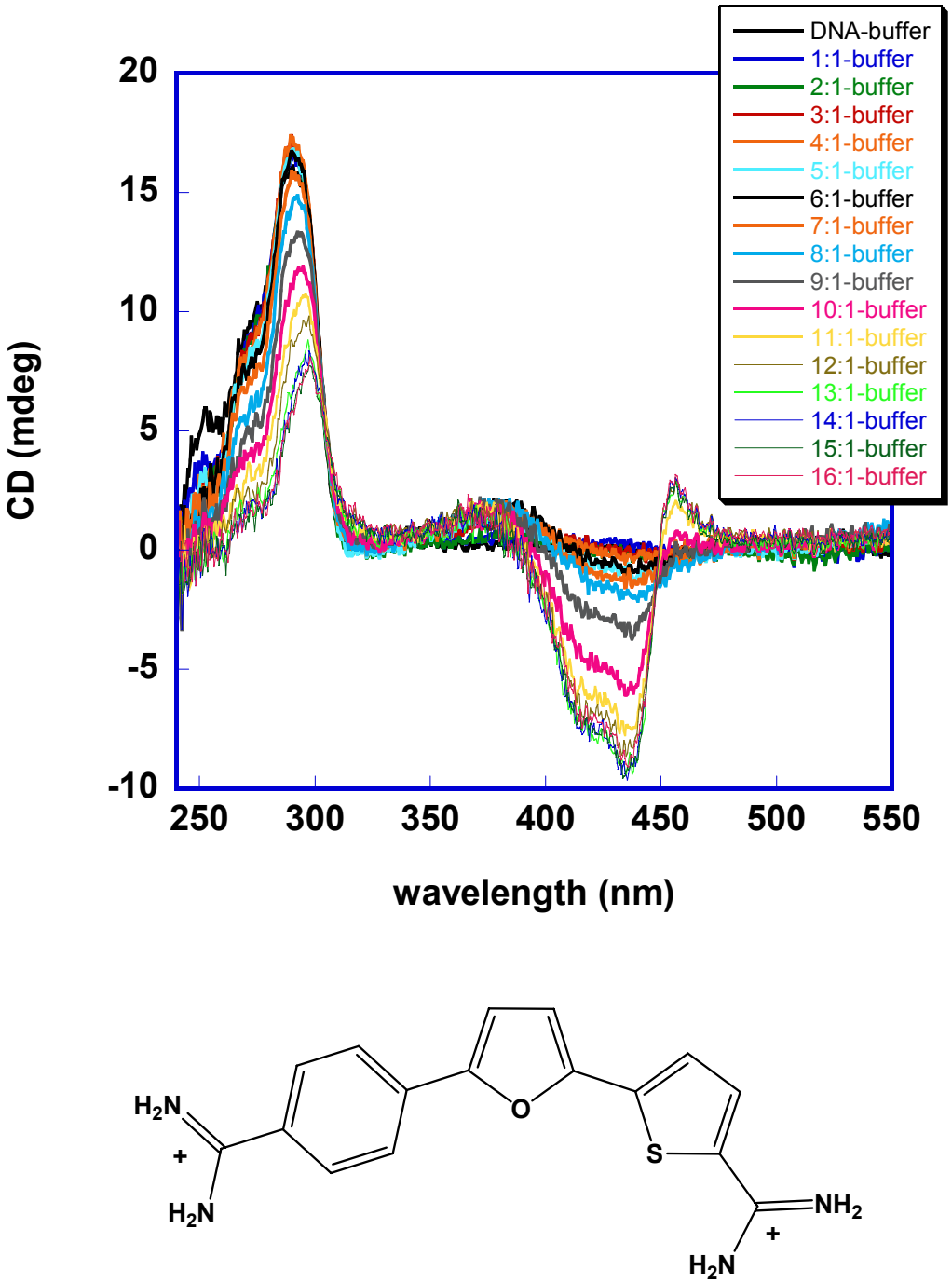


Figure 4.14 CD spectra of DB 1438 titrated into 5.1 μM human telomeric sequence, d[$AG_3(T_2AG_3)_3$], in HEPES buffer containing 50 mM KCl. Compound:DNA ratios ranged from 1:1 to 16:1.

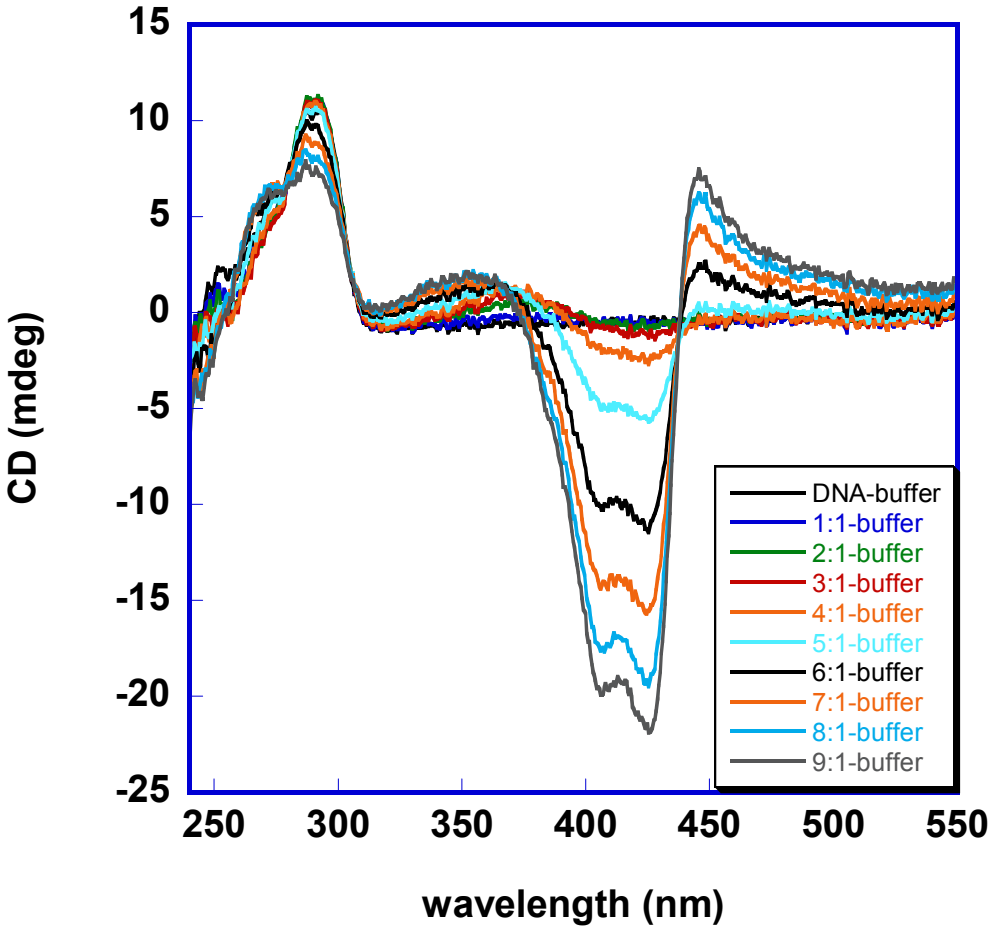


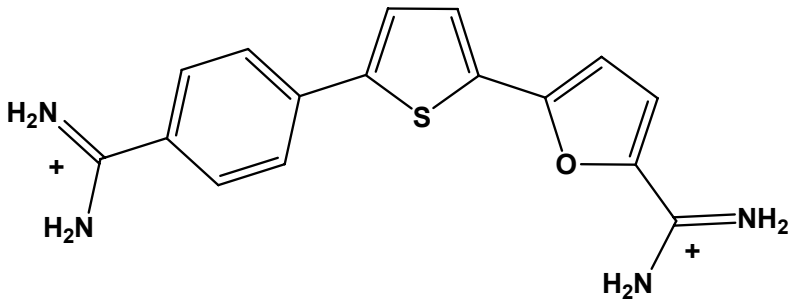


Figure 4.15 CD spectra of DB 1463 titrated into 3.6 μM human telomeric sequence, d[$AG_3(T_2AG_3)_3$], in HEPES buffer containing 50 mM KCl. Compound:DNA ratios ranged from 1:1 to 9:1.

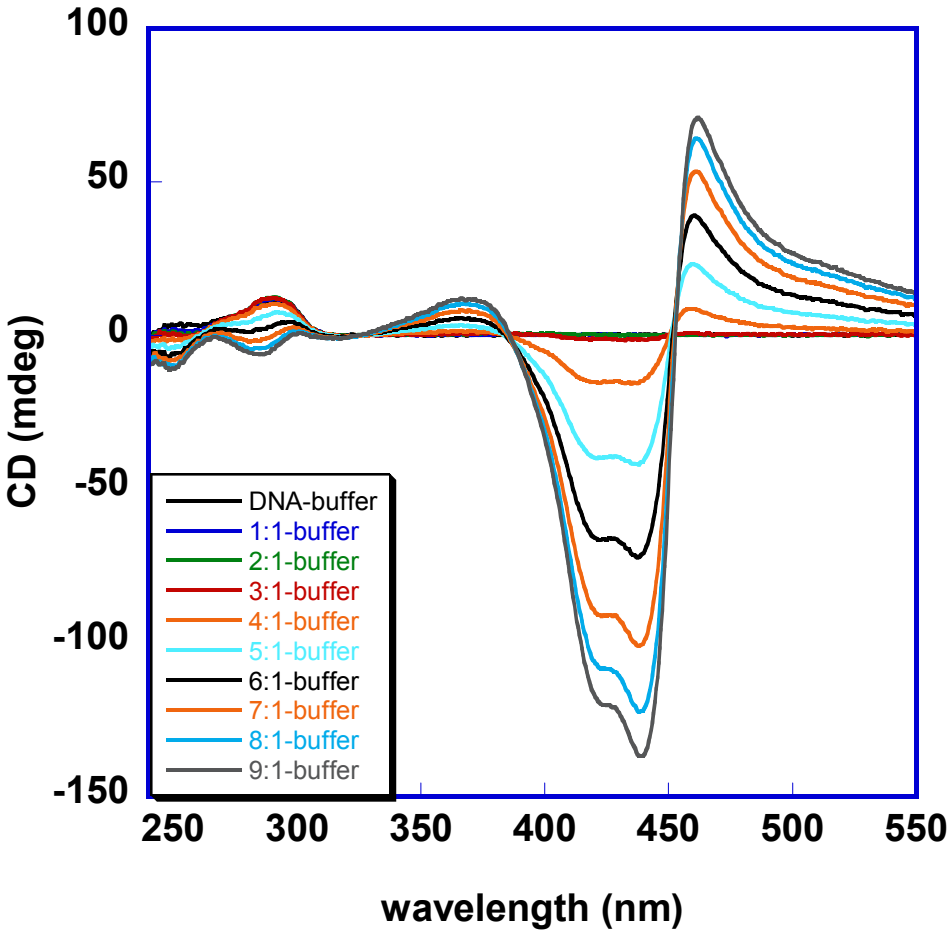


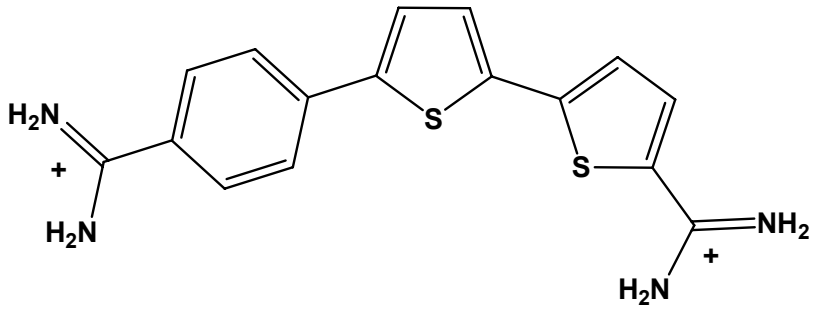


Figure 4.16 CD spectra of DB 1450 titrated into 3.6 µM human telomeric sequence, d[$AG_3(T_2AG_3)_3$], in HEPES buffer containing 50 mM KCl. Compound:DNA ratios ranged from 1:1 to 9:1.

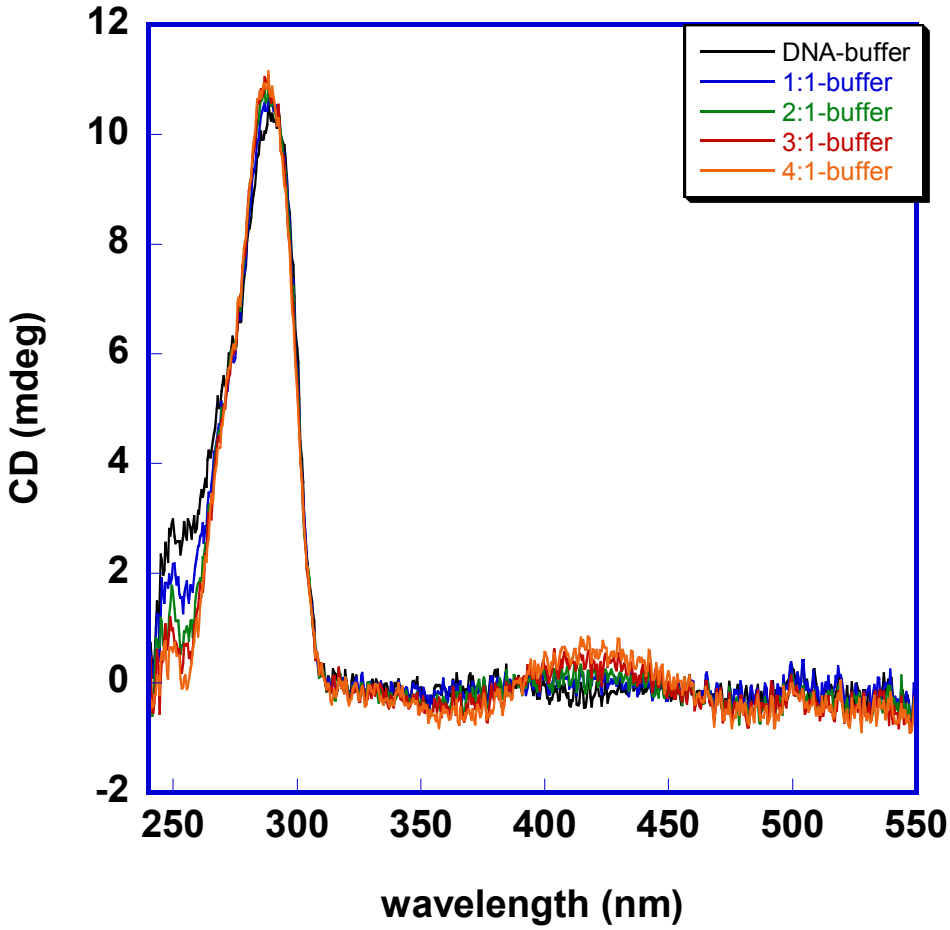


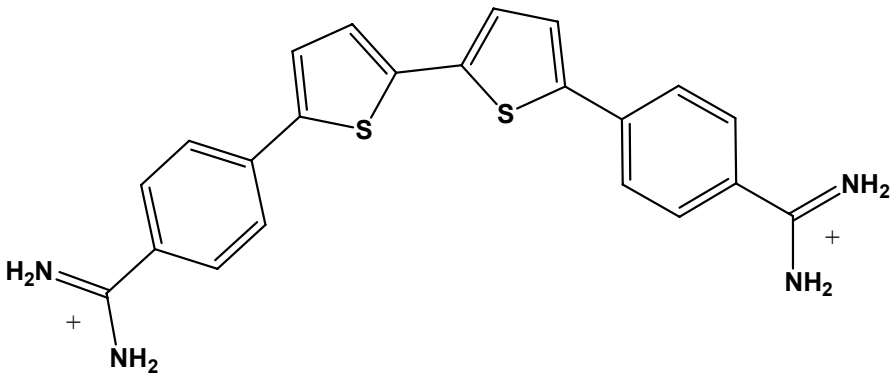


Figure 4.17 CD spectra of DB 1255 titrated into 3.6 μM human telomeric sequence, $d[AG_3(T_2AG_3)_3]$, in HEPES buffer containing 50 mM KCl. Compound:DNA ratios ranged from 1:1 to 4:1.

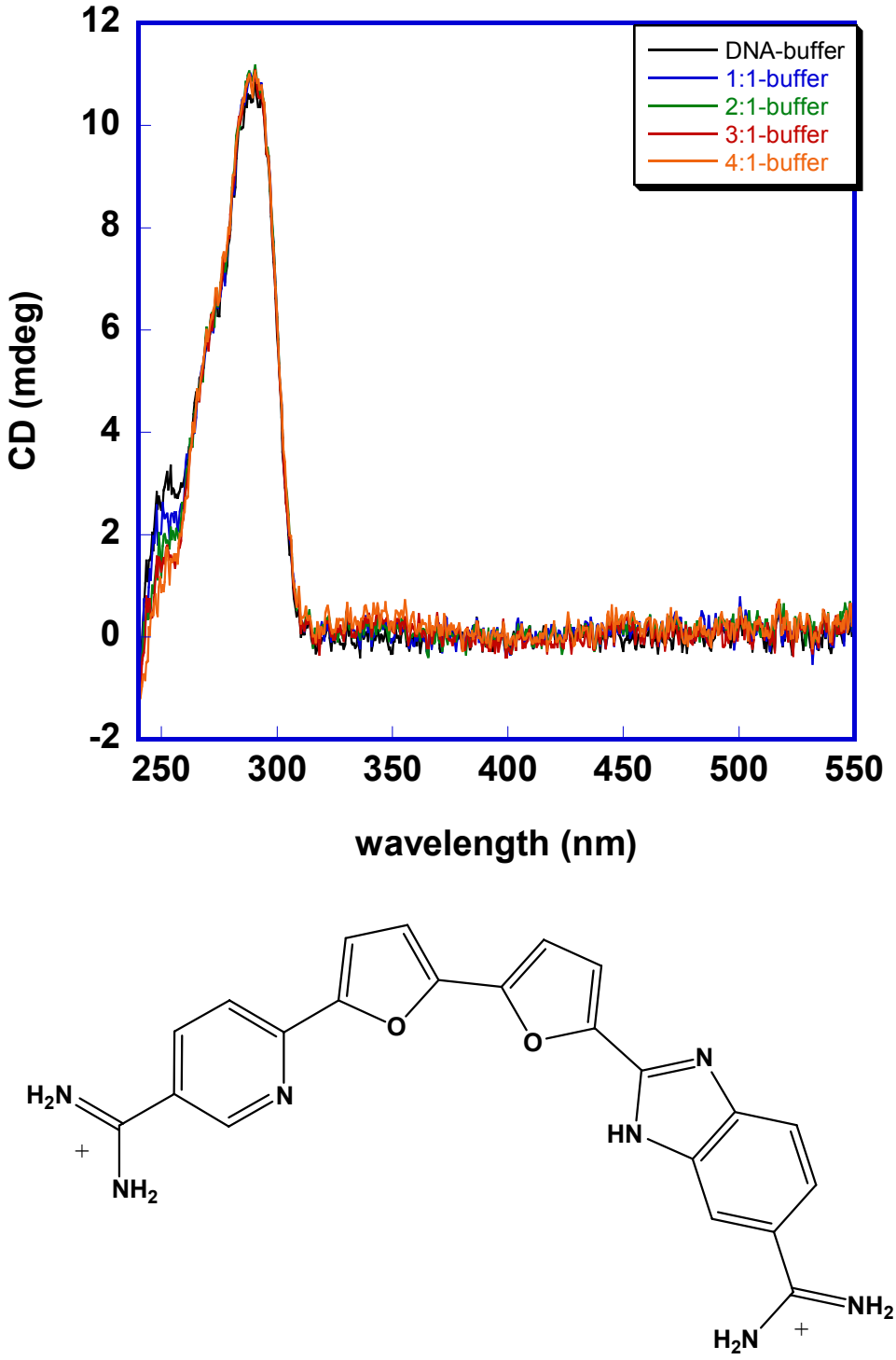


Figure 4.18 CD spectra of DB 1256 titrated into 3.7 μM human telomeric sequence, d[$AG_3(T_2AG_3)_3$], in HEPES buffer containing 50 mM KCl. Compound:DNA ratios ranged from 1:1 to 4:1.

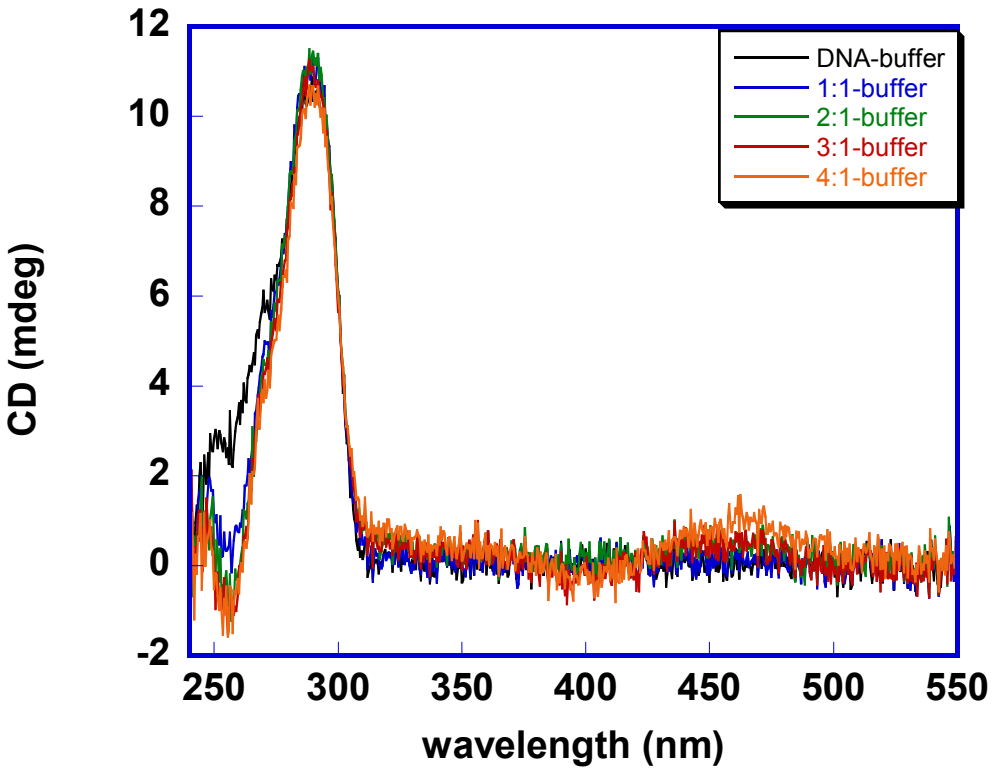


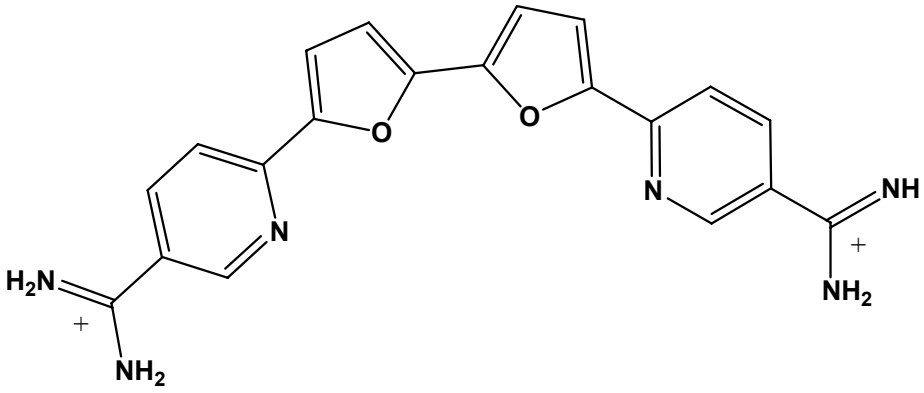


Figure 4.19 CD spectra of DB 1246 titrated into 3.6 µM human telomeric sequence, d[$AG_3(T_2AG_3)_3$], in HEPES buffer containing 50 mM KCl. Compound:DNA ratios ranged from 1:1 to 4:1.

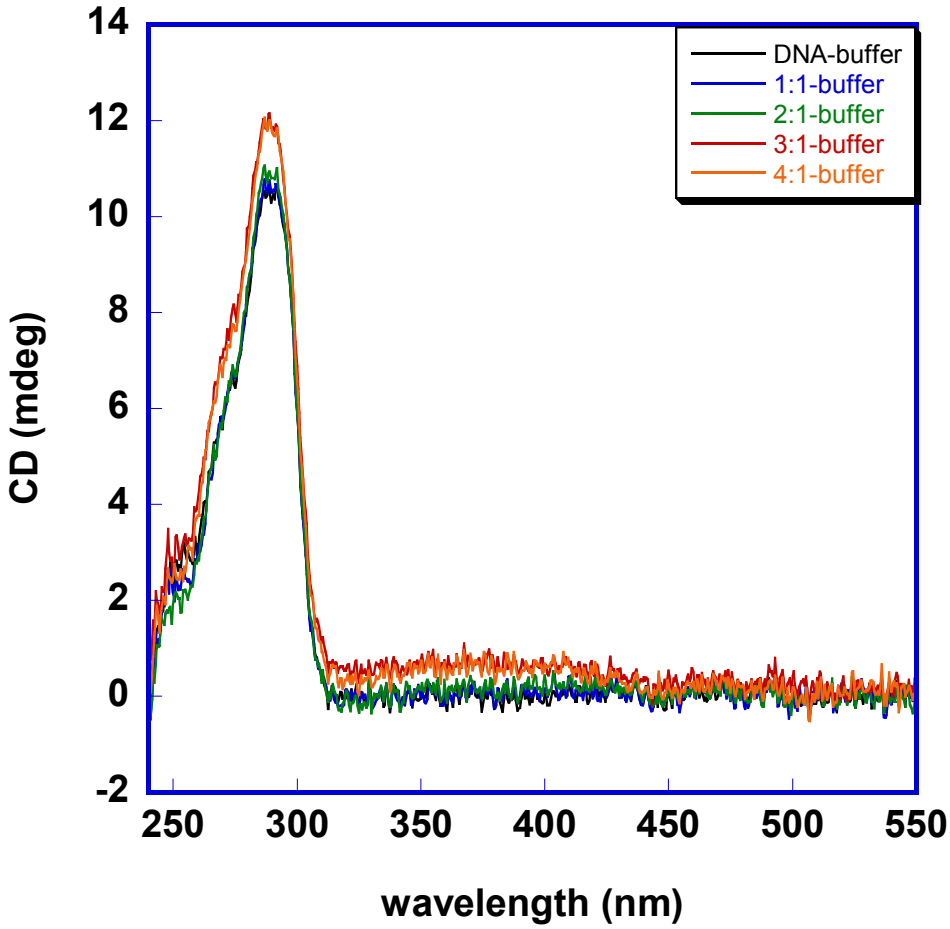


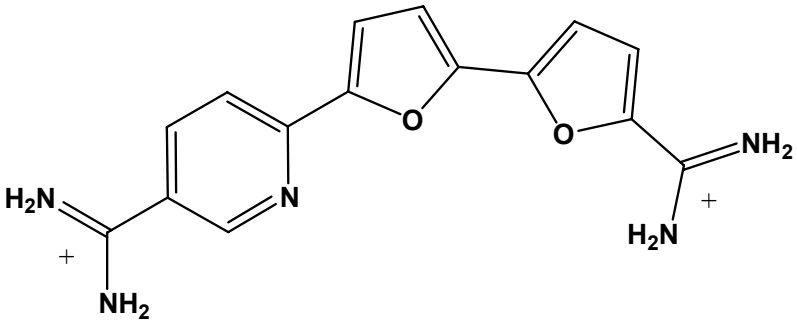


Figure 4.20 CD spectra of DB 934 titrated into 3.6 μM human telomeric sequence, d[$AG_3(T_2AG_3)_3$], in HEPES buffer containing 50 mM KCl. Compound:DNA ratios ranged from 1:1 to 4:1.

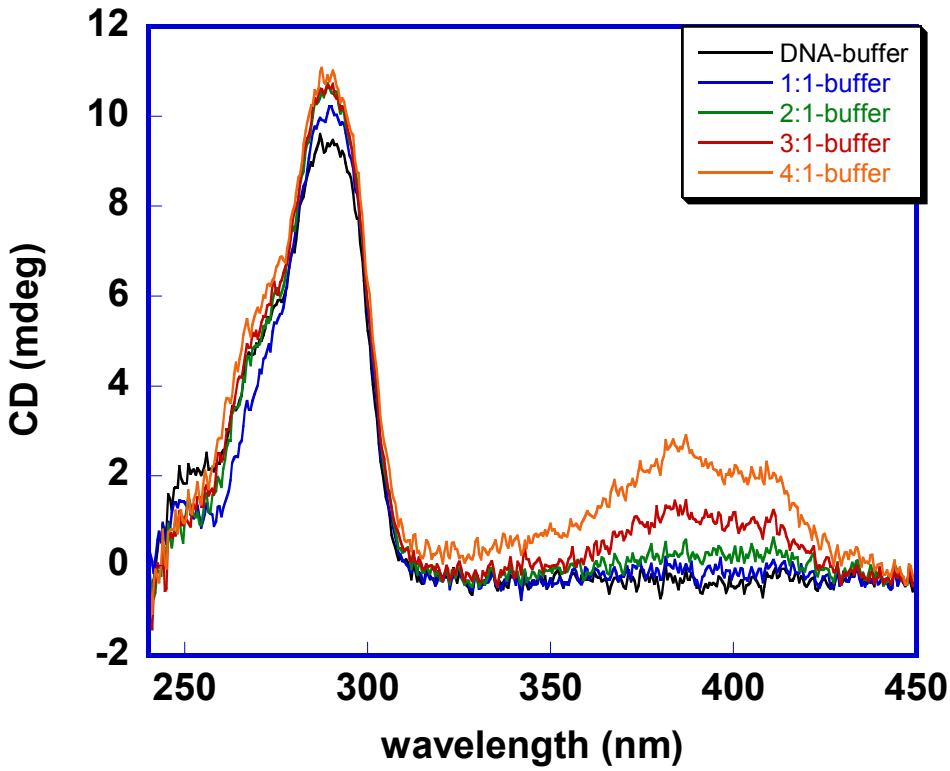


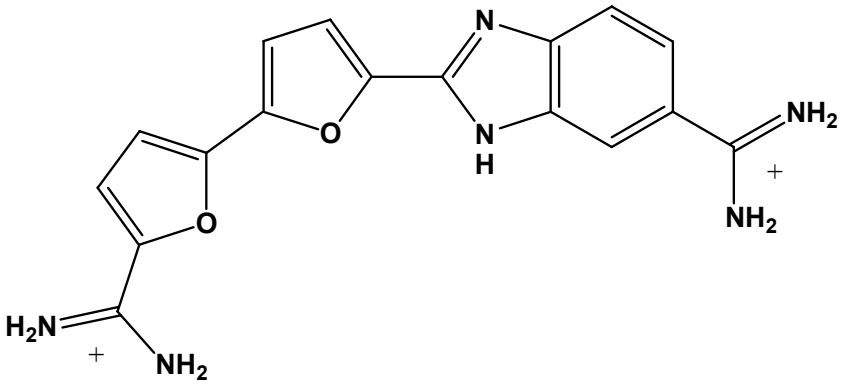


Figure 4.21 CD spectra of DB 1003 titrated into 3.3 μM human telomeric sequence, d[$AG_3(T_2AG_3)_3$], in HEPES buffer containing 50 mM KCl. Compound:DNA ratios ranged from 1:1 to 4:1.

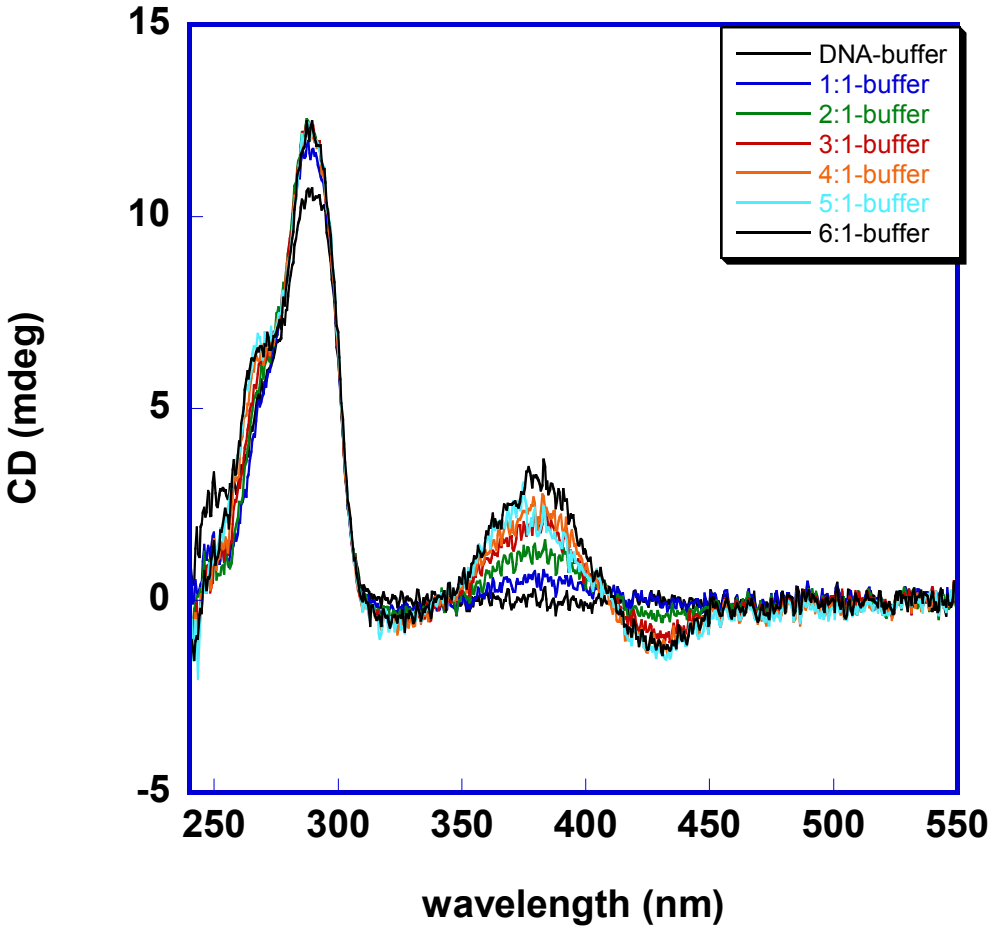


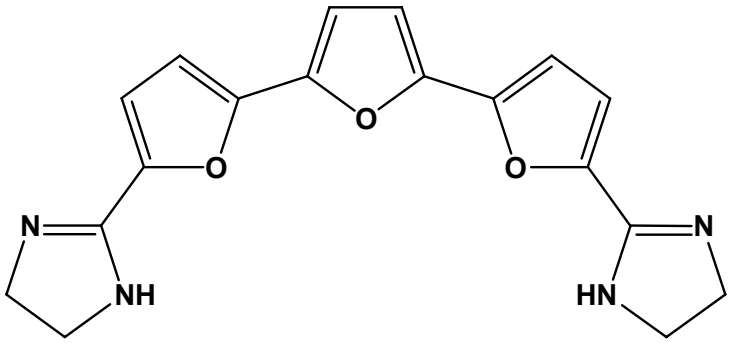


Figure 4.22 CD spectra of DB 657 titrated into 3.7 μM human telomeric sequence, d[$AG_3(T_2AG_3)_3$], in HEPES buffer containing 50 mM KCl. Compound:DNA ratios ranged from 1:1 to 6:1.

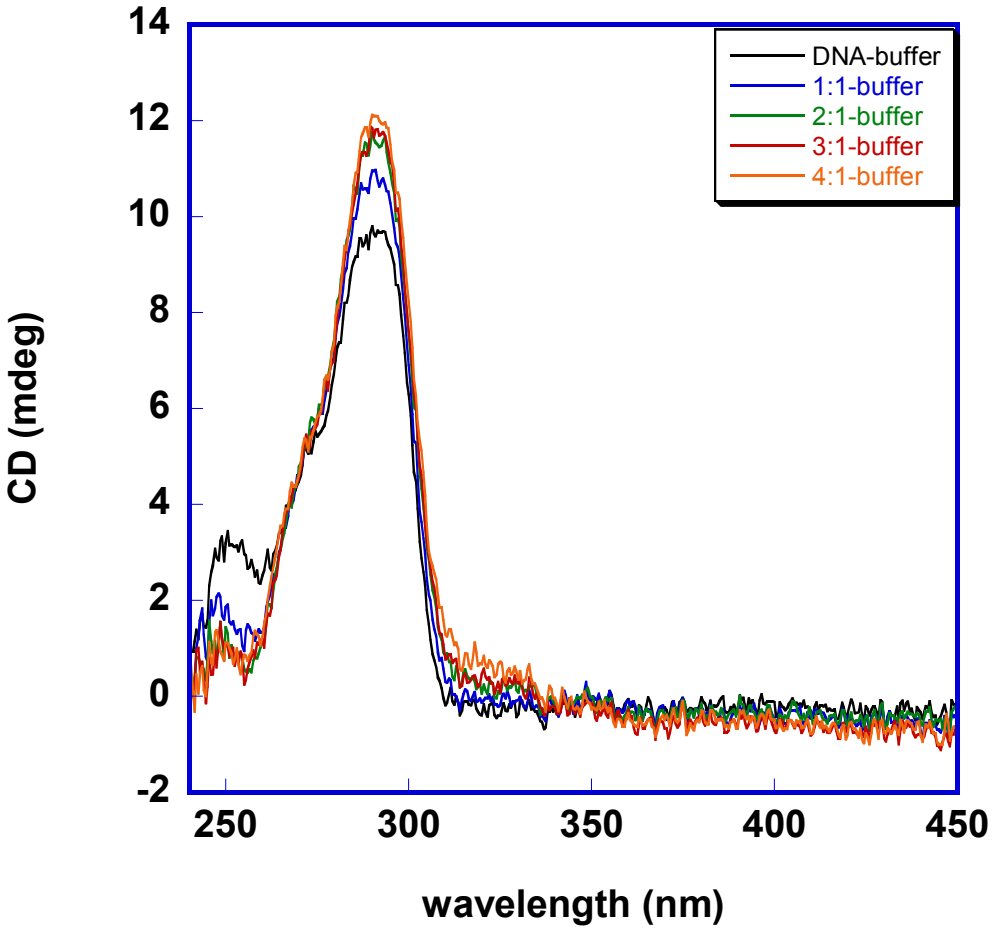


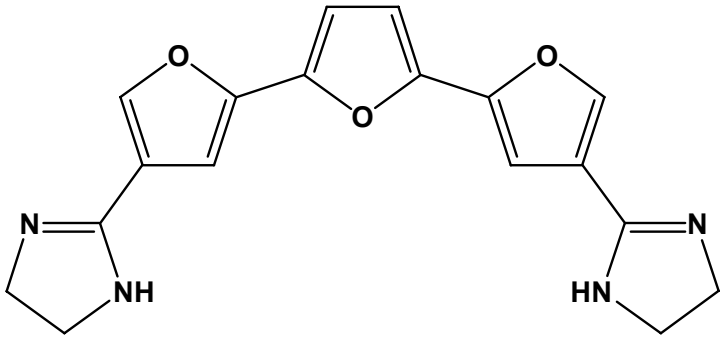


Figure 4.23 CD spectra of DB 659 titrated into 3.6 μM human telomeric sequence, d[$AG_3(T_2AG_3)_3$], in HEPES buffer containing 50 mM KCl. Compound:DNA ratios ranged from 1:1 to 4:1.

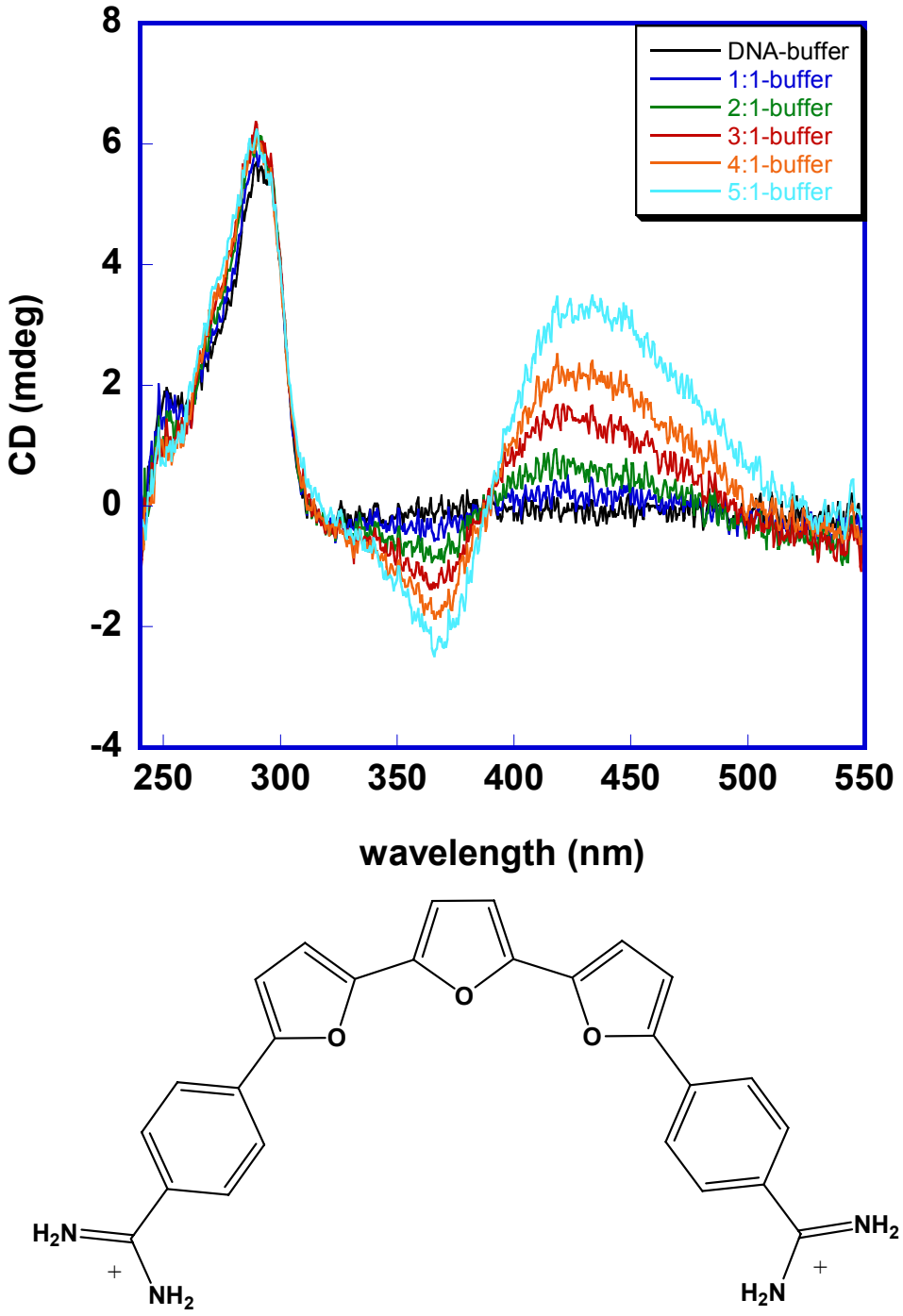


Figure 4.24 CD spectra of DB 1315 titrated into 2.6 μM human telomeric sequence, d[$AG_3(T_2AG_3)_3$], in HEPES buffer containing 50 mM KCl. Compound:DNA ratios ranged from 1:1 to 5:1.

## References


1. Miyoshi, D., H. Karimata, and N. Sugimoto, *Drastic effect of a single base difference between human and tetrahymena telomere sequences on their structures under molecular crowding conditions.* Angew Chem Int Ed Engl, 2005. **44**(24): p. 3740-4.
2. Chen, F.M., *Sr2+ facilitates intermolecular G-quadruplex formation of telomeric sequences.* Biochemistry, 1992. **31**(15): p. 3769-76.
3. Keniry, M.A., *Quadruplex structures in nucleic acids.* Biopolymers, 2000. **56**(3): p. 123-46.
4. Sen, D. and W. Gilbert, Nature, 1990. **344**: p. 410.
5. Sen, D. and W. Gilbert, *Guanine quartet structures.* Methods Enzymol., 1992. **211**: p. 191-199.
6. Ludwig, A., et al., *Ribozyme cleavage of telomerase mRNA sensitizes breast epithelial cells to inhibitors of topoisomerase.* Cancer Res., 2001. **61**: p. 3053-3061.
7. Macaya, R.F., et al., *Thrombin-binding DNA aptamer forms a unimolecular quadruplex structure in solution.* Proc. Natl. Acad. Sci. U S A, 1993. **90**(8): p. 3745-9.
8. Phan, A.T., et al., *Small-molecule interaction with a five-guanine-tract G-quadruplex structure from the human MYC promoter.* Nat. Chem. Biol., 2005. **1**(3): p. 167-73.
9. Wang, Y. and D.J. Patel, *Solution structure of the human telomeric repeat d[AG3(T2AG3)3] G-tetraplex.* Structure, 1993. **1**(4): p. 263-82.

10. Wang, Y. and D.J. Patel, *Solution structure of the Tetrahymena telomeric repeat d(T2G4)4 G-tetraplex.* Structure, 1994. **2**(12): p. 1141-56.

11. Wang, Y. and D.J. Patel, *Solution structure of the Oxytricha telomeric repeat d[G4(T4G4)3] G-tetraplex.* J. Mol. Biol., 1995. **251**(1): p. 76-94.

12. Yokoyama, Y., et al., *The 5'-end of hTERT mRNA is a good target for hammerhead ribozyme to suppress telomerase activity.* Biochem. Biophys. Res. Commun., 2000. **273**(1): p. 316-21.

13. Marsh, T.C. and E. Henderson, *G-wires: self-assembly of a telomeric oligonucleotide, d(GGGGTTGGGG), into large superstructures.* Biochemistry, 1994. **33**(35): p. 10718-24.

14. Seenisamy, J., et al., *The dynamic character of the G-quadruplex element in the c-MYC promoter and modification by TMPyP4.* J Am Chem Soc, 2004. **126**(28): p. 8702-9.

15. Dai, J., et al., *An intramolecular G-quadruplex structure with mixed parallel/antiparallel G-strands formed in the human BCL-2 promoter region in solution.* J Am Chem Soc, 2006. **128**(4): p. 1096-8.

16. Dexheimer, T.S., D. Sun, and L.H. Hurley, *Deconvoluting the structural and drug-recognition complexity of the G-quadruplex-forming region upstream of the bcl-2 P1 promoter.* J Am Chem Soc, 2006. **128**(16): p. 5404-15.

17. Phan, A.T. and D.J. Patel, *Two-repeat human telomeric d(TAGGGTTAGGGT) sequence forms interconverting parallel and antiparallel G-quadruplexes in solution: distinct topologies, thermodynamic properties, and folding/unfolding kinetics.* J. Am. Chem. Soc., 2003. **125**(49): p. 15021-7.

18. Xu, Y., Y. Noguchi, and H. Sugiyama, *The new models of the human telomere d[AGGG(TTAGGG)3] in K+ solution.* Bioorg Med Chem, 2006. **14**(16): p. 5584-91.

19. Phan, A.T., K.N. Luu, and D.J. Patel, *Different loop arrangements of intramolecular human telomeric (3+1) G-quadruplexes in K+ solution.* Nucleic Acids Res, 2006. **34**(19): p. 5715-9.

20. Seenisamy, J., et al., *Design and synthesis of an expanded porphyrin that has selectivity for the c-MYC G-quadruplex structure.* J. Am. Chem. Soc., 2005. **127**(9): p. 2944-59.

21. Catasti, P., et al., *Structure-function correlations of the insulin-linked polymorphic region.* J Mol Biol, 1996. **264**(3): p. 534-45.

22. Sen, D. and W. Gilbert, *Formation of parallel four-stranded complexes by guanine-rich motifs in DNA and its implications for meiosis.* Nature, 1988. **334**(6180): p. 364-6.

23. Siddiqui-Jain, A., et al., *Direct evidence for a G-quadruplex in a promoter region and its targeting with a small molecule to repress c-MYC transcription.* Proc. Natl. Acad. Sci. U S A, 2002. **99**(18): p. 11593-8.

24. Simonsson, T., P. Pecinka, and M. Kubista, *DNA tetraplex formation in the control region of c-myc.* Nucleic Acids Res., 1998. **26**(5): p. 1167-72.

25. Smith, F.W., P. Schultze, and J. Feigon, *Solution structures of unimolecular quadruplexes formed by oligonucleotides containing Oxytricha telomere repeats.* Structure, 1995. **3**(10): p. 997-1008.

26. Han, F.X., R.T. Wheelhouse, and L.H. Hurley, *Interactions of TMPyP4 and TMPyP2 with Quadruplex DNA. Structural Basis for the Differential Effects on Telomerase Inhibition.* J. Am. Chem. Soc., 1999. **121**(15): p. 3561-3570.

27. Schultze, P., R.F. Macaya, and J. Feigon, *Three-dimensional solution structure of the thrombin-binding DNA aptamer d(GGTTGGTGTGGTTGG).* J Mol Biol, 1994. **235**(5): p. 1532-47.

28. Dapic, V., et al., *Biophysical and biological properties of quadruplex oligodeoxyribonucleotides.* Nucleic Acids Res, 2003. **31**(8): p. 2097-107.

29. Phan, A.T., Y.S. Modi, and D.J. Patel, *Propeller-type parallel-stranded G-quadruplexes in the human c-myc promoter.* J Am Chem Soc, 2004. **126**(28): p. 8710-6.

30. Laughlan, G., et al., *The high-resolution crystal structure of a parallel-stranded guanine tetraplex.* Science, 1994. **265**(5171): p. 520-4.

31. Blackburn, G.M. and M.J. Gait, *Nucleic acids in chemistry and biology*. Second ed. 1996, New York: Oxford University Press. 528.

32. Ambrus, A., et al., *Human telomeric sequence forms a hybrid-type intramolecular G-quadruplex structure with mixed parallel/antiparallel strands in potassium solution.* Nucleic Acids Res., 2006. **34**(9): p. 2723-35.

# Chapter 5

# Binding of Modified Porphyrins and Sapphyrins to Quadruplex DNA: SPR-Biosensor Studies

## Introduction

Porphyrins are a class of heterocyclic macrocycles composed of pyrrole subunits linked through methine bridges. Cationic porphyrins are known to bind to and stabilize different types of G-quadruplexes and, in some cases, to facilitate G-quadruplex formation [1-5]. 5,10,15,20-tetra-(N-methyl-4-pyridyl)porphine (TMPyP4) is a commercially-available cationic porphyrin that has been widely studied and shown to bind to quadruplex DNA sequences (Figure 5.1). TMPyP4 has been shown experimentally to bind to human telomeric DNA with a 2:1 stoichiometry [6]. Molecular modeling with human telomeric DNA suggests that one TMPyP4 molecule is stacked externally on each of the terminal quartets, with the positively charged groups oriented toward the sugar-phosphate DNA backbone [2]. TMPyP4 has been shown to stabilize the quadruplex conformation of telomeres, preventing recognition of the telomere by telomerase and resulting in effective inhibition of the enzyme [3, 7]. TMPyP4 also binds to and stabilizes the G-rich strand of the intramolecular c-MYC sequence with a 2:1 stoichiometry, with each molecule stacked externally on the G-quartet surface, in a similar manner as TMPyP4 binds to the human telomere [4]. However, when TMPyP4 binds to c-MYC, it induces a conformation change in the DNA to a mixed parallel/antiparallel structure. This conformational change of the DNA renders the

accessory protein NM23-H2 unable to recognize the NHEIII1 and convert it to the transcriptionally active form, which leads to repression of transcriptional activity [8] and inhibition of tumor growth *in vivo* [9].

Despite the effective quadruplex-binding and enzyme inhibition exhibited by TMPyP4, this compound has several drawbacks that would prevent it from being used therapeutically. Porphyrins are known to produce photoinduced cytotoxicity [10, 11]. Upon excitation, singlet oxygen is generated, resulting in indiscriminant cell damage. This feature of porphyrins has been exploited advantageously through the use of photodynamic therapy for treatment of some cancers including lung, esophageal and bladder cancers [12]. However, the phototoxicity of porphyrins would prevent them from being used as telomerase inhibitors or c-MYC repressors. TMPyP4 also binds preferentially to intermolecular quadruplexes over the biologically relevant intramolecular quadruplexes. This intermolecular binding has been demonstrated through the TMPyP4-induced formation of anaphase bridges in sea urchins [3]. Binding to intermolecular quadruplexes not only results in compound loss due to binding of non-targeted sequences, but is undesirable because it can result in end-to-end fusion of chromosomes. Also, the binding of TMPyP4 to the human telomere and c-MYC sequence is not as strong as some of the newer quadruplex-interactive compounds which have been discovered. The porphyrin core of TMPyP4 is smaller (10.1 Å) than the size of the G-quartet (13.2 Å) which results in the molecule binding with an offset from the center of the quartet [2]. TMPyP4 only overlaps with two out of four of the guanines in the terminal G-quartets. The binding of TMPyP4 to the quadruplex could potentially be

improved if it were modified to increase the contact surface between the compound and the G-quartets, in order to maximize stacking interactions.

Telomestatin (Figure 5.1), a natural product isolated from *Streptomyces anulatus* 3533-SV4 [13], has a larger ring system than TMPyP4. The ring system is similar in size to the G-quartet structure (Figure 5.1) which increases π-π stacking, electrostatic and hydrogen-bonding interactions as compared to TMPyP4. Telomestatin has been shown to bind strongly to and stabilize intramolecular basket-type G-quadruplex structures [14]. Telomestatin is also able to induce and stabilize G-quadruplexes in the absence of added monovalent cations, which is a unique characteristic among small molecules [14]. DB 832 is the only other G-quadruplex-interactive compound that has been shown to induce quadruplex formation in the absence of salt. Modeling studies of Telomestatin suggest that it binds to the ends of the basket conformation of the intramolecular human telomeric sequence with a 2:1 stoichiometry [15].Telomestatin is the strongest telomerase inhibitor ever reported of any G-quadruplex interactive small molecule, with an $IC_{50}$ of .005 μM [16]. In comparison, TmPyP4 has an $IC_{50}$ of 0.63 μM [3]. Telomestatin is also a very specific inhibitor of telomerase. It does not inhibit other DNA polymerases or reverse transcriptases [16].Telomerase is also 70 times more selective for binding to quadruplex DNA over duplex DNA [14], likely due to the close match between the size and shape of the macrocyclic structure of telomestatin to that of the G-quartet. This is important because indiscriminant duplex binding is associated with cytotoxicity.

Since Telomestatin is a natural product, it is very difficult to obtain, especially in quantities needed for widespread therapeutic use. Its complicated ring system is difficult to synthesize, and at present would be cost-prohibitive to produce commercially. Also,

since telomestatin is an uncharged molecule, it has low solubility in water, which is not only undesirable from a therapeutic standpoint, but also makes it difficult to study. The ease of synthesis of porphyrins and the ability to create modified porphyrins with different ring systems and substituents as well as their solubility makes porphyrins desirable to work with from a drug design standpoint. On the basis of modeling and comparative analysis of the binding of TMPyP4 and telomestatin to G-quadruplex, a series of metal-substituted porphyrins and expanded porphyrins, (Figure 5.2), were designed and synthesized by Dr. Laurence Hurley's research group at the University of Arizona. The larger ring systems were designed to overlap the G-quartet more effectively than the ring system of TMPyP4, in hopes of improving binding and selectivity. The substitution of metals in the porphyrin cores eliminates the photocytotoxicity associated with porphyrins through rapid quenching of singlet oxygen [10, 11]. To investigate the effect of these modifications on binding and selectivity, surface plasmon resonance (SPR) was used to quantify the interactions between TMPyP4 as well as the modified compounds with different quadruplex DNA sequences.

**Materials and Methods**

**Sample Preparation**

The oligonucleotides 5'-biotin-d[$AG_3(T_2AG_3)_3$], 5'-biotin-d($AG_3TG_4AG_3TG_4A$), 5'-biotin-d(CGAATTCG), 5'-biotin-d[$(G_2T_4)_3$], 5'-biotin-d[$(T_2G_4)_4$], and 5'-biotin-d($G_2T_2G_2TGTG_2T_2G_2$) were purchased with HPLC purification and mass spectrometry characterization from Midland Certified Reagent Company. TMPyP4 was purchased from Midcentury. Stock solutions containing 1 mM of each compound were prepared in double distilled water and diluted to working concentrations immediately before use with

buffer. S2SAP, Se2SAP, Se2Py3, SHPy3, SeHPy3, and S2Py3 were synthesized by Dr. Laurence H. Hurley's group at the University of Arizona. The synthesis of Se2SAP has been previously described [17]. The synthesis of the other modified porphyrin compounds will be described elsewhere.

**Immobilization of DNA and Biosensor SPR Experiments**

Biosensor SPR experiments were performed with a four-channel BIAcore 3000 optical biosensor system (BIAcore, Inc.) and streptavidin-coated sensor chips (BIAcore SA with linked streptavidin). All DNA samples, for either duplex- or quadruplex-binding experiments, were used as single strands (fold-back structures) to prevent dissociation in the SPR flow system. The concentration in all cases refers to the strand concentration, which is also the duplex or quadruplex concentration. The chips were prepared for use by conditioning with three to five consecutive 1 min injections of 1 M NaCl in 50 mM NaOH followed by extensive washing with buffer. 5'-Biotinylated DNA samples (25 nM) in HBS buffer were immobilized on the flow cell surface by noncovalent capture as previously described [18-22]. Three flow cells were used to immobilize DNA oligomer samples, and a fourth cell was left blank as a control. Interaction analysis was performed by using both kinetics and steady-state methods with multiple injections of different compound concentrations over the immobilized DNA surface at 25 ºC. DNA-binding experiments were performed in sterile filtered and degassed HBS buffers: 0.01 M HEPES, (pH 7.4), 3 mM EDTA, and 0.005% surfactant P20 with either 0.1 M KCl, 0.2 M KCl, 0.1 M NaCl, or 0.2 M NaCl. Compound solutions were prepared in the desired buffer by serial dilutions from stock solution and injected from 7 mm plastic vials with

pierceable plastic crimp caps (BIAcore, Inc.). To remove any remaining bound compound after the dissociation phase of the sensorgram, a low-pH glycine regeneration buffer was used (10 mM glycine at pH 2). The baseline was then reestablished, and the next compound concentration sample was injected.

The instrument response (RU) in the steady-state region is proportional to the amount of bound drug and was typically determined by linear averaging over a 10-20 s or longer time span, depending on the length of the steady-state plateau. The predicted maximum response per bound compound in the steady-state region ($RU_{max}$) was determined from the DNA molecular weight, the amount of DNA on the flow cell, the compound molecular weight, and the refractive index gradient ratio of the compound and DNA, as previously described [23]. In most of the cases, the observed RU values at high concentrations were greater than $RU_{max}$, pointing to more than one binding site in these DNA sequences. The number of binding sites was estimated fitting plots of RU versus $C_{free}$. These methods can also be used to determine an empirical $RU_{max}$ value. The $RU_{max}$ value is required to convert the observed response (RU) to the standard binding parameter *r* (moles of drug bound per moles of DNA hairpin)

$$r = RU/RU_{max}$$

which is useful for comparison of a compound binding to different DNAs. To obtain the affinity constants, the data were fitted to the following interaction model using Kaleidagraph for nonlinear least-squares optimization of the binding parameters:

$$r = (K_1C_{free} + 2K_1K_2C_{free}^2)/(1 + K_1C_{free} + K_1K_2C_{free}^2)$$

where $K_1$ and $K_2$ are equilibrium constants for two types of binding sites and $C_{free}$ is the concentration of the compound in equilibrium with the complex and is fixed by the concentration in the flow solution. For a single dominant binding site model, $K_2$ is equal to zero. Errors in fitting two $K$ values within any experiment were ±10%, while errors in $K$ values in replicate experiments were ±25%. Errors in fitting results that required only a single $K$ value were ±10%.

After injection of the compound and prior to reinjection of buffer, the association kinetics of compound binding to immobilized DNA can be monitored, and after reinjection of buffer the dissociation kinetics can be determined. To minimize possible mass transport effects, SPR kinetics experiments were conducted at flow rates of 50-100 μL/min with low surface densities of immobilized DNA. Global fitting (BIA Evaluation Software, BIAcore, Inc.) of the association and dissociation curves was done in a concentration range where the compound binds significantly only to the strongest binding site: up to 400 nM for $G_2T_4$ and 100 nM for TetTel and TBA. Both the association rate constant, $k_a$, and the dissociation rate constant, $k_d$, could be obtained for these complexes, and the calculated equilibrium constant ($K_{kin} = k_a/k_d$) was within a factor of 2 of the steady-state value. For binding of Se2SAP to duplex DNAs, the kinetics of association and dissociation are too fast for accurate analysis by SPR methods. For binding of the compound to the c-MYC sequence, we were unable to obtain satisfactory global fits, on the basis of the analysis of residuals and quality of fit values, for the lowest concentrations required in the 1:1 binding region with this strong interaction. In the low-

concentration c-MYC association region, the curves were initially slightly concave, which may be due to a fraction of the compound adsorbing to the flow system at injection. This problem becomes much less significant at the higher concentrations used for the weaker binding DNAs. Since the compound is discarded on dissociation, the adsorption problem is less significant, and a $k_d$ value can be accurately determined for the c-MYC complex. With the steady-state $K$ and the $k_d$ value, a $k_a$ value can be calculated, but with less confidence than for the experimentally determined values.

**Results**

**SPR Screening of Modified Porphyrins**

Surface plasmon resonance (SPR) is a useful technique for the screening of small molecules in order to determine their relative binding affinities and selectivity for a target DNA sequence. TMPyP4 and the modified porphyrins were evaluated against a 19-mer c-MYC sequence, d($AG_3TG_4AG_3TG_4A$), and the human telomeric sequence, d[$AG_3(T_2AG_3)_3$], using SPR. These two oligonucleotides were immobilized in different flow cells on the same sensor chip, and a range of compound concentrations were injected to monitor the interactions with DNA. Suitable blank control injections with running buffer (HEPES buffer containing 200 mM KCl at pH 7.4) were also performed, and the resulting sensorgrams were subtracted from the compound sensorgrams to obtain the final concentration-dependent graphs. The binding stoichiometry arises naturally from the RU as saturation of binding sites is approached in SPR experiments. During SPR titration, the increase of RU values is directly proportional to the amount of drug bound to DNA molecules immobilized on the sensor chip. The plot of RU versus the unbound concentration of each of the compounds was fitted to a two-site binding model

(Experimental Section). Direct steady-state binding plots were constructed by averaging the observed SPR responses in the steady-state region, and the responses were plotted against the free compound concentration in the flow solution. The binding plots for the concentration-dependent binding of the porphyrins on the c-MYC sequence and the telomeric DNA are shown in parts A and B, respectively, of Figure 5.3. The equilibrium binding constants (K values) are shown for each compound in Table 5.1. Only TMPyP4 exhibited two strong binding sites with each sequence. The other compounds exhibited weaker, secondary binding with $K_2$ values (not shown) at least ten times lower than $K_1$. Of the compounds studied, a diseleno sapphyrin compound, Se2SAP, had the strongest binding to both the c-MYC sequence ($K = 6.2 \times 10^7\ M^{-1}$) and to the human telomeric sequence ($K = 1.01 \times 10^7\ M^{-1}$). This compound represents a significant improvement in binding to these sequences over TMPyP4. TMPyP4 binds to c-MYC at two sites, with $K_1 = 1.4 \times 10^7\ M^{-1}$ and $K_2 = 5.4 \times 10^6\ M^{-1}$ and to the human telomere, with $K_1 = 3.5 \times 10^6\ M^{-1}$ and $K_2 = 3.7 \times 10^5\ M^{-1}$. These results are in agreement with polymerase stop assay results from Laurence Hurley's group at the University of Arizona which shows that Se2SAP binds more strongly to the c-MYC sequence than TMPyP4 or the other modified porphyrins (unpublished data). On the basis of these results, Se2SAP was chosen for further study using SPR.

**Selectivity of Se2SAP for the c-MYC Sequence over Duplex DNA by Surface Plasmon Resonance Experiments**

Surface plasmon resonance (SPR) experiments were conducted to independently determine the selectivity of binding of Se2SAP with the 19-mer c-MYC sequence relative to a duplex sequence (CGAATTCG, as a hairpin duplex). These two oligonucleotides

were immobilized in different flow cells on the same sensor chip, and a range of Se2SAP concentrations were injected to monitor the interactions with DNA. Suitable blank control injections with running buffer (HEPES buffer containing 200 mM KCl at pH 7.4) were also performed, and the resulting sensorgrams were subtracted from the compound sensorgrams to obtain the final concentration-dependent graphs. Sensorgrams [resonance units (RU) versus time] for the concentration-dependent binding of Se2SAP on the c-MYC sequence and the duplex DNA are shown in parts A and B, respectively, of Figure 5.4. The plot of RU versus the unbound concentration of Se2SAP was fitted to the binding models with one or two binding sites (Experimental Section). The best fit to the interaction results for the c-MYC sequence is for a single, strong binding site, and the expected $RU_{max}$ was obtained for the single binding site (on the basis of the amount of DNA on the chip). At higher concentrations, additional Se2SAP binds to the DNA through a significantly weaker second site. The binding constant for the second site is over a factor of 10 less than for the strong site, and the dissociation rate is much faster, a characteristic of weak, nonspecific binding. The measured steady-state equilibrium binding constant, $K = 6.2 \times 10^7\ M^{-1}$, indicates the high affinity of Se2SAP for the c-MYC sequence. The dissociation rate constant $k_d = 0.0029\ s^{-1}$ obtained from the kinetics analysis of the sensorgrams also further confirmed the single, strong binding site of Se2SAP with the c-MYC G-quadruplex.

The binding of Se2SAP with the duplex DNA sequence showed much faster kinetics ($k_d > 0.2\ s^{-1}$) than binding with the c-MYC sequence. The very fast off kinetics and the multisite binding at higher concentrations clearly show the nonspecific, weaker binding of Se2SAP to the duplex DNA rather than the c-MYC G-quadruplex. The steady-

state *K* value calculated for the binding of Se2SAP with duplex is on the order of $10^6$. SPR experiments confirm the selectivity (~50-fold) of Se2SAP for the c-MYC G-quadruplex over the duplex DNA.

**SPR Demonstrates That Se2SAP Binds More Selectively to the c-MYC and Similar G-Quadruplexes Than to Other G-Quadruplex Structures.**

Recent studies indicate that biologically relevant parallel c-MYC G-quadruplexes can exist as a mixture of four loop isomers [8]. Se2SAP has been shown through electromobility shift assays (EMSA) with mutant c-MYC sequences to selectively trap out the single-loop hybrid 1:2:1 loop isomer of the G-quadruplex [17]. Circular dichroism results suggest that upon binding to Se2SAP, this parallel c-MYC structure is converted to a mixed parallel/ antiparallel hybrid structure [17]. The strong binding of this molecule, as implied from the modeling studies, and confirmed by SPR suggested that this molecule may be selective for this G-quadruplex structure, which has the tetrad arrangement *syn-anti-anti-anti* associated with the one-base lateral loop. To compare the selectivity of Se2SAP with the c-MYC G-quadruplex versus other G-quadruplex structures, an SPR experiment was performed using three established and different G-quadruplex-forming sequences. The $G_2T_4$ sequence was used to determine the binding of Se2SAP to the basket structure. $G_2T_4$ is known to form the basket-type G-quadruplex structure in both NaCl and KCl solutions [24, 25]. For comparison with the chair-type G-quadruplex, thrombin-binding aptamer (TBA) was used [26]. Finally, the Tetrahymena telomere (TetTel) sequence, which forms a G-quadruplex structure with a mixed parallel/antiparallel hybrid structure [27] was used to mimic the G-quadruplex structure

formed upon addition of Se2SAP to the parallel c-MYC G-quadruplex. One end of this G-quadruplex has a structure with a tetrad arrangement similar to that proposed to be trapped out by Se2SAP. The three G-quadruplex-forming oligonucleotides, TetTel, TBA, and $G_2T_4$, were immobilized in different flow cells on the same sensor chip, and the SPR experiments were conducted as described above with a range of Se2SAP concentrations. HEPES buffer containing 200 mM KCl or 200 mM NaCl at pH 7.4 was used for all the sequences. Since the NMR structure of the mixed parallel/antiparallel G-quadruplex for the TetTel sequence was obtained in NaCl [27], the SPR experiment was conducted in HEPES buffer containing 200 mM NaCl for the TetTel sequence. The SPR experiment showed similar results for the binding of Se2SAP with the TetTel sequence in the presence of buffer containing KCl or NaCl. The final concentration-dependent sensorgrams for the binding of Se2SAP to these three sequences are shown in Figures 5.5-5.7.

In all cases, the G-quadruplexes exhibited two binding sites: a single strong binding site and a site that is at least 10-fold weaker. Since the second binding site in all cases exhibited much faster dissociation kinetics, which is characteristic of weak, nonspecific binding, only the results from the primary strong binding site are considered for further discussion. The dissociation rate constant ($k_d$) obtained from the kinetics method and the equilibrium binding constant ($K$) derived from the steady-state method for the different sequences are tabulated in Table 5.2 (for comparison, the values for c-MYC and hairpin duplex DNA are also included). The differences in the dissociation of Se2SAP from that of the TetTel, TBA, and $G_2T_4$ sequences can be easily visualized from their corresponding sensorgrams (Figures 5.5-5.7). Among the G-quadruplexes, the c-

MYC G-quadruplex showed the highest equilibrium constant ($K = 6.2 \times 10^7$ $M^{-1}$) and the slowest dissociation rate constant ($k_d = 0.0029$ $s^{-1}$) indicative of the strongest binding of Se2SAP with this sequence. The kinetics ($k_d = 0.0041$ $s^{-1}$) and the steady-state ($K = 4.2 \times 10^7$ $M^{-1}$) values for the TetTel sequence indicate that Se2SAP also binds very strongly to a single site in the double-loop hybrid G-quadruplex with a slightly lower binding constant than with the c-MYC G-quadruplex. With the $G_2T_4$ sequence, Se2SAP showed a much faster dissociation rate ($k_d$ value is ~12 times larger than that for the c-MYC sequence), and its $K$ value is similar to that of the duplex DNA (Table 5.1), indicating the very weak binding of Se2SAP to the basket-type G-quadruplex structure. In contrast, the SPR experiments indicated that Se2SAP showed moderate binding to the chair-type G-quadruplex formed in the TBA sequence. In comparison to the c-MYC sequence, TBA showed an approximate 3-fold increase in the dissociation constant value for Se2SAP and a 4-fold decrease in the equilibrium constant value. The SPR results for the binding of Se2SAP to the four different G-quadruplex-forming sequences were converted to steady-state binding isotherm plots and are shown in Figure 5.8. The steady-state isotherms were constructed by averaging the observed SPR responses in the steady-state region, and the responses were then converted to $r$, moles of Se2SAP bound per mole of G-quadruplex DNA ($r = RU_{obs}/RU_{max}$), and plotted against the free Se2SAP concentration in the flow solution. The fitting results shown in Figure 5.8 are for the single strong binding site. As seen in Table 5.2, the plots clearly indicate the order of binding of Se2SAP to the G-quadruplex as c-MYC ≥ TetTel »TBA » $G_2T_4$, i.e., single-loop hybrid ≥ double-loop hybrid » chair-type » basket-type G-quadruplexes.

**Se2SAP Binds Selectively to the Hybrid Conformation of the Human Telomere**

To date, multiple G-quadruplex structures have been characterized for the human telomeric sequence. Wang and Patel reported that a DNA oligonucleotide with a human telomeric sequence forms an intramolecular basket-type G-quadruplex structure in the presence of $Na^+$ [28]. Basket-type G-quadruplexes have one diagonal and two lateral, or edgewise, loop regions, with the guanine columns in an antiparallel arrangement [29]. Parkinson et al. reported a solid-state, intramolecular propeller-type G-quadruplex structure that forms in the presence of $K^+$ [30]. However, more recent solution-based studies suggest that the human telomere forms other structures including a mixed parallel/antiparallel hybrid structure [31, 32]. Circular dichroism spectroscopy has been used to demonstrate that for the human telomeric $d[T_2AG_3]_4$ oligonucleotide, Se2SAP binds to a hybrid G-quadruplex structure [17]. We provide further experimental evidence for the structure-based selectivity of Se2SAP by using SPR under varied salt conditions.

To quantitatively determine the equilibrium constant and stoichiometry of binding of Se2SAP to the 5'-$d[AGGG(TTAGGG)_3]$-3' oligonucleotide under different salt conditions, SPR experiments were carried out as described (experimental section). The human telomeric oligonucleotide was immobilized in a sensor chip flow cell, and a range of Se2SAP concentrations with $Na^+$- or $K^+$-containing buffers were injected to quantitatively evaluate the interactions with DNA. The signal in RU was determined as a function of time as the compound flow solution passes over a blank flow cell and the DNA cell. The signal from the blank flow cell was subtracted from that of the DNA cell to provide the final concentration-dependent sensorgrams in Figure 5.9. As flow continued, a steady-state plateau was reached in which the rates of compound binding to and dissociation from the immobilized DNA were equal. The response values in the

steady-state region of the sensorgrams were plotted versus the unbound concentration of Se2SAP from the flow solution ($C_f$) to obtain the binding constants. The stoichiometry of binding arose from the RU value approached with increasing Se2SAP concentration. The significant difference in the limiting RU value for $K^+$ and $Na^+$ defined the binding stoichiometry of 2:1 in $Na^+$ and 1:1 in $K^+$.

Binding plots were constructed by averaging the observed SPR response in the steady-state region, and the responses were plotted against $C_f$ (Figure 5.10). The RU versus $C_f$ plots were fitted to binding models with one or two binding sites (Experimental Procedures). In the case of $Na^+$, the telomeric G-quadruplex sequence binds two molecules of Se2SAP with binding constants that are identical within experimental error, $K_1 = K_2 = 4.9 \times 10^6\ M^{-1}$. In contrast, only one strong binding site with $K_1 = 1.8 \times 10^7\ M^{-1}$ for the binding of Se2SAP with the human telomeric sequence in $K^+$ containing buffer was observed. The binding isotherms of Se2SAP in $K^+$ can be fitted to a two-site binding model, but the $K_2$ is at least 10 times less than the $K_1$, characteristic of weak, nonspecific binding, and cannot be determined accurately. The primary equilibrium constant ($K_1$) showed a 4-fold increase in $K^+$ solution compared to $Na^+$, indicating preferential binding of Se2SAP with the hybrid structure rather than with the basket structure. Although the binding constant in $K^+$ is higher than that in $Na^+$, the fitting results do not show a striking visual difference because of the larger second site binding affinity in $Na^+$. The SPR results confirm that Se2SAP binds to different G-quadruplex structures formed in the human telomeric sequence in the $Na^+$ (basket) and the $K^+$ (hybrid) ions and has a preference for the hybrid structure.

**Conclusions**

Surface plasmon resonance was used to screen a series of metal-substituted and expanded porphyrins for binding to c-MYC and human telomere G-quadruplex sequences. A diseleno sapphyrin compound, Se2SAP, was identified as the compound with the strongest binding to both sequences. SPR not only confirmed the strong binding ($K = 6.2 \times 10^7\ M^{-1}$) of Se2SAP to the novel c-MYC G-quadruplex structure but also provided solid quantitative information regarding the selectivity of Se2SAP for the single-loop hybrid G-quadruplex over the chair- and basket-type G-quadruplex structures and duplex DNA. The analysis of the steady-state binding isotherms from SPR further established the order of selectivity for binding of Se2SAP to G-quadruplexes, as single-loop hybrid (c-MYC) ≥ double-loop hybrid (TetTel) » chair-type (TBA) » basket-type ($G_2T_4$) and duplex DNA (Table 1 and Figure 5.8). Thus, the results from SPR experiments confirmed the selective and strong binding of Se2SAP to the c-MYC G-quadruplex structure in comparison to other G-quadruplex structures (parallel, basket, and chair) or duplex DNA. SPR studies with the human telomere further confirm the selectivity of Se2SAP for mixed parallel/antiparallel hybrid structures. In the presence of $Na^+$, the human telomere adopts a basket structure and Se2SAP binds to this conformation with two binding sites, $K_1 = K_2 = 4.9 \times 10^6\ M^{-1}$. However, in the presence of $K^+$, the human telomere forms a mixed parallel/antiparallel hybrid structure and Se2SAP binds it with one stronger binding site, $K = 1.8 \times 10^7\ M^{-1}$. The selectivity for mixed parallel/antiparallel quadruplex structures exhibited by Se2SAP establishes the important principle that it is possible to design molecules that are selective for different G-quadruplex DNA structures.

A.

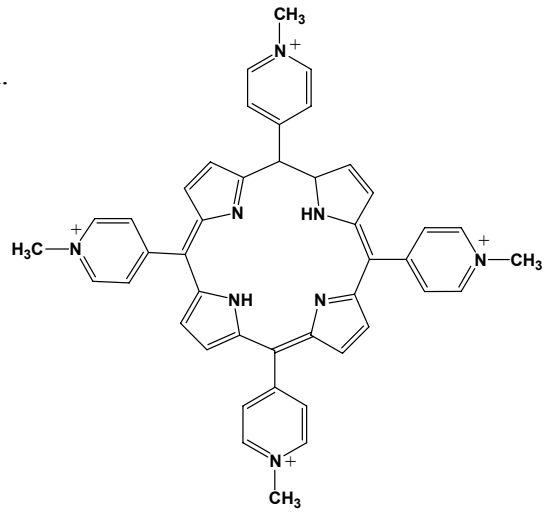

B.

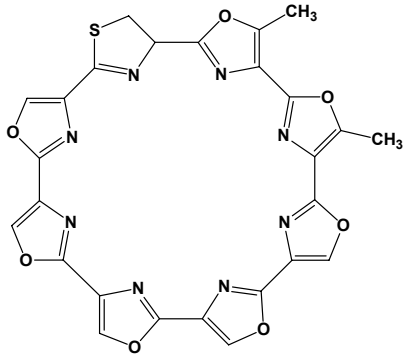

C.

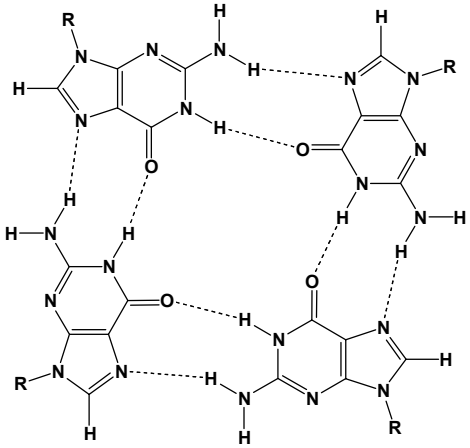

Figure 5.1 Structures of (A) TMPyP4, (B) Telomestatin, and (C) G-quartet.

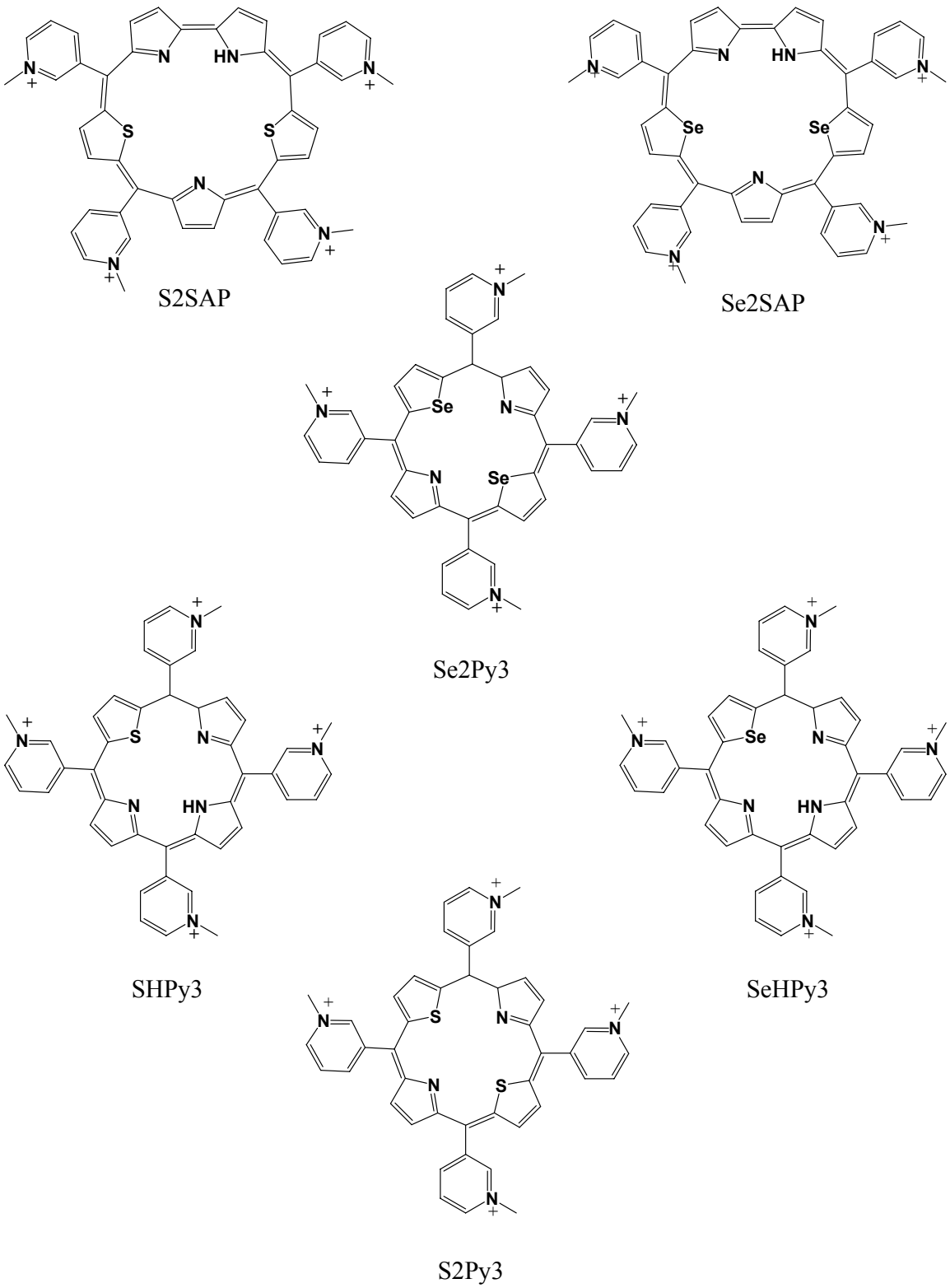


Figure 5.2 Structures of metal-substituted porphyrins and expanded porphyrins studied.

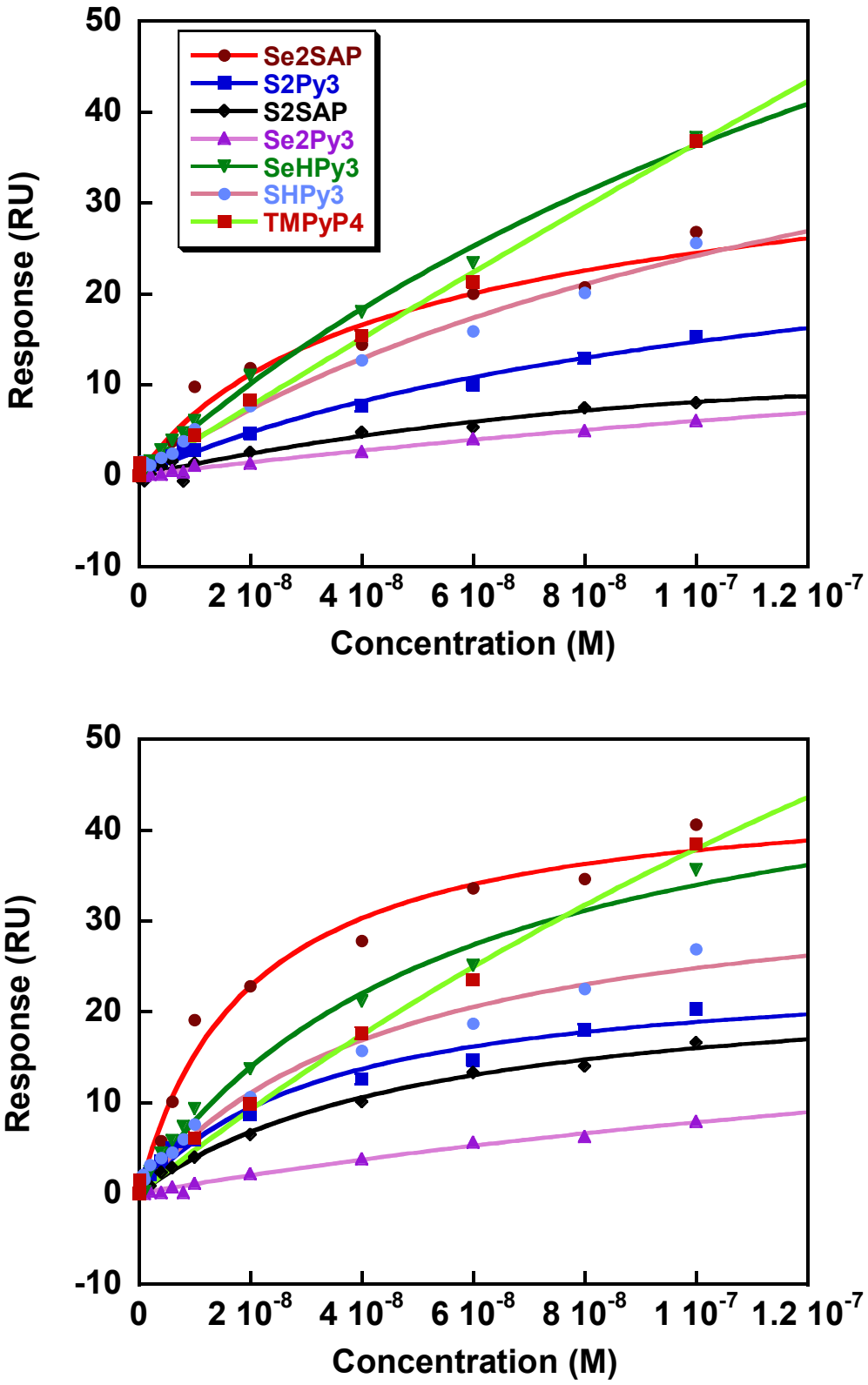


Figure 5.3 Steady-state binding plots for the modified porphyrins studied with human telomeric sequence (top) and c-MYC sequence (bottom) fit to a two-site model. The concentration values are for unbound compound concentration in the flow solution.

Table 5.1 Equilibrium binding constants for modified porphyrins with human telomere and c-MYC sequences obtained by SPR

| Compound | Human Telomere $K \times 10^{-6}$ ($M^{-1}$) | | c-MYC $K \times 10^{-6}$ ($M^{-1}$) | |
|---|---|---|---|---|
| | $K_1$ | $K_2$ | $K_1$ | $K_2$ |
| TMPyP4 | 3.5 | 0.37 | 14 | 5.4 |
| Se2Py3 | 0.57 | | 1.0 | |
| S2Py3 | 2.0 | | 5.3 | |
| S2SAP | 1.5 | | 4.5 | |
| Se2SAP | 10 | | 62 | |
| SHPy3 | 6.9 | | 22 | |

All experiments were performed in HEPES buffer containing 200 mM KCl at 25°C. Fitting errors due to random point scatter in any experiment are less than ±5%. The binding plots for each compound were fit with a two-site model. Only TMPyP4 exhibited two strong binding sites. The other compounds exhibited weaker, secondary binding with $K_2$ values (not shown) at least ten times lower than $K_1$.

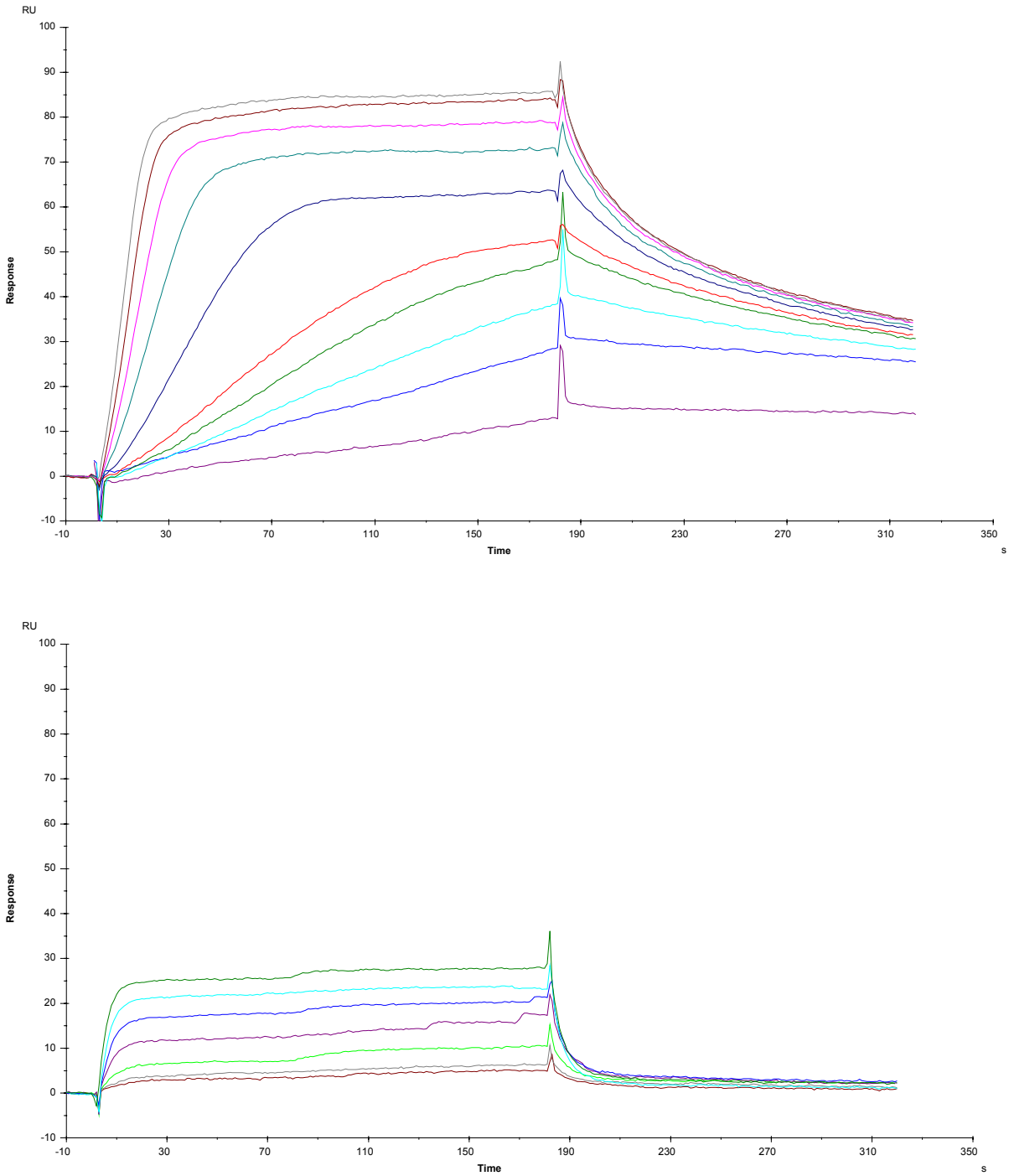


Figure 5.4 SPR sensorgrams for binding of Se2SAP to the immobilized G-quadruplex formed by a 19-mer c-MYC sequence (top) and CGAATTCG (bottom) as a hairpin duplex in HEPES buffer containing 200 mM KCl at 25°C. The c-MYC curves range in Se2SAP concentration from 2 nM for the lowest curve to 100 nM for the top curve, and for the duplex, they range in Se2SAP concentration from 8 to 100 nM, from bottom to top.

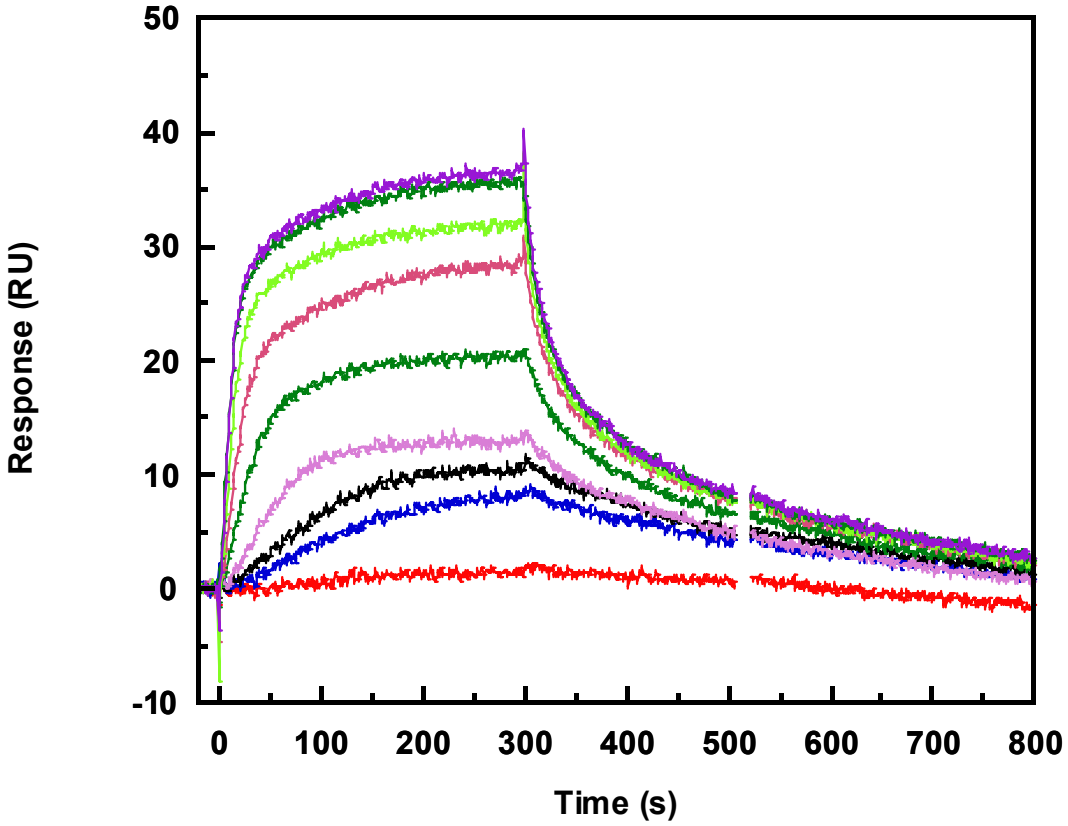


Figure 5.5 SPR sensorgrams for the binding of Se2SAP to Tetrahymena telomere sequence (TetTel). Binding experiments were performed at 25ºC in HEPES buffer containing 0.2 M NaCl. The concentration range is from 0.1 to 100 nM.

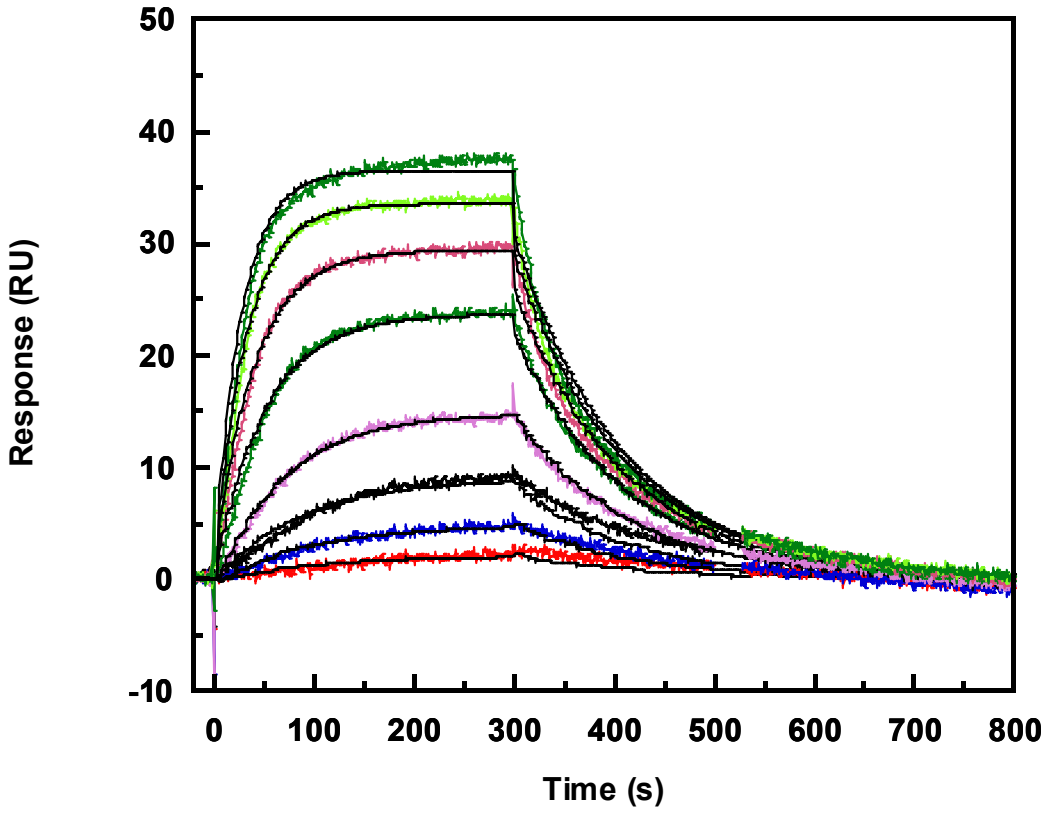


Figure 5.6 SPR sensorgrams for the binding of Se2SAP to thrombin binding aptamer (TBA). Binding experiments were performed at 25ºC in HEPES buffer containing 0.2 M KCl. The concentration range is from 0.1 to 100 nM. The black solid lines represent the results of the global kinetics fit.

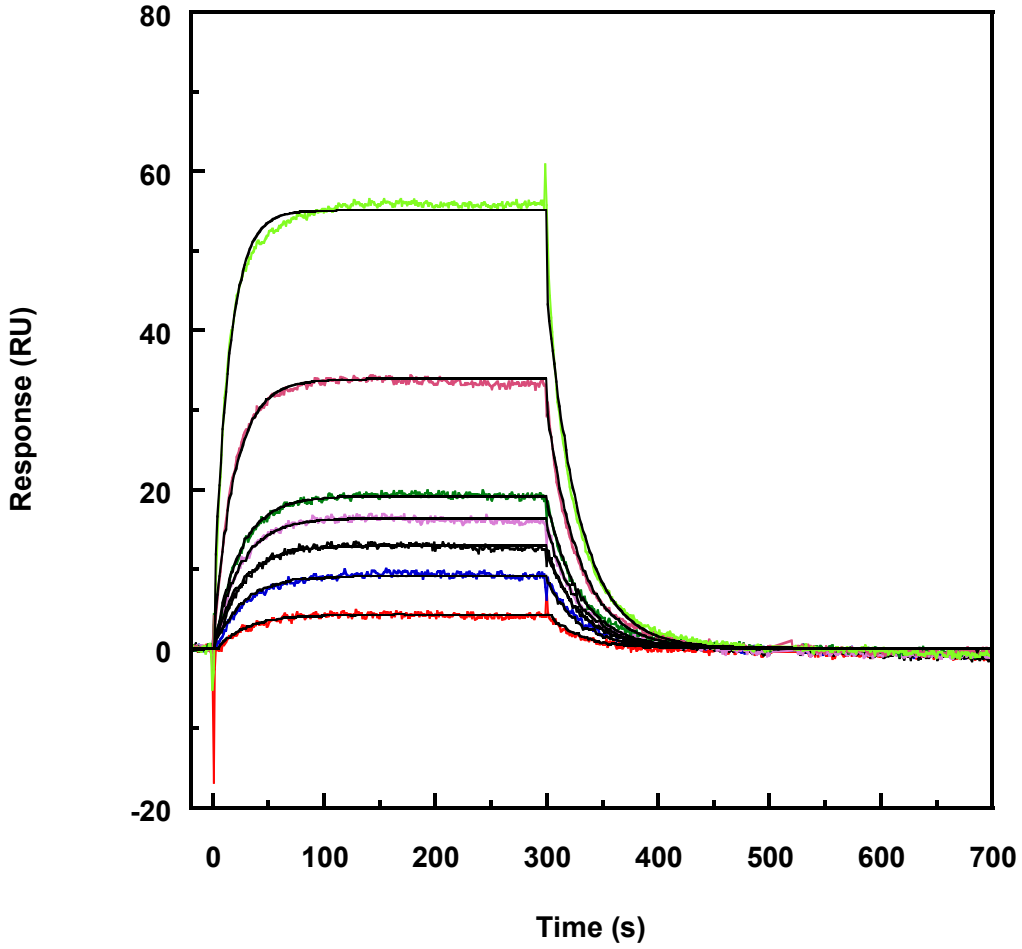


Figure 5.7 SPR sensorgrams for the binding of Se2SAP to G2T4. Binding experiments were performed at 25ºC in HEPES buffer containing 0.2 M KCl. The concentration range is from 0.1 to 100 nM. The black solid lines represent the results of a global kinetics fit.

Table 5.2 Equilibrium and Dissociation Kinetics Constants for Se2SAP Binding to G-Quadruplex and Hairpin Duplex DNA determined by SPR

| DNA | K x $10^{-7}$ ($M^{-1}$) | $k_d$ ($s^{-1}$) | $k_a$ x $10^{-3}$ ($M^{-1}s^{-1}$) |
|---|---|---|---|
| c-MYC | 6.2 | 0.0029 | 1.8 |
| TetTel | 4.2 | 0.0041 | 1.7 |
| TBA | 1.4 | 0.0094 | 1.3 |
| $G_2T_4$ | 0.31 | 0.034 | 1.1 |
| hairpin duplex | 0.16 | >0.2 | >3 |

All experiments were performed in HEPES buffer containing 200 mM KCl at 25°C and were repeated at least twice with fresh samples. Fitting errors due to random point scatter in any experiment are less than ±5%. Experimental errors estimated from reproducibility of results are ±10% for K values between 1 x $10^6$ and 2 x $10^7$ $M^{-1}$ and for $k_d$ values between 0.1 and 0.001 $s^{-1}$. Errors increase to ±20% for K values between 3 x $10^7$ and 1 x $10^8$ $M^{-1}$. It is difficult to accurately determine $k_d$ values that are significantly greater than 0.1 $s^{-1}$ by biosensor SPR methods. Because of some adsorption of Se2SAP in the biosensor flow system on initial injection, the $k_a$ values are difficult to determine directly and the values in the table are estimated from K and $k_d$.

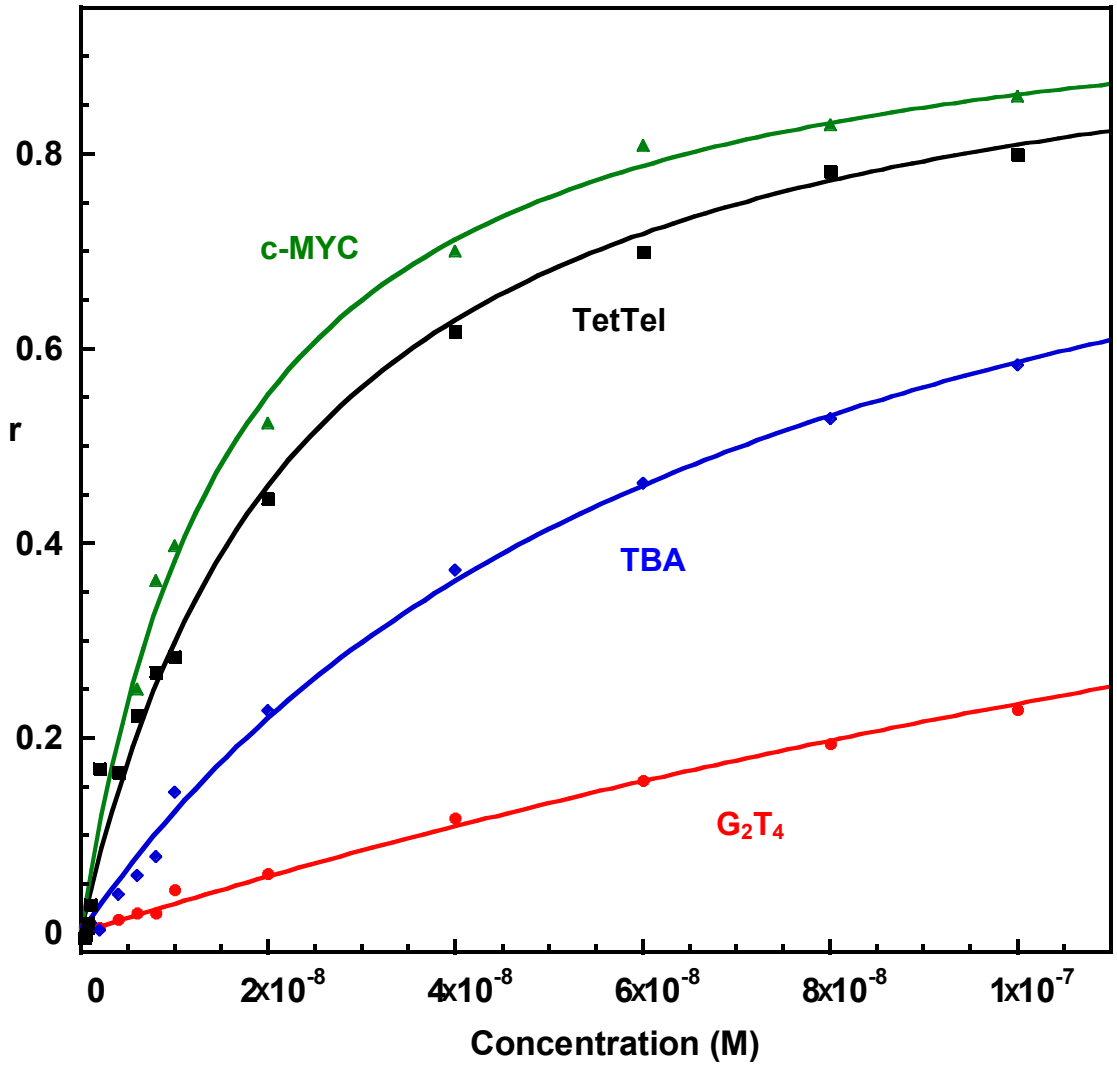


Figure 5.8 SPR steady-state binding plots. The concentration axis is for Se2SAP in the flow solution and is the unbound compound concentration; r represents the moles of compound bound per mole of G-quadruplex DNA. The points are for experimental data and the lines are the best-fit results for nonlinear least squares application of a single-site model to the data. Fitting errors due to random point scatter in any experiments are less than ±5%. The equilibrium constants determined from fitting data sets for each DNA are collected in Table 5.1. The buffer for all DNAs except TetTel was HEPES with 200 mM KCl. TetTel results are for the same buffer but with the KCl replaced by 200 mM NaCl.

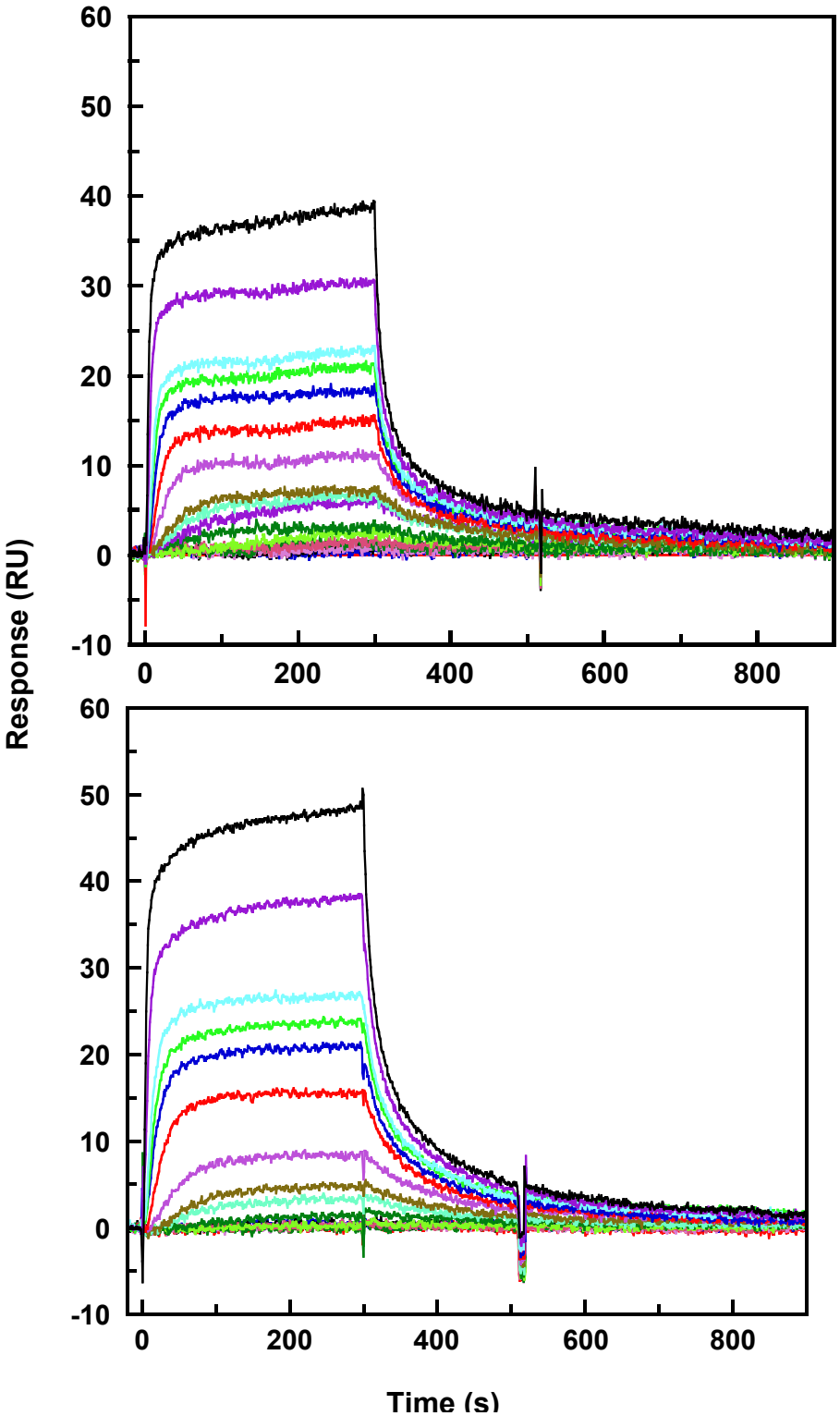


Figure 5.9 Sensorgrams for Se2SAP binding to the human telomere, d[$AG_3(T_2AG_3)_3$], in HEPES buffer containing 100 mM $K^+$ (top) and 100 mM $Na^+$ (bottom). The concentration range in both plots is from 0.0 μM to 0.4 μM.

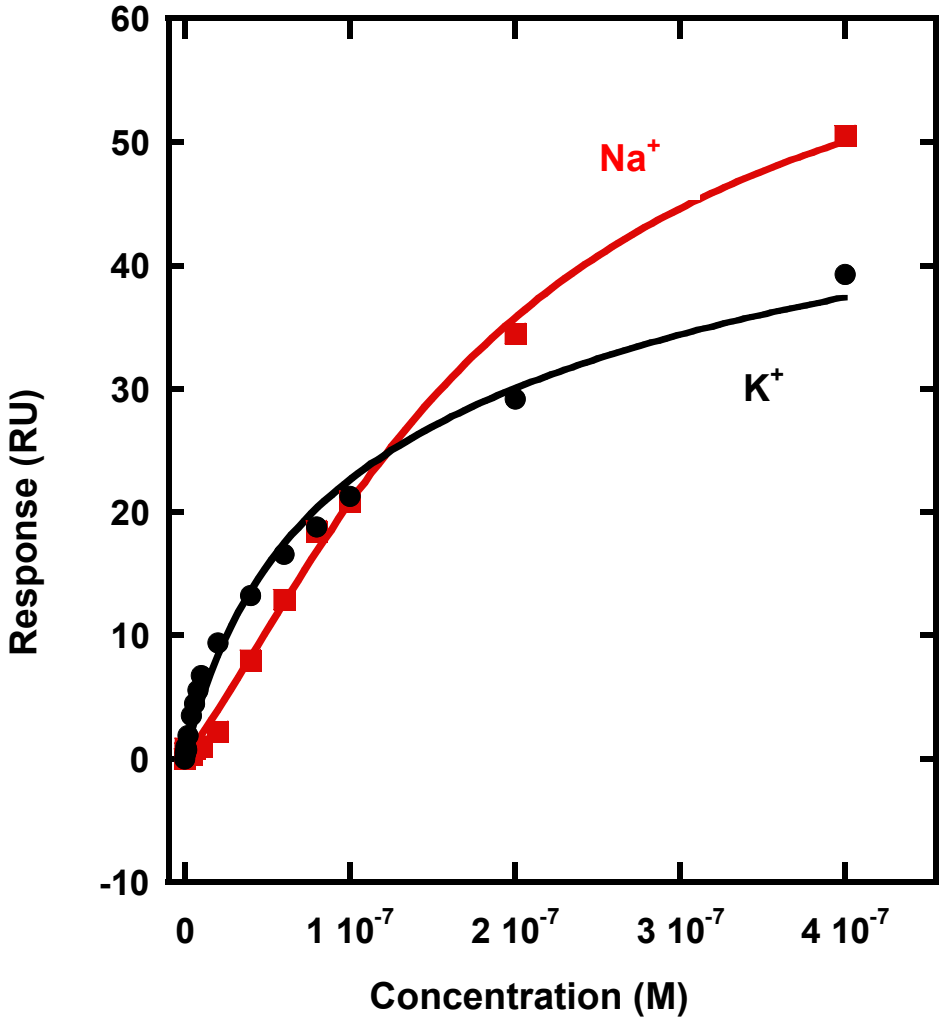


Figure 5.10 Direct binding plots for Se2SAP to the human telomere, d[$AG_3(T_2AG_3)_3$], in 100 mM $K^+$ (black) and 100 mM $Na^+$ (red). The concentration axis is for Se2SAP in the flow and is the unbound compound concentration. Direct plot curves from all experiments were fitted to a two-site binding model. The agreement in all experiments was within ±25% for both K values.

## References


1. Han, H., C.L. Cliff, and L.H. Hurley, *Accelerated assembly of G-quadruplex structures by a small molecule.* Biochem., 1999. **38**(22): p. 6981-6.
2. Han, H., et al., *Selective interactions of cationic porphyrins with G-quadruplex structures.* J. Am. Chem. Soc., 2001. **123**(37): p. 8902-13.
3. Izbicka, E., et al., *Effects of cationic porphyrins as G-quadruplex interactive agents in human tumor cells.* Cancer Res., 1999. **59**(3): p. 639-44.
4. Siddiqui-Jain, A., et al., *Direct evidence for a G-quadruplex in a promoter region and its targeting with a small molecule to repress c-MYC transcription.* Proc. Natl. Acad. Sci. U S A, 2002. **99**(18): p. 11593-8.
5. Shi, D.F., et al., *Quadruplex-interactive agents as telomerase inhibitors: synthesis of porphyrins and structure-activity relationship for the inhibition of telomerase.* J Med Chem, 2001. **44**(26): p. 4509-23.
6. Han, F.X., R.T. Wheelhouse, and L.H. Hurley, *Interactions of TMPyP4 and TMPyP2 with Quadruplex DNA. Structural Basis for the Differential Effects on Telomerase Inhibition.* J Am Chem Soc, 1999. **121**: p. 3561-3570.
7. Wheelhouse, R.T., et al., *Cationic Porphyrins as Telomerase Inhibitors: the Ineraction of Tetra-(N-methyl-4-pyridyl)porphine with Quadruplex DNA.* J Am Chem Soc, 1998. **120**: p. 3261-3262.
8. Seenisamy, J., et al., *The dynamic character of the G-quadruplex element in the c-MYC promoter and modification by TMPyP4.* J Am Chem Soc, 2004. **126**(28): p. 8702-9.

9. Grand, C.L., et al., *The cationic porphyrin TMPyP4 down-regulates c-MYC and human telomerase reverse transcriptase expression and inhibits tumor growth in vivo.* Mol. Cancer Ther., 2002. **1**(8): p. 565-73.

10. Hilmey, D.G., et al., *Water-soluble, core-modified porphyrins as novel, longer-wavelength-absorbing sensitizers for photodynamic therapy. II. Effects of core heteroatoms and meso-substituents on biological activity.* J Med Chem, 2002. **45**(2): p. 449-61.

11. Stilts, C.E., et al., *Water-soluble, core-modified porphyrins as novel, longer-wavelength-absorbing sensitizers for photodynamic therapy.* J Med Chem, 2000. **43**(12): p. 2403-10.

12. Dolmans, D.E., D. Fukumura, and R.K. Jain, *Photodynamic therapy for cancer.* Nat Rev Cancer, 2003. **3**(5): p. 380-7.

13. Shin-Ya, K., *Novel antitumor and neuroprotective substances discovered by characteristic screenings based on specific molecular targets.* Biosci. Biotechnol. Biochem., 2005. **69**(5): p. 867-72.

14. Kim, M.Y., et al., *The different biological effects of telomestatin and TMPyP4 can be attributed to their selectivity for interaction with intramolecular or intermolecular G-quadruplex structures.* Cancer Res., 2003. **63**(12): p. 3247-56.

15. Kim, M.Y., et al., *Telomestatin, a potent telomerase inhibitor that interacts quite specifically with the human telomeric intramolecular g-quadruplex.* J Am Chem Soc, 2002. **124**(10): p. 2098-9.

16. Shin-ya, K., et al., *Telomestatin, a novel telomerase inhibitor from Streptomyces anulatus.* J Am Chem Soc, 2001. **123**(6): p. 1262-3.

17. Seenisamy, J., et al., *Design and synthesis of an expanded porphyrin that has selectivity for the c-MYC G-quadruplex structure.* J. Am. Chem. Soc., 2005. **127**(9): p. 2944-59.

18. Lacy, E.R., et al., *Influence of a terminal formamido group on the sequence recognition of DNA by polyamides.* J. Am. Chem. Soc., 2002. **124**(10): p. 2153-63.

19. Mazur, S., et al., *A thermodynamic and structural analysis of DNA minor-groove complex formation.* J. Mol. Biol., 2000. **300**(2): p. 321-37.

20. Nguyen, B., et al., *Influence of compound structure on affinity, sequence selectivity, and mode of binding to DNA for unfused aromatic dications related to furamidine.* Biopolymers, 2002. **63**(5): p. 281-97.

21. Wang, L., et al., *Specific molecular recognition of mixed nucleic acid sequences: an aromatic dication that binds in the DNA minor groove as a dimer.* Proc. Natl. Acad. Sci. U S A, 2000. **97**(1): p. 12-6.

22. Wang, L., et al., *Evaluation of the influence of compound structure on stacked-dimer formation in the DNA minor groove.* Biochem., 2001. **40**(8): p. 2511-21.

23. Davis, T.M. and W.D. Wilson, *Determination of the refractive index increments of small molecules for correction of surface plasmon resonance data.* Anal Biochem, 2000. **284**(2): p. 348-53.

24. Dapic, V., et al., *Biophysical and biological properties of quadruplex oligodeoxyribonucleotides.* Nucleic Acids Res, 2003. **31**(8): p. 2097-107.

25. Marathias, V.M. and P.H. Bolton, *Determinants of DNA quadruplex structural type: sequence and potassium binding.* Biochemistry, 1999. **38**(14): p. 4355-64.

26. Schultze, P., R.F. Macaya, and J. Feigon, *Three-dimensional solution structure of the thrombin-binding DNA aptamer d(GGTTGGTGTGGTTGG).* J Mol Biol, 1994. **235**(5): p. 1532-47.

27. Wang, Y. and D.J. Patel, *Solution structure of the Tetrahymena telomeric repeat d(T2G4)4 G-tetraplex.* Structure, 1994. **2**(12): p. 1141-56.

28. Wang, Y. and D.J. Patel, *Solution structure of the human telomeric repeat d[AG3(T2AG3)3] G-tetraplex.* Structure, 1993. **1**(4): p. 263-82.

29. Patel, D.J., *Structural biology: a molecular propeller.* Nature, 2002. **417**(6891): p. 807-8.

30. Parkinson, G.N., M.P. Lee, and S. Neidle, *Crystal structure of parallel quadruplexes from human telomeric DNA.* Nature, 2002. **417**(6891): p. 876-80.

31. Ambrus, A., et al., *Human telomeric sequence forms a hybrid-type intramolecular G-quadruplex structure with mixed parallel/antiparallel strands in potassium solution.* Nucleic Acids Res., 2006. **34**(9): p. 2723-35.

32. Xu, Y., Y. Noguchi, and H. Sugiyama, *The new models of the human telomere d[AGGG(TTAGGG)3] in K+ solution.* Bioorg Med Chem, 2006. **14**(16): p. 5584-91.

# Chapter 6

## Binding of Fluoroquinolone Derivatives to Quadruplex DNA

### Introduction

Topoisomerase II is an enzyme that transiently cuts both strands of double-helical DNA, allowing another duplex strand to pass through. In bacteria, this enzyme serves as a target for antibacterial agents [1, 2]. In humans, topoisomerase II is a target for anti-cancer therapies. Fluoroquinolones (Figure 6.1) are a class of well-studied anti-bacterial agents that have exhibited activity as bacterial topoisomerase II inhibitors [3, 4]. They have large, planar aromatic structures which bind to single-stranded DNA and act by trapping the topoisomerase enzyme on the DNA to form a "cleaved complex" [5]. They have weak interactions with duplex and quadruplex DNAs [6]. The quinobenzoxazines are synthetic analogs of fluoroquinolones with extended ring systems that act as potent inhibitors of mammalian topoisomerase II [7]. They bind preferentially to duplex DNA by intercalation of one molecule, with another molecule bound externally through chelation with two $Mg^{2+}$ ions. It is likely that the external portion of the complex is responsible for the interaction with topoisomerase. A-62176 (Figure 6.1) is a fluoroquinobenzoxazine which has shown activity against human tumors *in vivo* including multi-drug resistant lines [8-10]. Because of its limited ability to form π- π stacking interactions, it does not bind strongly to G-quadruplexes and is a weak inhibitor of telomerase. This compound served as the basis of the design of a subsequent generation of fluoroquinophenoxazine and fluoroquinoanthroxazine compounds that were designed and synthesized to have selectivity for either topoisomerase II or G-quadruplex

interactions (Figure 6.1). It was believed that these compounds would likely bind G-quadruplex DNA better due to the larger ring systems that can stack better on the G-quartet surface. QQ58 and FQA-CR were shown to interact with G-quadruplexes, but have little activity against topoisomerase II [11, 12]. A stereoisomer of FQA-CR, FQA-CS was shown to be a potent topoisomerase II inhibitor that has little interaction with G-quadruplex DNA [12]. The trans FQA isomers (FQA-TR and FQA-TS) were also synthesized and studied, but they inhibited topoisomerase II and telomerase to a lesser degree than the other compounds [12].

This work with fluoroquinophenoxazine and fluoroquinoanthroxazine compounds served as the basis for the design of a new generation of fluoroquinolone derivatives developed by Cylene Pharmaceuticals [13]. One of these compounds, CX-3543 (structure not shown for proprietary reasons), demonstrates potent *in vivo* efficacy against a broad range of human tumors with a broad safety window. It is the first quadruplex-interactive compound to be evaluated in clinical trials. Currently it is in a Phase I trial of patients with advanced solid tumors or lymphomas. So far it has been well tolerated in humans with no toxicity to bone marrow, heart, liver or kidneys. This trial will determine the maximum tolerated dose (MTD), identify dose limiting toxicities (DLT), and establish the recommended dose for future Phase II studies.

CX-3543 was designed to selectively bind to the structural class of parallel quadruplexes as found in the G-rich strand of the promoter region of the c-MYC oncogene. However, intracellularly, CX-3543 demonstrates no direct effect on c-MYC transcription. It is believed that CX 3543 may be targeting a different G-quadruplex

structure, possibly the telomere or the ribosomal DNA template. Stabilization of the quadruplex conformation of the rDNA template would disrupt the interaction between nucleolin and the template. This would inhibit rRNA biogenesis in cancer cells, inducing apoptosis. Surface plasmon resonance (SPR) was attempted with CX 3546 in order to quantitatively measure its binding interactions with a series of quadruplex-forming DNA sequences, in order to gain insight into which quadruplex sequence it is targeting. Due to solubility problems, a full set of sensorgrams could not be obtained with this compound. A limited amount of kinetics data was collected, but the data had problems with errors and reproducibility. CX 2406 (structure not yet disclosed) is a second-generation Cylene compound that is closely related in structure to CX 3543. However, it exists as a dimesylate salt, making it more water-soluble than CX 3543. Therefore CX 2406 was used as a model system for studying CX 3543, allowing a full range of SPR experiments with six different quaduplex DNAs and one duplex DNA to be performed. In addition, SPR binding studies were performed with the earlier generation fluoroquinophenoxazine and fluoroquinoanthroxazine compounds A-62176, QQ58, FQA-CR, FQA-CS, FQA-TR and FQA-TS as a basis for comparison.

## Materials and Methods

### Sample Preparation

The oligonucleotides 5'-biotin-d[$AG_3(T_2AG_3)_3$], 5'-biotin-d($AG_3TG_4AG_3TG_4A$), 5'-biotin-d(CGAATTCG), 5'-biotin-d[$(G_2T_4)_3$], 5'-biotin-d[$(T_2G_4)_4$], and 5'-biotin-d($G_2T_2G_2TGTG_2T_2G_2$) were purchased with HPLC purification and mass spectrometry characterization from Midland Certified Reagent Company. Stock solutions containing 1

mM of each compound were prepared in double distilled water or DMSO and diluted to working concentrations immediately before use with buffer. A-62176, FQA-CS, FQA-CR, FQA-TR, FQA-TS and QQ58 were synthesized by Dr. Laurence H. Hurley's group at the University of Arizona. CX 3546 and CX 2406 were synthesized by Cylene Pharmaceuticals (San Diego, CA).

**Immobilization of DNA and Biosensor SPR Experiments**

Biosensor SPR experiments were performed with a four-channel BIAcore 2000 optical biosensor system (BIAcore, Inc.) and streptavidin-coated sensor chips (BIAcore SA with linked streptavidin). All DNA samples, for either duplex- or quadruplex-binding experiments, were used as single strands (fold-back structures) to prevent dissociation in the SPR flow system. The concentration in all cases refers to the strand concentration, which is also the duplex or quadruplex concentration. The chips were prepared for use by conditioning with three to five consecutive 1 min injections of 1 M NaCl in 50 mM NaOH followed by extensive washing with buffer. 5'-Biotinylated DNA samples (25 nM) in HBS buffer were immobilized on the flow cell surface by noncovalent capture as previously described. Three flow cells were used to immobilize DNA oligomer samples, and a fourth cell was left blank as a control. Interaction analysis was performed by using both kinetics and steady-state methods with multiple injections of different compound concentrations over the immobilized DNA surface at 25 ºC. DNA-binding experiments were performed in sterile filtered and degassed HBS buffers: 0.01 M HEPES, (pH 7.4), 3 mM EDTA, and 0.005% surfactant P20 with either 0.1 M KCl or NaCl. Compound solutions were prepared in the desired buffer by serial dilutions from stock solution and

injected from 7 mm plastic vials with pierceable plastic crimp caps (BIAcore, Inc.) at a flow rate of 25 μL/min for steady state experiments. To remove any remaining bound compound after the dissociation phase of the sensorgram, a low-pH glycine regeneration buffer was used (10 mM glycine at pH 2). The baseline was then reestablished, and the next compound concentration sample was injected.

The instrument response (RU) in the steady-state region is proportional to the amount of bound drug and was typically determined by linear averaging over a 10-20 s or longer time span, depending on the length of the steady-state plateau. The predicted maximum response per bound compound in the steady-state region ($RU_{max}$) was determined from the DNA molecular weight, the amount of DNA on the flow cell, the compound molecular weight, and the refractive index gradient ratio of the compound and DNA, as previously described. The number of binding sites was estimated fitting plots of RU versus $C_{free}$. These methods can also be used to determine an empirical $RU_{max}$ value. The $RU_{max}$ value is required to convert the observed response (RU) to the standard binding parameter *r* (moles of drug bound per moles of DNA hairpin)

$$r = RU/RU_{max}$$

which is useful for comparison of a compound binding to different DNAs. To obtain the affinity constants, the data were fitted to the following interaction model using Kaleidagraph for nonlinear least-squares optimization of the binding parameters:

$$r = (K_1C_{free} + 2K_1K_2C_{free}^2)/(1 + K_1C_{free} + K_1K_2C_{free}^2)$$

where $K_1$ and $K_2$ are equilibrium constants for two types of binding sites and $C_{free}$ is the concentration of the compound in equilibrium with the complex and is fixed by the concentration in the flow solution. For a single dominant binding site model, $K_2$ is equal to zero. Errors in fitting two $K$ values within any experiment were ±10%, while errors in $K$ values in replicate experiments were ±25%. Errors in fitting results that required only a single $K$ value were ±10%.

Kinetics data were obtained for the human telomeric sequence, the c-MYC sequence and the Tetrahymena telomere sequence in buffer containing 100 mM KCl. After injection of the compound and prior to reinjection of buffer, the association kinetics of compound binding to immobilized DNA were monitored, and after reinjection of buffer the dissociation kinetics were determined. To minimize possible mass transport effects, SPR kinetics experiments were conducted at flow rates of 50-100 μL/min using a different sensor chip with low surface densities of immobilized DNA. Global fitting using a one-site model (BIA Evaluation Software, BIAcore, Inc.) of the association and dissociation curves was done in a concentration range where the compound binds significantly only to the strongest binding site in order to obtain the association rate constant, $k_a$, and the dissociation rate constant, $k_{d,}$ for the first binding site for these complexes. For the compounds that did not reach steady state at low concentrations, a fit of the kinetics data was used to estimate the RU at equilibrium for the lower concentration region in order to determine a steady-state binding constant.

## Results and Discussion

### Human Telomeric DNA is the likely target for CX 2406

SPR was used to quantitatively evaluate the interaction between CX 2406 and a series of quadruplex-forming DNA sequences in order to provide insight into the selectivity of this compound for different types of quadruplexes. A hairpin duplex sequence was also studied in order to evaluate the selectivity of CX 2406 for quadruplex DNA vs. duplex DNA. The sequences, d[$AG_3(T_2AG_3)_3$] (HTel), d($AG_3TG_4AG_3TG_4A$) (c-MYC), d(CGAATTCG) (duplex), d[$(G_2T_4)_3$] (G2T4), d[$(T_2G_4)_4$] (TetTel), and d($G_2T_2G_2TGTG_2T_2G_2$) (TBA) were immobilized using two different SPR sensor chips. For all DNA sequences, the sensorgrams were obtained using buffer containing 100 mM KCl. Because the conformation of the human telomere is dependent on the type of cation present, sensorgrams for the binding of CX 2406 to the HTel sequence were also obtained in buffer containing 100 mM NaCl. A range of CX 2406 concentrations (0.1 nM to 90 nM) were injected to quantitatively evaluate the interaction with the DNA. Blank injections with running buffer were also performed, and the resulting sensorgrams were subtracted from the compound sensorgrams to obtain the final concentration-dependent graphs (Shown in Figures 6.2-6.4). The plot of RU versus the unbound concentration of each of the compounds was fitted to a two-site binding model (Experimental Section). The response values in the steady-state region of the sensorgrams were converted to r and plotted versus the unbound concentration ($C_f$) of CX 2406 in the flow solution (Figure 6.5). The equilibrium binding constants (K values) are shown for each compound in Table 6.1.

Because the sensorgrams had not reached steady state in the lower concentrations for the HTel (in KCl), c-MYC, and TetTel sequences, binding plots that use this data may underestimate the K values for CX 2406 binding with these DNAs. To obtain a more accurate value of the binding constant for the first strong binding site ($K_1$) with these three DNAs, a one-site global kinetics fit was performed for the lower concentration ranges of sensorgrams for CX 2406 with each of these DNAs (Figure 6.6). These values are shown in Table 6.1. The steady-state response at low concentrations was calculated from a fit of these kinetics curves and used to calculate the steady-state binding constants for these DNAs.

Fits of the binding data show that CX 2406 binds the strongest to the human telomeric sequence in KCl. The first, strong binding site has a kinetics binding constant of $K_1 = 2.8 \times 10^8\ M^{-1}$. This is among the highest binding constants reported for small molecule binding to human telomeric DNA to date [14].Several quadruplex structures have been proposed for the human telomere in potassium. However, recent studies suggest that it likely forms a mixed parallel/antiparallel hybrid structures under these salt conditions [15, 16]. CX 2406 also exhibits strong binding with TetTel ($K_1 = 2.2 \times 10^8\ M^{-1}$). TetTel also has been shown by NMR to form a mixed parallel/antiparallel quadruplex structure [17]. CX 2406 also binds strongly ($K_1 = 1.7 \times 10^8\ M^{-1}$) to the c-MYC sequence, but this sequence has been ruled out as a target for the biological action for this class of compounds. The binding of this compound is lower to the TBA sequence, which forms an antiparallel chair-type quadruplex [18], G2T4, which forms an antiparallel basket quadruplex [19, 20] and HTel in the presence of sodium, which also forms a basket-type structure [21].

These results suggest that CX 2406 may be selective for the mixed parallel/antiparallel hybrid type of quadruplex structure, and not the parallel quadruplex structure formed by c-MYC that it was initially designed to target.

**CX 2406 is Selective for Quadruplex Over Duplex DNA**

These results show also that CX 2406 is selective for quadruplex over duplex DNA. CX 2406 binds to two equivalent sites of the duplex DNA with $K_1 = K_2 = 1.1 \times 10^7$ $M^{-1}$. Although this binding constant is very high, the binding constant for the strong site of the human telomere as determined by kinetics is 25 times higher ($2.8 \times 10^8$ $M^{-1}$). As seen from the sensorgrams of CX 2406 with duplex DNA, it also has very fast dissociation kinetics. This high degree of selectivity for quadruplex over duplex DNA is consistent with the absence of cytotoxicity seen so far with CX 3543 in the Phase I clinical trials.

**CX 2406 Shows Improved Binding Over Other Fluoroquinolone Derivatives**

To quantitatively compare quadruplex binding affinity of CX 2406 to that of the previous generation of modified fluoroquinolones, SPR binding studies were performed with A-62176, QQ58, FQA-CR, FQA-CS, FQA-TR and FQA-TS. A sensor chip containing HTel, c-MYC and the duplex sequence was used. For all compounds, the amount of binding with each of the DNA sequences was too low to be measured using SPR. Sensorgrams for FQA-CR, the compound from this set that was previously shown to have the strongest degree of interaction with quadruplex DNA [12], are shown in Figure 6.7 as an example.

**Conclusion**

CX 3543 is a fluoroquinolone derivative that was initially designed to bind specifically to the quadruplex structure formed by the G-rich strand of the c-MYC oncogene. Although this compound has shown potent anti-cancer activity against a broad range of tumors, evidence suggests that c-MYC is not actually the biological target. A CX 3543 derivative, CX 2406, was evaluated against different quadruplex-forming DNA sequences using SPR. It exhibited extremely high binding with the human telomere ($2.8 \times 10^8\ M^{-1}$), which suggests that this sequence might actually be the target, and that its mode of action is telomerase inhibition. CX 2406 also was found to have a 25-fold selectivity for the human telomere over duplex DNA, consistent with the absence of cytotoxic side effects seen so far in patients receiving CX 3543 in Phase I clinical trials. CX 2406 also binds much stronger to quadruplex sequences than the fluoroquinolone compounds that CX 2406 and CX 3543 were based on. This suggests that the structural modifications that differentiate CX 2406 and CX 3543 from the earlier compounds play a very significant role in the selective recognition of quadruplex DNA.

The identification of the human telomere as the probable quadruplex target for CX 2406 (and thus CX 3543), provides evidence that specific quadruplex structures can be targeted selectively. Knowing the structure of the target will also aid in the design and evaluation of new compounds that may target this sequence with even higher affinity and selectivity.

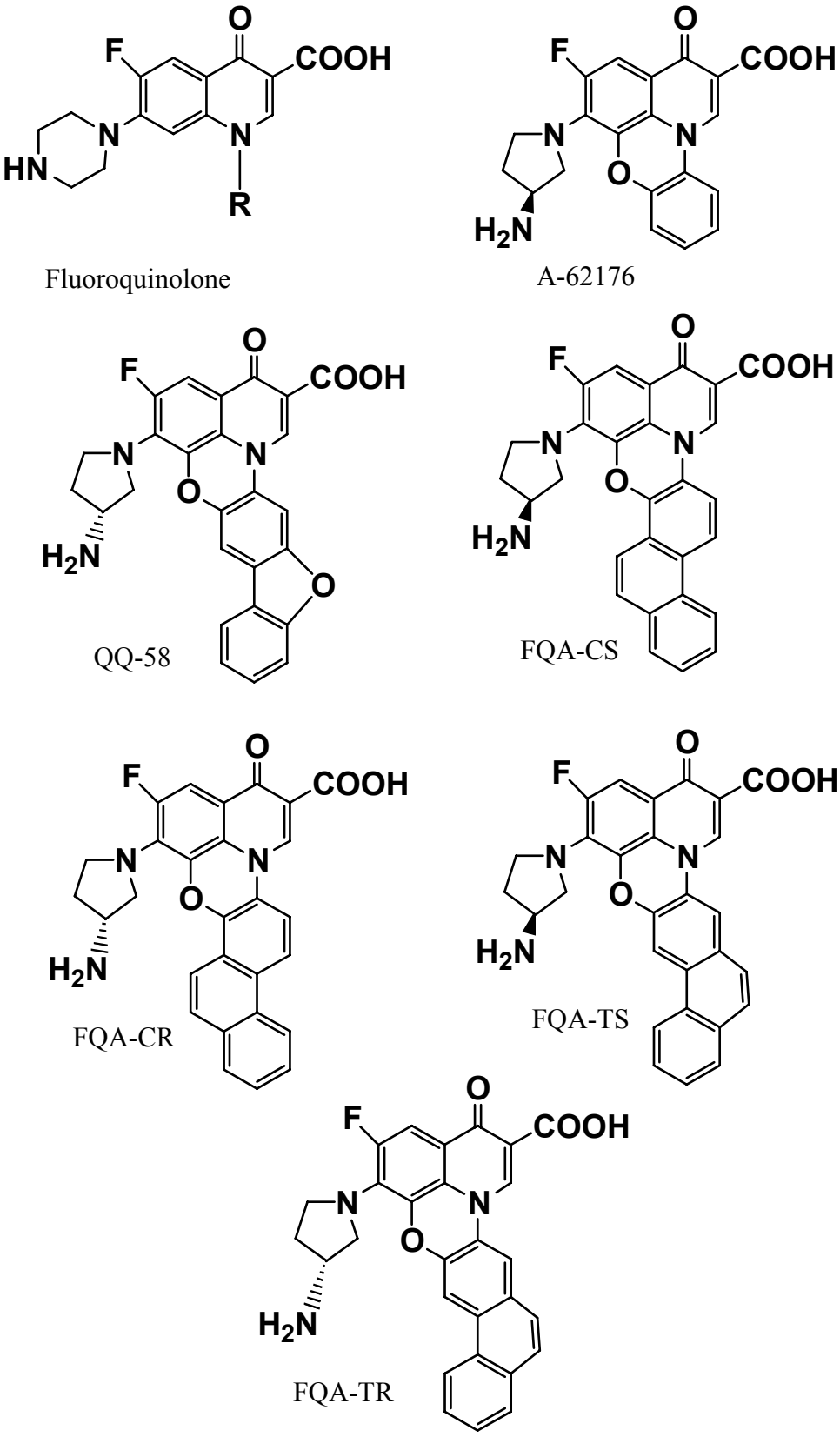


Figure 6.1 Structures of fluoroquinolone and fluoroquinolone derivatives

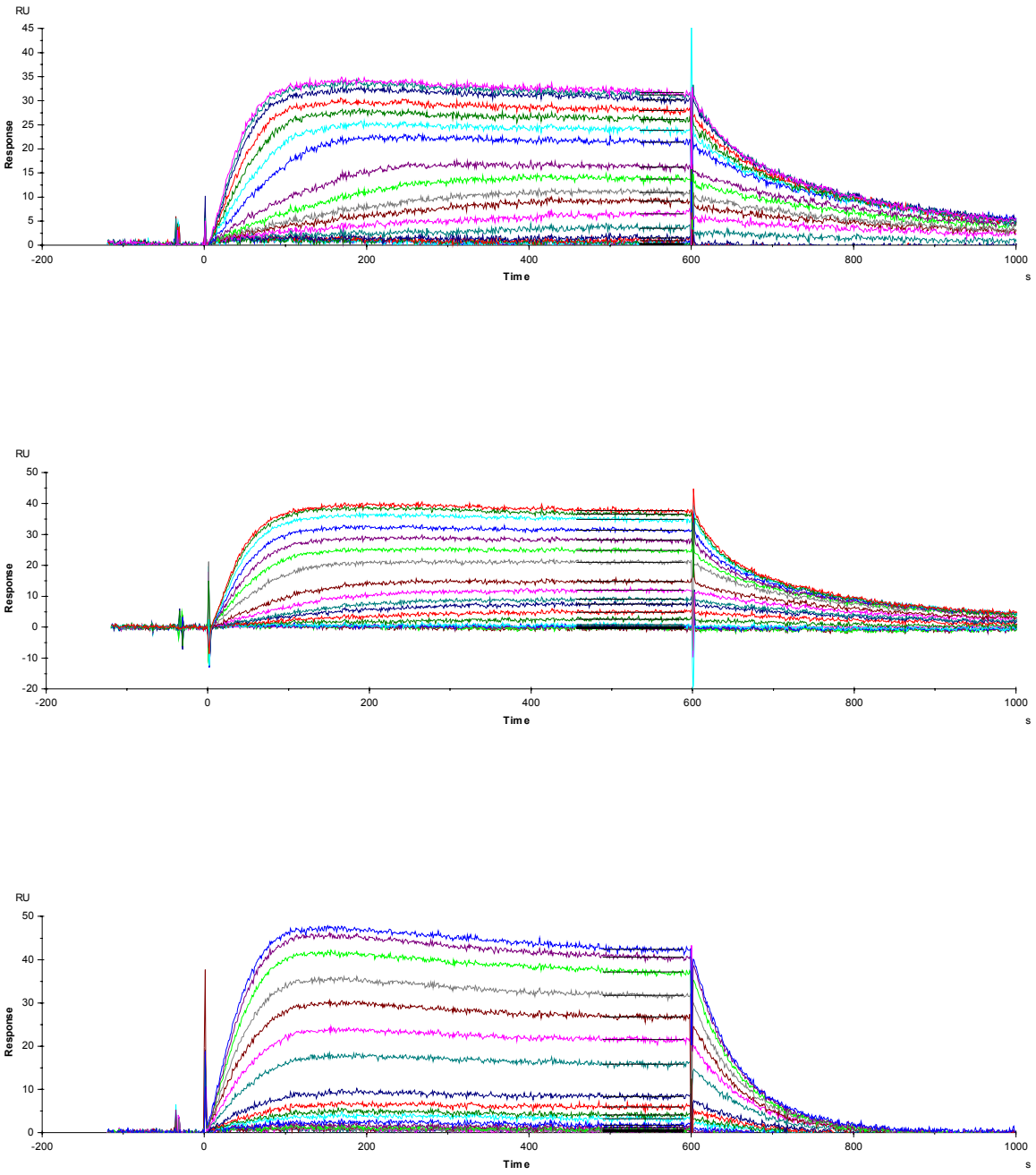


Figure 6.2 SPR sensorgrams for binding of CX 2406 to the immobilized G-quadruplex formed by c-MYC (top), human telomere (middle) and duplex DNA (bottom) as a hairpin dimer in HEPES buffer containing 100 mM KCl at 25°C. Each sensorgram ranges in concentration from 0.1 nM for the lowest curve to 90 nM for the top curve.

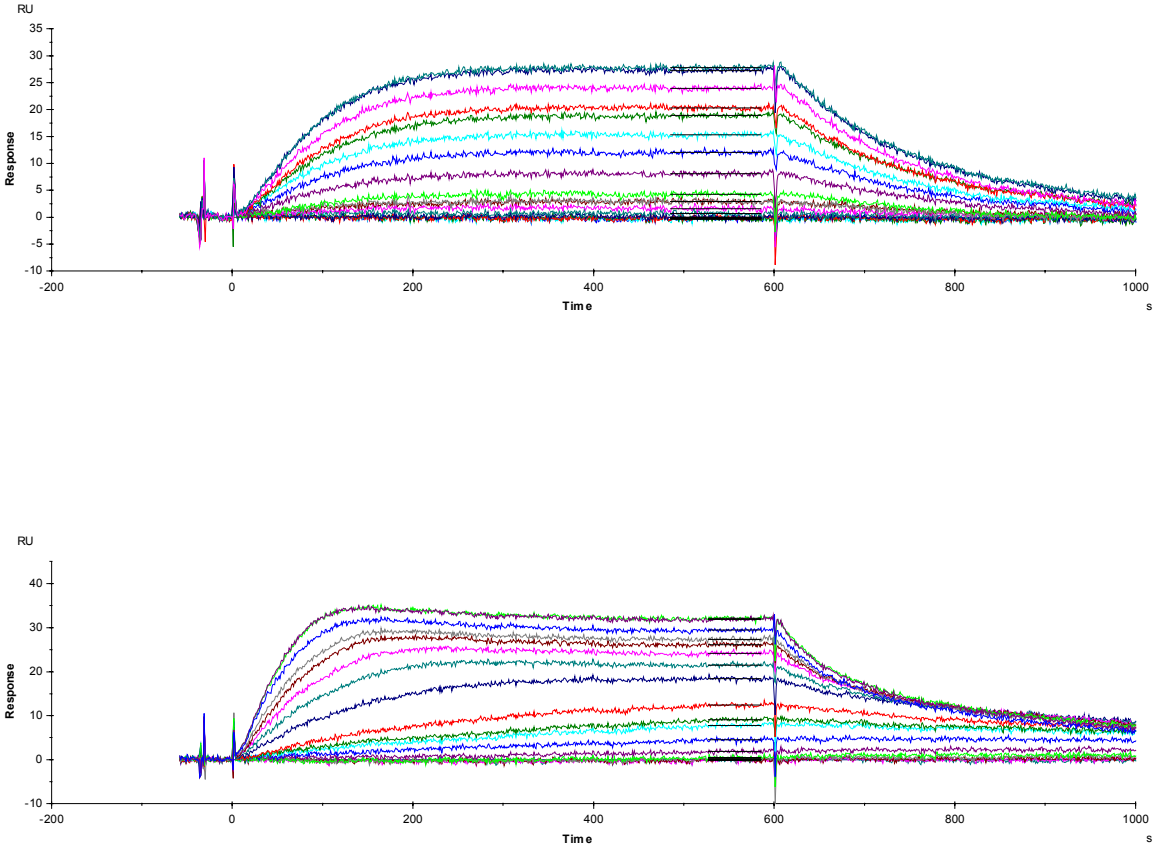


Figure 6.3 SPR sensorgrams for binding of CX 2406 to the immobilized G-quadruplex formed by G2T4 (top), and TetTel (bottom) in HEPES buffer containing 100 mM KCl at 25°C. Each sensorgram ranges in concentration from 0.1 nM for the lowest curve to 90 nM for the top curve.

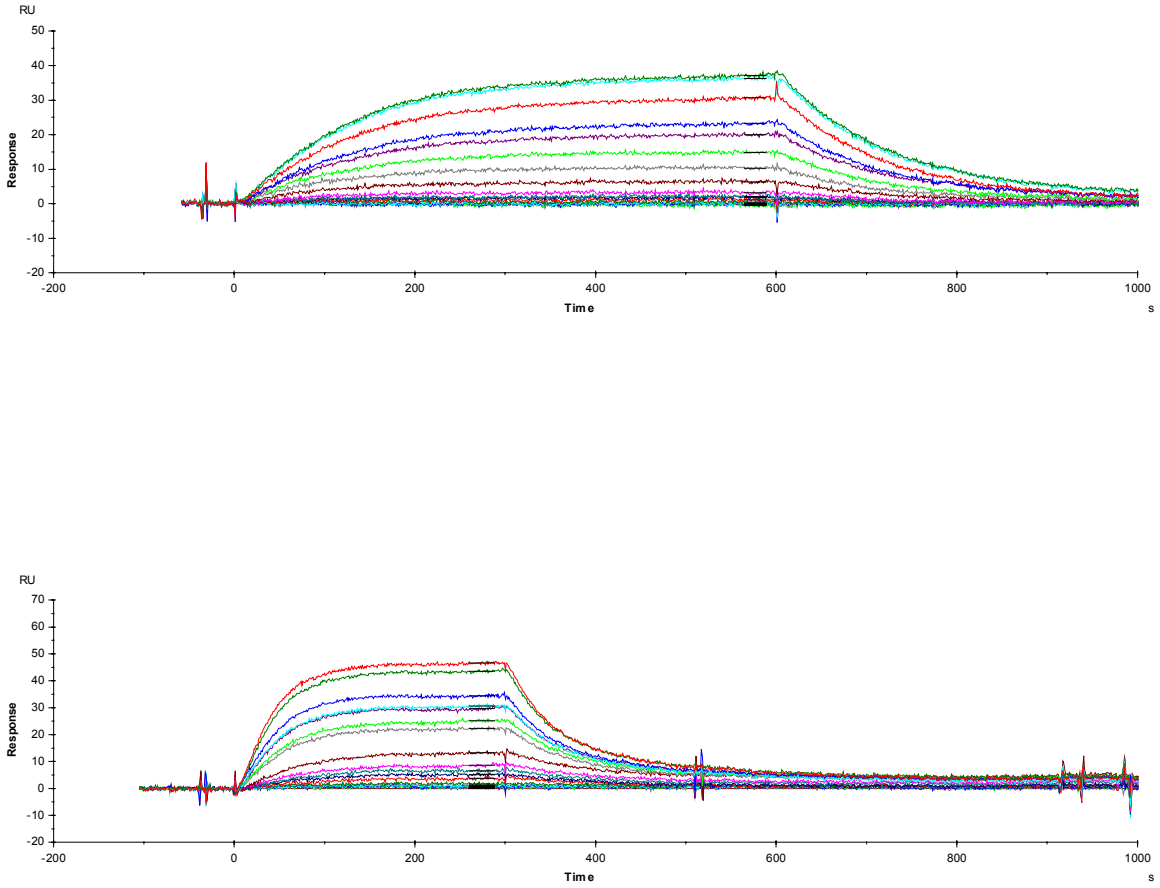


Figure 6.4 SPR sensorgrams for binding of CX 2406 to the immobilized G-quadruplex formed by TBA (top) in HEPES buffer containing 100 mM KCl, and human telomere DNA (bottom) in HEPES buffer containing 100 mM NaCl at 25°C. Each sensorgram ranges in concentration from 0.1 nM for the lowest curve to 90 nM for the top curve.

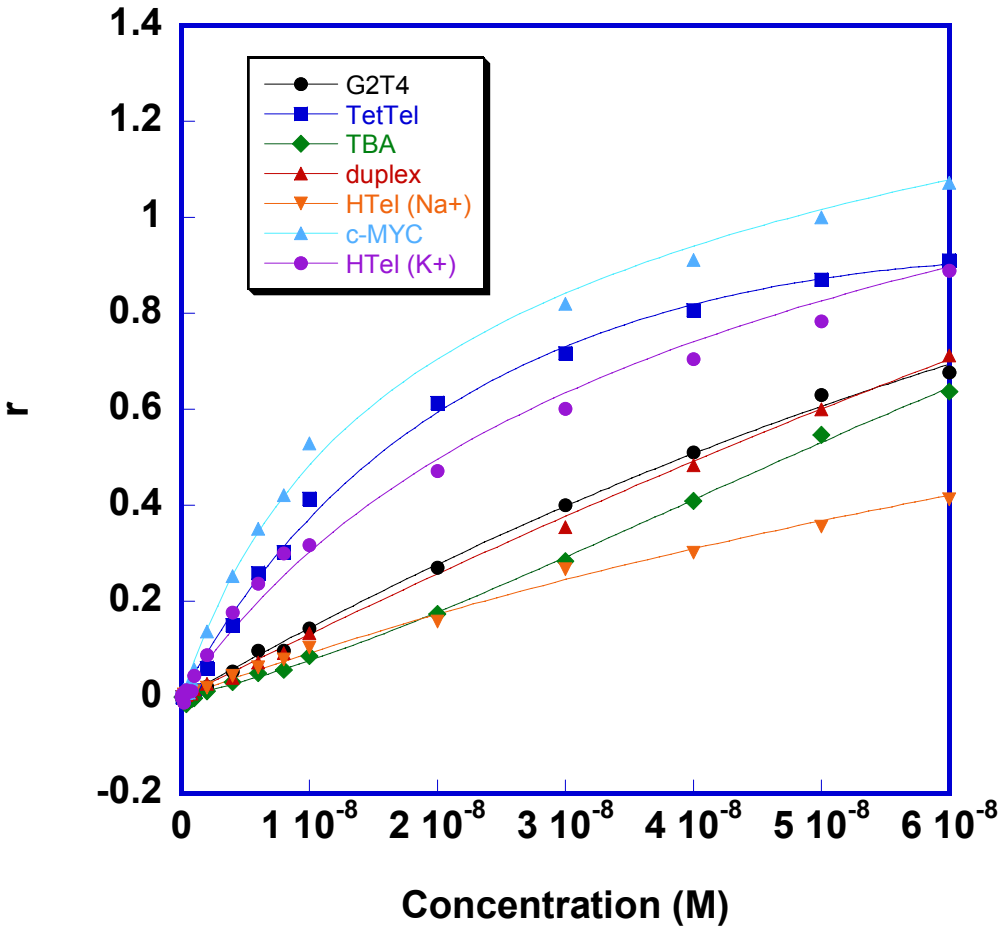


Figure 6.5 SPR steady-state binding plots for CX 2406. The concentration axis is for CX 2406 in the flow solution and is the unbound compound concentration; r represents the moles of compound bound per mole of G-quadruplex DNA. The points are for experimental data and the lines are the best-fit results for nonlinear least squares application of a two-site model to the data. Fitting errors due to random point scatter in any experiments are less than ±5%. The equilibrium constants determined from fitting data sets for each DNA are collected in Table 6.1. All experiments were performed in HEPES buffer containing 100 mM KCl at 25°C except HTel ($Na^+$) which was performed in 100 mM NaCl.

Table 6.1 Steady-State and Kinetics Binding Constants for CX 2406 as Determined by SPR

| DNA | Steady-State Binding Constants | | Kinetics Binding Constants | | |
|---|---|---|---|---|---|
| | $K_1 \times 10^{-6}$ ($M^{-1}$) | $K_2 \times 10^{-6}$ ($M^{-1}$) | $K_1 \times 10^{-6}$ ($M^{-1}$) | $k_a$ ($M^{-1}s^{-1}$) | $k_d$ ($s^{-1}$) |
| HTel ($K^+$) | 140 | 2.2 | 280 | $8.3 \times 10^5$ | $3.0 \times 10^{-3}$ |
| HTel ($Na^+$) | 9.8 | 1.4 | | | |
| Duplex | 11 | 11 | | | |
| TetTel | 160 | 12 | 220 | $2.0 \times 10^5$ | $8.8 \times 10^{-4}$ |
| TBA | 6.1 | 1.7 | | | |
| c-MYC | 190 | 12 | 170 | $3.3 \times 10^5$ | $1.9 \times 10^{-3}$ |
| G2T4 | <0.1 | | | | |

All experiments were performed in HEPES buffer containing 100 mM KCl at 25°C except HTel ($Na^+$) which was performed in 100 mM NaCl. Fitting errors due to random point scatter in any experiment are less than ±5%. The steady state binding plots for each compound were fit with a two-site model. Kinetics data was fit with a one-site global fitting model.

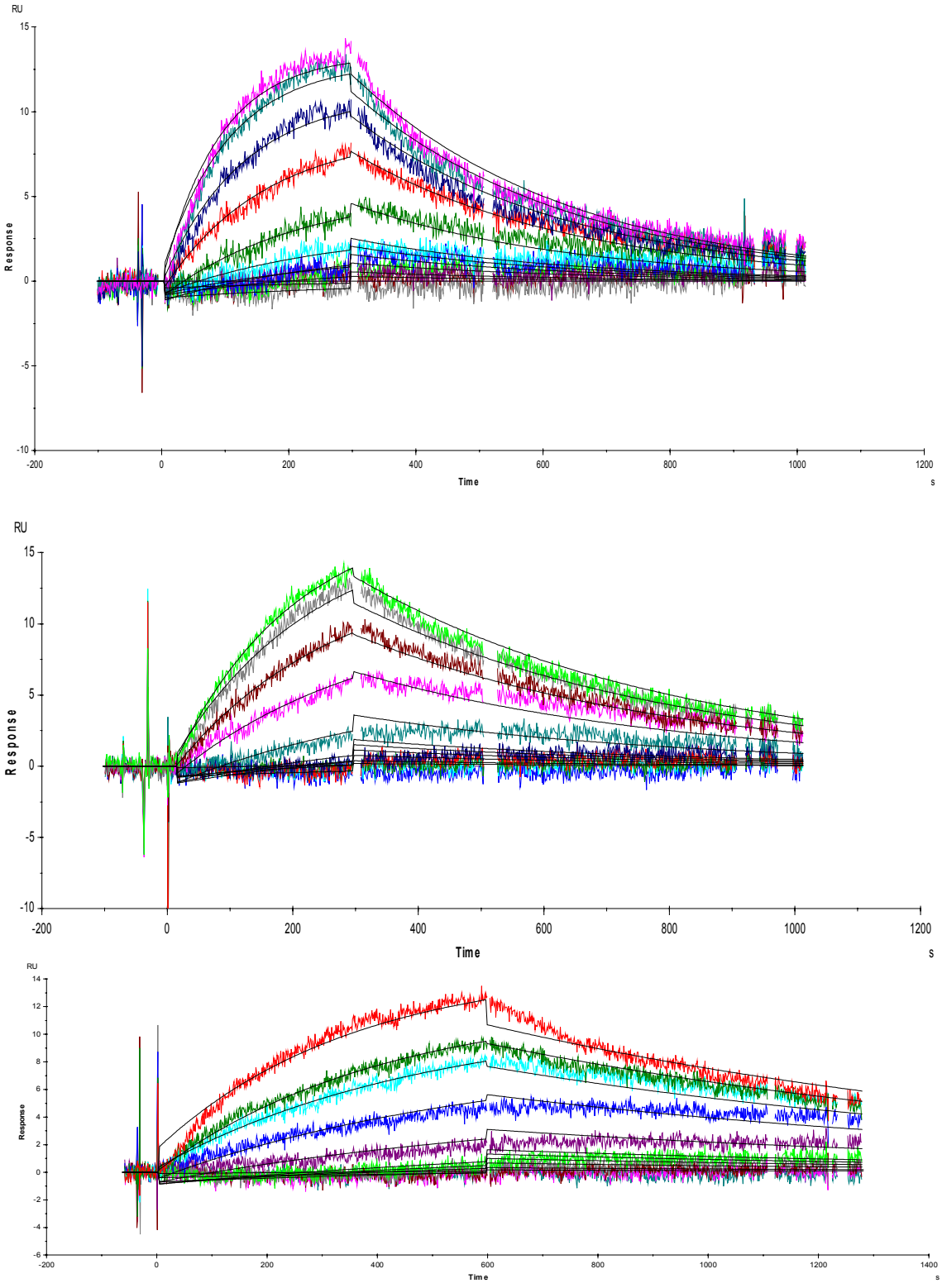


Figure 6.6 SPR sensorgrams for binding of CX 2406 to Htel (top), c-MYC (middle) and TetTel (bottom). Concentration ranges from 0.1 nM to10 nM. The black solid curves represent a 1:1 global kinetics fit.

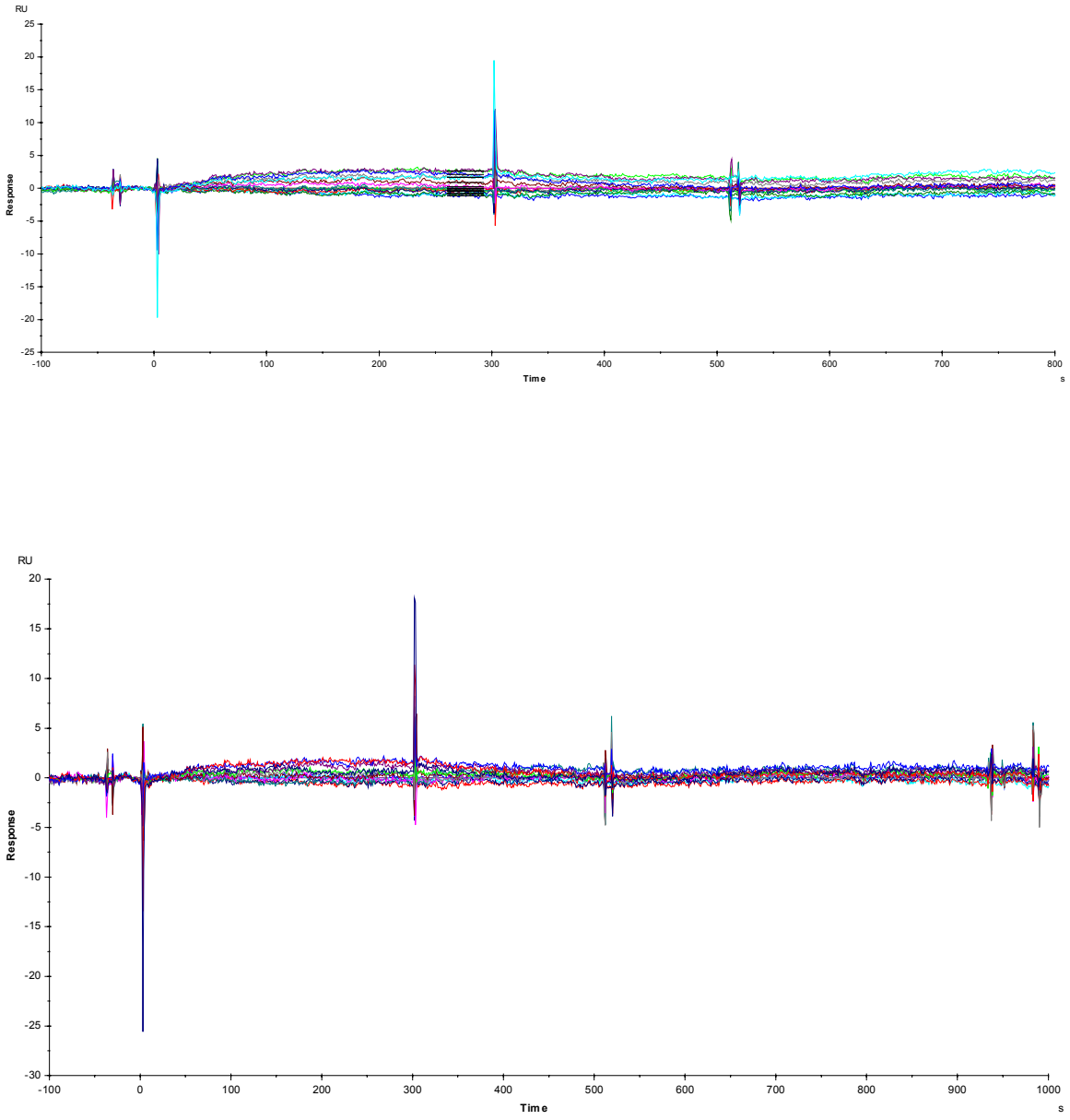


Figure 6.7 SPR sensorgrams for binding of FQA-CR to the immobilized G-quadruplex formed by HTel (top) and c-MYC (bottom) in HEPES buffer containing 100 mM KCl at 25°C. Each sensorgram ranges in concentration from 0.1 nM for the lowest curve to 0.2 μM for the top curve.

## References


1. Nitiss, J.L., *Investigating the biological functions of DNA topoisomerases in eukaryotic cells.* Biochim Biophys Acta, 1998. **1400**(1-3): p. 63-81.
2. Wang, J.C., *Cellular roles of DNA topoisomerases: a molecular perspective.* Nat Rev Mol Cell Biol, 2002. **3**(6): p. 430-40.
3. Reece, R.J. and A. Maxwell, *DNA gyrase: structure and function.* Crit Rev Biochem Mol Biol, 1991. **26**(3-4): p. 335-75.
4. Wang, J.C., *DNA topoisomerases.* Annu Rev Biochem, 1996. **65**: p. 635-92.
5. Chen, A.Y. and L.F. Liu, *DNA topoisomerases: essential enzymes and lethal targets.* Annu Rev Pharmacol Toxicol, 1994. **34**: p. 191-218.
6. Willmott, C.J. and A. Maxwell, *A single point mutation in the DNA gyrase A protein greatly reduces binding of fluoroquinolones to the gyrase-DNA complex.* Antimicrob Agents Chemother, 1993. **37**(1): p. 126-7.
7. Permana, P.A., et al., *Quinobenoxazines: a class of novel antitumor quinolones and potent mammalian DNA topoisomerase II catalytic inhibitors.* Biochemistry, 1994. **33**(37): p. 11333-9.
8. Chu, D.T., et al., *Synthesis and structure-activity relationship of 1-aryl-6,8-difluoroquinolone antibacterial agents.* J Med Chem, 1987. **30**(3): p. 504-9.
9. Chu, D.T., et al., *Synthesis and antitumour activities of quinolone antineoplastic agents.* Drugs Exp Clin Res, 1992. **18**(7): p. 275-82.
10. Clement, J.J., et al., *Biological characterization of a novel antitumor quinolone.* Cancer Res, 1995. **55**(4): p. 830-5.

11. Duan, W., et al., *Design and synthesis of fluoroquinophenoxazines that interact with human telomeric G-quadruplexes and their biological effects.* Mol Cancer Ther, 2001. **1**(2): p. 103-20.

12. Kim, M.Y., et al., *Design, synthesis, and biological evaluation of a series of fluoroquinoanthroxazines with contrasting dual mechanisms of action against topoisomerase II and G-quadruplexes.* J Med Chem, 2003. **46**(4): p. 571-83.

13. *www.cylenepharma.com*. [cited.

14. Moore, M.J., et al., *Trisubstituted acridines as G-quadruplex telomere targeting agents. Effects of extensions of the 3,6- and 9-side chains on quadruplex binding, telomerase activity, and cell proliferation.* J Med Chem, 2006. **49**(2): p. 582-99.

15. Ambrus, A., et al., *Human telomeric sequence forms a hybrid-type intramolecular G-quadruplex structure with mixed parallel/antiparallel strands in potassium solution.* Nucleic Acids Res., 2006. **34**(9): p. 2723-35.

16. Xu, Y., Y. Noguchi, and H. Sugiyama, *The new models of the human telomere d[AGGG(TTAGGG)3] in K+ solution.* Bioorg Med Chem, 2006. **14**(16): p. 5584-91.

17. Wang, Y. and D.J. Patel, *Solution structure of the Tetrahymena telomeric repeat d(T2G4)4 G-tetraplex.* Structure, 1994. **2**(12): p. 1141-56.

18. Schultze, P., R.F. Macaya, and J. Feigon, *Three-dimensional solution structure of the thrombin-binding DNA aptamer d(GGTTGGTGTGGTTGG).* J Mol Biol, 1994. **235**(5): p. 1532-47.

19. Dapic, V., et al., *Biophysical and biological properties of quadruplex oligodeoxyribonucleotides.* Nucleic Acids Res, 2003. **31**(8): p. 2097-107.

20. Marathias, V.M. and P.H. Bolton, *Determinants of DNA quadruplex structural type: sequence and potassium binding.* Biochemistry, 1999. **38**(14): p. 4355-64.

21. Wang, Y. and D.J. Patel, *Solution structure of the human telomeric repeat d[AG3(T2AG3)3] G-tetraplex.* Structure, 1993. **1**(4): p. 263-82.